

**Palaeomagnetic Analyses
of the Leaf Rapids Area in Manitoba**

by

Guye Strobel

A Thesis
presented to the University of Manitoba
in partial fulfillment of the requirements for the
Degree of Master of Science
in
Geophysics

Department of Geological Sciences
University of Manitoba
Winnipeg, Manitoba

Winnipeg, Manitoba, 1988

(c) Guye Strobel, 1988

Permission has been granted
to the National Library of
Canada to microfilm this
thesis and to lend or sell
copies of the film.

The author (copyright owner)
has reserved other
publication rights, and
neither the thesis nor
extensive extracts from it
may be printed or otherwise
reproduced without his/her
written permission.

L'autorisation a été accordée
à la Bibliothèque nationale
du Canada de microfilmer
cette thèse et de prêter ou
de vendre des exemplaires du
film.

L'auteur (titulaire du droit
d'auteur) se réserve les
autres droits de publication;
ni la thèse ni de longs
extraits de celle-ci ne
doivent être imprimés ou
autrement reproduits sans son
autorisation écrite.

ISBN 0-315-48051-3

PALAEOMAGNETIC ANALYSES OF THE
LEAF RAPIDS AREA IN MANITOBA

BY

GUYE STROBEL

A thesis submitted to the Faculty of Graduate Studies of
the University of Manitoba in partial fulfillment of the requirements
of the degree of

MASTER OF SCIENCE

© 1988

Permission has been granted to the LIBRARY OF THE UNIVERSITY OF MANITOBA to lend or sell copies of this thesis, to the NATIONAL LIBRARY OF CANADA to microfilm this thesis and to lend or sell copies of the film, and UNIVERSITY MICROFILMS to publish an abstract of this thesis.

The author reserves other publication rights, and neither the thesis nor extensive extracts from it may be printed or otherwise reproduced without the author's written permission.

ABSTRACT

Conventional methods of analyses of palaeomagnetic data, leave a lot to be desired. Fisher statistics, by far the most popular technique, is a method that was developed long before computers were widely available. Understandably, it is not specifically a computer application. Furthermore, the necessary selective procedures used to identify "valid" palaeomagnetic samples, introduce a subjective form of analysis. In order to answer to these shortcomings in current analysis, two digital computer methods were developed. In one method, Gaussian distributions representing the probability of a position corresponding to the true value were fitted to measurements made at each cleaning field strength. The most probable orientation was taken from the location of the highest amplitude. In the second method, the same measurements were summed using vector addition. The final vector sum was assumed to the most probable orientation.

Rock core samples used in this study were obtained from the Leaf Rapids area and are of mid-proterozoic age (1800-1900Ma). These samples were analyzed in the laboratory and the results were used to test the above methods. The equipment used was a Schonstedt model DSM-1 spinner magnetometer, while magnetic cleaning was done by using an alternating frequency demagnetizer. The rock samples were collected during a reconnaissance survey carried out in 1974. The methods used in this study offers a better interpretation of the results than fisher statistics would allow.

ACKNOWLEDGMENTS

I would like to express my extreme gratitude to Dr. D.H. Hall for his assistance in supervising this project.

I would like to acknowledge Dr. G. Clark, and Dr. H.C. Palmer for reviewing the manuscript and offering suggestions for improvement. I would also like to thank Dr. Brisbin for keeping my feet on the ground regardless of what approach he used to achieve this. Dr. C.D. Anderson also deserves a special mention for the moral support he has provided to me.

I would also like to thank my wife Karen who through thick and thin, supported this endeavour and helped out where ever and whenever she could (some times more enthusiastically than at others).

CONTENTS

Abstract	ii
Acknowledgments	iii
Chapter I: Introduction	1
Chapter II: The Magnetic Properties of Solids and Rock Magnetism	4
Magnetic Properties of Solids	4
Magnetic Minerals	5
Rock Magnetism	6
Remanent Magnetization	6
Forms of Remanent Magnetization	7
Secondary Magnetization	9
Metamorphic Effects	10
Self-Reversals	11
Stability of Remanence	11
Chapter III: Palaeomagnetism	13
Principles of Palaeomagnetics	13
Fundamental Assumptions of Palaeomagnetic Studies	13
Applications of Palaeomagnetism	17
Problems in the Interpretation of Palaeomagnetic Data	19
Interpretation of Palaeomagnetic Results	24
Applying Palaeomagnetic Theory	28
Rock Magnetism and Palaeomagnetism	28
Measurement Devices used in Palaeomagnetic Studies	29
Chapter IV: Statistical Analyses of Palaeomagnetic Data	31
Statistical Methods in Data Analysis	31
A New Approach	31
Approaching the Problem	32
Two-Dimensional Representation	35
Probability Distribution Representation	38
Mean Magnetization by Vector Addition	45
Consideration of this Method on the Physical Level	46
Resolution of Multiple Components	48
DGTL and Fisher Analysis; Comparison of the Uncertainties	52

Least Squares Fitting to Palaeomagnetic Data	52
Chapter V: The Earth's Magnetic Field	56
Secular Variations	56
Reversals	58
Apparent Polar Wandering	59
Chapter VI: Geology of the Study Area	60
Regional Setting	60
Isotopic Ages	65
Chapter VII: Processing and Sampling Methods	66
Chapter VIII: Discussion of Results	112
Consistency within Sites	118
Conclusions	120
References Cited	122
Appendix A: Suggestions on updating the current Magnetometer	128
Commodore to PDP 11/04 Interface: The RS-232.	129
Appendix B: Mainframe Analysis	132
Computer Analysis on the Amdahl at the University of Manitoba	133
CALCOMP and SAS Plotting	133
Compilation of CALCOMP Procedures	145
Execution of the Multi Step Program	145
Eigenvalue Analysis	147
Sun-Sight Corrections	151
Appendix C: Raw Data used in this Study	155
Appendix D: Apparent Pole Positions	202
Appendix E: Latitude and Longitude Positions of the Sample Sites.	228

Appendix F: Compass Error Corrections	232
Appendix G: Results of the Eigenvalue Analysis	236
Appendix H: Coring Tool Orientation	237
Appendix I: Data Corrections Due to Compass Errors	241

FIGURES

1. The positioning of the hemispheres used in this representation	37
2. The gaussian distribution	39
3. Preprocessed data used to illustrate the DGTL analysis . . .	41
4. Total probability	43
5. Half maximum of the total probability density distribution	44
6. Suggested criterion of resolvableability	50
7. Half-maximum distributions	51
8. The Geological Domains of Manitoba	62
9. Geology of the Study Area	63
10. The sampling sites for this study	67
11. Plots of remanence for sample 8021B	78
12. Plots of remanence for sample 8022B	79
13. Plots of remanence for sample 8611B	80
14. Plots of remanence for sample 8612B	81
15. Plots of remanence for sample 8613B	82
16. Plots of remanence for sample 8621B	83
17. Plots of remanence for sample 8622B	84

18. Plots of remanence for sample 8623B	85
19. Plots of remanence for sample 8621A	86
20. Plots of remanence for sample 8622A	87
21. Plots of remanence for sample 8623A	88
22. Plots of remanence for sample 8011B	91
23. Plots of remanence for sample 8012B	92
24. North pole positions determined by using conventional methods	94
25. South pole positions determined using conventional methods	95
26. North pole positions for CNVL analysis using unit weight over the full spectrum	96
27. South pole positions for CNVL analysis using unit weight over the full spectrum	97
28. North pole positions for DGTL analysis using unit weight over the full spectrum	98
29. South pole positions for DGTL analysis using unit weight over the full spectrum	99
30. North pole positions for CNVL analysis using magnitude weight over the full spectrum	100
31. South pole positions for CNVL analysis using magnitude weight over the full spectrum	101
32. North pole positions for DGTL analysis using magnitude weight over the full spectrum	102
33. South pole positions for DGTL analysis using magnitude weight over the full spectrum	103
34. North pole positions for digital analyses using magnitude weight over the reduced spectrum	104
35. South pole positions for digital analysis using magnitude weight over the reduced spectrum	105
36. North pole positions for CNVL analysis using magnitude weight over the reduced spectrum	106
37. South pole positions for CNVL analysis using magnitude weight over the reduced spectrum	107

38. The North pole positions for CNVL analysis, using unit weight and the reduced spectrum	108
39. South pole positions for CNVL analysis using unit weight over the reduced spectrum	109
40. North pole positions for digital analysis using unit weight over the reduced spectrum	110
41. South pole positions for digital analysis using unit weight over the reduced spectrum	111
42. The Distributions of significant palaeomagnetic poles . .	116
43. Apparent polar wander path	117

TABLES

1. Raw palaeomagnetic data used to illustrate the DGTL approach.	42
2. Susceptibilities of the rock cores.	68
3. Pole Groupings	119
4. Raw data used in this report.	156
5. Apparent pole positions using the DGTL method using magnitude over the reduced spectrum.	202
6. Apparent pole positions using the CNVL method, and magnitude weight over the reduced spectrum.	205
7. Apparent polar positions using conventional analysis over the reduced spectrum.	208
8. Apparent polar positions using DGTL analysis with unit weighting over the reduced spectrum.	210
9. Apparent polar positions using CNVL analysis with unit weighting over the reduced spectrum.	213
10. Apparent polar positions using DGTL analysis with unit weighting over the full spectrum.	216
11. Apparent polar positions using CNVL analysis with unit weighting over the full spectrum.	219
12. Apparent polar positions using DGTL analysis with	

magnitude weighting over the full spectrum.	222
13. Apparent polar positions using CNVL analysis with magnitude weighting, over the full spectrum.	225
14. Latitudinal and longitudinal positions of the sites . . .	228
15. Compass error due to local field abnormalities.	232
16. Eigenvalue analysis of selected samples.	236
17. Coring tool orientation in situ.	237

Chapter I

INTRODUCTION

This study was done on a set of rock core samples obtained from outcrops in the Canadian Shield in Northern Manitoba. The original intent of the study was to determine the apparent pole positions indicated by this sample set and to interpret the results. The author, in the early stages of the study, made investigations into the potential for resolving multiple components of remanence in individual samples. A significant amount of information is available describing the use of eigenvalue methods to accomplish such tasks in palaeomagnetic studies.¹ However, the conditions necessary for the success of this approach are very restrictive, and the results are very limited. In anticipation of applying an eigenvalue analysis, the samples were cleaned at intervals of field strengths that were finer than are usually applied. The intent of this was to provide more data and, potentially better information on the sample.

In resolving multiple components in palaeomagnetic samples, one must take great care that the individual components have some geological significance. There can be two sources of pitfalls. First, a resolved remanence may be due to an event that does not have any associated geological cause that would be considered interesting in

¹ Eigenvalue techniques are widely applied in the fields of mathematics ,the physical sciences, and engineering sciences. It has a very general formulation. When applied to palaeomagnetics, it is restricted to the specific case of geometric forms in three-space.

a palaeomagnetic study. Remanences that are due to one or more lightning strikes, or due to weathering would be cases of no interest to the palaeomagnetist. Secondly, a remanence may be due to a flaw in the method by which the sample was analyzed. The resolved "apparent" remanence, may be the resultant partial sums of component remanences. Such a remanence would have no geological significance and would lead to faulty interpretations.

In consideration of the complexity of the general problem of resolving multiple components in palaeomagnetic samples, this thesis reviews the broader subject of material magnetizations, the behavior of the earth's magnetic field through history, and other general ideas on the topic of palaeomagnetics. This is particularly important for samples from Precambrian rocks that have had a complex geological history. This is both a detailed look that considers the immediate environment of the samples, as well as a broader picture that considers the behavior of the cratons and blocks in which the geological setting is located. Events occurring on both these scales can have profound effects upon the positions of the final apparent poles.

This thesis also presents and applies a new approach for the analyses of palaeomagnetic data. It was originally conceived as a method to represent palaeomagnetic data by using computer methods. It was later found, by application to the real data, to have significantly different computational results. As with any new method, until it has been repeatedly tested on real data and found to produce results that are consistent with both the palaeomagnetic and

the geological perceptions, this method can only be accepted with a certain degree of scepticism.

Chapter II

THE MAGNETIC PROPERTIES OF SOLIDS AND ROCK MAGNETISM

2.1 Magnetic Properties of Solids

The study of magnetic materials is a quantum mechanical study. This is due to the fact that the magnetic properties of solids are primarily derived from the electron spins of orbiting electrons, the orbital angular momentum about the nucleus and changes of these motions due to externally applied fields. Contributions due to subatomic particles are insignificant (Kittel, 1976).

Microscopic principles of magnetic behavior have macroscopic expressions in the magnetic properties of materials. These include such things as spontaneous magnetic material, described in terms of its "magnetization" per unit volume (M), the magnetic susceptibility (χ) of the sample, which is the ratio of the magnetic moment to an applied external field as well as other properties. If $\chi < 0$ then it is termed as negative susceptibility and the sample is considered to be a "diamagnetic". If $\chi > 0$ it is termed as positive susceptibility, and the material is considered to be "paramagnetic" (Cracknell, 1975).

Paramagnetic behavior is exhibited by materials made up of atoms or ions with permanent magnetic moments. These moments are due to spins of unpaired electrons, the orbital motions of the electrons, or a combination of both (Cracknell, 1975).

Ferromagnetic materials are materials that exhibit a spontaneous magnetic moment for sufficiently low temperatures. This can occur both with or without an external magnetic field being applied.

Ferrites are materials composed of moments from two types of sources that co-exist on different sub-lattice planes. The alignment between planes is anti-parallel. If the magnetization of the moments are different then there will be a net magnetic moment over the entire sample.

Antiferromagnetic crystals are similar to ferrimagnetic materials with the exception that with antiferromagnetic materials, the net contribution between planes is zero. This behavior is often temperature dependent.

A particularly useful property of ferromagnetic materials is that they can be ordered into domains of parallel alignment. These regions are defined by their "bloch walls". Magnetic behavior of the material can then be considered in terms of the behavior of these domains (Williams, 1966).

2.1.1 Magnetic Minerals

There are many forms of magnetic materials in nature. The particular minerals that are abundant, which are included in this class, are the oxides and the sulfides of iron. These minerals generally are found in compounds with titanium, but this is not necessarily the case (Parkinson, 1983). Often these minerals can be found in ore bodies in sufficient quantities and strengths that their fields dominate the local magnetic field.

Of all magnetic minerals, magnetite is the most common, and is also the dominant mineral where magnetic properties are concerned. Magnetite (Fe_3O_4) contains iron in both ferrous and ferric oxidation states. Other frequently occurring magnetic minerals include titano-magnetites, oxidized titanomagnetites, hematite, titanomaghemite, and pyrrhotite.

When discussing optical and electron beam methods for studying magnetic materials, it should be noted that magnetic minerals can generally be easily detected. However, single domain grains can occur down to dimensions of .5 microns and these are barely within range of easy detection.

2.2 Rock Magnetism

2.2.1 Remanent Magnetization

Although there are many forms of remanent magnetization, the primary and most useful form for geological palaeomagnetic analysis are the thermal remanent components. This is the most common remanence found in igneous rocks and is directly related to thermal history of the rock formation.

The "blocking temperature" is that temperature at which the decay time of the remanence moment is at a macroscopic level.² The Curie temperature is that temperature above which the alignment of the magnetic dipoles become random (Williams, 1966). In the case of most igneous rocks, the blocking temperature is of the order of 50°C below the Curie temperature.

² It can be measured in a time frame of minutes (at least).

The actual processes which magnetically influence the rocks internally, are very complex. As they cool, reactions occur which change the crystal structures of the component minerals. Minerals which were stable at high temperature may become unstable and break down. Exsolution takes place at different rates. It is difficult to predict the properties of the individual samples as they undergo these changes. As far as the remanence is concerned, orientation of the domains is related to the external fields which are present while the rock mass cools below the blocking temperature. Long period cooling tends to average out short term fluctuations. Generally speaking, remanence grows as crystals grow beyond the blocking volume.

The remanence found in igneous rocks can usually be successfully applied to palaeomagnetic studies. Since igneous rocks generally have a less complex thermal history when compared to metamorphic rocks, it is safer to assume that the remanence reflects the earth's field at the time of emplacement; if the remanence has been correctly determined.

2.2.2 Forms of Remanent Magnetization

There are many terms used to describe remanent magnetization in rock samples. These terms relate to the way the magnetization was originally acquired.

Thermal remanent magnetism (T.R.M) is acquired when the temperature of the material is raised above the Curie point, and then subsequently lowered to below the blocking temperature. Above the Curie point, the magnetic domains are purely random (superparamagne-

tism). As the sample is cooled to below the blocking temperature, a magnetic ordering may be imprinted on the sample.

Many subaqueous sediments have weak remanences. This is due to the orientation of magnetic grains, by an external field, that was applied during the settling process. Once deposited, the orientation is preserved by cementation. This particular form of remanence is called detrital remanence (D.R.M.).

A material undergoing a chemical reaction in the presence of a magnetic field, often acquires a remanence parallel to that field. A material may acquire an individual moment in this manner which is due to a new crystal structure. This is called chemical remanent magnetism (C.R.M.).

Viscous remanent magnetism (V.R.M.), can be viewed as a change in the remanence under normal conditions of temperature and pressure. If the sample is left in an environment such as is found under field conditions or under laboratory conditions, then the remanence will change as it is subjected to the subtle influences of a magnetic and thermal origin. These changes may be rapid and large as would be the case for a "poor" palaeomagnetic sample, or small and over large geological time spans as would be found in a good palaeomagnetic sample. This change involves magnetic fields which have an internal or external origin. Since it is a change which is occurring in a rock sample under common in-situ conditions, its presence masks the primary remanence which is the remanence of interest. The "cleaning process" (which is to be discussed later), is directed primarily to the removal or identification of this particular form of remanence.

Two other forms of remanence are anhysteretic remanence (A.R.M.), and isothermal remanence (I.R.M.). They are commonly formed under laboratory conditions. Anhysteretic remanence is acquired by a sample which is subjected to simultaneously applied A.C. and D.C. fields. The A.C. field tends to imitate thermal agitation while the D.C. field provides an alignment that is favoured through energy considerations. Isothermal remanence is acquired due to the influence of an imposed D.C. field. Basically, this is similar to A.R.M. where thermal agitation at low temperature provides the impetus for change (room temperature is considered low in this context).

2.2.3 Secondary Magnetization

A rock with a primary magnetic remanence, is further subjected to processes that alter this magnetic remanence or superimposes others upon it. Viscous remanence is the alteration most often found in samples. It has a tendency to align itself with current magnetic fields.

Lightning strikes represent intense localized magnetic effects. The radius of alteration is of the order of 20 metres. Therefore, individual strikes have a minimal range of influence (Tarling, 1971).

Both mechanical and chemical weathering can form secondary magnetic remanences. Mechanical weathering produces little effect beyond the upper few millimeters. Chemical weathering, however, can cause extensive alterations to depths of hundreds of meters in porous material due to extensive solution and recrystallization. The primary chemical reaction is the oxidation of magnetic minerals.

2.2.4 Metamorphic Effects

Rocks that are subjected to pressures and/or temperatures which are sufficiently severe, will not retain their primary remanence. The processes involved can "wipe" the rocks clean of any of the original magnetic ordering, and then superimpose a new remanence associated with this latest event. This remanence can be considered primary in itself. Metamorphic influences can impose secondary remanences in a sample. Although there is no limit on the number of remanences that a sample can contain, generally the number of remanences that can be resolved is limited by the effectiveness of the laboratory and analytical procedures.

This research project found that some statistical methods can in many cases, resolve multiple remanences in single samples. It seems possible that the more severe the conditions were under which the particular remanence was imposed, the harder and more stable that remanence is (to a limit determined by the physical properties of the sample). This can be an extremely important property for the resolution of multiple components of remanence in a single sample. Since the total energy state of the Earth has decreased continually throughout history, the chance that an old remanence will survive increases with time. As well, the chance that the severity of the conditions under which the remanence is imposed is less, also increases with time. This increases the likelihood of resolving older remanences even though the sample has been reprinted with a new remanence. Since the energy of formation of a sample is usually the highest, subsequent remanences can usually be cleaned while

still leaving the primary remanence. Of course it is local conditions alone determine the palaeomagnetic characteristics of a sample.

2.2.5 Self-Reversals

Generally speaking, the orientation of the primary remanence of a sample is aligned with the externally applied field that was present at the time of its imprinting. This is not the case for all mineral assemblages. It has been predicted that the orientation could be anti-parallel in particular cases. This prediction was made by Neel (1955), based on theoretical considerations, and is called "self-reversals". It has been supported by actual findings of such cases for example, Uyeda (1958). This is an effect which is due to a "negative exchange interaction". One phase of the sample is magnetized parallel to the external field, which causes the second phase to magnetize in response to this arrangement in an anti-parallel orientation. As the crystal evolves, the magnetic contributions due to the second phase dominate the magnetic properties of the sample.

2.2.6 Stability of Remanence

There are several ways to determine the stability of magnetization in a sample. One test, for example, is to compare rock specimens before and after storage in the laboratory. The time scale involved in comparison to the geological scale is very small, and any change in the magnetic properties of the sample will indicate gross instabilities (Tarling, 1971).

A particularly revealing test is to compare the orientations of rocks of a similar age and from a similar region. Because of their temporal and spatial correlation, their thermal and magnetic history and hence magnetic remanences can generally be expected to be similar. This comparison indicates a stability in the samples that better corresponds to the geological time scale which is involved in palaeomagnetic measurements.

Demagnetization processes can be used to study stability. More stable materials show smaller changes due to these processes. There are several types of demagnetization processes that are commonly used. Alternating field (A.F.) demagnetization utilizes an alternating field to cause random disordering of the magnetic moments. Thermal demagnetization utilizes the thermal effect to provide the disordering influence, while steady field demagnetization involves a D.C. field which opposes the direction of a particular remanence. The characteristic behavior of a stable remanence is very distinct when compared to an unstable remanence. When a "magnetically stable" sample is demagnetized, using an A.C. field, it maintains its direction and magnitude at stronger cleaning field strengths. An unstable sample shows a great deal of random fluctuations even at low cleaning field strengths. Conventional analysis requires the selection of one (or possibly two), magnetization vectors to represent the magnetic orientation(s) of a sample. In the case of unstable samples, it is difficult to select a particular vector in an objective manner and in the past such samples were discarded. However, this study has produced a method that effectively utilizes these samples. This method is described in Chapter III.

Chapter III

PALAEOMAGNETISM

3.1 Principles of Palaeomagnetics

3.1.1 Fundamental Assumptions of Palaeomagnetic Studies

The most fundamental principle underlying the use of palaeomagnetic measurements, is that the earth's geomagnetic pole provides a point of reference on the surface of the earth and that this reference point is consistent for observations made for any position on the earth's surface at a particular time. Measurements which do not correlate in time can be compared by using the apparent polar wandering paths to determine motion relative to this reference. Accompanying this principle are many assumptions that are necessary to make it use feasible. The value to determine is the virtual pole. This is the field source, axial dipole position, that by definition, is aligned with the axis of rotation; the geographic pole at that time.³ The virtual pole is considered in terms of its position in the present-day geographical reference frame. It is described relative to the present location and orientation of the sample's magnetic moment. However, there are assumptions made as to the relationship which existed between the dipole component of the magnetic field and the axis of rotation, namely that they are, on average,

³ The geomagnetic pole is the vector sum of the "axial" dipole and the "equatorial" dipole.

co-linear. However, it is not critical to abide by these assumptions to obtain significant results. The choice to use the present day geographical reference frame provides a generally available frame of reference to describe the "Apparent Polar Wandering Path" (APWP).

A particularly intriguing feature of the palaeomagnetic method is that it provides information throughout the geological record. Rock magnetizations can be found that have been stable over time long periods (from as far back as the early Archean). In associating these remanent magnetizations with acceptable polar positions, it is critical to assume that over geological time, the magnetic field possessed many of the properties which are observed at the present time.

The current model of the magnetic field being considered when discussing the earth's magnetic field is one that consists of an axial dipole, a non-axial dipole, and higher order multiple components. All of which are superimposed to make up the total magnetic field. The axial dipole dominates the other two components, although they all contribute significantly to the total field. Since it is the axial field which is of interest, methods have been devised to isolate that particular component (Parkinson, 1983). Contributions due to the other sources are considered as dispersions in the statistical sense. Removal of their influence is done using statistical analysis which assumes that they are random over an acceptable time frame and an acceptable spatial frame.

It is not essential to have a full understanding of the behavior of the equatorial dipole. If its influence can be removed by whatever manner, then the remaining dipole component can be related to the geographical pole position (present at the time of magnetization). This particular component is referred to as dipole wobble about the axial position (McElhinny and Merrill, 1975). It has been shown that in recent time this particular component does average to zero (Bullard et al, 1950) but it is questionable as to whether this observation applies over geological time. It will remain an open question until the relationship which exists between the dipole moment and the axis of rotation is fully explained.

Variations of the non-dipole moment are also currently observed. These are both variations in intensity and direction, where changing directions are observed as drifting behavior (McElhinny and Merrill, 1975). The behavior of these higher order components are understood better than the behavior of the equatorial dipole. According to some authors, the ratio of the non-dipole to dipole field intensity has not shown much variation from its average value over the last two billion years: for example, Beck, 1970. For more recent time, time periods of approximately 10,000 years are sufficient, according to some authors, to statistically remove the higher order components (Creer, 1962a). Other authors, however, report that considerably more time is required (Doell, 1969). Generally speaking, given sufficient time, variations due to both these effects will average of zero , leaving an axial dipole model representation (McElhinny and Merrill, 1975).

The axial dipole exhibits variation of its own, although "wobble" which in other representations is accounted for by changes in the equatorial dipole component (McElhinny and Merrill, 1975). Considerable fluctuations in magnitude are recorded throughout geological time, including periods of reversal. Reversals are not significant in discussing tectonic activities using palaeomagnetic results, although they must be recognized for what they are. They can still be used in determining the apparent dipole orientation as opposed to actual apparent pole locations.

Palaeomagnetic results usually assume to be significantly influence by the effects of dispersion, including errors in measurement. The approach in dealing with this is to obtain a large number of samples taken over a long geological time frame and a large spatial area. As the sampling increases, so will the confidence in the results. Two factors that are commonly used to provide a measure of this confidence are dispersion (k), and angular dispersion (S), defined as follows (Wilson, 1959);

- $k = (N-1)/(N-R)$ ----- 1)
 - where $R = 0$ for observations randomly distributed.,
 - and $R = N$ for perfectly parallel observations
- $S = \arccos(R/N)$ ----- 2)

For the fisherian distribution, S is the best estimate of the standard deviation.

Palaeomagnetic results do not incorporate the complete tectonic history of the sample, nor do they consider the complete behavior of the sample in terms of its crystalline properties. The specific

details of the magnetic fields that were present when remanence was acquired, cannot be determined with the method. Instead, by using statistical reasoning based on workable assumptions, a virtual pole can be determined. Accuracy of any individual pole that is based on results from samples that are up to five million years old, cannot be considered to be more accurate than five degrees from the true mean, although statistically, the results can be greatly enhanced (McElhinny and Merrill, 1975). As the age of the rock increases and errors in dating increase, confidence in a measurement will degrade. In spite of all these complicating factors, information can be obtained from samples that have been magnetically unaffected since the early Precambrian.

3.1.2 Applications of Palaeomagnetism

Palaeomagnetics can play a very enlightening role in geological studies. In general, as the data base increases in size, the amount of information that can be obtained increases. Although there is considerable controversy over the validity of the reference frames which are used, palaeomagnetism provides an accurate measure of relative motion between geological units. This is particularly important in considering the behavior of "plates" in the "plate tectonic" model of the Earth.

Using palaeomagnetic data to represent a time profile of pole positions, an APWP can be constructed. When the APWP's associated with the units correspond, the bodies can be considered to have not undergone any relative motion (Cavanaugh, 1977). If there is divergence, then the plates have undergone relative motion.

These observations can lead to deductions regarding plate boundaries and plate-to-plate interactions. Zones where convergence or divergence phenomenon were occurring can be identified, and the tectonic effects can be identified as well (McElhinny and Merrill, 1975). Closely grouped palaeomagnetic directions in widespread older rocks may indicate that there were no occurrences of any deformational events after remanence was acquired (Evans and Bingham, 1975; 1973). Furthermore, the age that is determined from APWP paths can be compared to isotopic ages, or it can be used to provide a date where one is not available (Fahrig and Larochelle, 1972). Both approaches could yield valuable information to be used in reconstructing the geological history of the area (Dunlop, 1979).

A superficial analysis of palaeomagnetic observations determined from Precambrian rocks, and the subsequent conclusions based upon these observations, does not inspire much confidence in palaeomagnetic methods (Dunlop, 1979). Basing conclusions upon the complicated sequence of events and conditions the rock samples were likely subjected to, strongly offends most scientific instincts. It is because of the success of statistical analysis that palaeomagnetic results have proven to be consistent between studies. These methods have given researchers the continuing ability to reproduce results and produce a general, although sparse,⁴ picture of the tectonic history of a rock unit. Once a complete data base is constructed, questions related to prevalent geological conditions and global positions of the unit can be answered.

⁴ The term sparse is used in consideration of the fact that the very complicated tectonic sequences of events, that can be determined in a geological analysis, are not revealed.

In order to provide an accurate data base, close coordination between geochronologists, geologists, and palaeomagnetists is required. Accurate age determinations of the sampled sites are necessary to minimize dating errors. Palaeomagnetic results provide an overview of a situation that is free of the focused perspective inherent in geological observation. Palaeomagnetic results cannot provide a complete model of the local history of an area, however, they can furnish information to complement other studies.

3.1.3 Problems in the Interpretation of Palaeomagnetic Data

Palaeomagnetic results from samples within the early Precambrian leave themselves open to considerable question. The most fundamental assumption, that statistical analysis exposes significant geological information in all cases, can lead to pitfalls for the unaware. As rock samples increase in age, the probability that significant complicating events have magnetically influenced them increases in likelihood. Geological dispersion⁵ for example, increases in likelihood while significant individual tectonic events may go undetected. Metamorphic events may have occurred causing partial or complete remagnetization and thus problems in associating an age to a particular event (Creer, 1962b).

The Precambrian contains problems that are characteristic of the early time periods associated with it (Roy, 1983). These time ranges are considerably larger than any other and the density of measurements is much less. There are also considerable gaps in the palaeohistory due to a lack of data. Since plate boundaries are

⁵ For example, the dispersion of remanences due to tectonic activity.

generally considered to have been regions that are more tectonically active, this is where the bulk of the data must be obtained. On the other hand, this causes more complications for palaeomagnetic analysis since reworking will complicate the magnetic properties of the rocks. Sedimentary rocks that provide the best conditions for palaeomagnetic work are present, (Burke et al, 1976, Engle et al, 1974, Sutton and Watson, 1974) however, they are rare since most strata have undergone major metamorphism. Although these are potential problems in working with palaeomagnetic samples of any time period, this is especially true when considering data from the early Precambrian.

There are problems inherent in the technique itself (Creer, 1962a). Experimental errors account for a small portion of the dispersion. Although this is a problem, proper statistical techniques will minimize it. Inhomogeneities in the distribution of the magnetic material within the sample can cause significant error. This can be avoided by using proper experimental techniques. In the particular case of the spinner magnetometer, increasing the distance between the sensor coil and the sample causes the non-dipole signal of the sample to decrease disproportionately in comparison to the dipole field source. Errors that are incurred also include errors due to non-alignment of the samples' moment to the ancient geomagnetic field. Correct statistical analysis also minimizes this factor.

Lightning strikes can be significant events when considering localized magnetic properties (Dunlop et al, 1984). The particular

problem with a sample that has been struck by lightning is that the coercivity is much larger and so cleaning only enhances the component due to the strike. Lightning events can be recognized by the properties within the specimen that cause the divergence of the magnetic vector during A.F. cleaning to be much greater than between specimen scatter at a given A.F. level. As well, remanences imposed by lightning strikes have a high intensity.

A very significant factor in the determination of polar position and the A.P.W path can be the error in the isotopic age of the rock unit under investigation (Larochelle, 1968). Methods that are currently used have errors in the range of tens of millions of years for samples obtained from rocks of early to middle Precambrian age, for example. Isotopic ages obtained by different methods from individual rock units can be found in the literature that vary by much more than this (Bingham and Evans, 1976). This introduces a considerable time error in mapping the polar wander path, as well as in using these results in making confident interpretations. Discordant ages from different isotopic methods are common because metamorphism may affect the isotopic systems in different ways.

Also, inconsistencies between isotopic and palaeomagnetic ages may arise in cases where tectonic motion may have occurred without re-heating the sample to a temperature that was adequate enough to reset, or partially reset the isotopic clock. This provides one of the most useful properties of palaeomagnetics. Characteristic features observed in dispersion can sometimes identify the type of motion. Where motion is apparent, or where the APWP is not well

known, the isotopic age would be considered more appropriate than the age indicated by the APWP.

A particular problem that is frequently observed in the Canadian Shield, is the recurrent nature of igneous activity. This makes long distance correlation between palaeomagnetic settings very hazardous. The difficulty in this is that it is unlikely that suitable units can be found in close proximity that span the large time intervals necessary to provide adequate analysis of secular variations (Creer, 1962b).

Although successful enough, there are major shortcomings in the methods currently used in palaeomagnetic analysis. Fisherian techniques, by which the majority of the data is analyzed, is based on representing the observations as a gaussian density distribution about a mean position on the surface of the sphere. Technically, this perception is invalid (Beck, 1970). The distribution due to dispersion of a dipole field is not azimuthally symmetrical, but will be oval in a manner that is latitude dependent (Creer et al, 1959). The resultant area of uncertainty will be centred on the mean value with major axis dD and minor axis dI oriented parallel and perpendicular to the meridian respectively. These values are determined by the relationships (Creer, 1962b);

$$\bullet \quad dD = \lambda / (1 + 3\sin^{*2}L)^{*1/2} \text{ and } dI = \lambda / (1 + 3\sin^{*2}L)$$

where λ is the radius of the area of certainty.

Fisherian analysis does not allow for non-symmetries in the sampling processes. The resultant distribution is one that has symmetry about the mean value which may not be representative of the

sampling population. Even assuming axial symmetry is generally invalid, since irregularities in the sample set can produce many kinds of dispersion. Dispersion along a path would be probable, due to polar and plate wandering.

There are inconsistencies in the approaches used to obtain mean values. Different weighting schemes are available in determining the virtual pole. Data pre-processing based upon geological information may be done. The particular problem introduced in this case is that an overall analysis of the data base is difficult since a determination of each position may be based on a different premise (Creer, 1962b).

Currently, the reliability of the APWP for the Precambrian is at issue (Roy, 1983). What is required is the development of a solid data base founded on information concerning local tectonic conditions, thermal history, accurate isotopic ages, and a consistent and accurate analysis. A world-wide data base is necessary to provide a spherical harmonic analysis to determine the earth's field, and thus allow a complete understanding of the palaeomagnetic field (Creer, 1962b). Motions of less than a few hundred kilometers are not likely to be resolved (Dunlop. 1979), which means that there is considerable uncertainty in the APWP's. The result is that there is a inaccurate smoothness in the paths due to these uncertainties. This smoothness is most likely not a valid representation (Beck, 1970). Palaeomagnetism is as yet a long way from being a completely effective approach in determining Precambrian tectonic history. What is necessary to make it a generally well respected study in this

respect, is a consistent and solid approach to the analysis of palaeomagnetic data.

3.1.4 Interpretation of Palaeomagnetic Results

Resolution and identification of individual components of remanences in a rock sample is a difficult procedure. The presence of multiple components which are the result of multiple events, can lead to difficulty in associating a particular palaeomagnetic event to a direction. If individual events can be associated with directions, and these directions have an alignment with the palaeomagnetic field at particular times, information about the palaeomagnetic field can then be inferred. Each component in such a case would have equal importance. It is not appropriate to consider a remanence as being "primary" or "secondary", but rather as "characteristic" (Zijderveld, 1967). If the approach to the problem of multiple components is not uniform, then the results will likely be incomprehensible. The lumping of these directions in a single treatment will lead to confusion.

The problem facing palaeomagnetists is to resolve and identify the individual components of remanence. Unfortunately, the individual values that are determined cannot be considered conclusive. Thus, tests that consider the reliability as a measure of confidence, of these results are necessary (Irving, 1964). If the cleaning process produces a stable end-point at which there is insignificant variation in direction values (orderly variations in magnitude are acceptable), then the result will probably be associated with a stable remanence. A verification of a result from several samples

is necessary (Dunlop et al 1984). These must include single site samples or samples from outcrops of the same lithologic unit. If sites have variations in the mineralogy, or are dissimilar in some other manner, yet lead to similar results, then this would be strong supporting evidence for the results.

Lack of correspondence does not necessarily imply that one or both of the results are wrong since a variable geological history could account for this outcome.⁶ Even after cleaning, specimens from a common rock unit may possibly show considerable dispersion. Such dispersion cannot be conclusively identified with either a geological event or a mineralogical property of the rock without an in-depth analysis of the geology of the area, as well as the mineral composition of the sample. Considerable dispersion can also result when the cleaning field rises above some minimum intensity of the sample. If this is the case, the demagnetization vector will not show any kind of regular behavior as the cleaning field is increased. Instead, it will fluctuate randomly and unpredictably in both magnitude and direction. It seems that at the minimum intensity, the magnetization is related to the cleaning parameters, and not to internal properties of the sample.

Geological settings provide informative tests relating to the sample. If a scheme can be devised to rotate samples that have been influenced by dispersion such that the remanences closely align, then it is possible that deformation or reorientation of the core

⁶ There are several aspects to the geological history of a sample that are important from a palaeomagnetic point of view. This list includes the thermal regime as one of the more important aspects.

has occurred since the remanence was acquired. In the case of conglomerates, if individual pebbles show a lack of correlation, then remanence was acquired before the pebbles were deposited. Relationships between intrusive bodies and the country rocks can be examined for clues. Immediately adjacent to the contacts, the remanence will be consistent with the intruded body. As the separation increases further into the country rock, the influence of the heating effect will diminish and the remanence approaches that of the uninfluenced country rock (Irving, 1964).

The degree of stability of a remanence does not identify it with primary or secondary events in the history of a rock. A remanence is considered stable in terms of the length of time that it maintains itself. On the other hand, the hardness or softness of a sample is related to the release forces that are required to clean the sample. If the magnetization is removed with fields up to 150 nT, then they are likely to be viscous and unrelated to geological events in the history of the rock. Gross physical properties of the rock can indicate reliability of the determined directions. A high coercivity suggests that the magnetization is most stable. Also, if the distribution of the magnetic material in a outcrop is isotropic, then this minimizes the potential of a result that is related to the sampling location and orientation in the outcrop. The absence of stress effects suggest a reliable sample (Zijderveld, 1967). It is also suggested that the higher the Curie temperature the more stable the magnetization of the rock (Kawai, 1955, as quoted by Irving, 1964).

In order to deal with the reliability of palaeomagnetic results, Irving (1964) suggested several criteria, three of which are listed here;

1. The determined results must be consistent in 5 or more separately oriented samples.
2. The circle of confidence, $p = .05$, associated with the measurement must not exceed 25 degrees.
3. Results from samples older than the Tertiary are not adequate unless the direction diverges significantly from the direction of the present field. This condition is applied because of the possible dominance of a remanence that is associated with the current magnetic field.

The current emphasis in palaeomagnetics is to resolve individual components and their associated events. In consideration of the complexity of Precambrian terranes, and current methods of statistical analysis, this is a very difficult approach. As Fisher statistics are currently applied, the behavior of the sample as it undergoes demagnetization is not considered other than in the procedure of selecting good from bad samples. More emphasis should be placed on the statistical analysis of the results, in particular, on finding a satisfactory method that utilizes all the readings of remanence obtained throughout the cleaning process. Also, efforts should be made during the field work to provide a large number of samples over a large area that represents a small age range, thus leading to an effective averaging of the influence of dispersion. Consistency of methods between researchers would provide a uniform

method of analysis and provide coherence between the results of different authors. It must be a scheme that is applied to all situations in a consistent manner. This avoids the possibility of any input of a subjective nature into the analysis, and gives other researchers easy understanding of the quality and consistency of the results.

3.2 Applying Palaeomagnetic Theory

3.2.1 Rock Magnetism and Palaeomagnetism

The properties and response of rocks on the microscopic level, to physical influence, is very complicated. Although much is known about the solid state physics of magnetic materials, the case in palaeomagnetism is complicated by the diverse combination of magnetic assemblages that are found. Those particular properties that are important in palaeomagnetics are related to the size and stability of the net magnetic remanence. Decay times must be long and blocking temperatures high so that the sample retains its remanence over long geological time periods.

The crystal properties of rocks (and in particular the properties of the magnetic domains) best suited for this work is controversial. It has been reported in localized studies (Dunlop, 1979), that metavolcanics (greenschist facies) are weakly magnetized, as well as being relatively unstable and that mafic intrusions are more stable and more strongly magnetized. Dunlop (1979), also found that it has not been possible to establish a relationship between magnetic intensity and stability, and either rock type or degree of meta-

morphism. Dunlop et al (1984) found that the unusual and distinct magnetic curves of granites which combine high blocking temperature with low coercivities make ideal specimens for use in palaeomagnetic work.

It seems possible that small grain size contributes disproportionately to remanence (Dunlop et al, 1984). This is possibly due to single domain behavior having only minor viscous components (Ermanovics and Fahrig, 1975). In this study, the author was unable to make any correlation between particular magnetic properties and any other macroscopic physical property.

It seems, however, that the stability and intensity of the magnetic moment does not determine the outcome of a carefully planned study. It can be assumed that a certain amount of information concerning the remanence is contained in the sample. Thus it can be assumed that adequate statistical analysis will reveal the "true" remanence. It has been found that samples that were to be rejected based on stability criteria caused no more significant variance than when these samples were not used in calculating the statistical mean (McElhinny and Merrill, 1975).

3.2.2 Measurement Devices used in Palaeomagnetic Studies

Generally, Palaeomagnetic analysis utilizes either the astatic magnetometer, or the spinner type magnetometer (Collinson and Creer 1967). Both methods have their own merits. The principles for their use is elaborated in Collinson et al, (1957) Collinson and Creer, (1967) Helsley, (1957) and Gough (1964). The reader is referred to Lorrain and Carson, (1970) Duckworth, (1965) and Pugh

and Pugh, (1972) in regards to principles of electromagnetics involved.

Chapter IV

STATISTICAL ANALYSES OF PALAEOMAGNETIC DATA

4.1 Statistical Methods in Data Analysis

The statistical method most commonly used in the analysis of palaeomagnetic data is that proposed by Fisher (1953). This method gives an expression of a measurements about a mean value plotted on a sphere. The method is an analysis of the gaussian distribution on the sphere.

Although the statistical distribution of a set of observations may possess the symmetrical distribution of the gaussian when mapped into corresponding virtual geomagnetic poles, in general the azimuthal symmetry is not present. This, in effect, indicates a weakness in fisherian statistics.

Fisher (1953), provides a complete description of his method, while Creer (1962b) provides an updated version which accounts for latitude dependent distortions in the probability distributions.

4.2 A New Approach

Current analyses of palaeomagnetic data relies on the mathematical methods developed over thirty years ago. The method that has been developed here, is referred to as the DGTL method.

4.2.1 Approaching the Problem

The approach that is pursued here is to consider a set of observations, each having been assigned an equal probability (or otherwise weighted).⁷ There is a considerable degree of uncertainty that any single observation is the mean value. A probability distribution associated with an observation expresses this fact mathematically. If a finite set of observations is considered, then each observation can be written as an element of that set;

$$o(i) \in \langle\!o\rangle \in \langle\!o\rangle'$$

where;

- $\langle\!o\rangle$ is the finite sample set of N elements.
- $\langle\!o\rangle'$ is the set of all possible measurements.

The set $\langle\!o\rangle$ is a subset of a larger set consisting of an infinite number of observations. Statistical analysis of this larger set will produce the mean value exactly. Assuming that the allowable states of the observations are not discrete, the mean value will be included in this set (to an infinite degree of certainty). The particular limitations of obtaining data necessarily requires that an unlimited set of data will not be available. Consequently, there is a limit to the certainty of any mean value that is determined.

⁷ An important asset of this approach is that weighting factors are easily introduced to emphasize confidence in specific values.

Once a single observation is made, that particular value has as much chance of being the mean value as any single observation that has been made or subsequently will be made. Alternatively that observation has as much chance of not being the mean value as any other observation of the set. Subsequently, in terms of the weighting of that measurement;

1. The degree of certainty of each measurements must be equal and,
2. The degree of uncertainty expressed as a probabilistic distribution about all observed values will also be equivalent.

The procedure is to associate a unit value with each observation to satisfy condition (1), and a normalized probability distribution about each potential mean value to satisfy condition (2). In principle, the probability contribution due to each observation at a particular point is considered in the sum. Then as the number of elements of the set «O» increases, if there is a statistical grouping within the set, the probability density in this area will increase favorably. The "tighter" this grouping is, the higher the probability density; in effect, a measure of the degree of certainty.

The user is not limited in this approach to any one particular weighting scheme which may not accurately reflect the degree of certainty of particular observations. A scheme that is indicative of the confidence that the experimenter has upon any particular measurements, may be effectively and easily introduced.

The user is also not limited to any particular form for the probability distribution. This allows total flexibility in intro-

ducing symmetry conditions. Conversely, there could be a total lack of symmetry: individual points may have associated distributions unique in that set.

The resulting distribution will contain an expression of the mean value where the probability density is the greatest. The degree of grouping of the density about the mean gives an expression of the degree of certainty in the mean. An expression of the symmetry of the data set is contained in terms of the symmetry of the resultant distribution.

The particular difficulty in collecting palaeomagnetic data is the length of time necessary for each measurement. A single virtual pole may represent the final measurement upon a single sample that required a field excursion, considerable manual labour as well as lengthy analysis. A survey under good conditions may produce as few as a dozen satisfactory measurements for a week of sampling; particularly true where Precambrian rocks are involved.⁸ As far as a pole position is concerned, it has a distinct value. Since influences of dispersion smear this true position, attempts to determine this "true value" are mathematically impossible. The consequence of this is that the statistical representation of an observation as a distinct point is inaccurate and requires alterations before it can be considered valid.

The probability distribution produces a smearing effect that reflects the uncertainty of the measurement. As a set of single observations, each reading occupies a unique position. This is due

⁸ This survey produced approximately 20 "good" samples for over two weeks of field work.

to the mathematical impossibility of the exact repetition of an element of an infinite set. As a distribution representation, each observation contributes a measure of probability to all positions. The magnitude of this measure at each position, is dependent on the distance from the observation itself.

4.2.2 Two-Dimensional Representation

The usual approach to representing palaeomagnetic data is to plot the orientations of the data on a stereo-net projection.⁹ The virtual pole is the "statistical average" position of multiple observations.¹⁰ Each observation corresponds to the virtual pole derived from the set of one observation. The measure of confidence is indicated by a ellipse centred about the point which contains a standard amount of the volume of probability within (for example, $a_{95} = 95\%$, see Fisher, 1953). The limitations of this approach are obvious (as discussed earlier). In order to represent a three dimensional distribution in three space the following scheme was developed. Let;

$$\Phi = \Phi(\theta', \phi', A, X, Y)$$

where;

- ϕ', θ' = longitude and co-latitude of the virtual pole.

⁹ Usually it will be remanence directions, but may in cases be a set of apparent pole postions.

¹⁰ A virtual pole can be determined from a single sample, a set of samples from one site, or from a set of sites.

- A = magnitude of the probability distribution.
- X, Y = arc distance of the distribution function from the mean (virtual pole).

The following transformations were made;

- $\Theta = \Theta' + X$
- $\phi = \phi' + Y$
- $A = A$

$$\Phi = \Phi(\Theta, \phi, A)$$

which were then followed by the transformation;

- $x = \cos\Theta * \cos\phi + a$
- $y = \cos\Theta * \sin\phi$
- $\Phi = \Phi(A, x, y)$

where $a = \begin{cases} 1 & \text{if } \Theta' < 90 \\ 0 & \text{if } \Theta' \geq 90 \end{cases}$

These series of transformations correspond to the division of the unit sphere into halves (north and south hemispheres), and with the probability amplitude values superimposed upon it, placing them side by side, and then projecting each hemisphere into the plane (see Figure 1).

The function used to represent the probability distribution or dispersion, is arbitrary. The more common forms would naturally be most popular since their properties are better understood. The par-

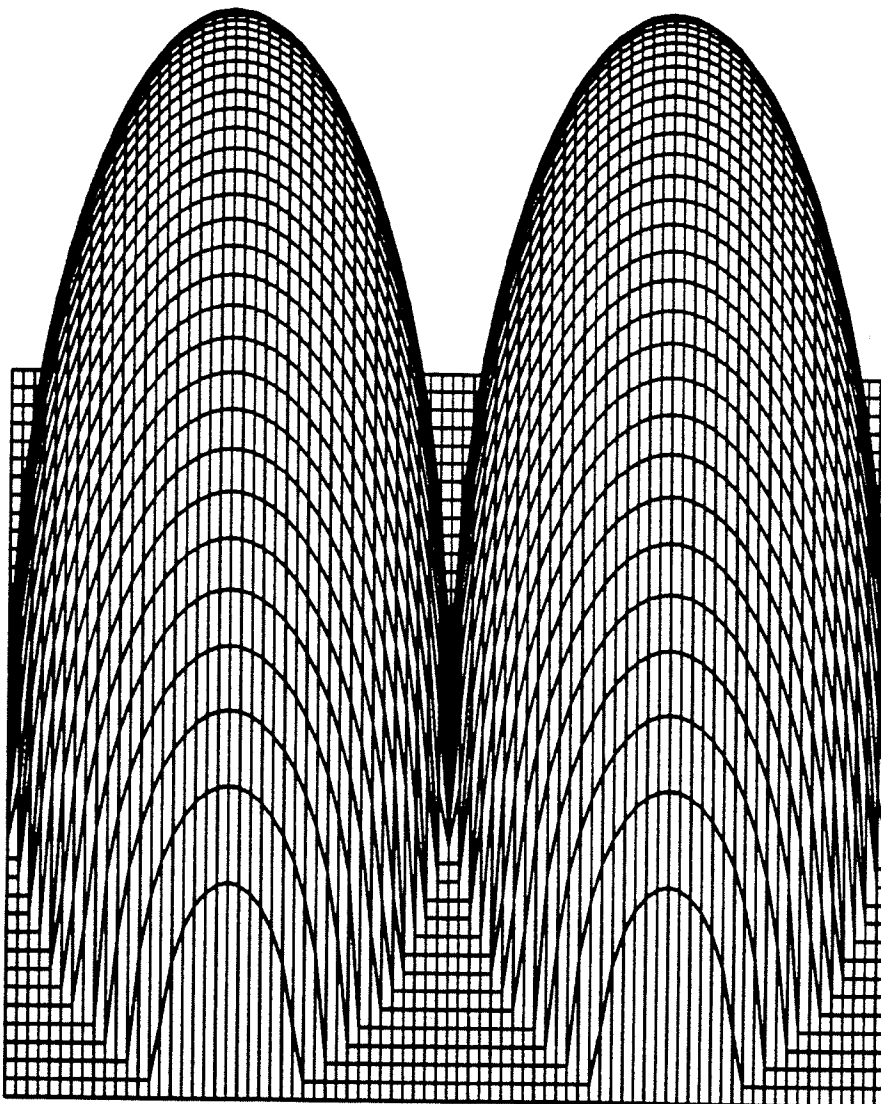


Figure 1: The positioning of the hemispheres used in this representation. The upper hemisphere is located on the left while the lower hemisphere is located on the right. East is on the left, while west is on the right. This method requires an effective way to represent four dimensional data. The positions on the surface of the globe require three dimensions, and the magnitude of the probability represents the fourth dimension. In polar coordinates the vector magnitude has unit value since these are positions on the sphere. This removes one of the dimensions.

ticular parameters that relate to symmetry (if symmetry is an acceptable property) and rate that the magnitude drops from the maximum (for example the standard deviation) can be assigned based on experience or insight into the problem (or it can be set to a universal standard).

The effect of assigning these distributions to each observation is to "smear" the observation so that each contributes an amount of probability to each position on the globe. The most probable value, (the virtual pole) would then correspond to the position of largest probability density. If the standard deviation of the function is chosen to be too large, then it may lead to difficulty in resolving the maximum density peak. If it is chosen to be too small, the resultant net distribution will indicate an excessively large uncertainty in the result.

4.2.3 Probability Distribution Representation

Although any function can be used to represent a distribution, the approach here has been to use the gaussian distribution. The gaussian or normal distribution is the most logical choice since by the "Central Limit Theorem" (Loveday, 1971), all statistical distributions approach the normal distribution for sufficiently large enough sample populations (20 is considered large enough).

The gaussian distribution can be expressed in the following equation (Miller, 1964);

$$\Phi = 1/((2\pi)^n/2^n |M|^{1/2}) \exp(-1/2(x-M)^T M^{-1} (x-M))$$

where M = covariance matrix

n = number of observations

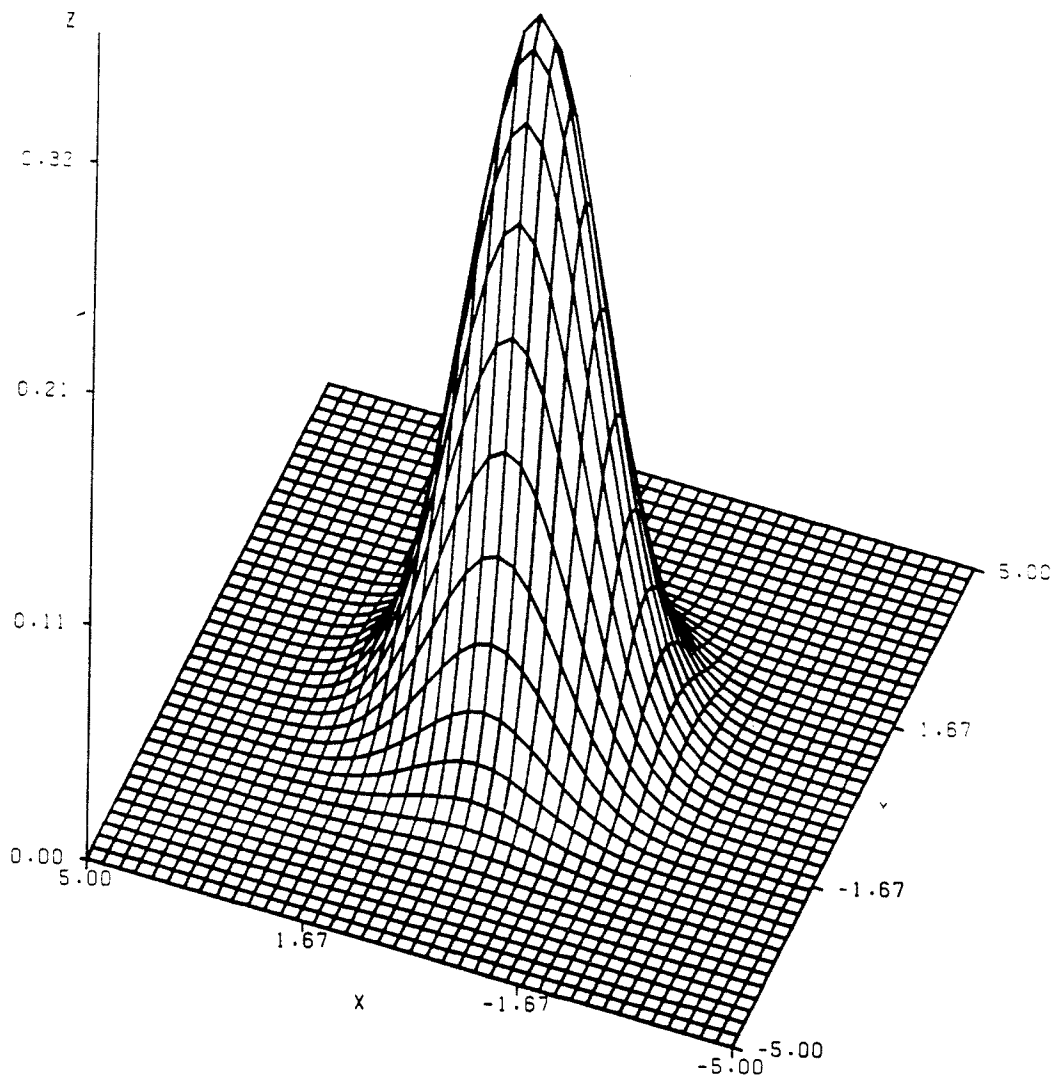


Figure 2: The gaussian distribution. This particular distribution is perfectly symmetrical about the mean value. There are no restrictions on the symmetry or skewness in the technique that is presented here. It is advantageous to be able to choose the parameters that determine the property of the distribution, such as shape, standard deviation, as well as other properties.

and is represented in Figure 2 on page 39. This particular representation is azimuthally symmetrical. However, symmetry is not a necessary requirement (non-symmetry is allowed in the equation above).

If the distribution is symmetrical when considered on the surface of the globe, the resulting projection onto the plane will distort the shape depending on its position on the globe and on the particular projection that is used. In the case of the projection used in this thesis, there is positionally dependent distortion.

Figure 3 is a representation of the data presented in Table 1. Distortion of the function can be observed as the values approach the edges of the hemispheres where $z = 0$. The negative hemisphere is projected onto the right surface while the positive hemisphere is projected on the left. The values plotted, are the maximum probabilities that are determined for each position. This particular presentation expresses the forms as they relate to each other and to locations on the globe.

The total probability is represented in Figure 4. The total contribution at each point, from every observation, is considered in the sum. It is clear that a "most probable" value has been determined and can be read from the plot. This value is the position on the globe where the total probability is maximum. It represents a most probable position in the usual statistical sense. A simple set of steps can be written into the computer program that generates the data for the plot to produce the positional value of the maximum in the print-out.

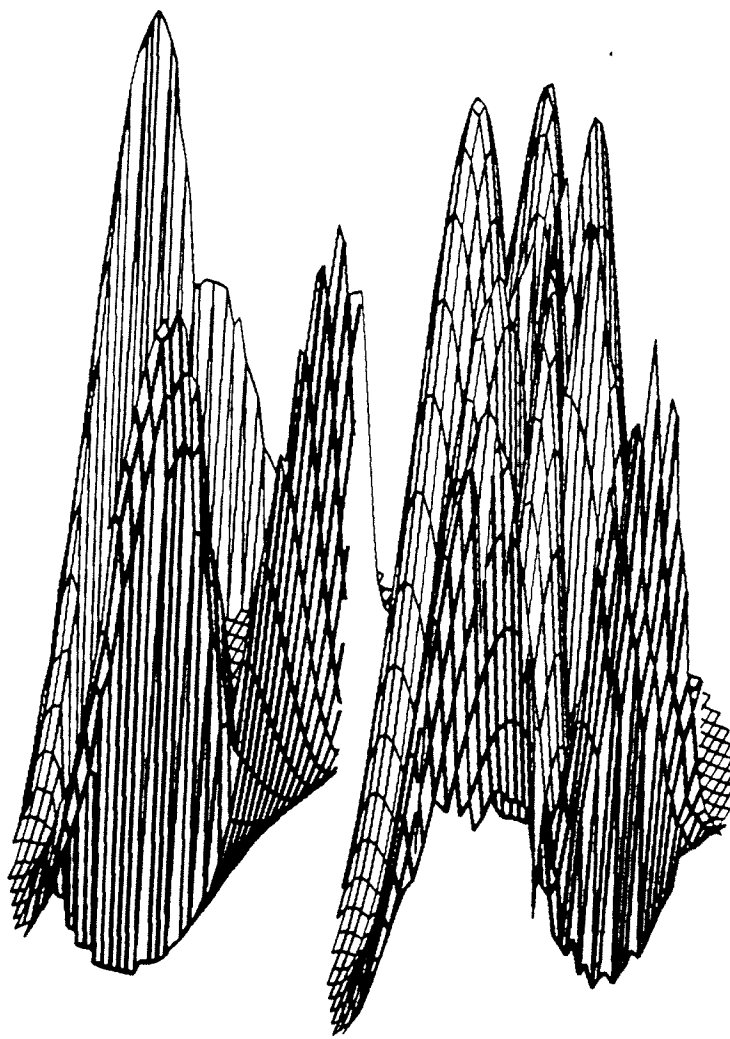


Figure 3: Preprocessed data used to illustrate the DGTL analysis. The representation presented here is of the data contained in Table 1. Note the distortion effecting the gaussian distributions due to the projection used. This is apparent as the data values approach the edges of the plots.

Table 1: Raw palaeomagnetic data used to illustrate the DGTL approach.

The data that is considered in this report was obtained by the author using samples cored in northern Manitoba. A small degree of preprocessing was done by the simple averaging of multiple measurements at individual values of the "cleaning" spectrum. The sample used to illustrate is 801, sample 1 taken from core b.

X-VALUE	SIGM-X	Y-VALUE	SIGM-Y	Z-VALUE	SIGM-Z
-9188	-6	9144	-6	-4276	-6
-1680	-6	3852	-6	-6163	-6
-9014	-7	1700	-6	2422	-7
1959	-6	5417	-6	-6612	-6
1312	-6	1233	-6	-6181	-6
2036	-6	4189	-6	-2030	-6
1946	-6	5922	-6	-1317	-6
6818	-6	5267	-6	6026	-6
6702	-6	5073	-6	6208	-6
-1700	-6	5837	-6	-3694	-6
-2297	-6	5845	-6	-3489	-6
3403	-6	1311	-5	3367	-6
2352	-6	1469	-5	3867	-6
3029	-7	4648	-6	7155	-7
-5218	-7	4543	-6	-7451	-8
5709	-7	1012	-5	4105	-6
9199	-7	1030	-5	3835	-6
8434	-6	6582	-6	2802	-6
8704	-6	8049	-6	2407	-6
				1828	-5
				1303	-5
				1335	-5
				9410	-6
				8755	-6
				9880	-6
				9800	-6
				1497	-5
				1532	-5
				1017	-5
				1017	-5
				1809	-5
				1725	-5
				1802	-5
				1917	-5
				2134	-5
				2054	-5
				9845	-6
				9886	-6
				1967	-6
				-2346	-6
				-1406	-5
				-1403	-5
				-1412	-5
				-2673	-5
				-2672	-5
				1210	-5
				1347	-5
				1860	-5
				1824	-5
				1089	-5
				1145	-5
				7557	-6
				7535	-6
				2047	-5
				2192	-5
				2269	-5
				1184	-5
				1541	-5
				1633	-5
				6338	-6
				7316	-6

The values tabulated contain multiple readings for individual cleaning field strengths. There are actually 11 unique observations in this data set; multiple readings are averaged. The components are un-normalized cartesian vectors. The second integer in each column represents the power (base 10) of the reading while the first integer in each column has been multiplied by 1000.

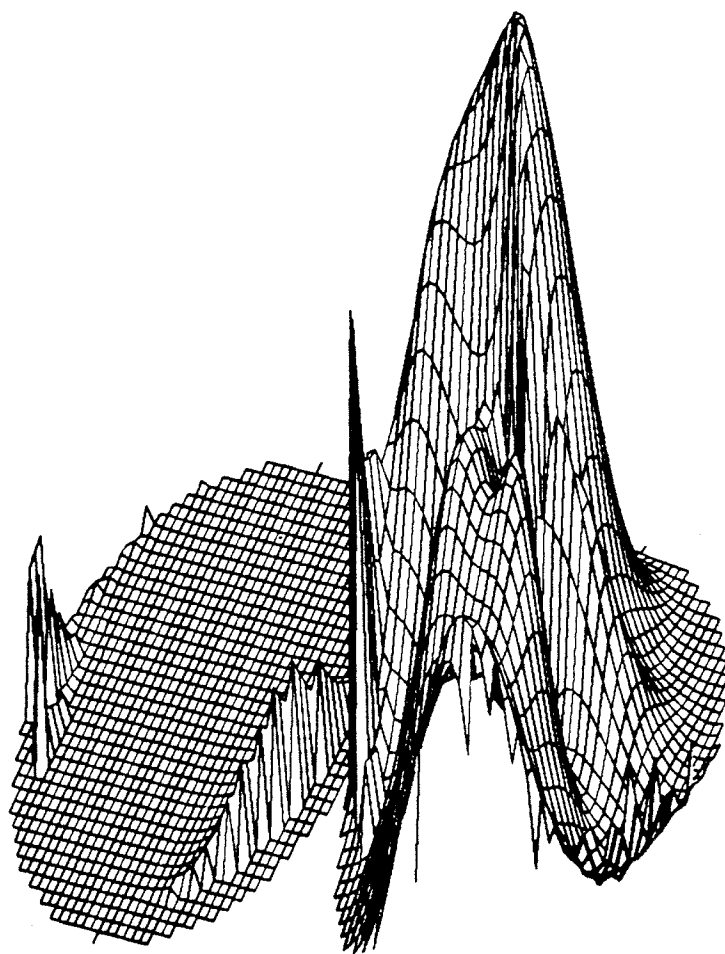


Figure 4: Total probability. The presentation here is of the total contribution from the individual distribution functions. The mean value is clearly represented. This plot is referred to as the total probability distribution.

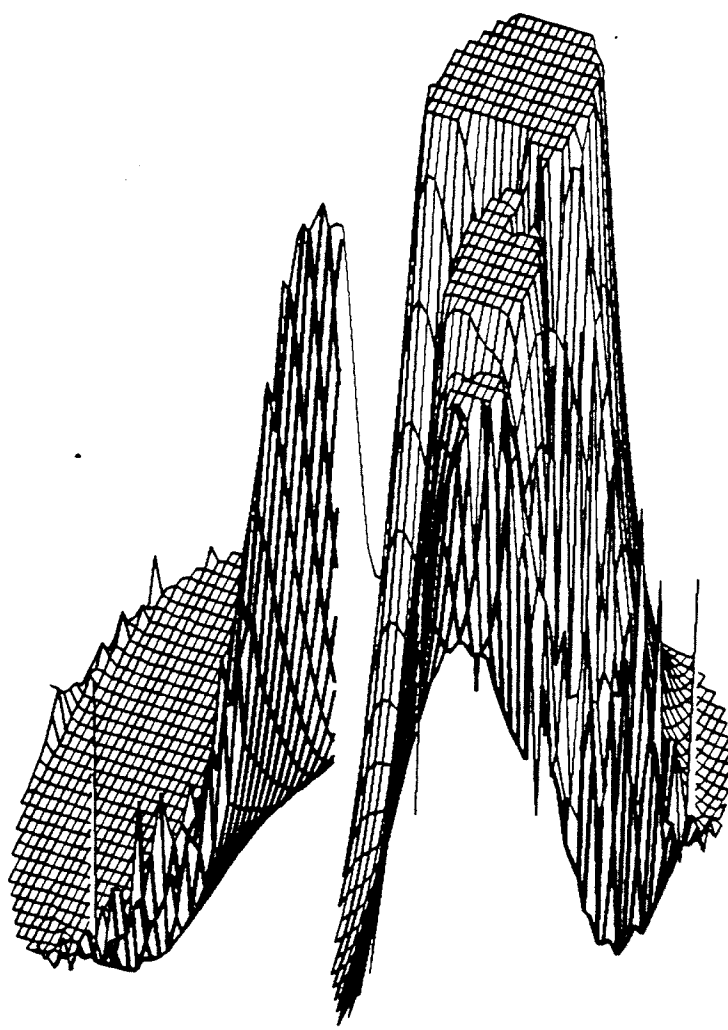


Figure 5: Half maximum of the total probability density distribution. This represents the area of confidence of the mean value. As can be clearly seen, there are no symmetry restrictions in the approach. It is allowable to have confidence in readings that are apparently otherwise unconnected to the mean value. This plot can be used to determine resolvable components in a sample set: once an acceptable criterion has been established.

Figure 5 on page 44 is a plot of the half-maximum value of the cumulative probability. It represents the degree of certainty of the reading. As can be seen, a considerable portion of the total probability is grouped about the mean value. However, there are two other groupings that can be observed for this data. This grouping does not absolutely determine the position of the true value but indicates an "area of confidence" in the conventional sense surrounding the mean value. It is important to note as a feature of this method of analysis, that this area is not restricted by the symmetry properties of conventional analysis, but has full freedom to represent the inherent properties of the data used. It is also important to note that this area of confidence does allow confidence in values that are not contained in the principle area that surround the mean value. It is a very simple matter to write into the computer programs steps to determine the percentage of total probability contained in this area and then to print it out as output. The particular value for this data set is 3% (not particularly good).

The failure to produce a single grouping about the mean value can be explained by inadequacies in the sampling set or by the presence of multiple components within the set of observations.

4.2.4 Mean Magnetization by Vector Addition

A second method was used here that represents a novel application of the conventional approach. The behavior of the magnetization vector (in particular, for soft components), was very erratic in many cases. Most samples did not reach a clearly defined stable end point. Instead, even at sufficiently high field strengths, the

direction and magnitude fluctuated in an apparently random manner. This makes it impossible to define any kind of objective approach in selecting the field strength that will represent the remanence of the sample. The question remains, "Is significant information contained in such a sample?" A repeatable method is necessary for successful resolution of this question.

Fisherian statistics deals with dispersion on a sphere. If in the statistical analysis of pole positions, the demagnetization vector directions are handled with fisherian statistics, an objective and well understood method is available. This particular approach is referred to here as the CNVL approach. This approach shares a common principle with the DGTL method. That is that each measurement for each field strength is composed of a vector component that represents the true magnetization, and a vector component that represents the dispersion in the measurement. As the statistical base increases, the random nature of the noise will average itself out, thus emphasizing the true value. The significant noise in each measurement will be due to instrument error and so it can be expected that this particular component will be random in nature.

4.2.5 Consideration of this Method on the Physical Level

The relationship between the physical behavior of materials and their representation by current methods is fairly well understood. As the sample is cleaned by A.F. demagnetization, the less stable, unwanted remanence is removed leaving a remanence that is due to a single natural remanence that can then be related to an event in the samples' history. This event could be extreme heating in-situ, or

injection of magma into the local rocks (as examples). If the cleaning process indicates that there are no apparent remanences in the sample, then the sample is useless from a palaeomagnetic standpoint. Also, if the character of the demagnetization, indicates that multiple remanences are present in the sample, and the demagnetization spectrums overlap, then only under special circumstances can this sample be used for palaeomagnetic analysis (the special cases are discussed below). The physical features and behaviors of the sample that are being considered in this new approach to palaeomagnetic analysis, are the same as those considered by conventional analysis. The chief advantage of this method is that statistical analyses is applied before a sample is evaluated. This analysis enhances the measurements done on the sample thus improving the statistical density of the points. Samples that would normally be discarded, can be used. This method is still subjected to the same pitfalls of conventional methods. If demagnetization spectrums of multiple components within a sample overlap, then the investigator needs to be aware of this and make the necessary adjustments. This problem applies to both the conventional and this new method. Cleaning a sample to the full extreme of the instruments' range and finding that the sample behaves "in an acceptable manner", ie, the initial remanence appears to be hard enough to be considered TRM, or that it appears to have reached a stable end point, does not imply that the sample has been fully cleaned of all, or all but a single component of remanence.

4.3 Resolution of Multiple Components

The issue of resolution in palaeomagnetics is a very important one. Multiple components can co-exist in single samples (as primary and secondary magnetizations). As well, multiple components can co-exist in sample sets. In order to accurately consider the resultant observations, it is important to recognize the presence of two separate directions, as opposed to inadequate sampling of a set dispersed about a single mean direction. If the former is encountered, additional information has been made available to the experimenter regarding the geological and magnetic history of the sample (such as the influence of multiple metamorphic events). Additional information is also available as to the history of the earth's magnetic field.

The DGTL approach being developed here is well supported by the mathematical theory related to optics. However, the analogy is not complete when using a gaussian distribution since it does not allow for the property of destructive interference (only constructive). As a result, optical theory can only be used with caution. In spite of this, the terminology of optics applies very well in consideration of such phenomenon as resolution.

In regards to resolution, the criteria used are arbitrary (Webb, 1969). It is enough to say that if two systems are individually discernable, then they are said to be resolved (Hecht and Zajac, 1974). Beyond this, there are generally applied criteria. The most commonly considered criterion in optics is that when the central maximum of one pattern is no closer to the nearest dark

fringe than it is to another maximum, then the images are then said to be resolvable (Slater, 1980). The problem in applying this particular criterion to the case of gaussian distributions is that there are no diffraction characteristics such as dark fringes.

Hecht and Zajac present Rayleigh's criterion that is based on maximum amplitudes. For multiple peaks, if the saddle point is less than $8/\pi^2$ times the maximum, then they are considered resolvable (see Figure 6). Criteria that are based upon extreme values are particularly attractive to computer techniques since the programming requires very simple procedures to determine their values.

Important to the issue of resolution is the particular representation that is used for an observation. "Sharply" defined distributions introduce a higher degree of distinction between observations. This may or may not be indicative of the properties of the observations in the set. The particular rate of decay of the function that best represents characteristics of the sampling set will depend on properties of the set, such as in the sampling, density of observations, and distribution of the data set (indicative of unidentifiable dispersion in the set).

Figure 7 is a plot of the half-maximum distributions. This applies the condition that a half-maximum separation is required for the resolution of two individual peaks. As can be seen, the eleven peaks of the data reduces to five resolvable peaks. The half-maximum condition is not the only condition that can be introduced in this manner; other criteria can be easily introduced into the calculations.

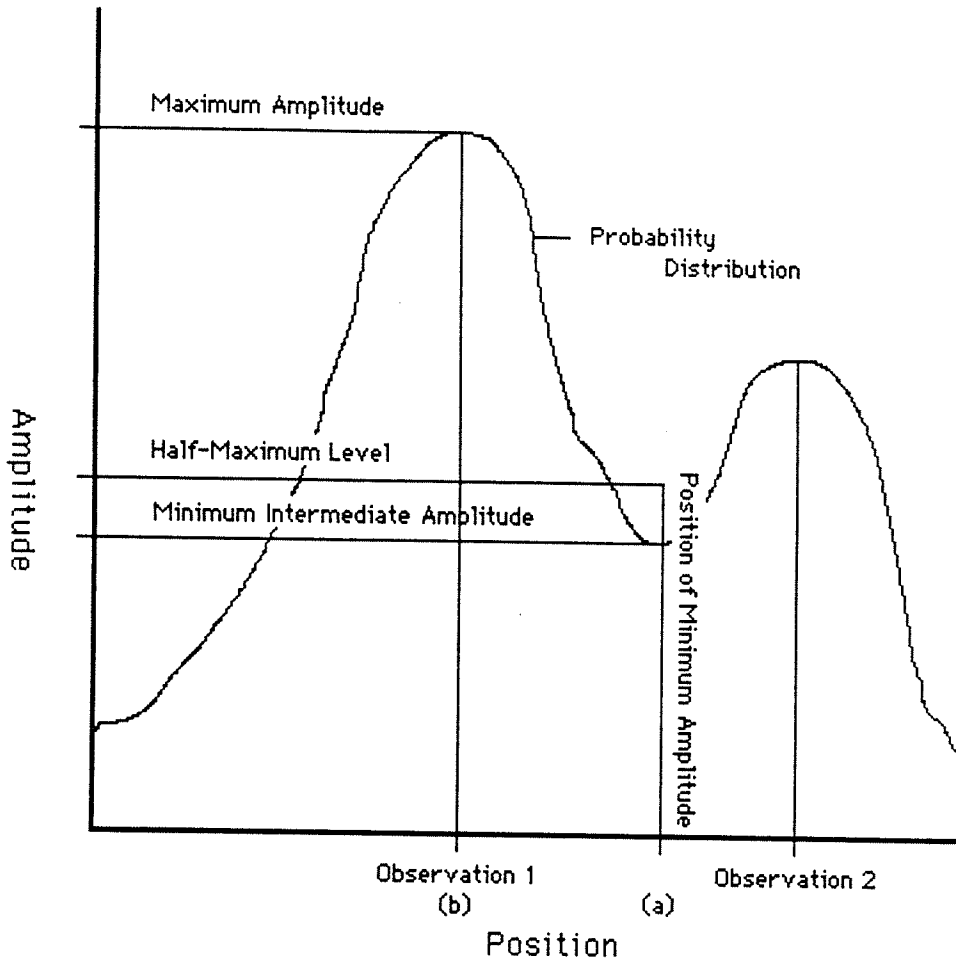


Figure 6: Suggested criterion of resolvableability. The relative positioning of multiple peaks. The saddle point at "a" must be of magnitude $8/\pi^2$ less than the maximum at "b". For peaks of differing magnitude, the author suggests that the maximum used would be the largest peak value.

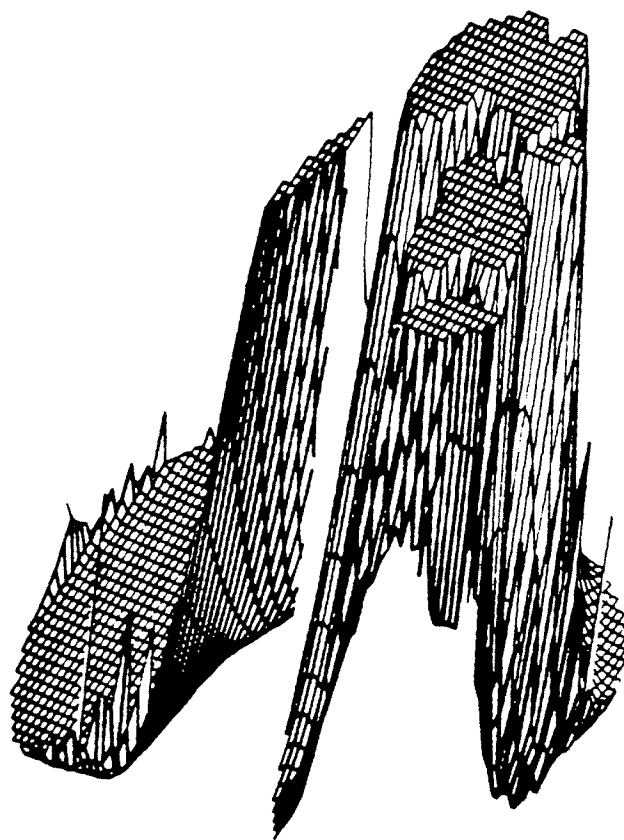


Figure 7: Half-maximum distributions. This representation of the sample data is of the half-maximum values. This presentation is important in considering the resolution of individual observations. Observations that cannot be resolved can be considered to indicate the same observation.

4.3.1 DGTL and Fisher Analysis; Comparison of the Uncertainties

Both fisher statistics and the DGTL method incorporate an area of certainty in their results. This is a measurement of area where the size of this area relates to the confidence in the result that it is associated with. There is no direct or easy way to relate the certainties of the two techniques. For a perfectly symmetrical gaussian distribution (as is the case for a fisher analysis), the half maximum contains 66% of the total probability and so corresponds to the α_{33} area of confidence. In consideration of the converse relationship, since for the probability distribution of the DGTL approach, the unlimited shapes and forms that are possible means that there is no general relationship between the amplitude of the maximum value and the closeness of the grouping of the distribution. There is in fact, no relationship between the position in the area of certainty of the maximum, and the properties of that area.

4.4 Least Squares Fitting to Palaeomagnetic Data

There are a host of different sources imposing a magnetic moment upon any particular rock. For practical purposes when dealing with samples, only a few, and usually only one, component is present. However, samples exist where multiple components are encountered. Where only one component exists, then the ideal demagnetization vector will map out a line which is collinear with the origin. This is also the case for samples where the coercivity spectrums do not overlap. In this case, the line will not be collinear with the origin. Where multiple components overlap, simple

vector analysis does not apply, and more intricate techniques are required (Halls, 1976).

The next level of simplicity occurs where two components exist, but the coercivity spectrums overlap. The remagnetization circle will, in this case, lie in a single plane. If samples from other sites contain the the same component, then the common magnetization component lies at intersection of the planes defined by the remagnetization planes. A certain amount of rotation, which is due to the imposition of a magnetization unique to each sample, is necessary to define this line. This requires that both components share a certain similar part of their history, as well as having a portion that is unique.

The error that must be associated with the intersection of the planes is dependent on the amount of dispersion in the magnetization vectors, and on the experimental errors. This requires that particular criteria are to be met in order to define an acceptable result. As well, an error or standard deviation should be assigned to the results.

A particularly useful criterion is the "least-squares-best fit". This approach demands that the squared value of the distance from the real data to the theoretical model be minimum. Although this can readily be determined for a plane, the stationary point is more difficult to determine. The variational principal lends itself well to this problem.

The method of variations is widely used and thus the theory is very well developed. Its use in problems relating to thermal con-

ductivity, leads to solutions that are boundary value dependent and free of spatial derivatives (Biot, 1970). It is also used as a method for fitting approximately co-planar sets of atoms in solid state and chemistry problems (Schomaker et al, 1959). The problem is equivalent to finding the principle plane of least inertia. It also has a very important application in the mechanics of physical bodies as it leads to Lagrange's equations (Goldstein, 1950).

When the coercivity spectrum of two components of magnetization are similar, the process of demagnetization does not resolve these components in an orderly fashion. Instead, the resultant vectors map a path in three space where all the points lie on a plane. There is considerable dispersion involved in the resultant plane due to dispersion and errors so it is impossible to match a perfect fit. A least-squares criterion can provide the condition for a best fit. When best-fit planes from various sample sites are compared, intersection lines define common vector components, if they are present. Once identified, vector addition will determine the second vector component in a two component case. For a complete discussion of the details of least-squares analysis and the calculus of variations, the reader is suggested to consult Arfken (1970). Schomaker et al (1959), discuss the problem as it refers to positions in three dimensions in physical problems.

Kirschvink (1980), provides an excellent reference regarding the issue of resolution of multiple components of remanence as it applies to palaeomagnetic data. This particular paper discusses the general limitations of current methods such as the limited use of the data available and the data that is potentially available. Also

provided by this paper is a numerical criterion for determining linearity or planarity. If a section of the path through space that the remanence vector maps out in three-space is linear, then this can be interpreted to be characteristic of a single component of remanence, and subsequently used to determine a characteristic remanence of the sample by vector translation of this section to the origin. Alternatively, if a portion of the path lies on a plane, then by an eigenvalue analyses as described above, it can be used to resolve components of remanence. A particular feature of these approaches is the identification of geometric objects. They provide criteria by which an object is determined to have been identified, such as the maximum angular deviation, as discussed by Kirschvink (1980). Schmidt (1982), has further refined this approach to resolve almost parallel components by the simultaneous analyses of multiple samples; provided the samples were obtained from a homogeneous source. This has the particular advantage that it eliminates the step of incorporating the results of multiple samples which may allow the introduction of subjective input by the researcher.

The first thing to note in comparing these approaches to the method developed here, is that the DGTL and CVNL methods are not geometric methods. They do not depend on any kind of geometric configuration. This can be extremely critical in the analyses of poor palaeomagnetic data as was the case for the samples used here, and as is often the case for data from the Precambrian. The methods described by Kirchvink place a error based upon the deviation of the path from that of the ideal path or plane and so necessary requires samples that are "geometrically good".

Chapter V

THE EARTH'S MAGNETIC FIELD

5.1 Secular Variations

A excellent and complete reference regarding the earth's magnetic field can be found in Parkinson (1983). A brief discussion follows as is relevant to this thesis.

The steady change that is occurring in the magnetic field over long periods (years) of time is referred to as secular variation. Rough compass measurements taken as early as the 15th century indicated that the earth's magnetic field varied in time at particular locations.

Although local fields vary due to local conditions, secular variation refers to changes associated with the earth's main field. This change can be adequately described by changes in the magnetic moment of the dipole component of the field, by westward drift of the non-dipole components, by northward shift of the axial dipole, and/or non-drifting secular variations (Nagata, 1965).

Areas of rapid rates of change (fractions of degrees each year) have been found. These are classed as isoporic foci and generally have a westward drift. Alternately there are areas of considerable stability, as are found over in the Pacific Ocean. To use westward drift exclusively to explain secular variations is an approach which is too simplistic since there exists eastward moving components.

The first measurement of declination was made in China in 720 A.D. (Parkinson, 1983). The first measurement of inclination was made in Europe in 1544. The secular variations in local fields were first discovered in 1634 by H. Gellibrand, based on measurements done in 1580, 1622, and 1634. Gilbert, in 1600, presented the notion that the earth could be viewed as a giant magnet yet it wasn't until 1849 that the first observations showed that rocks could be magnetized. Chevallier, (1925) took this one step further to initiate studies of the secular variation in the earth's field.

The sources of these variations are not clear. It is certain that the variations in the field are tied up with the field's source mechanism so it involves complicated interactions in the earth's interior. Variations could be due to the transfer of angular momentum between the earth, moon, and sun. Another possibility is that it is connected with the coupling between the core and the mantle. Because of energy considerations, secular variations must involve more rearranging of the magnetic lines of force than a process that creates or destroys them (Hide, 1966).

For the last million years, the motion of the dipole has had a reduced rate of acceleration. Recent variations can be determined using dated lavas and archaeological material. Material found in archaeological sites that have proven useful include kilns, furnaces, tiles, and pottery. In these cases, hematite constituents provide the magnetization, while dating using ^{14}C methods on the ashes have been accurate to about 100 years.

5.1.1 Reversals

Major events in the earth's dipole field are represented by field reversals (Parkinson, 1983). These reversals are supported in the geological record and are part of the popular dynamo model used to explain the earth's magnetic field. Instabilities trigger these reversals (Cox, 1969, Nagata, 1965). Analysis of magnetic anomalies in marine sediments show that such reversals in the field occurred as far back as 170 million years. Particularly striking are the magnetic stripes that are observed paralleling spreading oceanic ridges. Older events have been deduced from magnetostratigraphic reconstructions of sedimentary rock sequences.

Palaeomagnetic studies have provided some of the best evidence supporting plate tectonics during the Precambrian. Lack of correlation in the polar wander paths from various plates indicate relative motion. This conclusion is not dependent on the fundamental assumptions of the earth's magnetic field, past or present. Apparent polar wandering does not, in itself, conclusively indicate plate motion; singular lack of correspondence between the paths of individual plates does.

Periods where the polarity remains constant almost all the time (60-100Ma), are called normal polarity, or reverse polarity. Periods of mixed polarity occur where the field alternates more frequently.

5.2 Apparent Polar Wandering

Although higher order terms of the magnetic field show considerable motion, the geomagnetic poles move in relatively small regions close to the geographic poles. The field is relatively stable in magnitude and predominantly dipole in nature. However, periods have occurred in which there have been significant deviations from this model (Harrison and Ramirez 1975).

When a mean pole position is determined for several sites they trace out a path. This path represents time variations of the origin, and is called the apparent polar wandering path. This path may differ from region to region, indicating relative motion between these regions.

Chapter VI

GEOLOGY OF THE STUDY AREA

6.1 Regional Setting

The samples used in this study were collected in the Leaf Rapids area of north eastern Manitoba, Canada. The study area lies along 101 degrees west longitude between 56 degrees N latitude and 57 degrees N latitude. The survey was conducted along Manitoba Provincial Highway 391, between Adam Lake and Suwannee Lake. A total of 148 samples were analyzed, mostly taken from outcrops of granitic and tonalitic intrusions.

The study area lies in the Churchill Province, approximately one hundred and fifty kilometers northwest the Churchill-Superior boundary. The Churchill Province of Manitoba and Saskatchewan has been further divided into separate lithological and tectonic domains. These domains in Manitoba are shown in Figure 8. This particular lithotectonic partitioning has been devised by Lewry et al (1978, 1981, 1985), Ray and Wanless (1980), Lewry and Sibbald (1980), Lewry (1981), Fumerton et al (1984) and Green et al (1985). The study area is within the Leaf Rapids domain.

A generalized geological schematic of the local geology is included in Figure 9.

Leaf inserted to correct page numbering

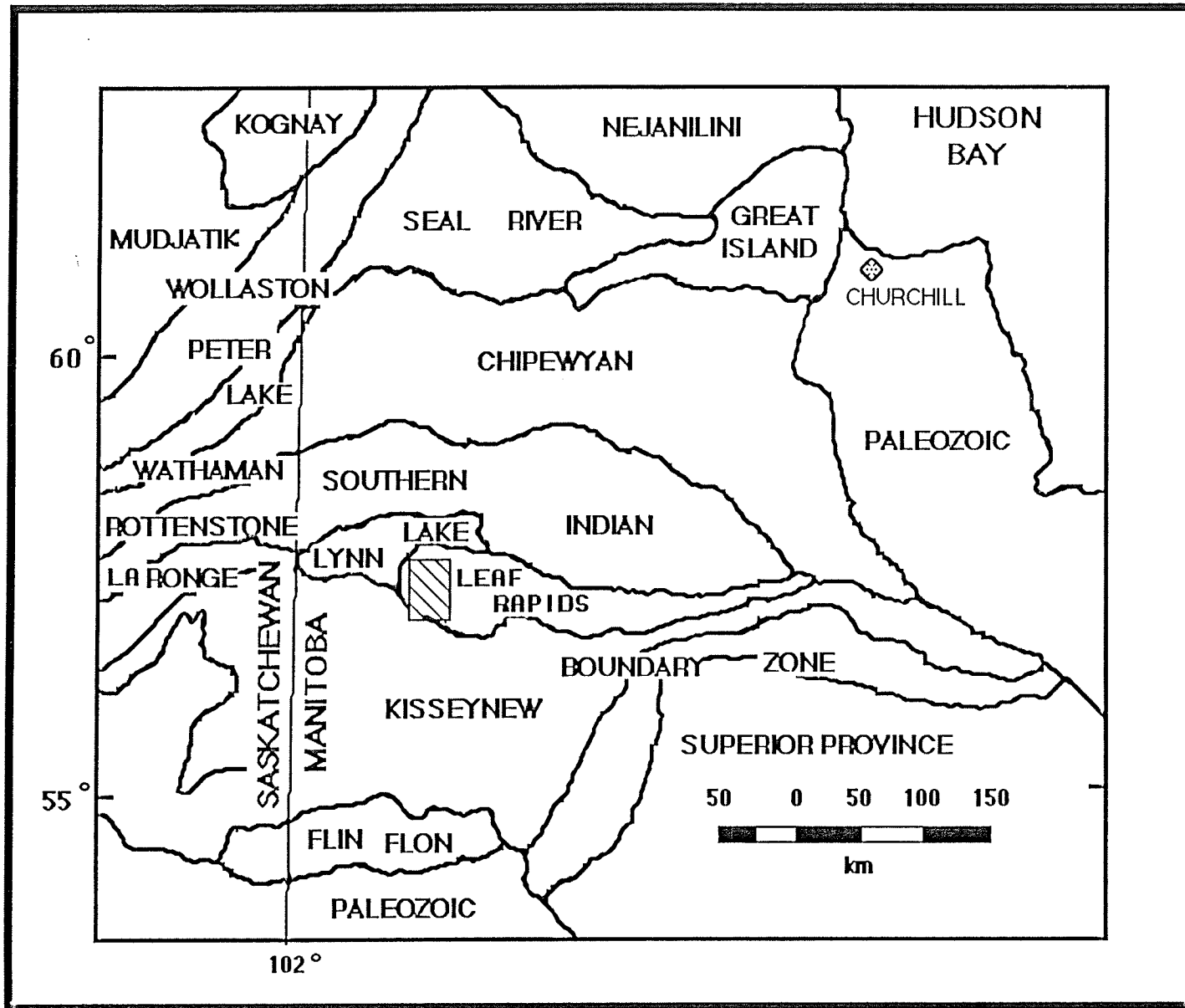
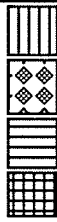


Figure 8: The Geological Domains of Manitoba. The following figure contains a schematic of the domains of Manitoba (from Clark and Schwedivitz, 1986). The Study area is marked by the shaded area.

Figure 9: Geology of the Study Area. The following figure (overleaf), contains a schematic of the geological configuration in the study area.



Tonalite-granodiorite
Greywacke and mudstone derived gneiss
Arkose, arenite and quartzite derived gneiss
Felsic metavolcanics
Migmatite, agmatite and gneiss complex



Granite-granodiorite
Mafic and intermediate volcanic flows
Meta-conglomerate
Amphibolite and mafic gneiss

scale 1:400000

The unit boundaries were determined from Barry and Gait (1966), Frohlinger (1979), Schledewitz (1972), Kendrick (1972), Campbell (1972), and Hinds (1972). A considerably large number of geological studies (e.g., Schledewitz, 1972, Barry and Gait, 1966, Kendrick, 1972) have been done in this area. The study area is predominantly underlain by gneisses and granites containing belts of greenstones of supra-crustal rocks that are cut by high level granitoid plutons. The granitic rocks generally show a gneissic or migmatitic layered gneissic structure on one hand, and nebulitic and homogeneous granitoid structure on the other. The predominant characteristic of the rocks in the region indicate that they were emplaced during the Hudsonian orogeny (1800 to 1950 Ma ago), under conditions of fairly uniform regional tectonic forces. It is generally agreed that the geological history of the study area is most closely related to the Hudsonian orogeny.

6.2 Isotopic Ages

The oldest rocks in the region appear to be metavolcanic rocks which yield U-Pb zircon ages ranging from 1.93 to 1.91 +15 -10 Ga, (Baldwin et al, 1985) while ages ranging from 1940 +/-75 to 1835 +/-75 Ma have been obtained in these zones using Rb/Sr methods (as reported by Lapoint et al, 1978).

Age determination of composite plutons emplaced into the Lynn Lake volcanics give ages of 1876 +6/-4 and 1876 +9/-7 Ma. (Baldwin et al, 1985). Post-Sickle intrusions are also reported to be of Age 1765 +/-100 Ma (Clark, 1980) using Rb/Sr methods.

Chapter VII

PROCESSING AND SAMPLING METHODS

Approximately 120 samples were obtained for this survey. They were cored from the Precambrian shield along Highway 391 in northern Manitoba, in the Leaf Rapids area (see Figure 10). The survey was strictly an initial reconnaissance survey with sampling completed where exposure of the bedrock allowed. The density of sample points varied dependent upon the terrain.

The field work was done during the summer of 1974 (by Tang and McGowan). The samples then remained at the University of Manitoba until cleaning and analysis in the autumn of 1984.

The method in sampling was to drill two cores at each site, then cut three samples from each core. In many cases this was not possible and so there were sites where fewer than six samples were available. Along with the cores, a sunsight reading was taken along with the local time, a compass bearing was taken, and the core was oriented relative to magnetic north and the vertical. The location was determined by odometer readings from the vehicle, and landmarks along the road.

The convention used in identifying the samples is to assign a three digit number to the sample site. The next single digit identifies the sample from each core while the final attached letter (either an A or a B) identifies the core.

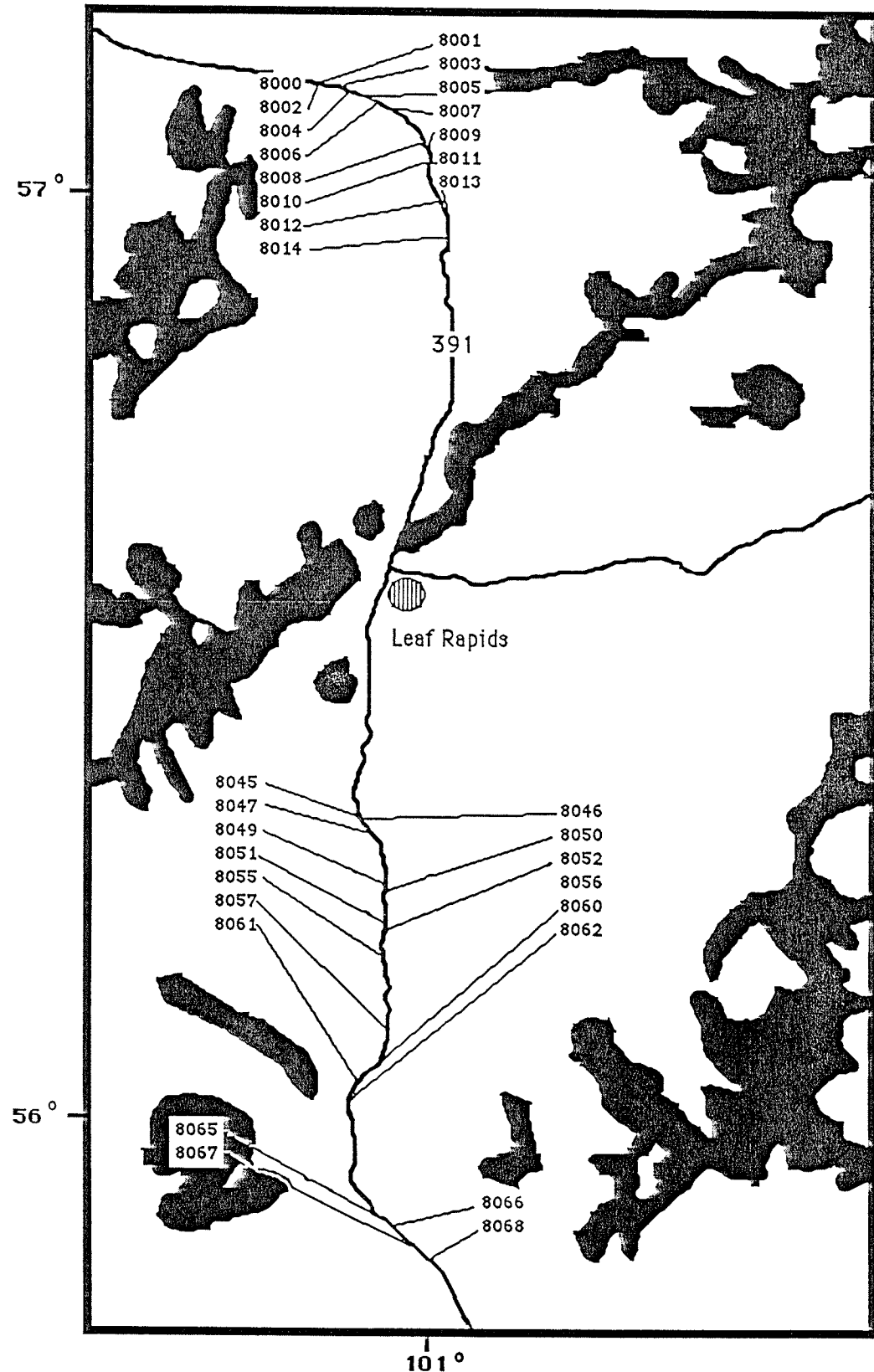


Figure 10: The sampling sites for this study. The sampling locations that were used in this study are contained in this figure. The sampling was done along highway 391 as conditions allowed. The values indicated at the sites are the magnetic susceptibility value as measured for each core. The samples and their associated susceptibilities are contained in Table 2

Table 2: Susceptibilities of the rock cores.

The following table contains the site identifier, and the susceptibility of the rock samples from that site. This table can be used to identify the sample locations from Figure 10.

Site	Core A	Core B
800	.11	.25
801	.12	.09
802	.34	.55
803	1.94	2.09
804	2.03	2.12
805	.94	1.86
806	.08	.09
807	.11	.08
808	.04	.04
809	.64	1.37
810	.55	1.26
811	.96	1.25
812	.08	1.07
813	.26	.14
814	.94	.92
815	.08	.02
816	1.12	1.08
817	.01	.01
818	.31	.37
819	.01	.04
820	.23	.23
821	.01	.29
822	.65	.65
823	1.65	1.15
824	4.62	.21
825	1.72	1.51
826	1.33	1.08
827	1.36	1.42
828	.17	1.33
829	1.60	1.32
830	1.19	.81
831	.44	n/a
832	.02	.02
833	.04	.02
834	.04	.03
835	.09	.09
836	.87	.48

Site	Core A	Core B
837	.98	.44
838	2.11	2.45
839	.11	.77
840	.49	.86
841	3.80	4.69
842	1.33	.97
843	1.36	2.17
844	1.38	.19
845	.13	.73
846	2.33	n/a
847	2.88	2.43
848	2.05	.93
849	.03	.14
850	.22	n/a
851	4.46	2.58
852	1.46	1.74
853	2.01	2.50
854	.84	1.25
855	1.75	1.93
856	3.11	2.18
857	1.55	2.37
858	4.36	2.68
859	4.62	5.22
860	2.41	3.01
861	.03	.02
862	.32	.72
863	.88	1.04
864	.04	.03
865	.08	.08
866	.02	.02
867	.02	.02
868	.02	n/a
869	.06	.06
870	.09	.06
871	.03	.03
873	.03	n/a

Due to the geological age of the samples, a great deal of care was taken in lab techniques, as well as in the computer analysis of the data. This is in reference to the care in making measurements on the samples. The samples were cleaned at 100 nT intervals. This was done for each core where sample one was cleaned on 50 nT, sample two was cleaned on 75 nT and sample three was cleaned on 100 nT, up to 975 nT (which is the limit of the instruments). By taking readings on three different values, one for each sample, three samples from each core, a large density of points was obtained. The original intention was to allow the potential for an improved eigenvalue analysis for resolution of multiple components, and also improve the statistical density of points. It is felt by this author, in consideration of the apparent success of the method presented here, that each sample should be cleaned on 25 nT intervals for all samples. The large volume of data that must be handled in this case is best done by improving the link between the PDP11 and the Amdahl.

The spinner magnetometer is controlled using a PDP 11/04 microprocessor. The software was set up to do six spins for each holder at different orientations of the sample, printing out the direction and magnitude of the moment relative to the shaft and then the inclination and declination of the average moment (from the six spins). A second reading was then done to verify the original result, and to verify that the operator had correctly positioned the sample holder. If the second measurement did not repeat the first, then the measurement was repeated until two readings were equal; to within approximately 4° . This criterion was flexible since the degree of reproducability was magnitude dependent.

The final output included the vector values in cartesian coordinates with standard deviations for each component, the same vector value in spherical co-ordinates without standard deviation, and an optional output of the orientation after correction to account for the orientation of the sample at site. The field sampling procedure provided this orientation of the core in site, and a sunsight orientation. As well, a GMT value was determined to correct the compass reading of the sample orientation.

The principle behind taking three samples from each core, and two cores from each sample site was to verify the magnetic homogeneity of the rock body. A second verification on the homogeneity of the sample was done by the machine based on the sinusoidal form of the signal output. If the signal was from a rotating dipole source, then the output would have the same frequency as the shaft rotation. If it was determined that the signal had significantly higher-order components, then the PDP 11/04 responded with the command to move the sample further away from the pick-up coil. This then improves the dipole signal/non-dipole signal (noise) ratio.

In order to avoid static build-up, anti-static dryer sheets were used to wipe the holder, sample and surrounding work area. Another precaution included cleaning the holder daily before use, and also measuring the magnetization of the holder regularly throughout the day (two or three times). No significant component could be detected from these measurements done on the sample holders. The author was careful to avoid inserting any metallic items into the magnetic shield to avoid static build-up in this element of

the instrument. As well, anti-static dryer sheets were inserted into the shield to minimize this influence.

The cartesian values of their vectors were used since they were output with their associated standard deviations. The principle behind this was to use the standard deviation as a weighting factor on the individual measurements. These values, unprocessed in any way, were then typed into the mainframe for subsequent calculations.

Due to the weak response of the samples, multiple readings were used for each sample. It was hoped that any instrument dispersion would be statistically removed in this approach. The number of readings used for each sample can be used as an indication of the certainty of the reading. The finite limitations of the demagnetizing machine requires that readings are only available between that limit and the point where the demagnetization vector becomes stable. This range will be variable for each sample, and hence so will the number of data points available in the calculations. Although there are qualitative measures of the certainty in the reading, they were not the only criteria used. In cases where the oscillations of the magnetization vectors were obviously random, these results were either discarded or appropriately weighted. In cases where the signal from the sample was so weak that the measurement was taking a significant amount of time, the density of measurements for that sample was decreased, or the sample was discarded.

The standard deviation was used to weight the pole positions in determining the final positions of the data set. The factor used was the inverse of the standard deviation. If the pole position was determined from n readings:

$$\sigma' = n/\sigma$$

This was not the only factor used. A quantitative measure was determined by examination of individual plots to determine how erratically the magnetization vector varied. Considered in this value was the number of points used. More points represent better statistics, while fewer points do not give a good perspective on the behavior of the magnetization vector. Digital plots, where few points are resolved (one in cases), represent samples where the cleaning field does not significantly alter the magnetization. Such a situation must necessarily be weighted very high.

The standard deviation produced by the instruments is as indicative of the magnetic isotropy of the sample as it is of the error in the values of the readings. Multiple moment distributions in the sample lead to large standard deviations.

The data processing involved operator interactive procedures. Once the data was entered into a "Mantes" file on the Amdahl 5850 at the University of Manitoba, a plot of the demagnetization vector and the magnitude of the demagnetization vector as a function of cleaning field, was done. The magnitude plots were inspected to investigate for regions of interest. This area, it is assumed, indicates the region where the viscous remanence is removed. This region of the data was then replotted. As well as this replotting, the mean value of the magnetization vector was determined for each sample from the multiple readings. This mean was corrected for compass error, and tilt of the coring tool. This value was then used to determine the apparent pole position for that sample.

A mean value using the cleaned vectors was also determined using the digital plots. These plots were also inspected for multiple resolvable components. Three particular plots were completed based upon this technique, a plot of the individual distributions, a plot of the total cumulative probability, and a plot of the half-maximum distribution of the total probability (for resolution criteria). The probability functions used in these applications were gaussian distributions, which are directly analogous to Fisher Statistics with a standard deviation of $1/5$. Until sufficient work has been completed that provides a standard and appropriate standard deviation, this author found that this value was adequate. Further calculations produce the half maximum surface area which provides an indication of the certainty of the mean value. The result of this value was dependent on the standard deviation of the probability distribution function, the number of points used, and the dispersion of the data set.

In a manner similar to the calculations performed in the Fisherian treatment, the mean value was corrected, then used to calculate an apparent pole position. Where the results warranted, multiple components were treated as such in the averaging process.

The final calculation involved the determination of pole positions, each associated with separate magnetic events, as indicated by multiple components in single samples and groupings in the total sample set.

The first step in the processing of the data was to average multiple measurements that were obtained at each field strength for

each sample. Usually there are two readings at each field strength, though this is not always the case. Where replication of readings was poor, more readings were taken at the individual field strengths. The magnetization behavior plots (magnetization vs. field, and orientation vector vs. field) were then plotted using these results. The magnitude values were normalized with the value of the uncleaned sample. The demagnetization vector was then plotted by projecting the three-dimensional plot onto the page. The three-dimensional character was preserved by projecting each vector into the x-y plane by a straight line, and then mapping the path of this projection as the field strength varied.

The mean value for each sample was determined in the manner presented here. The standard deviation was calculated as (Bevington, 1969);

$$\sigma' = \sigma_1 + \sigma_2 + \sigma_3 \dots$$

where σ' = standard deviation of the total

$\sigma_1, \sigma_2 \dots$ = the component σ 's

Each individual component was then used to produce an apparent pole position. This position was then weighted and used to determine the mean pole position for the sample set.

The dimensions of the ellipse of confidence was also determined in the calculations. This provides a measure of the confidence of the reading. An area of confidence is associated with the pole from each sample, as well as the final pole position.

In the application of the digital analysis, three plots were done. The distributions used were normalized gaussian distributions. The first plot was a plot of the remanence vector at each measurement, where a measurement was considered to be each set of six spins on the magnetometer. This gives a good perspective of the distribution of the set at a glance. The second plot is of the total probability. Each point in this plot is the contribution of the probability from each distribution. This plot produces the mean value for the sample. It also gives the shape of the probability distribution of the entire set. The third plot, plots the value;

Val = minimum (Total probability, 1/2 maximum)

The third plot is important in considering the resolution of multiple components in a sample. The shape of the flat surface also provides an indication of the symmetry (or lack thereof), in the distribution. Produced at this step is the value of area of this flattened surface, as a percentage of the total area of the sphere. The reader is cautioned to note that the graphic representation is not indicative of this value since the projection onto the plane is dependent on where the distribution lies in the sphere. A way to avoid this problem would be to rotate the sphere such that the mean value is positioned at the pole.

The mean value produced by these plots provides a pole position. Each value weighted by the formula;

$$\omega = N \times A / \sigma$$

where A = area of certainty

N = number of values used to determine
the position

was used to determine the pole positions for the sample set. This is done by plotting the weighted distributions to determine the mean value. The certainty of this result is determined simply by determining the area of the half-maximum surface.

The raw data obtained and used in this study contained in Table 4 in appendix C). The pole positions, (corrections considered) that were determined using CNVL techniques are contained in Table 6, Table 9, Table 11, and Table 13 in Appendix D). Sample orientations, as determined by the DGTL method presented here, are contained in Table 5, Table 8, Table 10, and Table 12, contained in the appendices. Included in this table are the multiple orientations contained in separate samples. Correction factors, the compass error, and coring tool orientations are contained in Table 14, Table 17, and Table 15. The pole positions determined using the oriented vectors are contained in Table 7.

As can be expected from real samples, behavior of the magnetization ranges from very poor to very good. Ideally, the magnitude should maintain itself at low cleaning strength (0nT to 200nT). The magnetization vector should maintain a steady direction. The digital plots will show clumping of both the observation plot and the total probability plot, with the half maximum area being small. Naturally, the opposite behavior as described here would represent a

poor sample. For low cleaning fields, the magnetization vector remains constant. This indicates a very stable magnetic property; the sample has failed to reflect the influence of recent viscous remanence.

An example of an excellent palaeomagnetic site is location 802. There are two cores from this sample site. The remanence remains constant in direction as the magnitude drops. The magnitude is relatively resistant to the cleaning effects. This behavior is consistent between samples. The probability distribution shows excellent grouping in the distribution form plot with the area of confidence restricted to a tight area about the mean position. Two magnetization readings were used to determine the final pole position.

Another excellent example is site 861. For this site, three samples are available. Characteristic of this site, is extreme hardness of the remanence. The magnitude is extremely resistant to cleaning for the full range of the A.C. demagnetization unit.

Sample site 862 must be considered a poor site by current palaeomagnetic standards. The magnetization vector exhibits wild random fluctuations. However, there are six samples available from this site. Both the magnitude and unit weighting schemes provide highly repetitive results. This supports the conclusion that significant palaeomagnetic evidence can be obtained from poor samples by using good statistical techniques.

Samples exist which provide only one or two points in a region of interest in the demagnetization spectrum. Dealing with these cases requires a weighting scheme which reflects the uncertainty

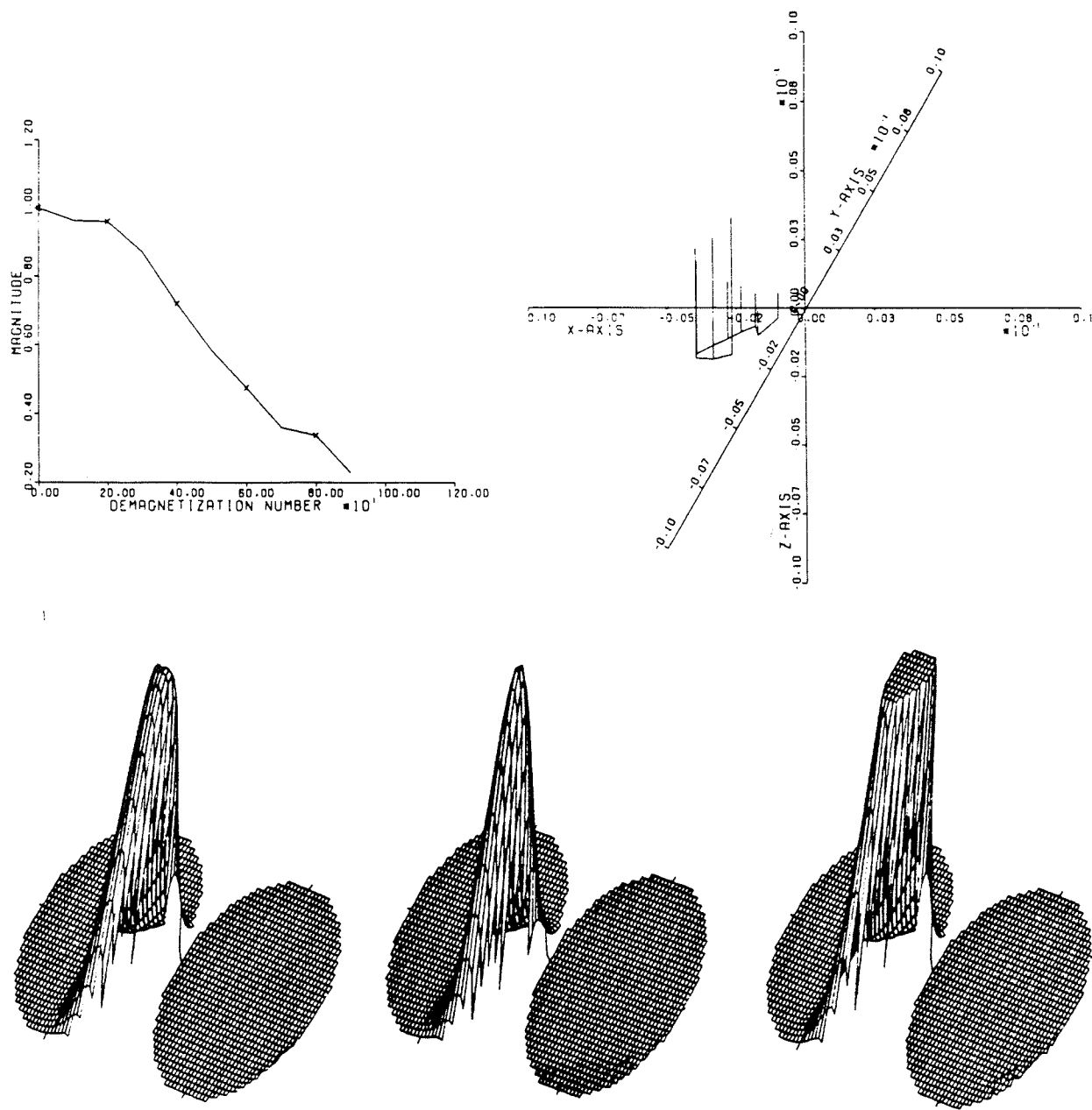


Figure 11: Plots of remanence for sample 8021B. This sample site is an example of an excellent palaeomagnetic sample. The demagnetization vector maintains the direction and strength relatively well. This sample was cut from one of two cores (coreB) that were taken from site 802.

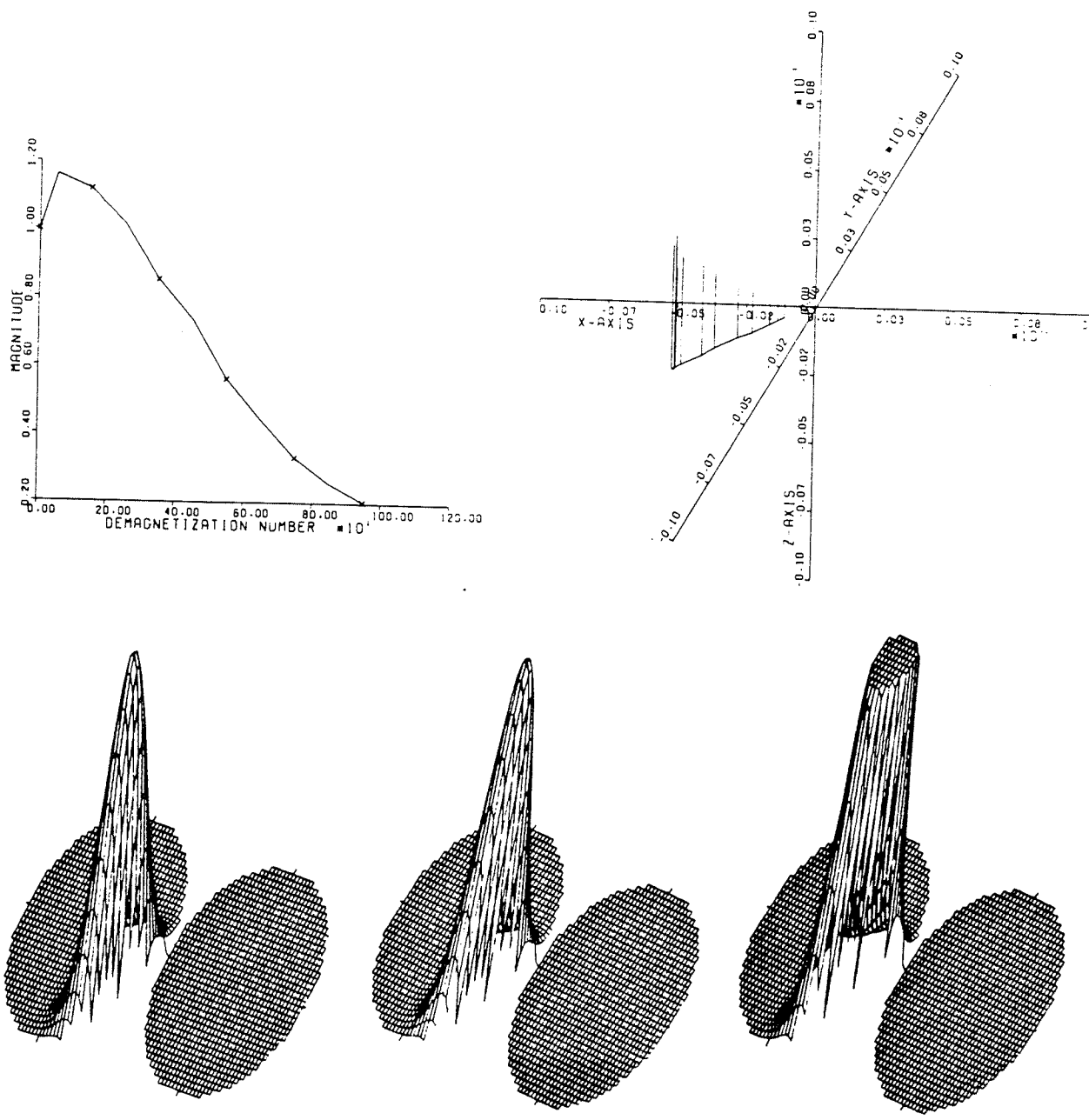


Figure 12: Plots of remanence for sample 8022B. As must be expected from a good palaeomagnetic core, all samples cut from it must show consistent results. This is a property of core 802B, as shown by sample 2.

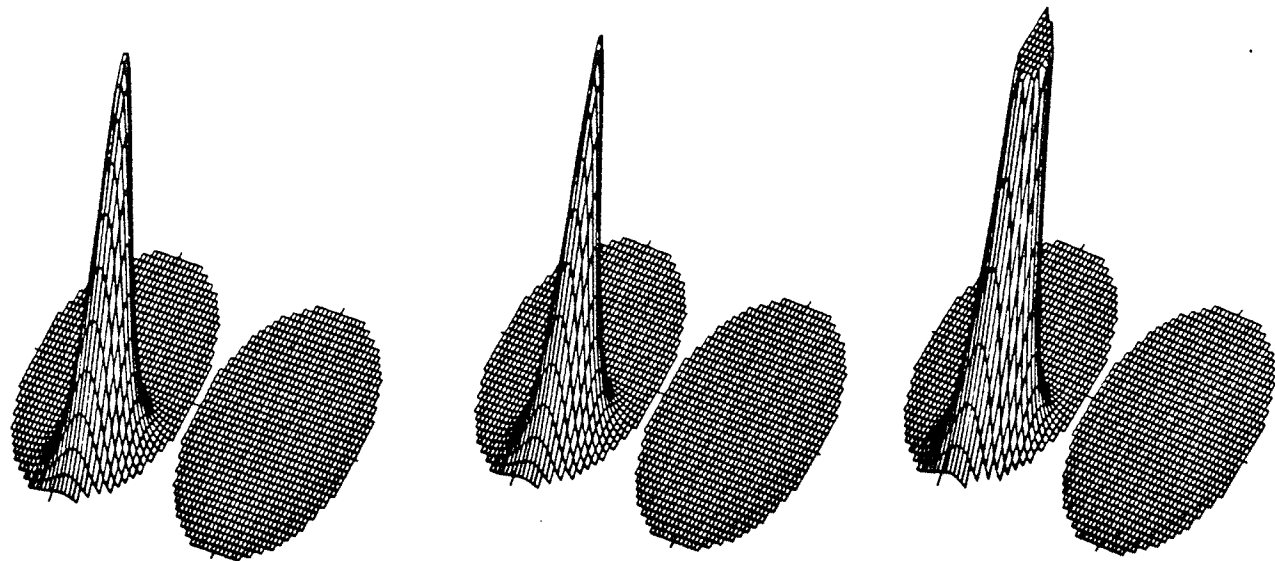


Figure 13: Plots of remanence for sample 8611B. As another example of a good palaeomagnetic sample, are those that were cored at site 861. Different in this case from those cored at 802 is the failure of a clear stable end point to express itself. In order to use this sample for conventional analysis, field measurements where the wild oscillations developed were ignored.

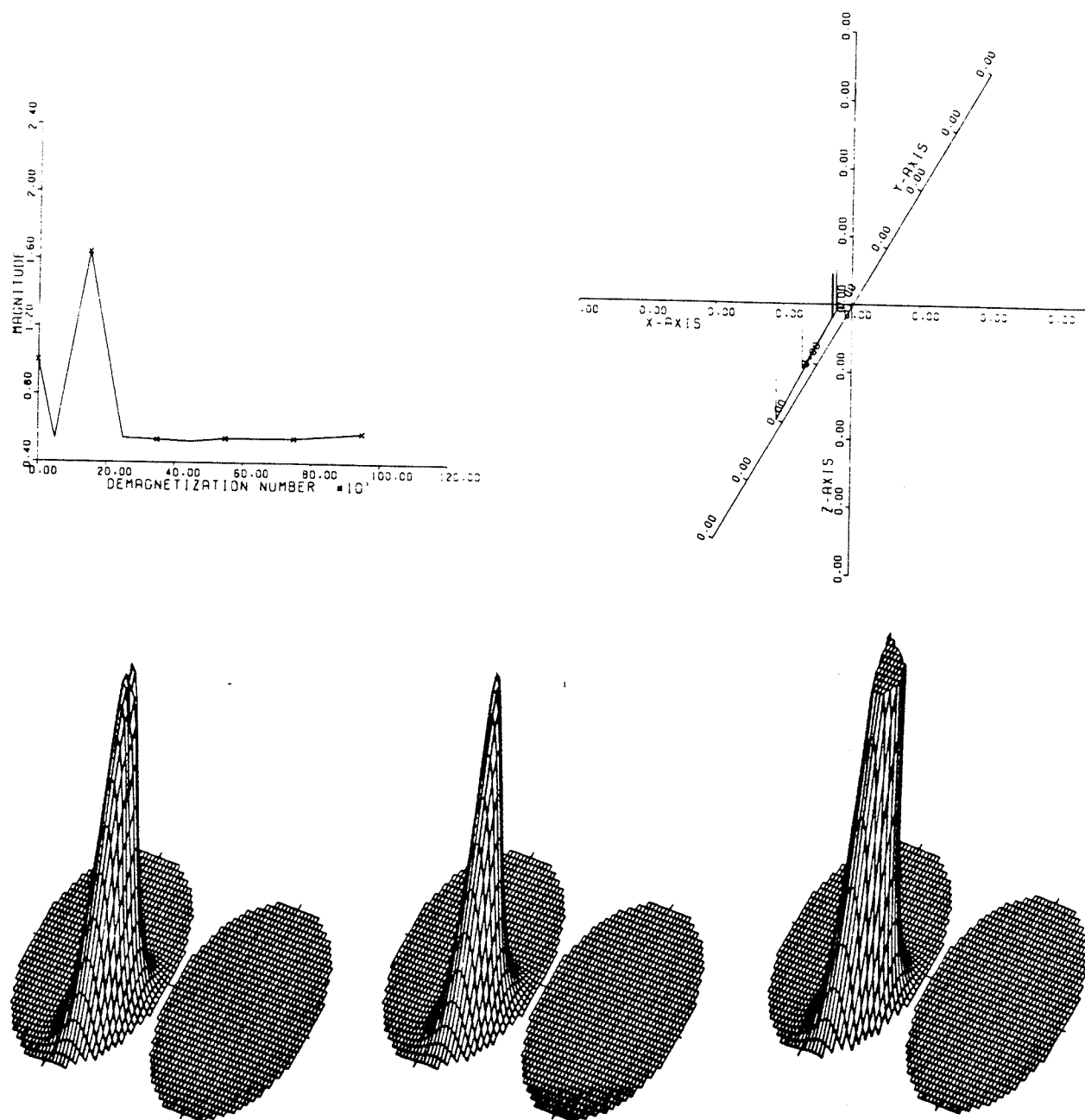


Figure 14: Plots of remanence for sample 8612B. This is the second sample cut from core B which was taken from site 861. This sample does not evolve into a clear stable end point.

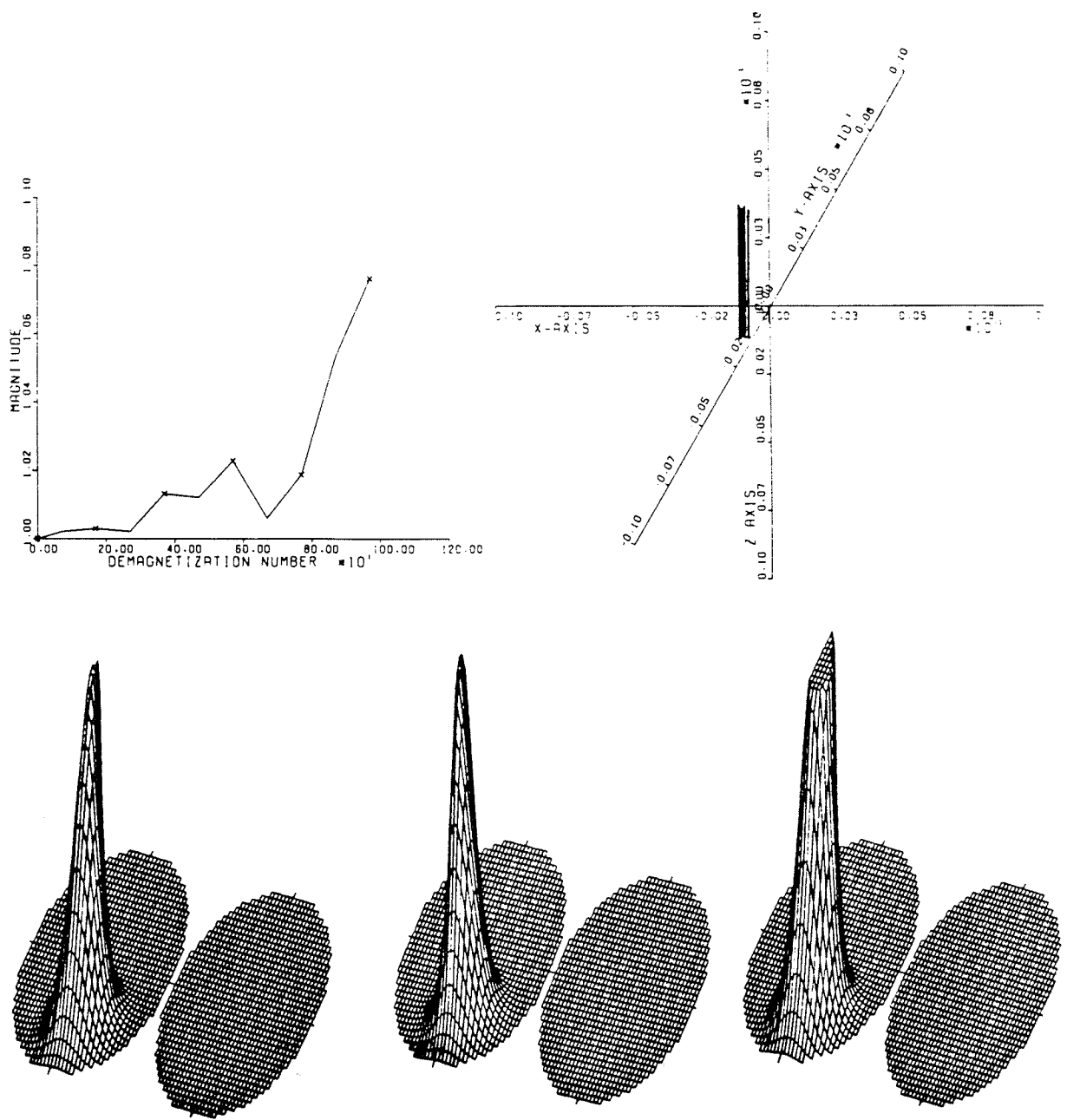


Figure 15: Plots of remanence for sample 8613B. This is the third sample cut from core B which was cored from sample site 861. No clear end point can be observed in any of the samples cut from this site.

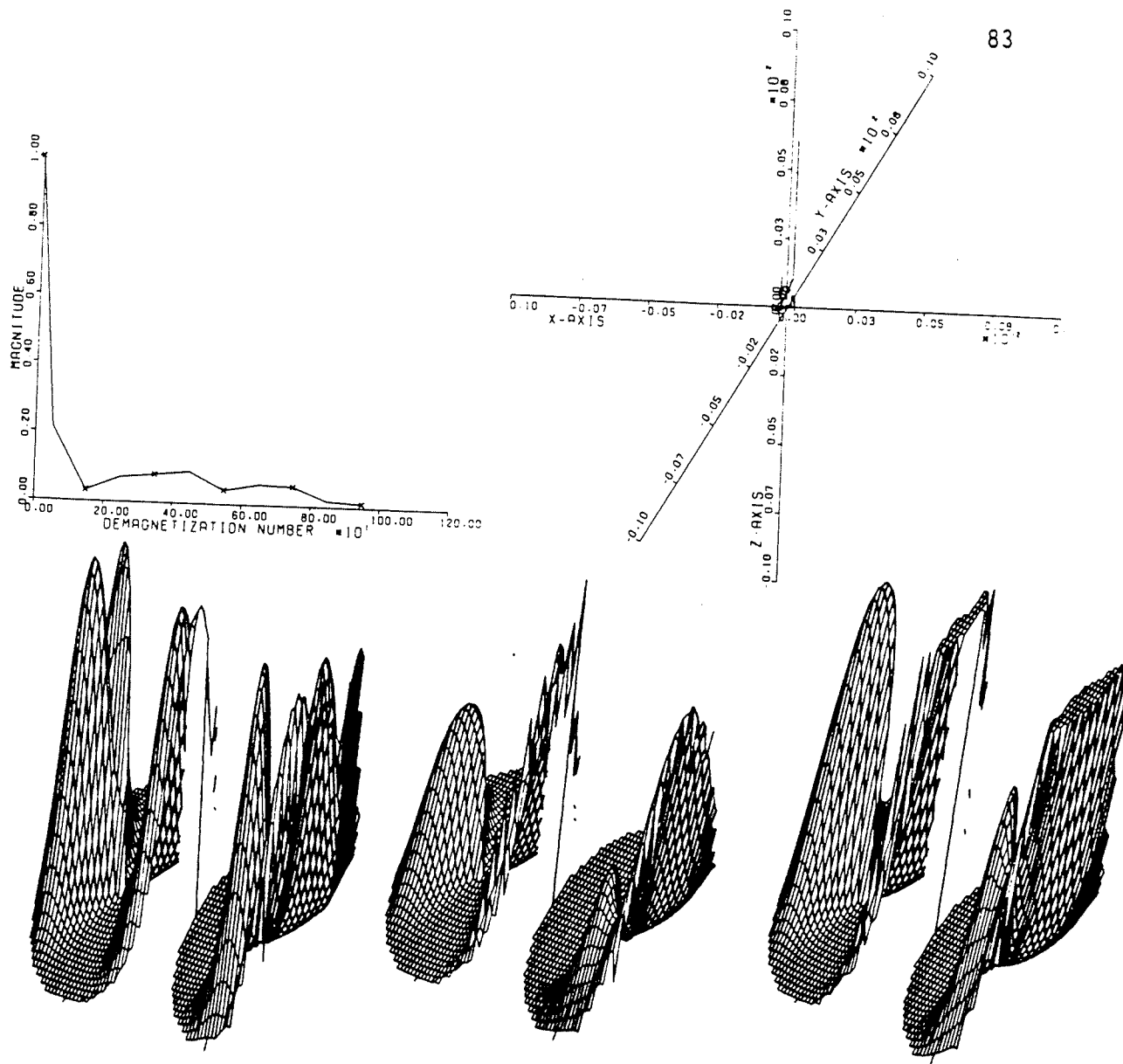


Figure 16: Plots of remanence for sample 8621B. Sample 8621B must be considered a poor palaeomagnetic sample by current standards. The magnetization vector drops sharply in magnitude(1) and fluctuates widely in direction(2) at low cleaning fields. The observation distribution functions are located at random locations around the sphere(3) without any significant bunching that would indicate a magnetization that can be determined by reading directly from these plots. The total probability distribution(4), reiterate these conclusions; the maximum value does not clearly identify a definite mean magnetization. The area of confidence(5), does not show a good grouping about the mean value. It covers a large area of the sphere.

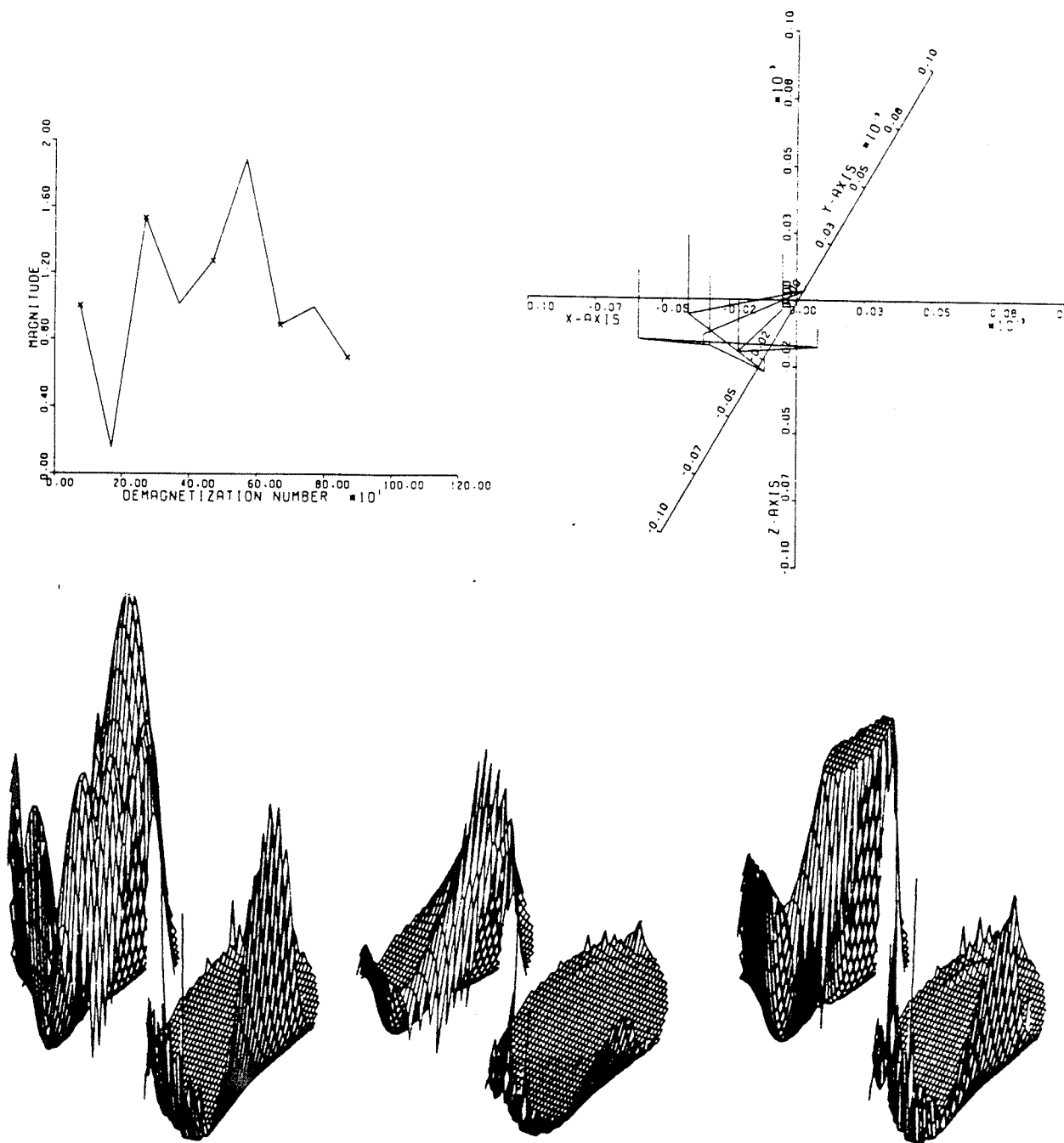


Figure 17: Plots of remanence for sample 8622B. Sample 8622B is the second sample cut from core B, which in turn, was drilled at sample site 862. The results from this sample reiterate the observations made for Figure 16).

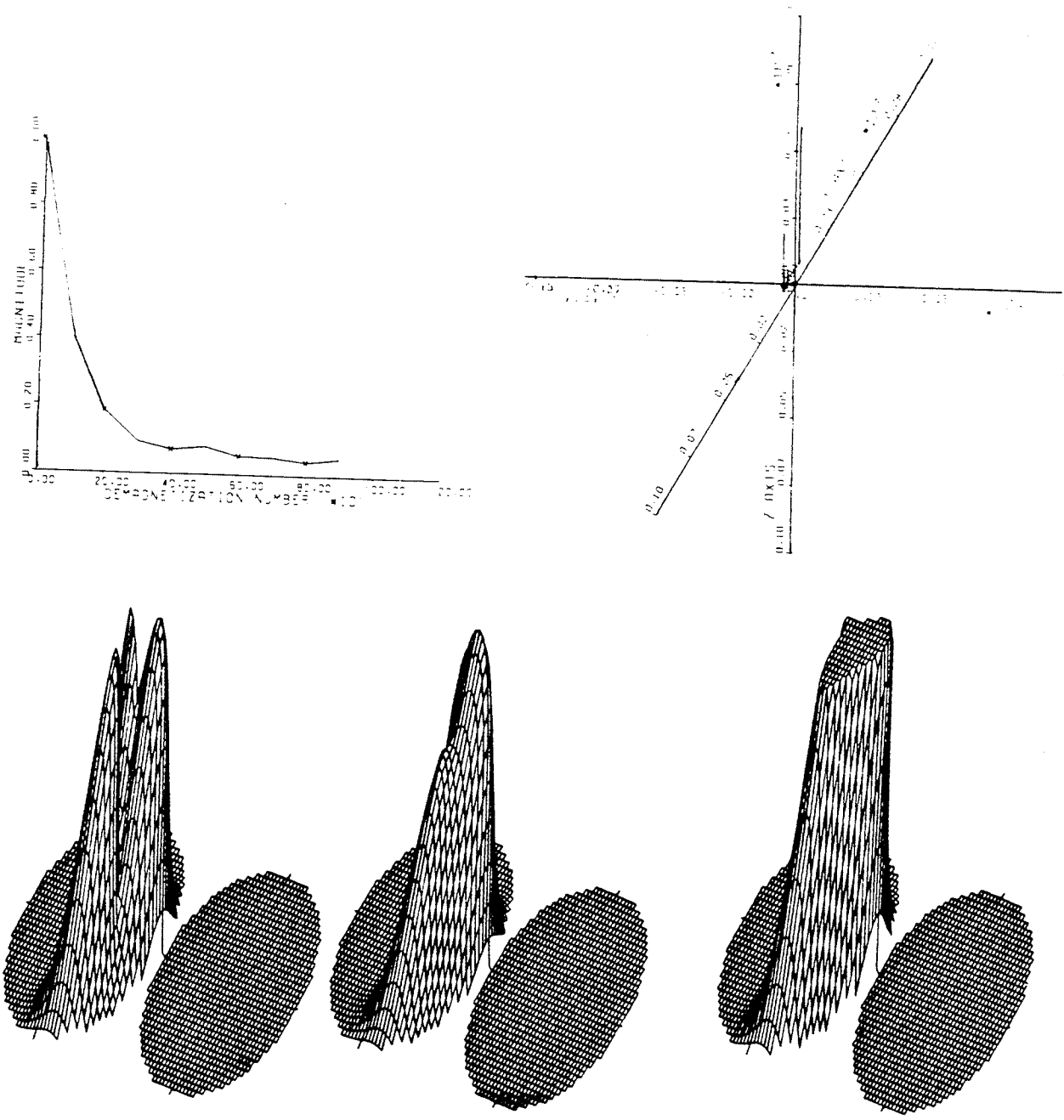


Figure 18: Plots of remanence for sample 8623B. Sample 8623B is the third sample cut from core B, which in turn, was drilled at sample site 862. The results from this sample support the observations made for Figure 16

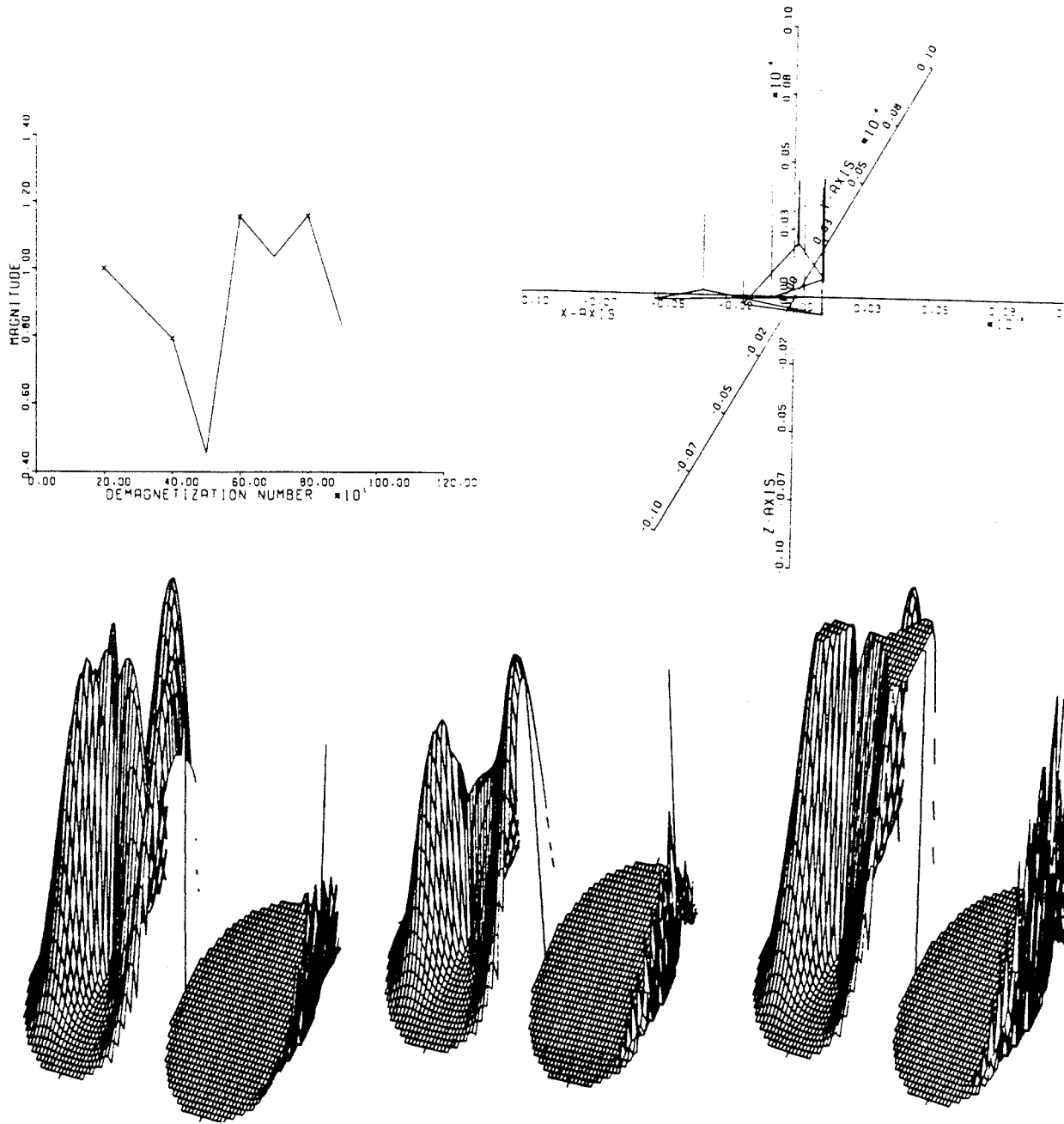


Figure 19: Plots of remanence for sample 8621A. Sample 8621A is the first sample cut from core A, which in turn, was drilled at sample site 862. The more samples that are available to verify a value for an observation the more confidence there is in that observation. The results from this sample reiterate the observations made for Figure 16

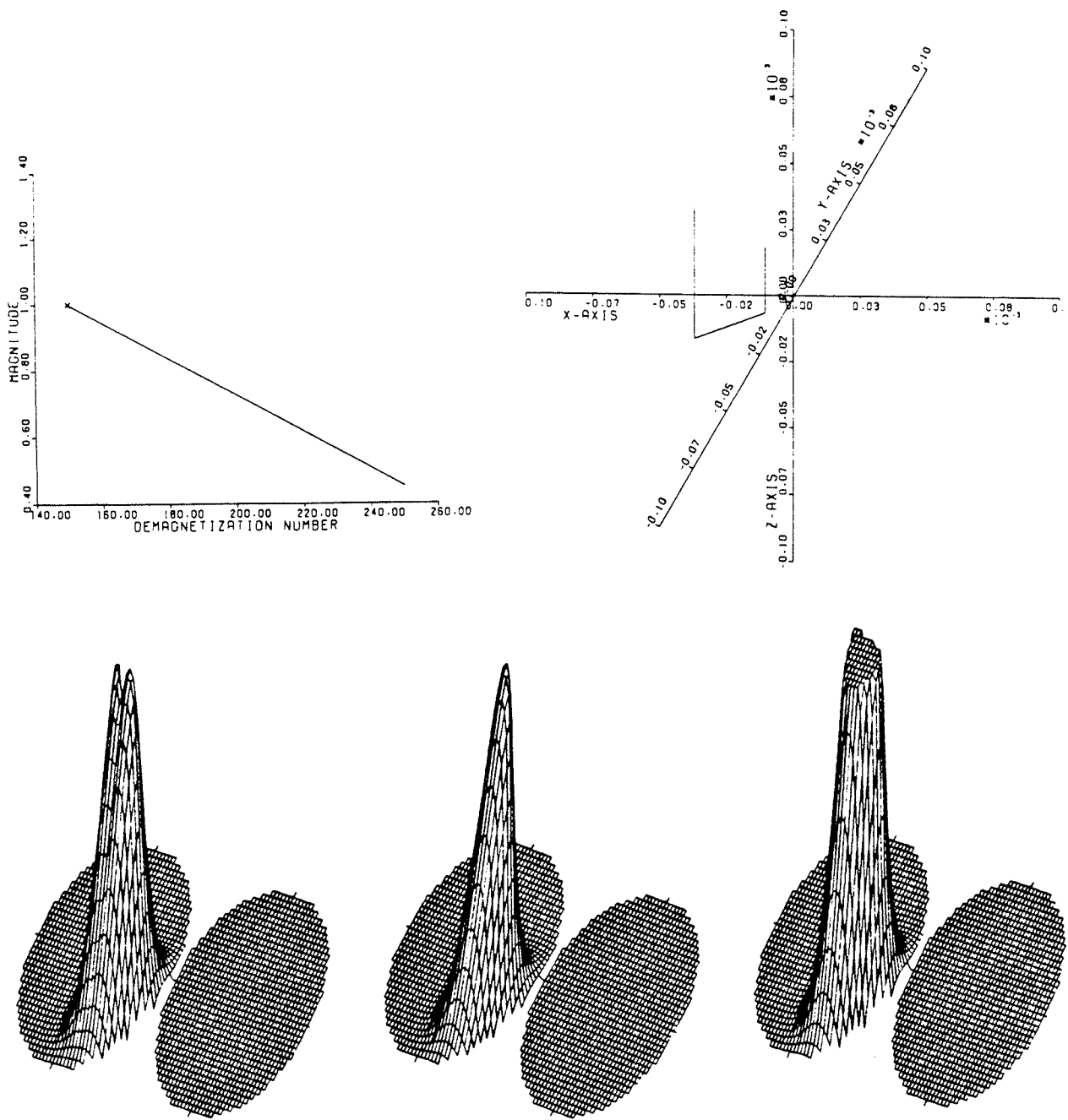


Figure 20: Plots of remanence for sample 8622A. Sample 8622A is the second sample cut from core A, which in turn, was drilled at sample site 862. The results from this sample reiterate the observations made for Figure 16

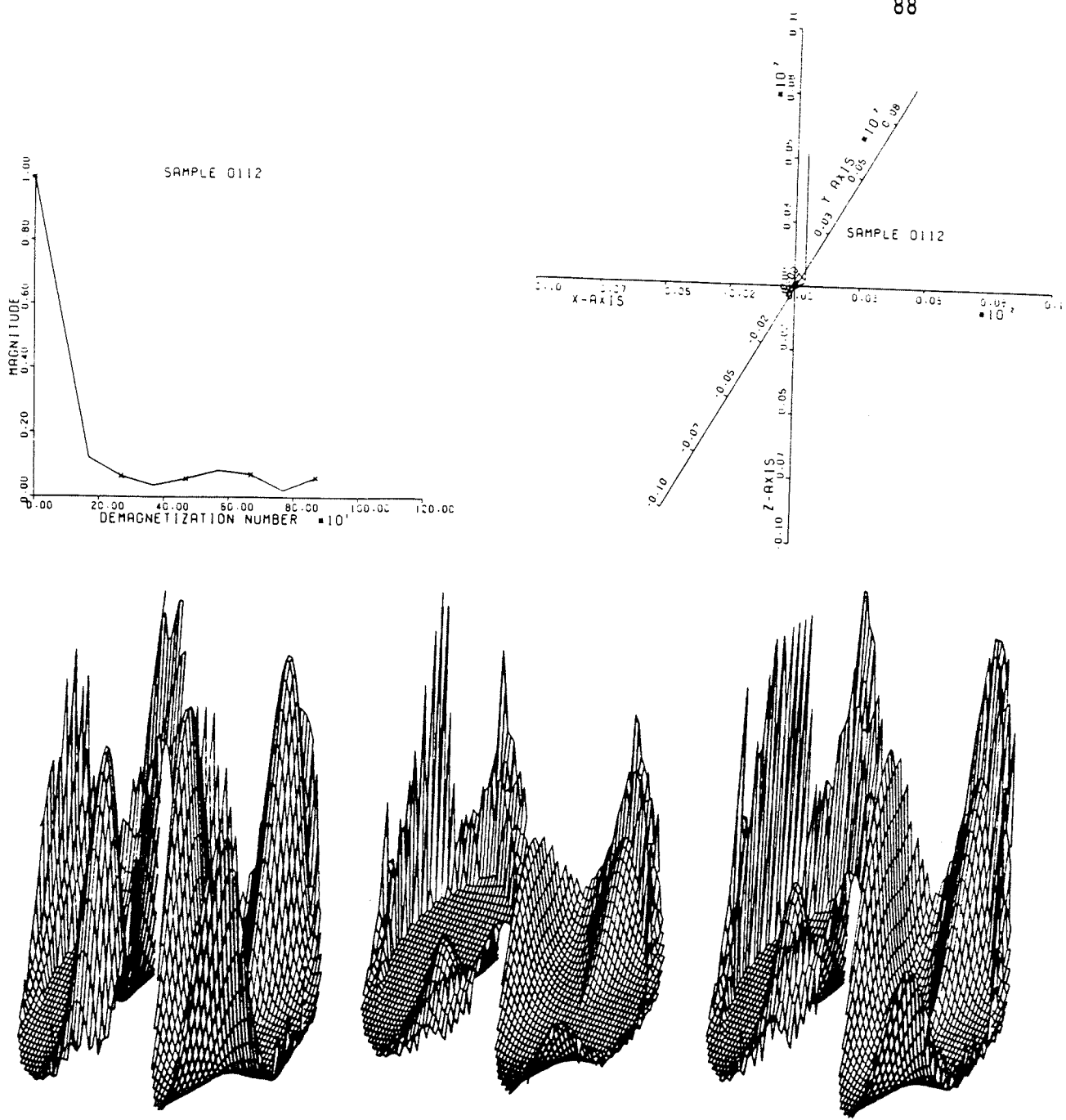


Figure 21: Plots of remanence for sample 8623A. Sample 8623A is the second sample cut from core A, which in turn, was drilled at sample site 862. The results from this sample reiterate the observations made for Figure 16

inherent in this fact. The more readings available that verify a value, or that are involved in determining a value, the more confident one can be with that value.

Processing of the data followed the approach currently used in palaeomagnetic analysis as well as the new approaches developed and presented here. The analysis can be further divided into subsequent sets of steps. Each field strength reading was given unit weight and then used in the calculation of the apparent pole for the sample. The principle of this approach was to allow all random influences to cancel themselves out which resulted in a very random distribution of pole positions. Second, the magnetization vectors were given magnitude weight. The purpose of this was to minimize the error introduced by the magnetometer. The results generally confirmed each other, except for one case; that being the DGTL analysis with magnitude weight.

The demagnetization spectra were divided into three regions and each region was analyzed by the methods discussed here. The first region considered is of the full demagnetization spectrum. A second analysis was done by selecting that part of the demagnetization spectrum between 100nT and 300nT. Restricting attention to the spectrum ranging for the first 300nT, the influence of purely random oscillations which are observed at high field strengths can be minimized. The third region analyzed was the spectrum beyond where any clear remanence could be observed. This region varied with each sample. The purpose of this was to determine whether any information was located in this region.

The conventional approach involved selecting samples where the remanence remained stable over the first several hundred nT. of field cleaning strength. Such samples were picked by examining the demagnetization vector and their magnitudes to determine a resistant magnitude and, (more importantly) a steady direction. Samples are present in the set which indicate multiple components with overlapping cleaning spectrums. These samples can be recognized by the sweeping behavior of the path of the demagnetization spectrum, see Figure 22, and Figure 23. An eigenvalue analysis was done on these particular samples in order to determine the components contained within them.

Once a stable end position was determined for the eigenvalue analysis, then the second component could be calculated by vector subtraction. The stable end point is indicated when the demagnetization vector maintains a constant direction. In many cases a stable end point could not be determined since the demagnetization vector fluctuated in an apparently random manner. In these cases, the point before where these fluctuations started was used.

Sample site 801 shows overlapping of two remanences. The sweeping behavior of the magnetic moment suggests this. Neither of the component remanences seem to be viscous since the pattern is maintained over a considerable range of cleaning and in both available samples. No stable end point is available, however, and the wild fluctuations that are apparent at the high cleaning fields indicate that there is a point where the remanence is fully cleaned.

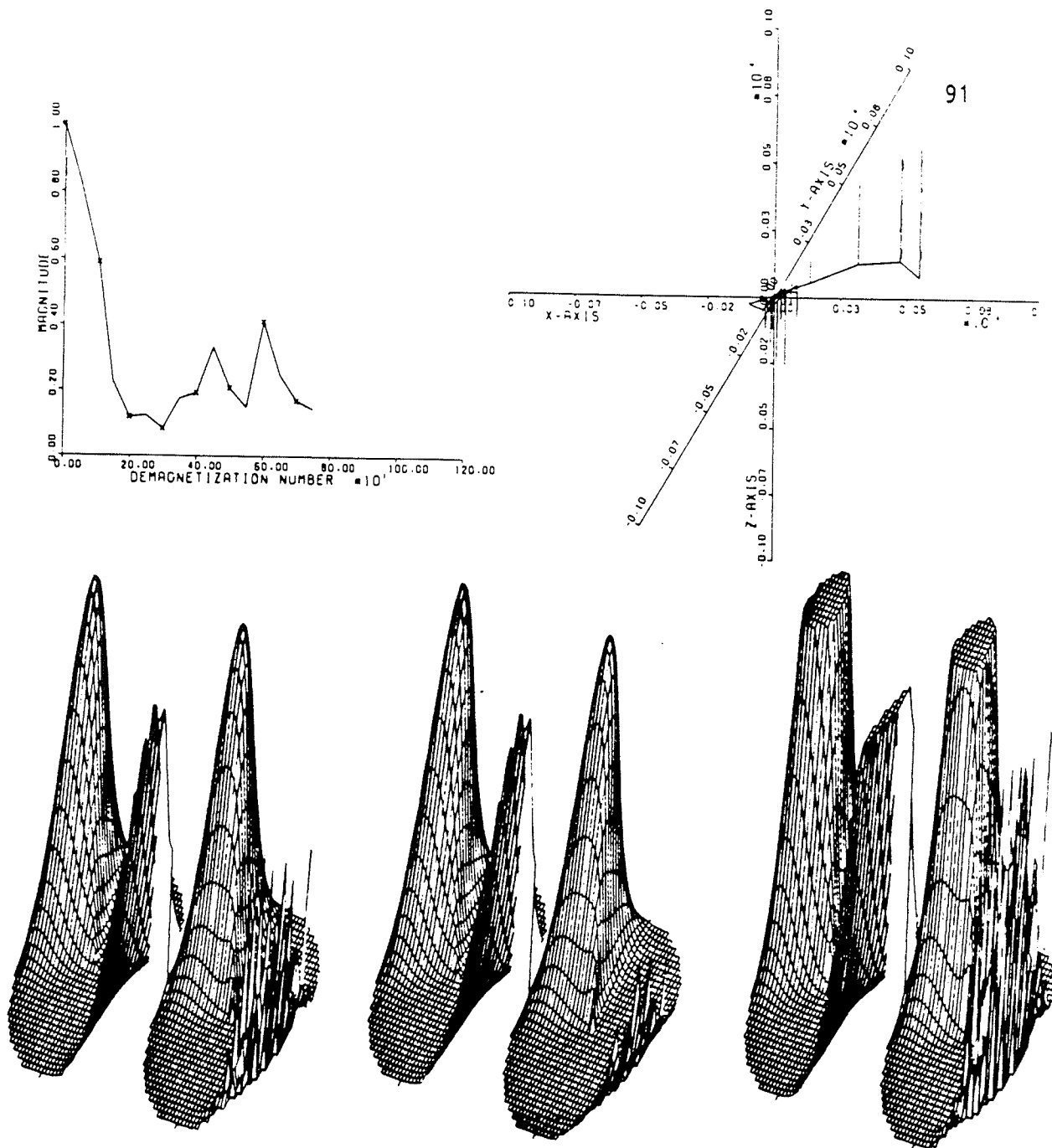


Figure 22: Plots of remanence for sample 8011B. The samples that were obtained from this core show sweeping behavior that is associated with overlapping remanences. The sweeping behavior referred to is of the magnetization vector with cleaning field strength. Both the samples that were available from this core support this conclusion. The fact that the remanence vector is very strong, and stable, for even reasonably strong cleaning fields, adds credence to this conclusion; making this a very good palaeomagnetic study of overlapping remanences.

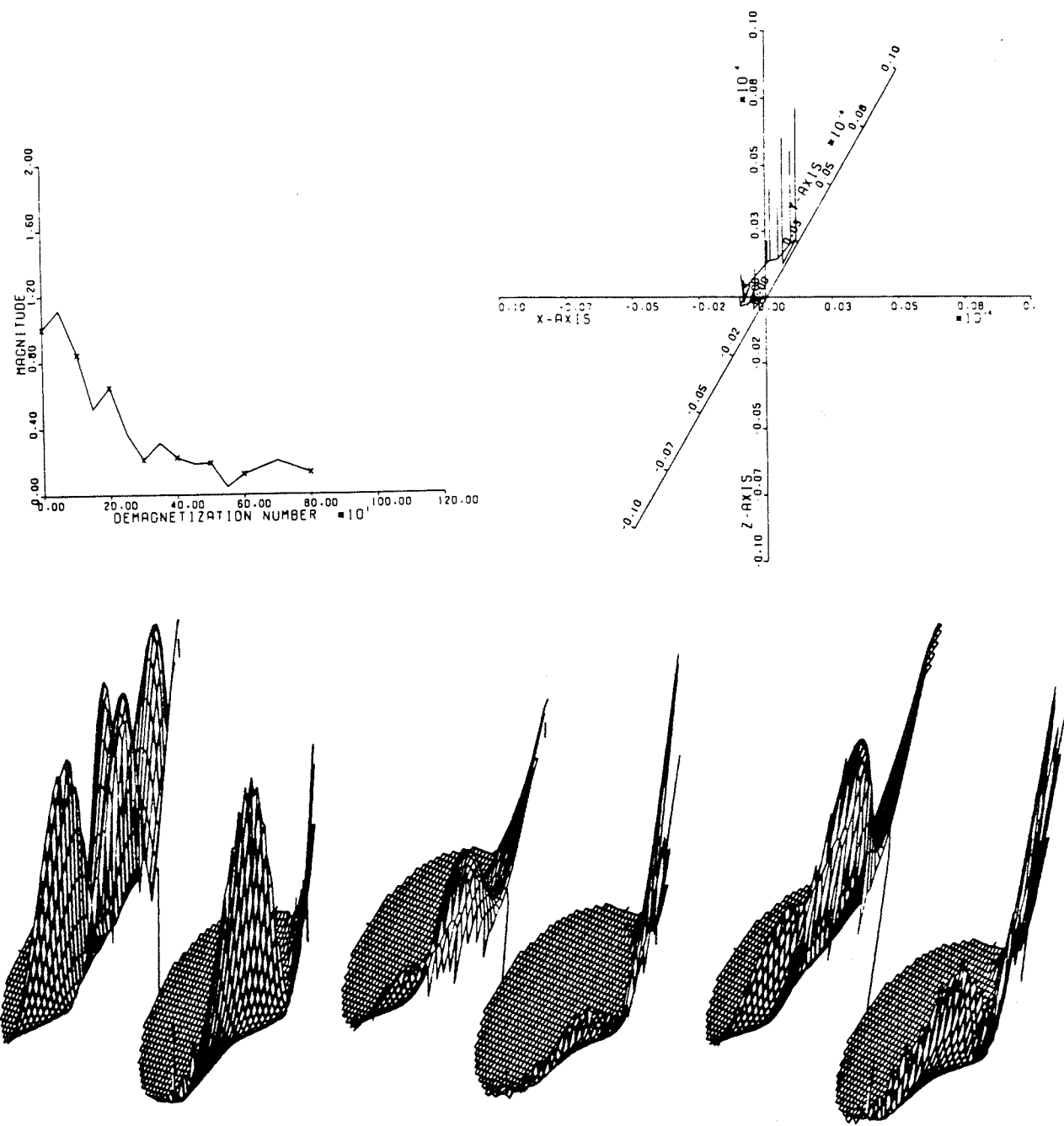


Figure 23: Plots of remanence for sample 8012B. Sample 8012B provides supporting evidence for the observations made about sample 8011B.

The differences between the unit weight scheme and magnitude weight scheme were not as expected. The magnitude weighting approach was intended to account for instrument error as field strengths decreased. The DGTL approach resulted in excellent groupings of the data set when applied using magnitude weight over the reduced spectrum. It did not reconfirm those poles determined by using unit weights, (see Figure 41).

Once these sets of poles are determined, conventional analysis requires that groups be selected as associated with a set dispersed about a single pole position. This is a very arbitrary and subjective approach and allows no criterion to be introduced which is based on resolution. The digital approach, on the other hand, introduces the option of carrying the analysis further. By using digital analysis on the data sets produced by all methods so far, multiple poles can be examined. This allows consideration of possible rotation of the samples, dates of events of metamorphic and igneous activity, as well as a finer determination of pole positions. Such an analysis was done, (pole positions were weighted) to produce the results contained in Figure 42.

In order to investigate the possible presence of reversals in the Earth's field, the south pole positions for each sample were plotted, see Figure 27, Figure 29, Figure 31, Figure 33, , Figure 35, Figure 37, Figure 39 and Figure 41. This is done at this step by considering the quality of the fit of the data to the known.

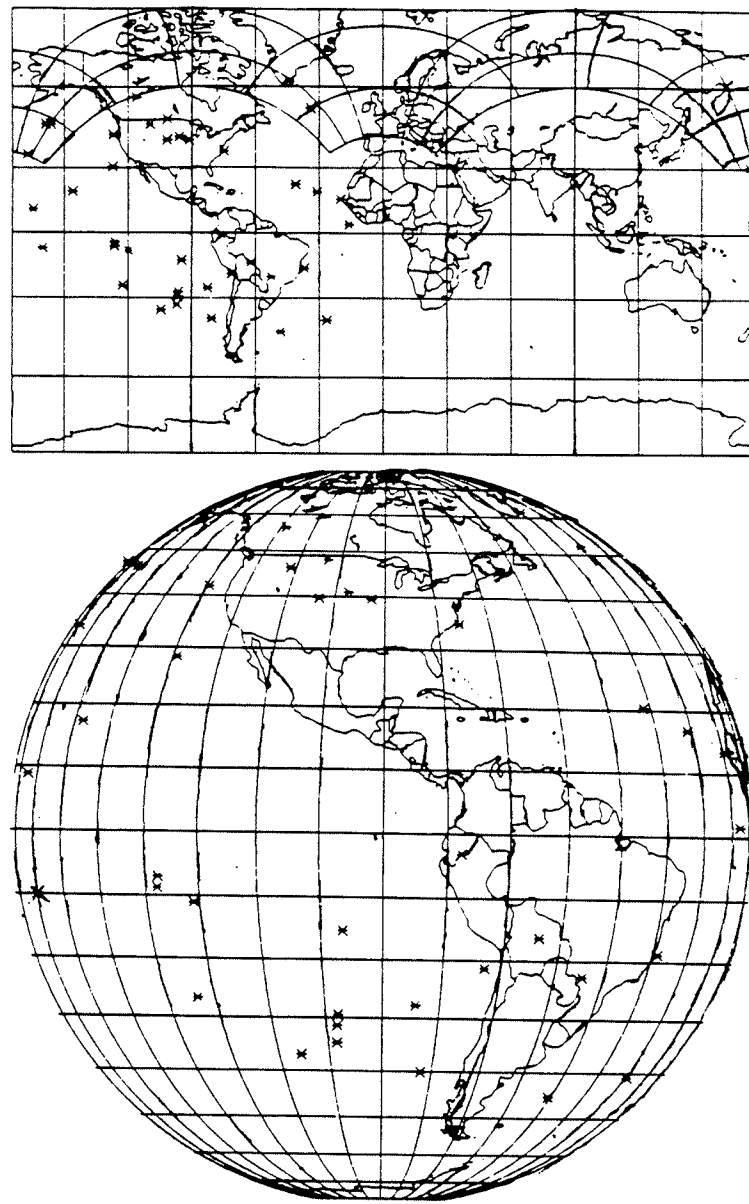


Figure 24: North pole positions determined by using conventional methods. This is the plot of the pole positions that were determined using currently popular statistical methods in palaeomagnetic analysis. As is clear from this plot, that the data set shows a great deal of dispersion. Although further criterion could be applied to remove many of the poles in this set, the fact remains that at best, there will be very few observations that would support any one pole position.

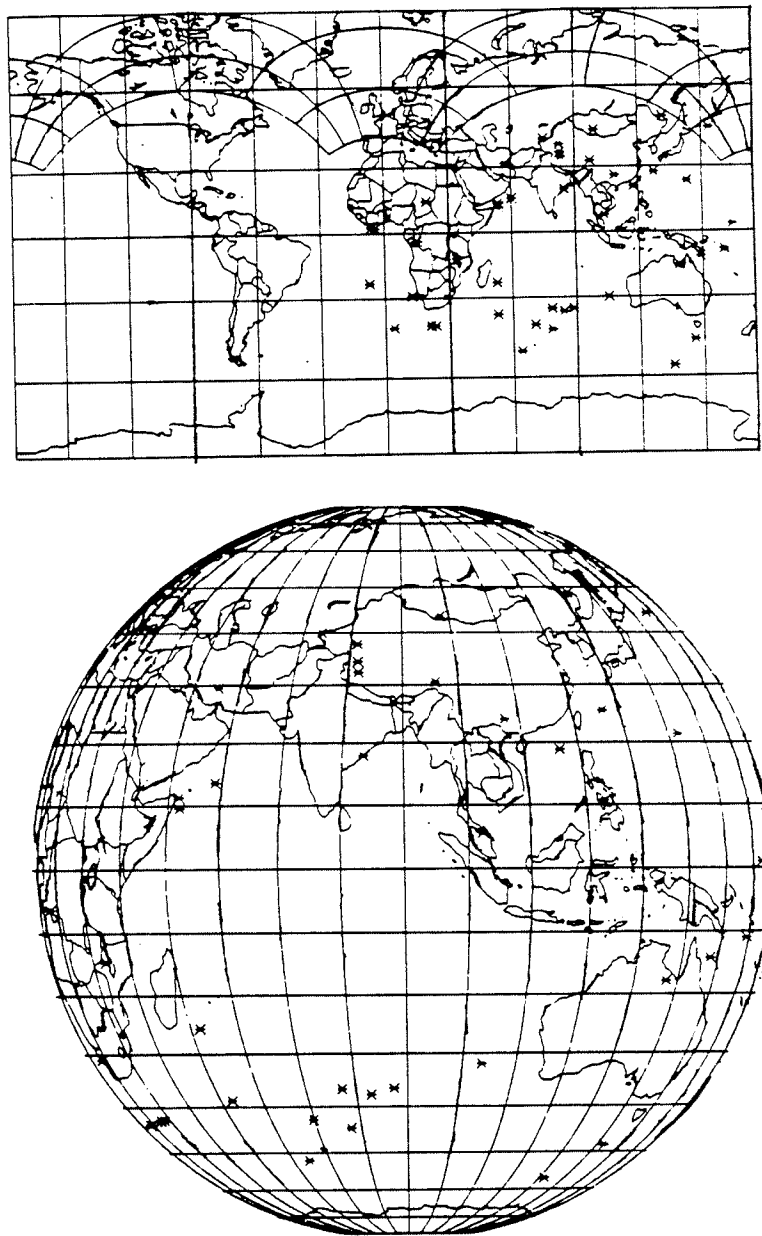


Figure 25: South pole positions determined using conventional methods. This is the plot of the south pole postions that were determined using conventional palaeomagnetic techniques.

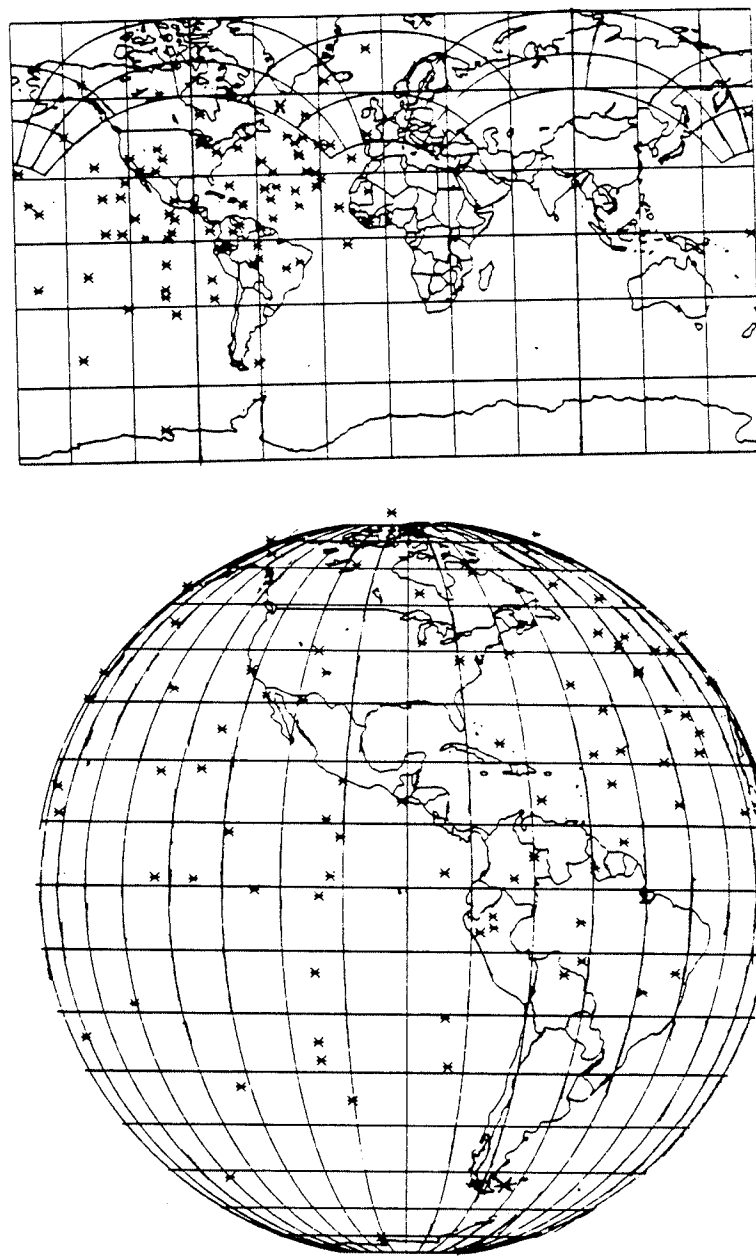


Figure 26: North pole positions for CNVL analysis using unit weight over the full spectrum.

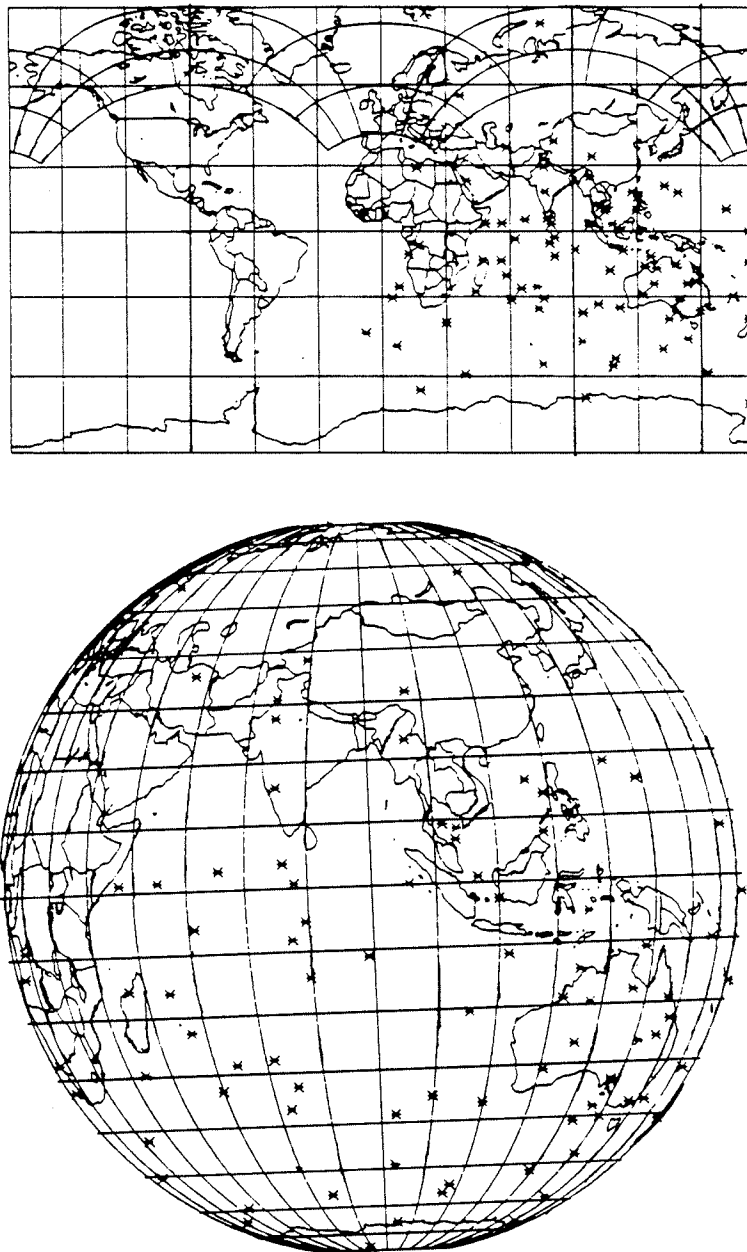


Figure 27: South pole positions for CNVL analysis using unit weight over the full spectrum. The data indicates a great deal of dispersion in the magnetization. The dispersion follows a linear trend that is consistent for all the remanences. It is clear that the dispersion in this set does not clearly identify a particular pole position.

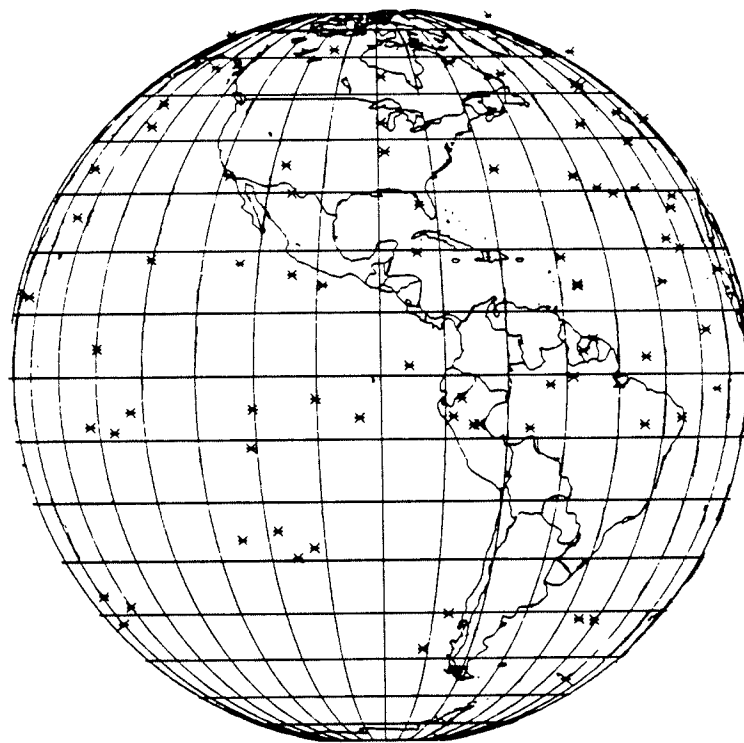
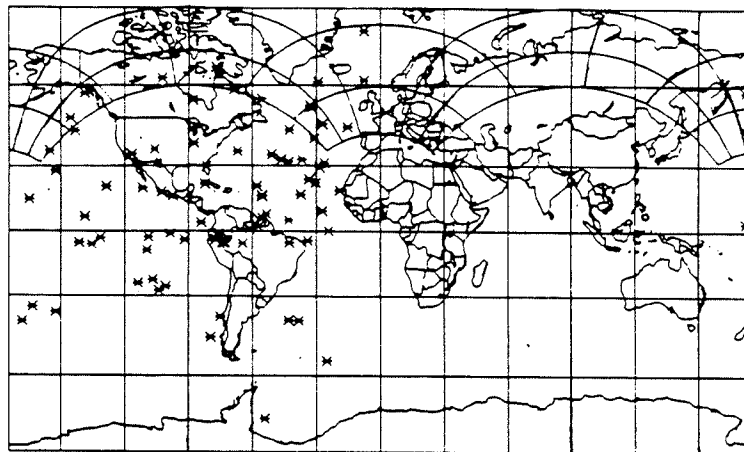


Figure 28: North pole positions for DGTL analysis using unit weight over the full spectrum. This is the plot of the full spectrum. It is clear that the dispersion in this set does not clearly identify a particular pole position.

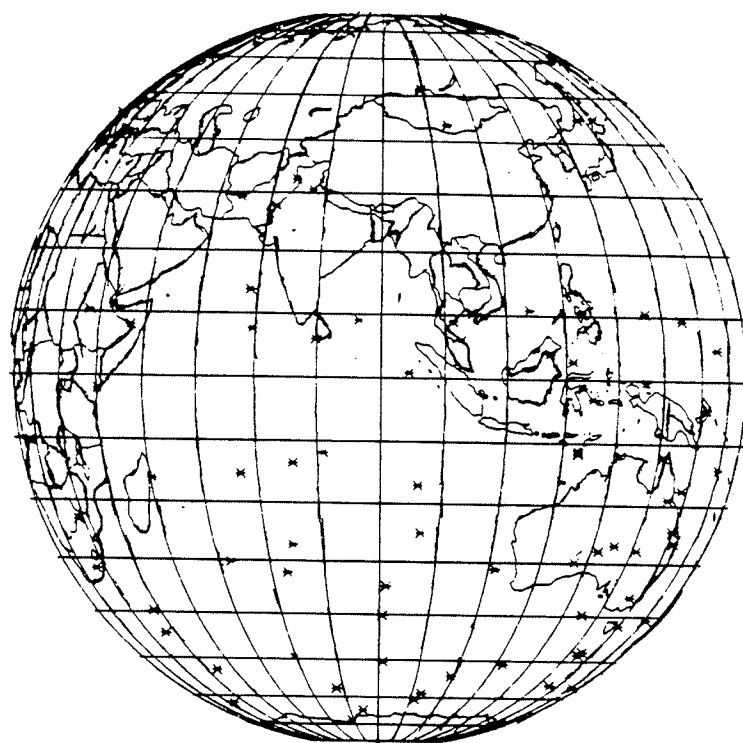
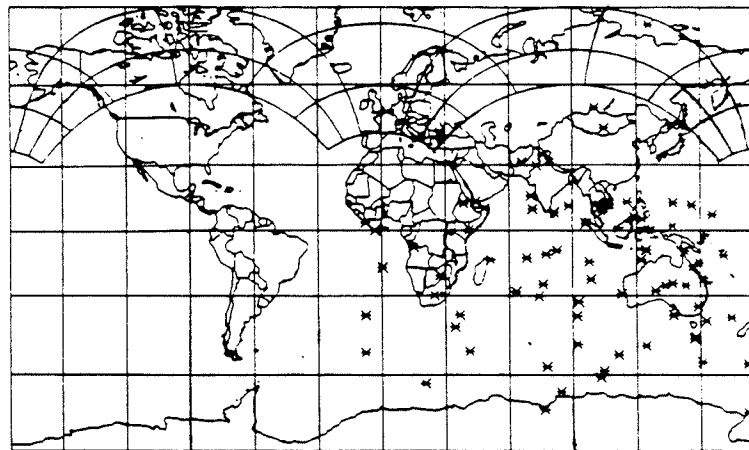


Figure 29: South pole positions for DGTL analysis using unit weight over the full spectrum. This is the plot of the full spectrum. It is clear that the dispersion in this set does not clearly identify a particular pole position.

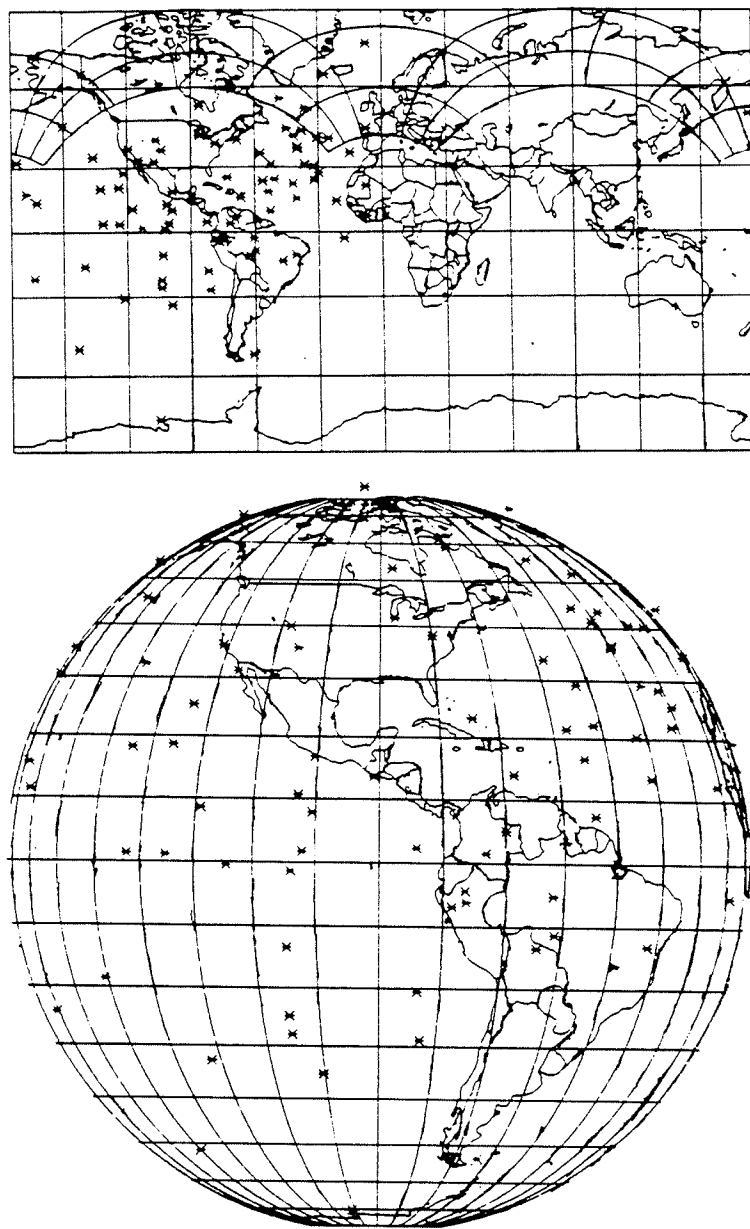


Figure 30: North pole positions for CNVL analysis using magnitude weight over the full spectrum. This is the plot of the full spectrum. It is clear that the dispersion in this set does not clearly identify a particular pole position.

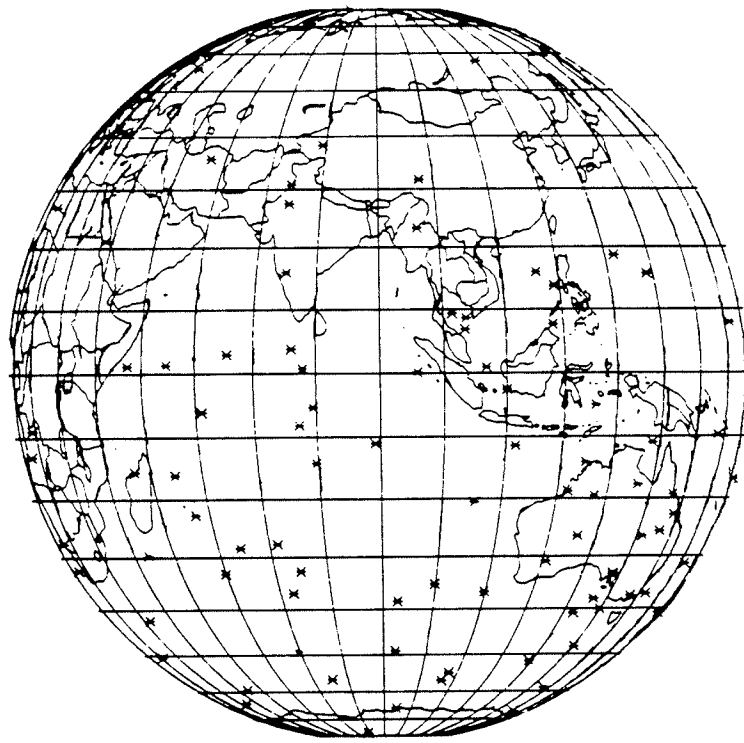
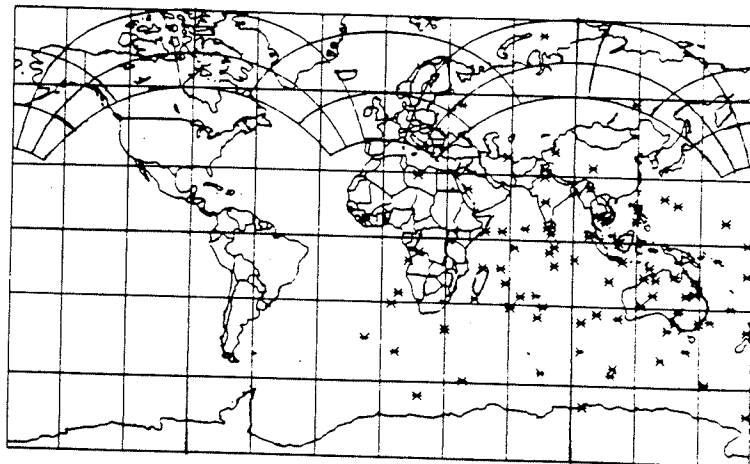


Figure 31: South pole positions for CNVL analysis using magnitude weight over the full spectrum. This is the plot of the full spectrum. It is clear that the dispersion in this set does not clearly identify a particular pole position.

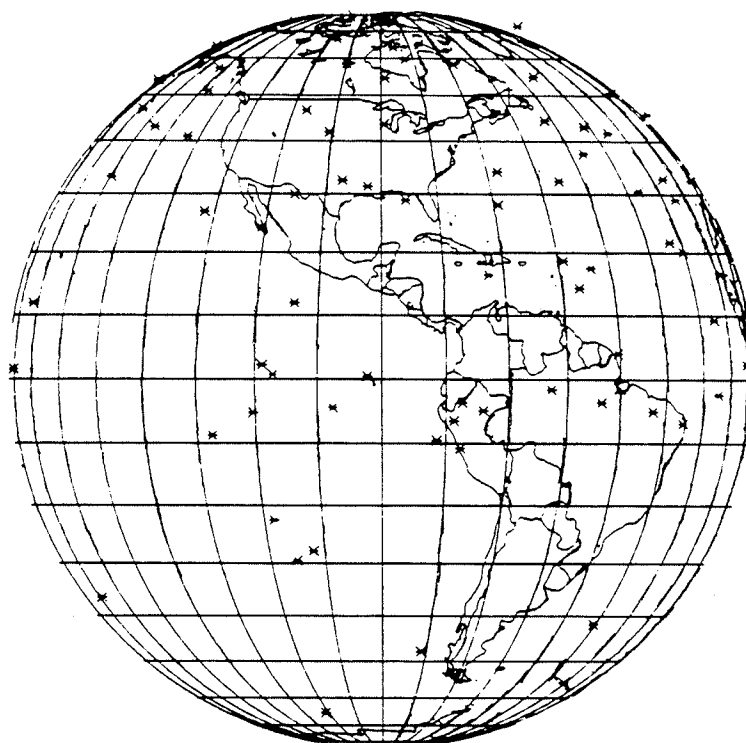
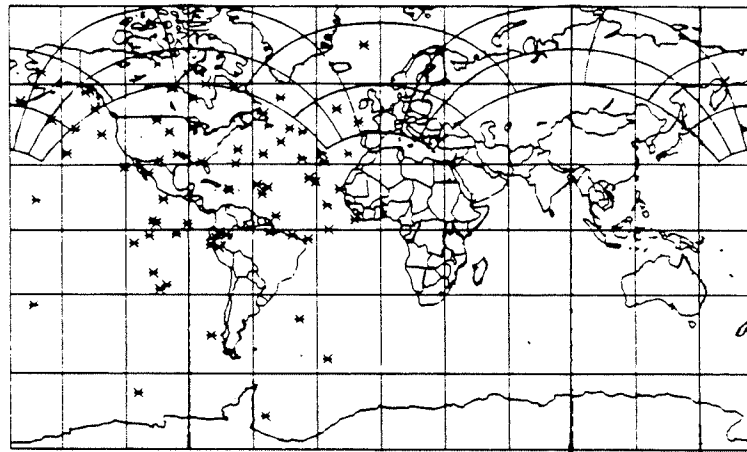


Figure 32: North pole positions for DGTL analysis using magnitude weight over the full spectrum. This is the plot of the full spectrum. It is clear that the dispersion in this set does not clearly identify a particular pole position.

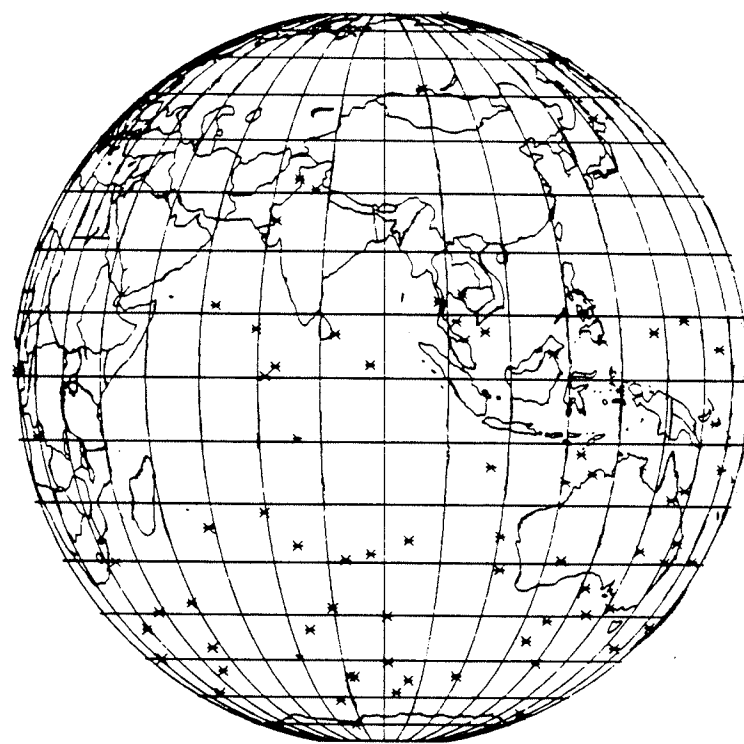
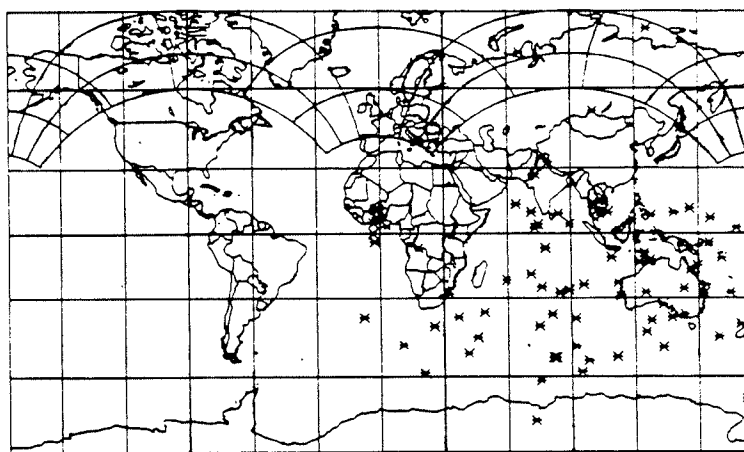


Figure 33: South pole positions for DGTL analysis using magnitude weight over the full spectrum. This is the plot of the full spectrum. It is clear that the dispersion in this set does not clearly identify a particular pole position.

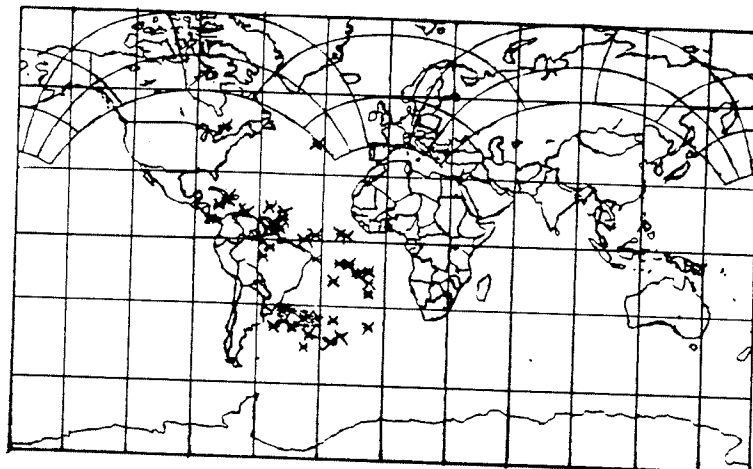


Figure 34: North pole positions for digital analyses using magnitude weight over the reduced spectrum. This plot is the north pole positions for the DGTL analysis.

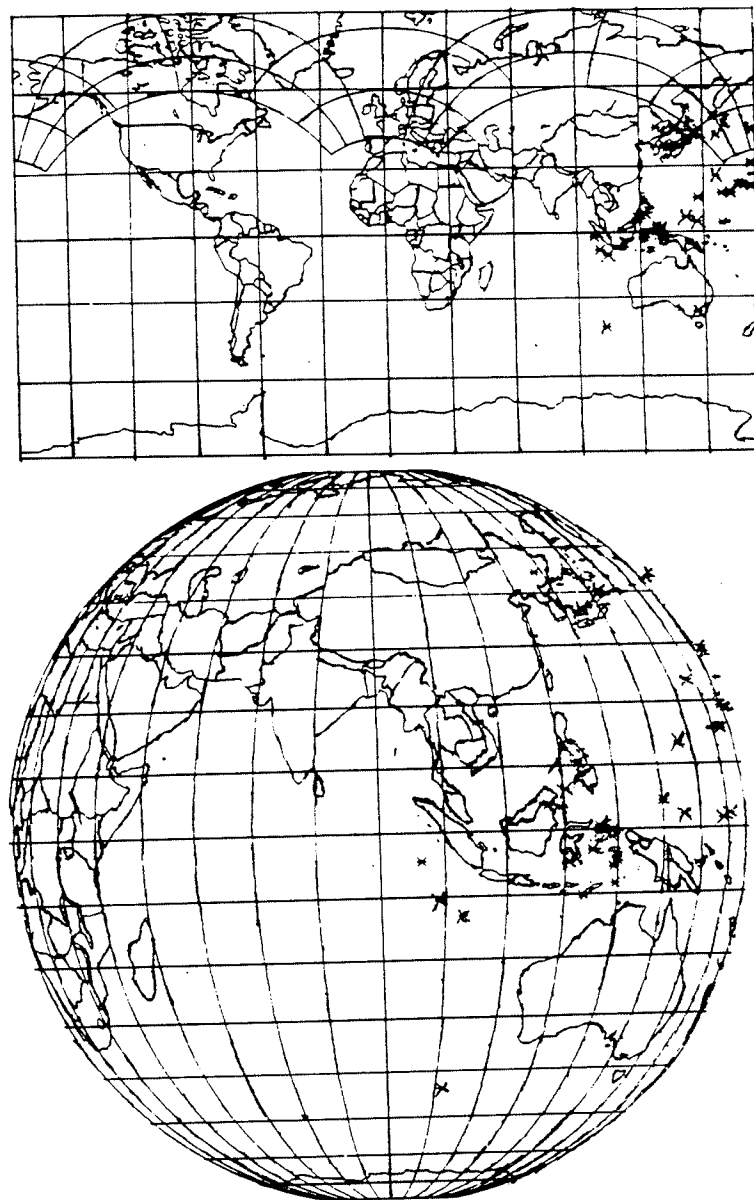


Figure 35: South pole positions for digital analysis using magnitude weight over the reduced spectrum. This representation of the south poles is important in considering the presence of reversals as indicated by a sample set. Where these poles correspond to the polar wandering path, after consideration of rotational influences that have been recognized it is possible to interpret the remanence as having been imposed during a period of reversed orientation of the dipole field.

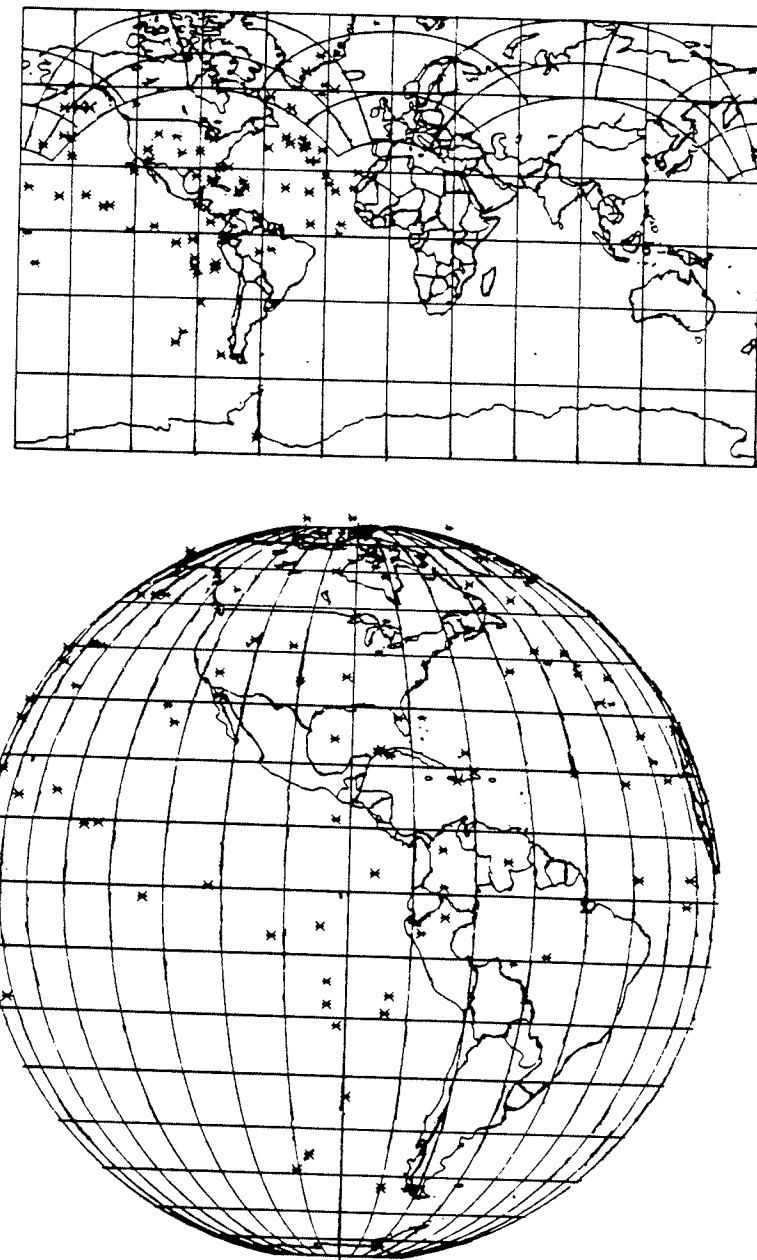


Figure 36: North pole positions for CNVL analysis using magnitude weight over the reduced spectrum.

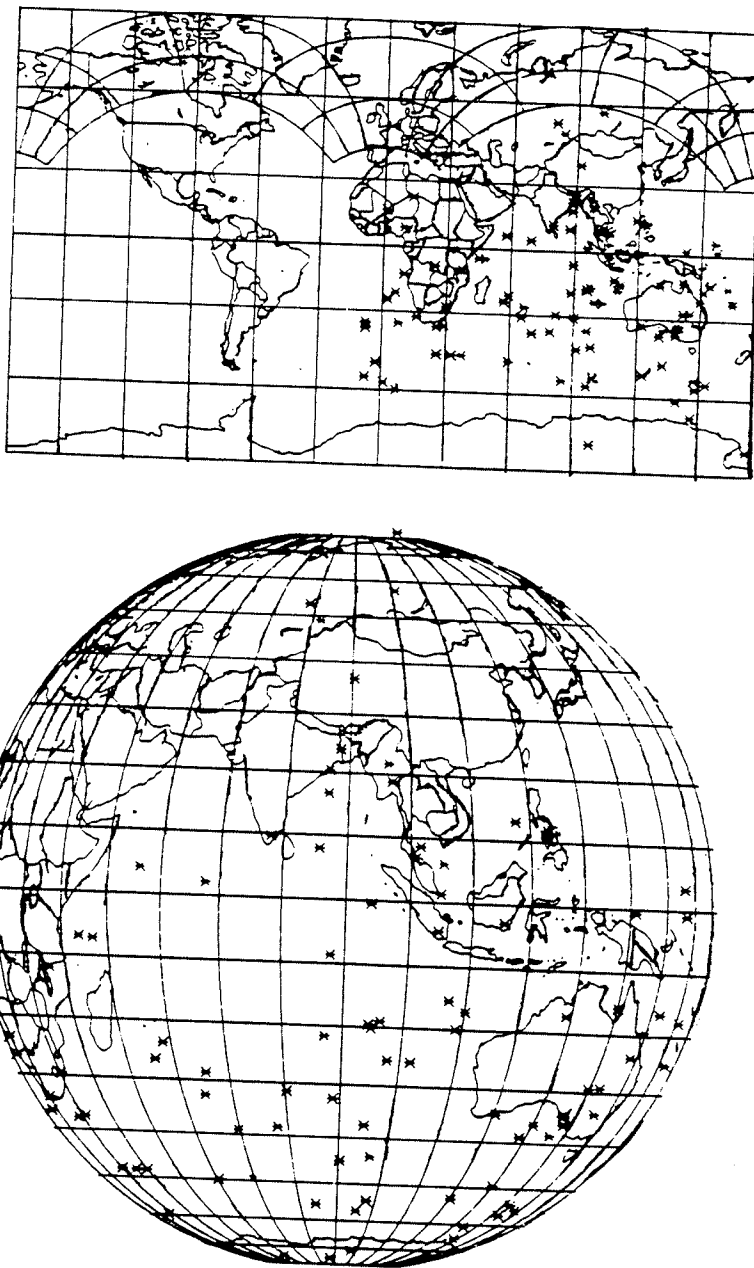


Figure 37: South pole positions for CNVL analysis using magnitude weight over the reduced spectrum.

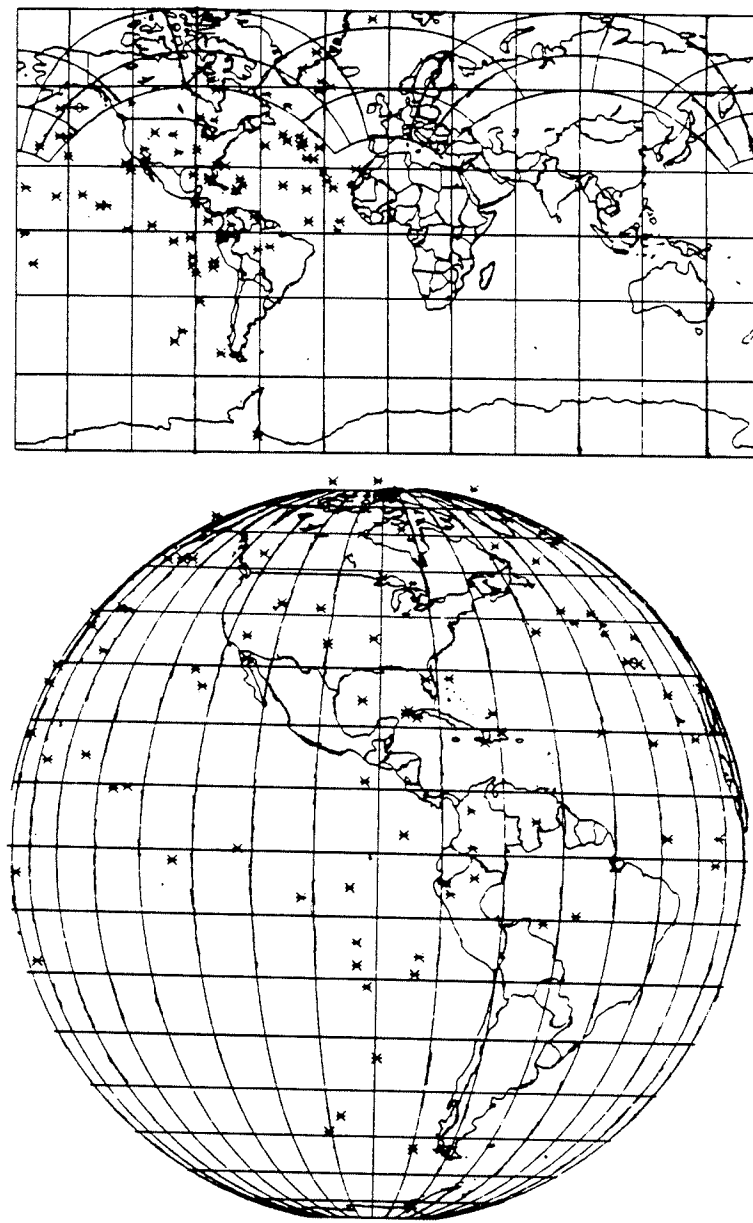


Figure 38: The North pole positions for CNVL analysis, using unit weight and the reduced spectrum. The weighting scheme, used unit weight. The positions correspond to the apparent north position as determined from each sample, in the sample set available to this author.

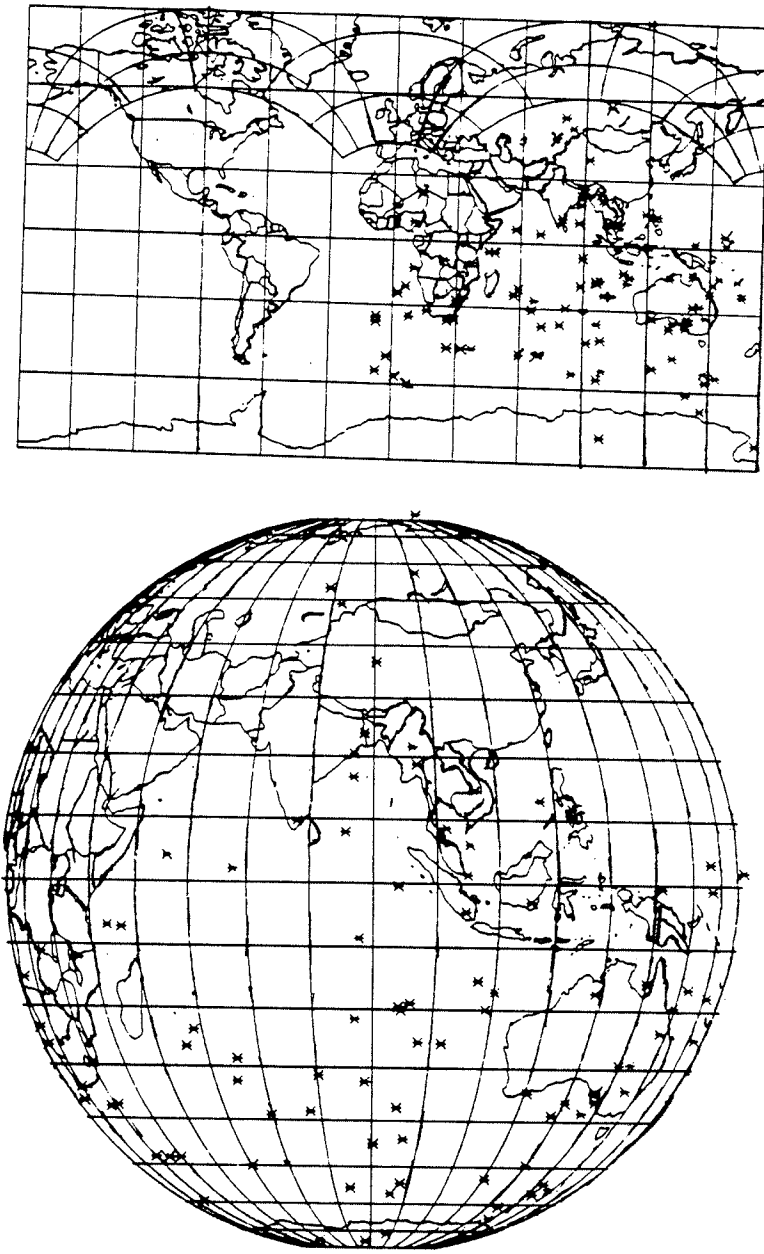


Figure 39: South pole positions for CNVL analysis using unit weight over the reduced spectrum.

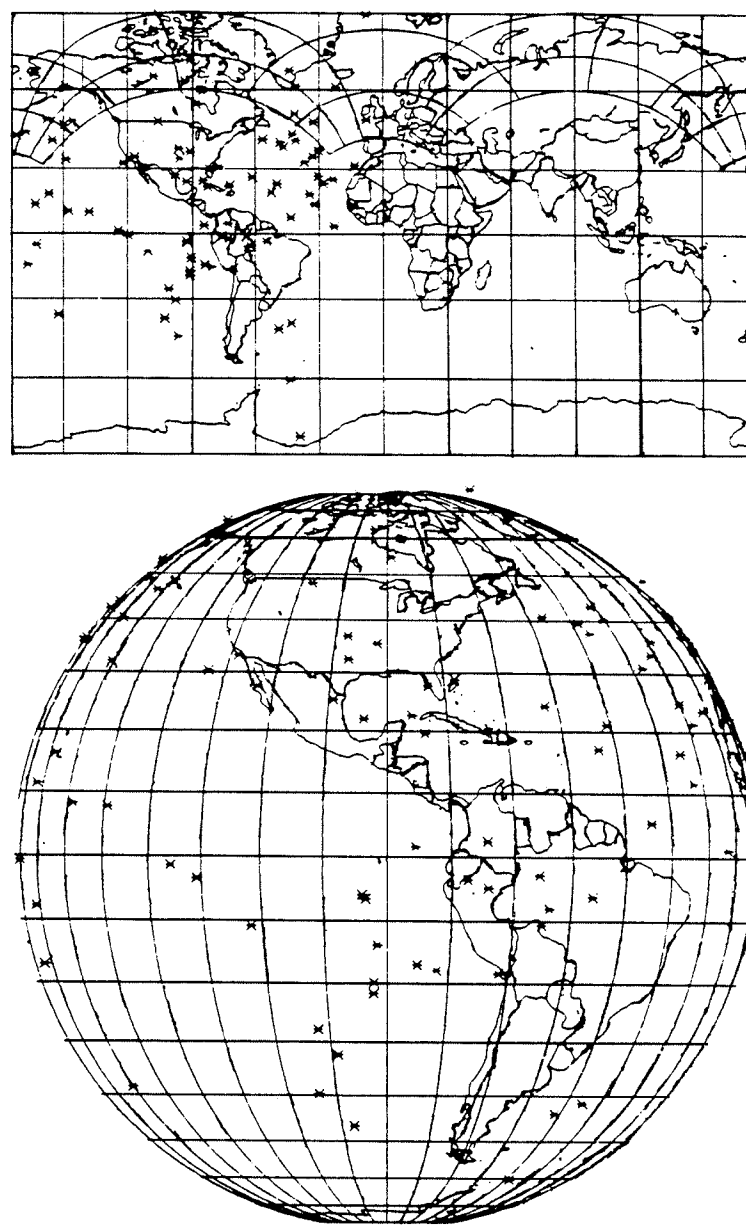


Figure 40: North pole positions for digital analysis using unit weight over the reduced spectrum.

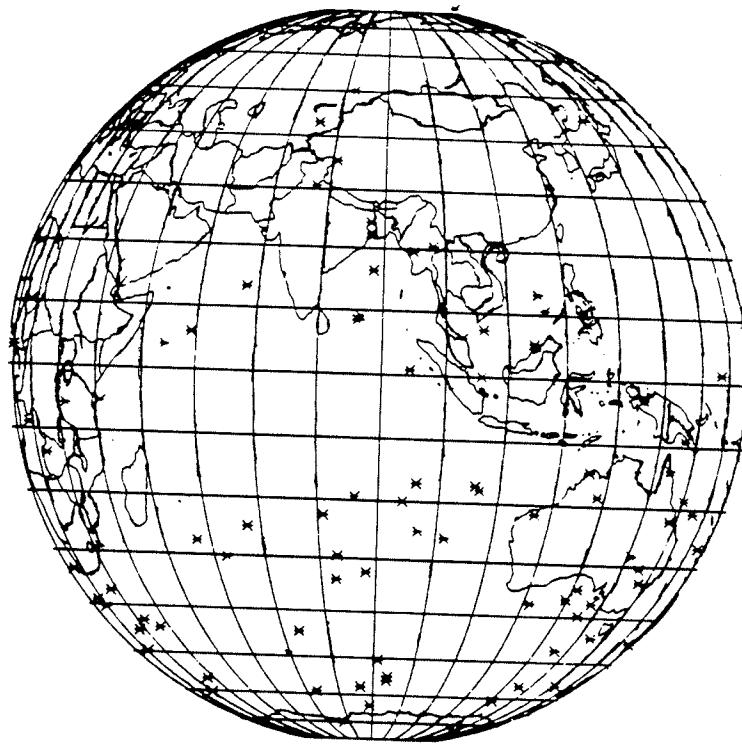
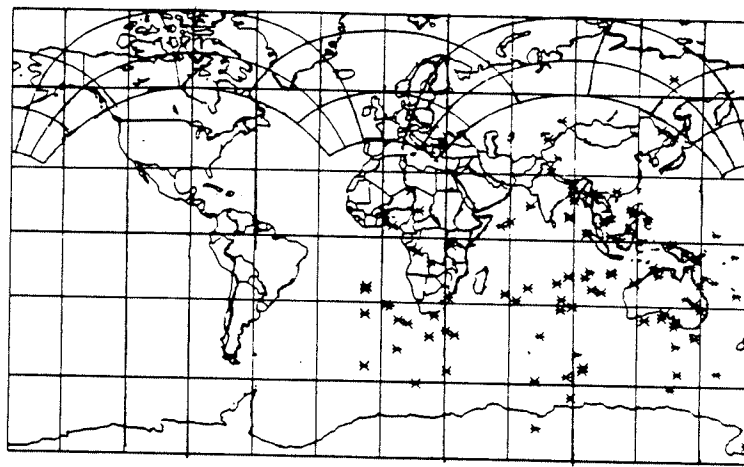


Figure 41: South pole positions for digital analysis using unit weight over the reduced spectrum.

Chapter VIII

DISCUSSION OF RESULTS

The results obtained by the different approaches has produced apparently contradictory results. The question is; "Are these discrepancies due to errors in the logic of the analysis, or are they interpretable as significant information?" If each is carefully considered, then it appears that all poles produced are significant.

The poles produced by conventional analysis, and those produced by weighting the magnetization vectors with unit values, complement each other with only very little discrepancy. The particular problem encountered in the poles indicated by these methods is that there has been a large amount of dispersion of the remanence direction. This problem is partially circumvented by the new approach since it utilizes more samples in determining the remanences, so potentially it provides more confidence in the final result.

The significance of using values selected as stable end points from demagnetization vector plots is that these values are characterized by being at higher cleaning field strengths in the spectrum. The magnitude of the values are characteristically low when compared to values measured at lower cleaning fields.

By choosing to weight the demagnetization observations as unit value, the influence of the later values in the spectrum is heightened. This emphasizes the components which are contained in the sample set and in the individual samples, which are more stable.

By using magnitude weight the components at low cleaning field strength are emphasized. These will be the stronger, softer components contained in the samples.

It appears by the results obtained in this analysis that the approach using unit weight produces poles that are of a lower magnitude of magnetization and more stable. This applies to the region of the spectrum being considered. This suggests that they are poles that are older. This conclusion is supported by the observation that the poles have undergone a great deal more dispersion about the mean value.

By using magnitude weight, the stronger, softer component is emphasized. This suggests a younger remanence produced by thermal conditions less severe than that of the older remanences. The conditions responsible for the younger poles would have imposed secondary remanence on the rock without completely rewriting the magnetic characteristics of the rock.

It is important to consider the influence of more stable remanences on the measurements obtained from the lower ranges of the demagnetization spectrum. If the magnitude of the magnetization at these lower ranges are great enough, then their values will dominate the final reading. Fisher statistics is not immune to this same problem. If we choose a sample as being "good" because it has shown itself to be stable over the range of the instrumentation, or because the remanence appears to be hard enough as to be due to thermal origins and not viscous in nature, then what is there to say that a remanence beyond the range of the instrumentation, and so not exposed, is not influencing the final result?

Three poles show a high degree of dispersion that takes on a linear distribution. This would be expected of samples that have been folded about a single axis. The one folding event was responsible for the dispersion of all the poles.

It is clear that conventional analysis fails to resolve and reveal interpretable information from this data set. The dispersion influencing it has had this effect. However, there is accurate information based upon the geological history of the area included in this set. A more powerful tool was necessary for confident evaluation.

The methods CNVL and DGTL, allow interpretation of this data set. It appears that there have been a total of three pole positions that have been smeared in a linear fashion; all in an exactly similar manner. This dispersion indicates a period of folding subsequent to the imposition of these remanences. The axis of folding has a north by north-east strike. Such a folding configuration has been mentioned in geological reports in this region (Taylor, 1978).

The Hudsonian orogeny was the latest significant metamorphic event to influence the area. Geochronological studies indicates that the earliest period of this occurring would be about 1.9 Ga. If the pole reported by Park (1975), and interpreted in this data, corresponds to the earliest events associated with the Hudsonian orogeny, then rotation to allow for this discrepancy orients the other two poles identified in these results to correspond with earlier events.

The DGTL plot with unit weight identifies three other poles unique from the other methods. Their position in the polar wander path, and the lack of dispersion characteristic of the other three poles, indicate this. Their location on the polar wander path corresponding with the Hudsonian orogeny indicate that the Churchill Superior boundary was effectively sutured after the early Hudsonian. The early Hudsonian included spreading and folding events. It appears that this time period was characterized by periodic metamorphic events, with three unique time periods characterized by a significant increase in this activity.

There is controversy regarding the APWP where it passes over the northern part of South America. The time period associated with this portion of the path includes the time period in which the Hudsonian orogeny had it's influence. Authors had identified a motion in a loop fashion, referring to it as the "Coronation Loop". The data results of this study seem to confirm this interpretation as far as the configuration of the poles is concerned. However, identification of the age of the component remanences is necessary to unequivocally verify whether or not the path actually crosses itself. The pole locations do indicate that there was a substantial deviation of the path, from the general trend at that time.

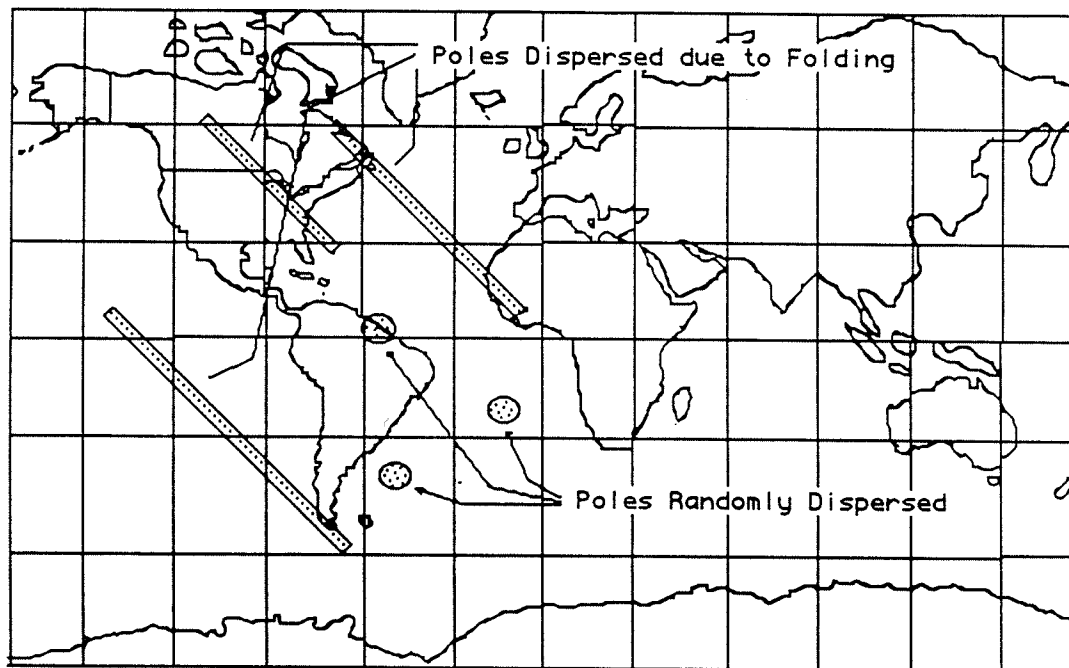


Figure 42: The Distributions of significant palaeomagnetic poles. This figure contains significant trends in the palaeomagnetic data set. As can be clearly seen, there are six pole positions readily interpreted from all analysis done so far. The three oldest poles are dispersed along a linear axis due to a folding event. The three youngest pole have been dispersed in a manner that can be expected from experimental error and inhomogeneities in the samples themselves.

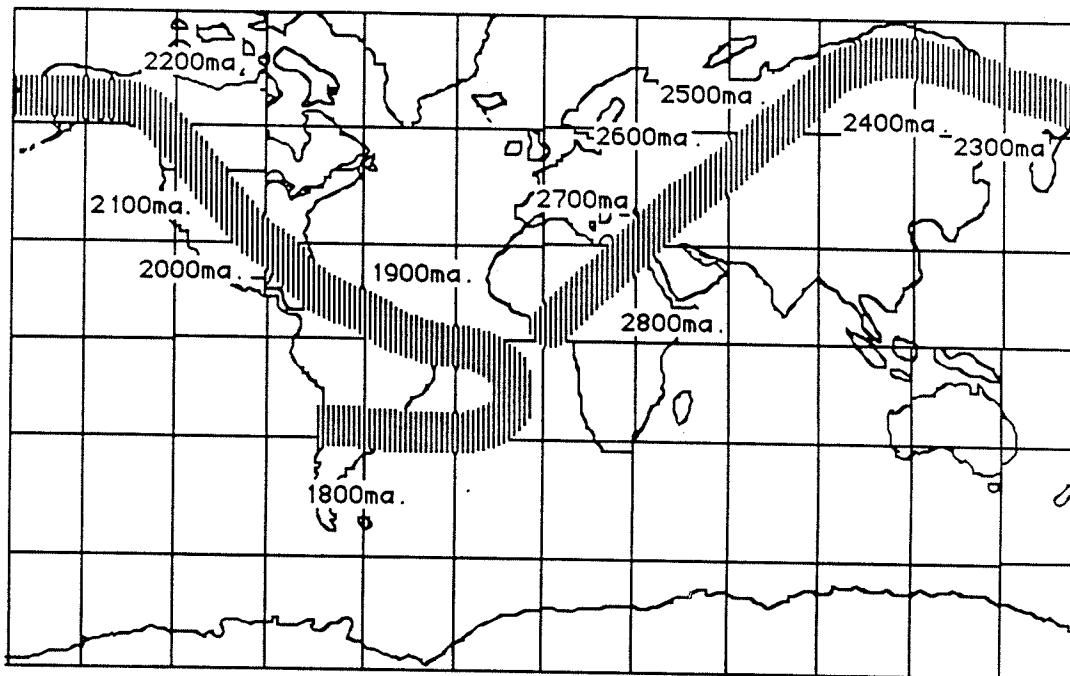


Figure 43: Apparent polar wander path. This figure contains an apparent polar wander path as has been constructed from the results of the literature and of this study (Kahn, 1982, Dunlop, 1984). It is currently very dangerous to consider these paths since there is little understanding of the plate boundaries that were active during the Pre-cambrian. This author also feels that the methods currently in wide use in palaeomagnetic analysis are highly inadequate. This polar wandering path is presented as a indication of the trends that the true path does take. There can be no certainty of the confidence in this path, however, as is usual for such representations, the path is given a width to indicate errors.

8.1 Consistency within Sites

Possibility of correlating rock units with pole groupings was considered as part of this study. This list was compiled using maps 71-2-5, 71-2-2, 71-2-6, and 71-2-11 provided by Manitoba Energy and Mines. The results are contained in Table 3

As can be clearly seen by these results, there is no apparent correlation. This introduces a very perplexing problem. Is it accurate to have faith in these results and these new methods, when this inconsistency is considered? Certainly, in consideration of current ideals it is not possible since such consistency is a necessary requirement for acceptance. However, conventional methods are not very efficient in handling multiple components in single samples. It is possible that due to the varying physical properties of the rock samples themselves, unique poles express themselves at variable cleaning conditions. Consistency within the cores themselves is far from perfect. This can be explained by overlapping of pole positions, which makes it difficult to associate samples to a particular cluster. This is supported by the fact that in the case of the DGTL method, consistency does improve. If these new approaches prove superior to current methods as the results of this study seem to indicate, it is necessary to re-examine the current premises by which palaeomagnetic results are studied (certainly for Precambrian terraines).

Table 3: Pole Groupings

This table contains the clustering of poles as was determined from the DGTL (magnitude weight, reduced spectrum-set one), and the CNVL (unit weight, reduced spectrum-set two) methods. The numbers one to three correspond to (3° S, 105° W), (30° S, 30° W) and (55° N, 100° W) for set one. For set two, the identifiers one to three correspond to the poles at (3° N, 55° W), (22° S, 15° W) and (40° S, 50° W).

Sample	Set One	Set Two
800 1A	1	1
2A	1	1-2
3A	3	1
801 1A	3	2
2A	3	1
3A	3	3
802 1A	3	1-2
2A	3	1-2
3A	n/a	1-2
803 1A	3	1-2
2A	3	1
3A	3	1-2
804 1A	3	1
2A	1	1
3A	3	1
805 1A	3	3
2A	1	3
1B	2	1-2
2B	2	3
3B	3	2
806 1A	n/a	3
3A	3	2
807 1A	2	2
2A	1	3
3A	2	1
808 1A	1	1
2A	2	n/a
3A	2	n/a
809 1A	2	1
2A	2	2
3A	2	1-2
810 1A	2	1-2
2A	2	2-3
3A	3	3
811 2A	1	1
812 1A	1	3
2A	1	1-2
3A	1	2
813 1A	1	1
2A	1	2
3A	2	2
814 1A	1	2-3
2A	3	1-2
3A	3	2
845 1A	2	2
2A	1	1
3A	1	2
846 1B	1	n/a
3B	2	3
849 3A	3	1
850 1B	3	2
2B	3	n/a
3B	1	n/a

Sample	Set One	Set Two
851 1B	3	3
2B	1	n/a
3B	1	3
1A	2	n/a
2A	2	n/a
3A	2	2
852 1B	3	2-3
2B	2	3
3B	3	1
1A	1	n/a
2A	1	n/a
3A	2	2-3
855 1A	3	n/a
2A	3	2
3A	1	3
2B	2	1
3B	1	1
856 2A	2	3
3A	1	3
856 2A	2	3
3A	1	3
1B	2	2-3
2B	2	2
3B	2	3
857 1A	1	1
2A	1	3
1B	2	n/a
2B	2	3
3B	2	3
860 2A	1	1
3A	n/a	3
860 2A	1	1
3A	n/a	1
861 1A	2	2-3
2A	2	n/a
3A	2	2
862 1A	3	n/a
2A	3	2
3A	3	2
1B	1	2
2B	2	2
3B	3	1
865 1A	1	1
2A	1	1
868 1B	2	3
3B	1	3
869 1B	3	2
2B	2	n/a
3B	1	1

8.2 Conclusions

When using conventional analysis, the results were very questionable due to the dispersion of the remanence and the quality of the sample set. In order to obtain better results, the analysis required the development of new and more effective statistical methods. One new approach used digital processing. The results produced by both methods developed in this study produced excellent results.

A total of six poles are indicated from methods that were used. Those poles are located at 20° S and 105° W, 30° S and 30° W and 25° N and 100° W for all methods, while the digital method indicated a further three poles at 3° N and 55° W, 22° S and 15° W and 40° S and 50° W. The pole located at 55° N and 100° W is identical to positions reported in the literature. It is indicative of the occurrence of a period of motion between the Superior and Churchill cratons. This conclusion is based on discrepancies between the older pole positions and the polar wandering paths that are currently available. In order to account for these results, the best interpretation states that spreading motion had rotational action.

Three poles produced by the digital analysis follow very close to those expected for the polar wandering path. This leaves very little room for any interpretation regarding the motion of these cratons after these remanences were imposed. If the results which were produced by this method are to be accepted, then the close grouping of these remanences gives great confidence in their positions. In fact they indicate a greater confidence in these mean positions than those produced by conventional analysis.

The interpretation which states that six apparent polar positions are contained in this sample set, is very attractive. Each could correspond to a separate metamorphic event. The dispersion affecting the oldest three poles is due to a folding event which occurred during the early Hudsonian Orogeny. This event is also reported in the literature. The positions of these poles on the polar wander path, indicate that soon after, or even during the period of folding, the cratons were undergoing relative motion.

REFERENCES CITED

- Arfken, G. (1970) Mathematical Methods for Physicists. New York: Academic Press.
- Baldwin, D.A., E.C. Syme, H.V. Zwanzig, T.M. Gordon, P.A. Hunt, and R.D. Stevens. (1985) "Zircon Ages From the Lynn Lake and Rusty Belts, Manitoba: Two ages of Proterozoic Magmatism." GAC-MAC, Joint annual meeting.
- Barry, G.S., and R.I. Gait. (1966) "Geology of the Suwannee Lake Area." Man. Mines Br. Pub., 64-2.
- Beck, M.E. (1970) "Palaeomagnetism of Keweenawan Intrusive Rocks, Minnesota." J. Geophys. Res., 75-6, 4985-4996.
- Bevington, P.R. (1969) Data reduction and error analysis for the physical sciences. New York: McGraw-Hill.
- Bingham, D.K., and M.E. Evans. (1976) "Paleomagnetism of the Great Slave Supergroup, Northwest Territories, Canada; the Stark Formation." Can. J. Earth Sci., 13, 536-578.
- Biot, M.A. (1970) Variational Principles in Heat Transfer. London: Oxford Press.
- Bullard, E.C., C. Freedman, H. Gillman, and J. Nixon. (1950) "The Westward Drift of the Earth's Magnetic Field." Phil. Trans. Roy. Soc. London, A243, 67-92.
- Burke, K., J.F. Dewey, and W.S.F. Kidd. (1976) "Precambrian Paleomagnetics and the Contemporary Operation of the Wilson Cycle." Ancient Plate Margins Tectonophysics, ed. J.C. Briden. New York: John Wiley and Sons.
- Cavanaugh, M.D. (1977) "Apparent polar wander paths and the joining of the Superior and Slave provinces during early Proterozoic time." Geology, 5, 207-211.
- Chevallier, R. (1925) "Laimantation des laves de l'Etna et L'orientation du champ terrestre en Sicile." Ann. Phys., 4, 5.
- Clark, G. (1980) "Rubidium-Strontium Geochronology in the Lynn Lake Greenstone Belt: Northwestern Manitoba." Man. Mines Br. Pub., GP80-2.

- Collinson, D.W. and K.M. Creer. (1967) Methods and Techniques in Geophysics. New York: McGraw-Hill.
- Collinson, D.W., K.M. Creer, E. Irving, and S.K. Runcorn. (1957) "The measurement of the permanent magnetism of rocks." Phil. Trans. Roy. Soc. London, A250, 73-82.
- Commodore 64 User's Guide. (1983) Indianapolis: Howard W. Sans and Co. Inc.
- Cox, A. (1969) "Geomagnetic Reversals." Science, 163, 237-245.
- Cracknell, A.P. (1975) Magnetism in Crystalline Materials. Toronto: Pergamon Press.
- Creer, K.M. (1962a) "A Statistical Enquiry into the Partial Remagnetization of Folded Old Red Sandstone Rocks." J. Geophys. Res., 67-5, 1899-1906.
- Creer, K.M. (1962b) "The Dispersion of the Geomagnetic Field due to Secular Variation and its Determination for Remote Times from Paleomagnetic Data." J. Geophys. Res., 67-9, 3461-3476.
- Creer, K.M., E. Irving, and A.E.M. Nairn. (1959) "The Paleomagnetism of the Great Whin Sill." Geophys. J., 2, 306-323.
- Doell, R.R. (1969) "Secular variations in the central Pacific during the last 10,000 years." Am. Geophys. Union Trans., 50-4, 129.
- Duckworth, H.E. (1965) Electricity and Magnetism. New York: Holt, Rinehart and Winston.
- Duffett-Smith, P. (1981) Practical Astronomy with your Calculator. Cambridge: Cambridge University Press.
- Dunlop, D.J. (1979) "A Regional Paleomagnetic Study of Archean Rocks from the Superior Geotraverse area, northwestern Ontario." Can. J. Earth Sci., 16, 1906-1919.
- Dunlop, D.J., L.D. Schutts, and J. Hale. (1984) "Paleomagnetism of Archean Rocks from Northwestern Ontario: 3. Rock Magnetism of the Shelley Lake Granite, Quetico Subprovince." Can. J. Earth Sci., 21, 879-886.
- Engle, A.E.J., S.D. Itsin, C.G. Engel, D.B. Stickney, and E.T. Cray. (1974) "Crustal Evolution and Global Tectonics: A Petrographic View." Geol. Soc. American Bull., 85, 843-858.
- Ermanovics, I., and W.F. Fahrig. (1975) "The Petrochemistry and Paleomagnetism of the Molson Dikes, Manitoba." Can. J. Earth Sci., 12, 1564-1575.

Evans, M.E., and D.K. Bingham. (1975) "Paleomagnetism of the Great Slave Supergroup, Northwest Territories, Canada: the Tochatwi Formation." Can. J. Earth Sci., 13, 555-562.

Evans, M.E., and D.K. Bingham. (1973) "Paleomagnetism of the Precambrian Martin Formation, Saskatchewan." Can. J. Earth Sci., 10, 1485-1492.

Fahrig, W.F., and A. Larochelle (1972) "Paleomagnetism of the Michael Gabbro and Possible Evidence of the Rotation of Makkevik Subprovince." Can. J. Earth Sci., 9, 1287.

Fisher, R.A. (1953) "Dispersion on a sphere." Proc. Roy. Soc., A-217, 295-305.

Frohlinger, T.G. (1979) "Hall Lake, Manitoba." Man. Mines Br. Pub., 78-3-4.

Fumerton, S.L., M.R. Stauffer and J.F. Lewry. (1984) "The Wathaman batholith: largest known Precambrian pluton." Can. J. Earth Sci., 21, 1082-1097.

Goldstein, H. (1950) Classical Mechanics. Don Mills: Wesley Publishing Co.

Gough, D.I. (1964) "A Spinner Magnetometer." J. Geophys. Res., 69-12, 2455-2463.

Green, A.G., Z. Hajnal and W. Weber. (1985) "An evolutionary model of the western Churchill Province and western margin of the Superior Province in Canada and the north-central United States." Tectonophysics, 116, 281-322.

Halls, H.C. (1976) "A Least-squares Method to Find a Remanence Direction From Converging Remagnetization Circles." Geophys. J. R. Astr. Soc., 45, 297-304.

Harrison, C.G.A., and E. Ramirez. (1975) "Areal coverage of spurious reversals of the Earth's magnetic field." J. Geomaq. Geoelect., 27, 139-151.

Hecht, E., and A. Zajac. (1974) Optics. Reading: Wesley Pub. Co.

Helsley, C.E. (1957) "Design of a Spinner Magnetometer." Phil. Trans. Roy. Soc. London, 250, 73.

Hide, R. (1966) "Free hydromagnetic oscillations of the Earth's core and the theory of the geomagnetic secular variation." Phil. Trans. Roy. Soc. London, A-259, 615-647.

Hinds, R.W. (1972) "Geology of the Opachuanau Lake-Fraser Lake-Lemay Island area." Man. Mines Br. Pub., 71-2G.

- Irving, E. (1964) Paleomagnetism and its Application to Geological and Geophysical problems. New York: Wiley and Sons.
- Kahn, S. (1982) "Palaeomagnetism of Archean Rocks from the English River and Uchi Subprovinces, North Western Ontario, and Polar Wandering Paths for North America." M.Sc. Thesis, University of Manitoba, unpublished.
- Kawai, N. (1955) "Instability of natural remanent magnetism of rocks." J. Geomag. and Geoelect., 6-4, 208-209.
- Kendrick, G. (1972) "Geology of the Turnbull Lake and Pemichigamau Lake Area." Man. Mines Br. Pub., 71-2E.
- Kirschvink, J.L. (1980) "The least-squares line and plane and the analysis of palaeomagnetic data." Geophys. J.R. Astr. Soc., 62, 699-718.
- Kittel, C. (1976) Introduction to Solid State Physics. Toronto: John Wiley and Sons.
- Lapointe, P.L., J.L. Roy, and W.A. Morris. (1978) "What Happened to the High Latitude Paleomagnetic Poles?" Nature, 273, 655-657.
- Larochelle, A. (1968) "Paleomagnetics of the Abitibi Dyke Swarm." Can. J. Earth Sci., 3, 671-683.
- Leeman, S. (1984) Mapping the Commodore 64. Greensboro: Compute Publications.
- Leibson, G. (1982) "The input/output primer; A look at one of the least understood interfaces -RS 232C- and one of the first instrument interfaces." Byte, May 1982.
- Lewry, J.F. (1981) "The age and geological history of the Wollaston, Peter Lake, and Rottenstone domains in northern Saskatchewan." Can. J. Earth Sci., 1, 178-180.
- Lewry, J.F., and T.I.I. Sibbald. (1980) "Thermotectonic evolution of the Churchill Province in northern Saskatchewan." Tectonophysics, 68, 45-82.
- Lewry, J.F., T.I.I. Sibbald and C.J. Rees. (1978) "Metamorphic patterns and their relation to tectonism and plutonism in the Churchill Province in northern Saskatchewan." Geol. Surv. Can., 78-10, 139-154.
- Lewry, J.F., T.I.I. Sibbald and D.C.P. Schledewitz. (1985) "Variation in character of Archean rocks in the western Churchill Province and its significance." Geological Association of Canada, 28, 239-261.

- Lewry, J.F., D.J. Thomas, K. Christopher and K. Roberts. (1981) "Geology of an area around Compulsion Bay Wollaston Lake; part of NTS area 64E NW." Report-Saskatchewan, Department of Mineral Resources, 205.
- Lorrain, P. and D. Carson. (1970) Electromagnetic fields and Waves. San Francisco: W.H.Freeman and Company.
- Loveday, R. (1971) Statistics. London: Cambridge University Press.
- Marx, A. (1983) "Interfacing with Parallel and Serial Ports." Computers and Electronics, Nov. 1983.
- McElhinny, M.W., and R.T. Merrill. (1975) "Geomagnetic Secular Variation Over the Past Five M.Y." Reviews of Geophys. and Space Phys., 13-5, 687-708.
- Miller, K.S. (1964) Multidimensional Gaussian distributions. New York: Wiley.
- Nagata, T. (1965) "Main Characteristics of Recent Secular Variation." J. Geomag. Geoelect., 17, 263-276.
- Neel, L. (1955) "Some Theoretical aspects of Rock Magnetism." Adv. Phys., 4, 191.
- Park, J.K. (1975) "Paleomagnetism of the Flin Flon-Snow Lake Greenstone Belt, Manitoba and Saskatchewan." Can. J. Earth Sci., 12, 1272-1290.
- Parkinson, W.D. (1983) Introduction to Geomagnetism. New York; Elsevier Science.
- Pugh, E.M. and E.W. Pugh. (1972) Principles of Electricity and Magnetism. Don Mills: Addison-Wesley Publishing Company.
- Ray, G.E. and R.K. Wanless. (1980) "The age and geological history of the Wollaston Peter Lake, and Rottenstone domains in northern Saskatchewan." Canadian Journal of Earth Sciences, 17, 333-347.
- Roy, J.L. (1983) "Paleomagnetism of the North American Precambrian: A Look at the Data Base." Precambrian Res., 19, 319-348.
- Sander, W.B. (1983) The Elementary Commodore 64. Reston: Reston Publishing Co. Inc.
- Schledewitz, D.C.P. (1972) "Geology of the Rat Lake Area." Man. Mines Br. Pub., 71-2B.
- Schmidt, P.W. (1982) "Linearity spectrum analysis of multi-component magnetizations and its application to some igneous rocks from south-eastern Australia." Geophys. J.R. Astr. Soc., 70, 647-665.

- Schomaker, V., J. Waser, R. Marsh, and G. Bergman. (1959) "To fit a plane to a set of points by least-squares." Acta.Cryst., 12, 600.
- Slater, P.N. (1980) Remote Sensing, Optics and Optical Systems. Reading Mass: Addison-Wesley Pub. Co.
- Sutton, J., and J.V. Watson. (1974) "Tectonic Evolution of Continents in Early Proterozoic Times." Nature, 247, 433-435.
- Tarling, D.H. (1971) Principles and Applications of Palaeomagnetism. London: Chapman and Hall.
- Taylor, J.R. (1978) "Structural Geology of the Sickle and Wasekwan Group, Mynarski Lake Manitoba." M.Sc. Thesis, University of Manitoba, unpublished.
- Uyeda, S. (1958) "Thermoremanent Magnetism as a medium of Palaeomagnetism with special reference to Reverse Thermoremanent Magnetism." Japan J. Geophys., 2, 1.
- Webb, R.H. (1969) Elementary Wave Optics. New York: Academic Press.
- Williams, D.E.G. (1966) The Magnetic Properties of Matter. New York: American Elsevier Publ. Co.
- Wilson, R.L. (1959) "Remanent Magnetism of Late Secondary and Early Tertiary British Rocks." Phil. Mag., 4, 750-755.
- Witten, I.H. (1983) "Welcome to the Standards Jungle; An in-depth look at the confusing world of computer connection." Byte, Feb. 1983.
- Zijderveld, J.D.A. (1967) "A.C. Demagnetization of Rocks: Analysis of Results." Developments in Solid Earth Geophysics, ed. D.W. Collinson, K.M. Creer and S.K. Runcorn. New York: Elsevier Publishing Co.

Appendix A

SUGGESTIONS ON UPDATING THE CURRENT MAGNETOMETER

The purpose of this appendix is to provide an outline for the conversion of the pdp 11/04 system currently in use at the University of Manitoba, from the Teletype DTE driver device, to a system that is driven by a Commodore 64. This system provides several advantages. First, since a 1541 disc drive can easily be added to the system, all output can be directly stored as it is obtained; thus, eliminating the need to type in the data as an intermediate step. The data can be processed directly by the Commodore, or it can be uploaded to the university's main frame (currently the Amdahl 5850) in a later step. The software could be made "smart" in the sense that options can easily be introduced to satisfy the needs of the operator. These options may include print-outs, interactive processing, etc.

The programming steps used here are Basic. Basic is able to work at rates up to 300 baud. This is satisfactory for the pdp 11/04. The necessary equipment was not available to this author to "set-up" a working system so the actual programming and "de-bugging" steps have not been done.

The C-64 has several features that make it attractive. Its power is more than adequate in this application and the price is low

(currently approximately \$329.) It is widely available and well serviced, with a wide range of peripherals and software. The 1541 disk drive (Device8), is currently priced at \$350., and provides an excellent data storage facility.

A.1 Commodore to PDP 11/04 Interface: The RS-232.

The RS-232 is a serial interface. Originally designed to handle modern devices, it has been altered in the past for application to various situations (for example, the RS-232C is software controlled).

The PDP 11 uses a "current loop" method for interfacing to the teletype. This particular method has gone through a period where it was out of vogue, although it is now making a comeback. The consequences of this, (Commodore uses a voltage signal) is that the RS232 needs a current to voltage adapter to handle this current configuration. The PDP 11/04 can be altered to a voltage system by swapping for the appropriate interface board, or simply tripping the appropriate internal switch.

The serial connector in the RS-232 has 25 pins. Of these, only three are used. They are pin 2, which transmits data; pin 3 which receives data; and pin 7, the logical ground. The configuration on the PDP 11/04 is; white=transmit(-), green=receive(-) blue=read(-), black=transmit(+), orange=read(+) and red=receive(+).

The Commodore contains the necessary software to emulate the operation of a 6551 UART chip. These program steps are located at \$293-\$297, and are accessed by the "opening" device2. The parame-

ters used in this communication process can be altered by changing bits located at these RAM locations.

The control register is located at \$293. The necessary parameters for use with the PDP 11/04 are:

- Bit 7: stop bits; 0=1 stop bit.
- Bits 6 through 5: word length; 01=7 data bits
- Bit 4: unused.
- Bit 3 through 0: Baud rate; 0110=300 Baud.

Locations \$298 to \$2A1 are used in this for the RS232. However, they do not directly concern the user. It is important to note that when the RS 232 is "opened", RAM \$293 to \$296 are set. Any variable previously contained here are rewritten. The user should open 2 before defining variables in order to avoid overwriting these locations.

The programming functions that are used, as far as the software is concerned, are the get print and print commands. Get is used to receive data from the RS-232, while print and print will send data to the screen and/or the 1541 disk drive. In order to avoid hanging the system up on a getcommand, register \$29B, (index to end of receive buffer) can be tested using the peek function against \$29C, (index to start of receive buffer) to see if data from the PDP 11/04 is being held. As far as the screen control is concerned, the key board at \$277 is monitored at \$C6 to determine if there is any data being input from the keyboard.

There are many good publications on the RS 232, and other interface devices, and on the Commodore 64. In particular, it is

suggested that the reader consult Marx (1983), Witten (1983), Leibson (1982), Leeman (1984), Sander (1983), and the Commodore 64 User's Guide (1983) for detailed information.

Appendix B

MAINFRAME ANALYSIS

The computer system at the University of Manitoba is an Amdahl 5850 (TSU 580) using an IBM 370 OS. The job control language on the system is JCL. This study used FORTRAN and SAS as the languages, along with the system packages CAM and CALCOMP routines. A certain degree of interaction between the processing and the operator was required so that it was not possible to create a one-step package. The result was a three-step procedure. CALCOMP routines produced a plot of the magnitude and vector path of the raw data from which the region of the spectrum which was cleaned of viscous remanence was selected by the user. In the second step, this region was replotted, plotted on the hemisphere projection using the SAS procedures, and then apparent poles were determined (along with confidence values). The resultant site of poles were then grouped into natural clusters and used to generate final apparent pole positions, (along with confidence values) in the third step.

B.1 Computer Analysis on the Amdahl at the University of Manitoba

B.1.1 CALCOMP and SAS Plotting

The following program is a multi-step procedure that produces the density distribution, the wave function distribution, the area of confidence, the magnetization spectrum and the magnetization vector plots. It also computes the apparent pole position for both methods developed here with the areas of confidences, magnitudes of the axes for poles that have not been corrected and poles that have been corrected using the sun sight postions. Required input is the components of the magnetization vectors as a function of the cleaning field, the standard deviation of each measure, the site latitude and longitude, correction factor from the sun sight data and the coring unit's orientation.

```

C This program takes the raw data that is generated from the
C PDP11/04 and determines the apparent pole position using
C conventional techniques and digital analytic techniques.
C This source file when driven by the JCL in file DRIVE produces
C a total of five plots. These plots are of the wave function
C distributions, the total probability, the half-maximum
C surface, the magnetization vector and the magnitude of the
C magnetization.
C The program writes the following intermediate and final
C calculations to defined data sets;
C FT10F001=Wave function distribution.
C FT21F001=Total wave function distribution.
C FT22F001=Half-maximum distribution.
C *These last three data sets are destroyed after execution*
C FT23F001=Mean value, written by updating the user defined dataset
C TSO.MEAN.
C FT24F001=Latitude and longitude (corrected and uncorrected) for
C digital techniques. Also included are the surfaces of confidence.
C These values are written to the user defined data set TSO.DGTL.
C FT16F001=Values of poles and confidences using conventional

```

C methods. Written to the user defined data set TSO.CVNL.
C FT17F001=The confidence area of the gaussian plot.
C The source code is compiled and link-edited using a simple
C series of JCL code and the object module is placed in the
C user defined data set LOAD(GO1).
C NPTS= First assignment to the number of measurements in a file.
C The second assignment is for the number
C Unique field strengths in the set of observations.
C X=West to East component of the measurement in the reference
C frame of the sample holder.
C Y=South to North component of the measurement in the reference
C frame of the sample holder.
C Z=Vertical component of the measurement in the reference frame
C of the sample holder.
C SX=Standard deviation associated with the X measurement.
C SY=Standard deviation associated with the Y measurement.
C SZ=Standard deviation associated with the Z measurement.
C T(L,K)=Array that contains the distribution of individual
C wave functions.
C TI(L,K)=Array that contains the total probability wave form.
C UM=Mean (X-component) value generated from the total
C probability distribution.
C VM=Mean (Y-component) value generated from the total
C probability distribution.
C D=Declination
C PI=Inclination
C SAZ=Azimuth of the core in situ (degrees)
C SDEC=Declination of the core insitu (degrees).
C SLONG=Site longitude (degrees).
C SLAT=Site latitude (degrees).
C CORR=Local deflection of the compass due to local magnetic
C conditions as determined from sun-sight (degrees).
C PLAT=Latitude position of the Apparent pole (degrees),
C uncorrected for sun-sight.
C PLONG=Longitude position of the Apparent pole (degrees),
C uncorrected for sun-sight.
C PLT=Latitude position of Apparent pole (degrees),
C Corrected for compass error.
C PLG=Longitude position of Apparent pole (degrees),
C corrected for compass error.
C BETA=Geomagnetic co-latitude.
C TMAG=Magnitude of the orientation vectors.
C PX,...,PSZ=Powers of the individual readings.
C IA=Sample identifier.
C M=Maximum cleaning field strength for reading.
C X2D,X2,Z2D,Z2=Arrays used in plotting.
C VAL=Maximum probability density.
C UM=X-value of the mean position.
C VM=Y-value of the mean position.
C ZM=Z-value of the mean position.
C DIMENSION X(40),Y(40),Z(40),M(40),PX(40),PY(40),PZ(40),
*TMAG(40),SX(40),SY(40),SZ(40),PSX(40),PSY(40),PSZ(40),T(100,60),
*TI(100,60),X2(40),X2D(40),Z2(40),Z2D(40),TM(40),TA(25)
COMMON/BLK1/X,Y,Z,PX,PY,PZ

```

COMMON/BLK2/SX,SY,SZ,PSX,PSY,PSZ
COMMON/BLK3/M
COMMON/BLK4/TMAG
COMMON/BLK5/T
COMMON/BLK6/TI
C   Read in the data set
C   CALL READAT(NPTS,IA)
C   Convert the data set from the format used in the input file
C   into real format
DO 20 I=1,NPTS
  X(I)=DECIML(X(I))
  Y(I)=DECIML(Y(I))
  Z(I)=DECIML(Z(I))
  SX(I)=DECIML(SX(I))
  SY(I)=DECIML(SY(I))
  SZ(I)=DECIML(SZ(I))
20  CONTINUE
C   Convert field values in the format of the input file into
C   correct readings.
CALL FUPDAT(NPTS)
DO 13 I=1,NPTS
  X(I)=POWER(X(I),PX(I))
  Y(I)=POWER(Y(I),PY(I))
  Z(I)=POWER(Z(I),PZ(I))
  SX(I)=POWER(SX(I),PSX(I))
  SY(I)=POWER(SY(I),PSY(I))
  SZ(I)=POWER(SZ(I),PSZ(I))
13  CONTINUE
C   End format conversion
C   Average multiple observations at field strengths.
CALL AVRMLT(NPTS)
C   Determine the magnitude of the vectors.
CALL AMGNTD(NPTS)
C   Initialize the Arrays T and TI.
CALL ZERO(NPTS)
CALL ZEROI(NPTS)
DO 21 N=1,NPTS
C   Determine the wave function values and array locations.
VAL=0.
UM=0.
VM=0.
DO 22 I=01,60
DO 23 J=01,60
L=I
K=J
CALL GAUSSN(L,K,X(N)/TMAG(N),Y(N)/TMAG(N),Z(N)/TMAG(N),ITEST,TINT)
IF(ITEST.EQ.1.AND.Z(N).LT.0.0)L=L+40
IF(ITEST.EQ.0.AND.Z(N).GT.0.0)L=L+40
C   PRINT*,I,L,FACT
TINT=TINT*TMAG(N)/TMAG(1)
T(L,K)=AMAX1(TINT,T(L,K))
TI(L,K)=TI(L,K)+TINT
VAL=AMAX1(VAL,TI(L,K))
IF(VAL.EQ.TI(L,K))UM=RCNVRN(L)

```

```

1 IF(VAL.EQ.TI(L,K))VM=RCNVRN(K)
23 CONTINUE
22 CONTINUE
21 CONTINUE
C Print the values to be plotted and determine the mean value
C as indicated by the wave distribution.
CALL RPRSNT(NPTS,UM,VM,VAL,IA)
C Input the position and correction values
READ*,SLAT,SLONG
READ*,CORR,SAZ,SDEC
C Determine the pole position using the wave functions
IF(UM.GT.1.)TEST=1.
IF(UM.LE.1.)TEST=-1.
UM=UM-(1.+TEST)
ZM=(1.-UM*UM-VM*VM)**(1./2.)*TEST
D=ATAN2(UM,VM)
PI=ATAN2((UM*UM+VM*VM)**(1./2.),ZM)
SAZ=SAZ*3.14152/180.
SDEC=SDEC*3.14152/180.
PI=PI+(3.14152/2.-SDEC)*COS(SAZ-D)
PI=3.141592/2.-PI
R=1.
TNPTS=1.
SLONG=100.
C CORR=CORR/100.
SLAT=SLAT/100.
SLAT=SLAT*3.14152/180.0
SLONG=SLONG*3.14152/180.0
CORR=CORR*3.14152/180.0
BETA=ATAN2((1./2.)*TAN(PI),1.)
BETA=3.14152/2.-BETA
C PRINT*,BETA
PLAT=ALAT(SLAT,D,BETA)
C PRINT*,SLONG,D,BETA,SLAT,PLAT
PLONG=ALONG(SLONG,D,BETA,SLAT,PLAT)
C PRINT*,PLONG
PIC=PI
D=D-CORR
BETA=ATAN2((1./2.)*TAN(PIC),1.)
BETA=3.14152/2.-BETA
PLG=ALONG(SLONG,D,BETA,SLAT,PLAT)
PLT=ALAT(SLAT,D,BETA)
PLONG=PLONG*180.0/3.14152
PLAT=PLAT*180.0/3.14152
PLG=PLG*180.0/3.14152
PLT=PLT*180.0/3.14152
CALL ZERO(NPTS)
C Determine the half-maximum surface area.
CALL GAUSNI(NPTS,UM,VM,ZM,IA,COU,VAL)
WRITE(24,7)IA,PLAT,PLONG,PLT,PLG,COU,NPTS
WRITE(17,10)IA,COU
10 FORMAT(5X,I5,5X,F9.6)
7 FORMAT(1X,I4,1X,4(F5.1,1X),1X,F8.4,2X,I2)
C This part of the program determines the pole postion using

```

```

C conventional analyses.
C It produces the latitude, longitude, radius, and major
C and minor axes of the ellipse of confidence.
C           VARIABLES
C A,AA=CIRCLE OF CONFIDENCE(95)
C A1,AA1=ERROR IN COLATITUDE
C A2,AA2=ERROR IN COLONGITUDE
C XC=0.0
C YC=0.0
C ZC=0.0
DO 9 I=1,NPTS
  XC=XC+X(I)/TMAG(I)
  YC=YC+Y(I)/TMAG(I)
  ZC=ZC+Z(I)/TMAG(I)
9  CONTINUE
C PRINT*, RA
  TNPTS=FLOAT(NPTS)
  R=(ABS(XC*XC+YC*YC+ZC*ZC))**(.1.0/2.0)
  D=ATAN2(XC,YC)
  PI=ATAN2((XC*XC+YC*YC)**(.1./2.),ZC)
  PI=PI+(3.14152/2.-SDEC)*COS(SAZ-D)
  PI=3.141592/2.-PI
C PRINT*,D,PI
  BETA=ATAN2((.1./2.)*TAN(PI),1.)
  BETA=3.14152/2.-BETA
C PRINT*,BETA
C Determine the confidence parameters.
  CALL CNFDNC(AA,AA1,AA2,BETA,PI,R,TNPTS)
C Determine the latitude and longitudes.
  PLAT=ALAT(SLAT,D,BETA)
  PLONG=ALONG(SLONG,D,BETA,SLAT,PLAT)
C PRINT*,PLONG
  PIC=PI
  D=D-CORR
  BETA=ATAN2((.1./2.)*TAN(PIC),1.)
  BETA=3.14152/2.-BETA
  CALL CNFDNC(A,A1,A2,BETA,PIC,R,TNPTS)
  PRINT*,SLONG,D,BETA,SLAT,PLAT
  PLG=ALONG(SLONG,D,BETA,SLAT,PLAT)
  PLT=ALAT(SLAT,D,BETA)
  PLONG=PLONG*180.0/3.14152
  PLAT=PLAT*180.0/3.14152
  PLG=PLG*180.0/3.14152
  PLT=PLT*180.0/3.14152
  WRITE(16,8)IA,PLAT,PLONG,AA,AA1,AA2,PLT,PLG,A,A1,A2
8   FORMAT(1X,I4,1X,2(2(F5.1,1X),3(F6.3,1X)))
  QQQ=-10.0
  DO 1 I=1,NPTS
    ZM=ABS(Z(I))
    YM=ABS(Y(I))
    XM=ABS(X(I))
    IF(XM.GT.QQQ)QQQ=XM
    IF(YM.GT.QQQ)QQQ=YM
    IF(ZM.GT.QQQ)QQQ=ZM

```

```

1 CONTINUE
FC=(2.0/QQQ)
DO 4 I=1,NPTS
X2D(I)=(X(I)+Y(I)*(1.0/2.0))*FC
Z2D(I)=(Z(I)+Y(I)*SQRT(3.0)/2.0)*FC
X2(I)=X2D(I)
Z2(I)=Y(I)*(SQRT(3.0)/2.0)*FC
TA(I)=FLOAT(M(I))
4 CONTINUE
DO 3 I=1,8
EX=FLOAT(I)
EX=-9.0+EX
E=EX+1.0
XH=10.0**E
XL=10.0**EX
IF(QQQ.GT.XL.AND.QQQ.LT.XH)VAL=XH
3 CONTINUE
OVAL=-VAL
DVAL=VAL/4.0
CALL PAPER(0.0,20.0,0.0,20.00)
CALL PLOTS(IBUFF,4000)
CALL PLOT(4.0,5.0,-3)
CALL AXIS(-4.0,0.0,'X-AXIS'
C',-43,8.0,0.0,OVAL,DVAL)
CALL AXIS(-2.00,-3.50,'Y-AXIS'
C,38,8.0,60.0,OVAL,DVAL)
CALL AXIS(0.0,-4.0,'Z-AXIS
C',44,8.0,90.0,OVAL,DVAL)
C CALL SYMBOL(0.8,0.8,.14,'SAMPLE 0112',0.0,11)
DO 2 I=1,NPTS
CALL PLOT(X2(I),Z2(I),3)
CALL PLOT(X2D(I),Z2D(I),2)
2 CONTINUE
CALL PLOT(X2(I),Z2(I),3)
DO 5 I=1,NPTS
CALL PLOT(X2(I),Z2(I),2)
5 CONTINUE
CALL PLOT(5.25,-4.0,-3)
DO 6 I=1,NPTS
TMAG(I)=(X(I)*X(I)+Y(I)*Y(I)+Z(I)*Z(I))**(.1/2.)
TM(I)=TMAG(I)/TMAG(1)
TA(I)=FLOAT(M(I))
6 CONTINUE
CALL SCALE(TM,5.0,NPTS,1)
CALL SCALE(TA,6.0,NPTS,1)
N1=NPTS+1
N2=NPTS+2
CALL AXIS(0.0,0.0,'DEMAGNETIZATION NUMBER',-22,6.0,0.0,TA(N1),TA(
CN2))
CALL AXIS(0.0,0.0,'MAGNITUDE',9,5.0,90.0,TM(N1),TM(N2))
CALL LINE(TA,TM,NPTS,1,2,4)
CALL SYMBOL(2.0,6.0,.14,'DEMAGNETIZATION CHARACTER',0.0,25)
C CALL SYMBOL(2.0,5.0,.14,'SAMPLE 0112 ',0.0,25)
CALL PLOT(12.0,0.0,999)

```

```

STOP
END
SUBROUTINE CNFDNC(A,A1,A2,BETA,PI,R,TNPTS)
A=ACOS(1.-((TNPTS-R)/R)*((1./.05)**(1./(TNPTS-1.))-1.))
A1=(1./2.)*A*(1.+3.*((COS(BETA))**2.))
A2=A*SIN(BETA)/COS(PI)
RETURN
END
FUNCTION ALAT(SLAT,D,BETA)
BLAT=ACOS(COS(BETA)*COS(3.14152/2.-SLAT)+SIN(BETA)*SIN(3.14152
@/2.-SLAT)*COS(D))
ALAT=3.14152/2.-BLAT
RETURN
END
FUNCTION ALONG(SLONG,D,BETA,SLAT,PLAT)
BITA=(SIN(BETA)*SIN(D)/SIN(3.14152/2.-PLAT))
IF(ABS(BITA).GT.1.)BITA=BITA/ABS(BITA)
BITA=ASIN(BITA)
PRINT15
15 FORMAT(1X,'OK')
IF(COS(3.14151/2.-SLAT).LE.SIN(SLAT)*SIN(PLAT))ALONG=SLONG+3.1415
@-BITA
IF(COS(3.14151/2.-SLAT).GT.SIN(SLAT)*SIN(PLAT))ALONG=SLONG+BITA
RETURN
END
SUBROUTINE READAT(NPTS,IA)
COMMON/BLK1/X,Y,Z,PX,PY,PZ
COMMON/BLK2/SX,SY,SZ,PSX,PSY,PSZ
COMMON/BLK3/M
DIMENSION X(40),Y(40),Z(40),PX(40),PY(40),PZ(40),SX(40),SY(40),
*SZ(40),PSX(40),PSY(40),PSZ(40),M(40)
READ*,NPTS
DO 10 I=1,NPTS
READ*,IA,M(I),Y(I),PY(I),SY(I),PSY(I),X(I),PX(I),SX(I),PSX(I),
*Z(I),PZ(I),SZ(I),PSZ(I)
10 CONTINUE
RETURN
END
FUNCTION DECIML(A)
SIGN=A/ABS(A)
P=0.0
11 FC=10.0**P
TEST=ABS(A)/FC
IF(TEST.LE.1.0)GOTO 15
P=P+1
GOTO 11
15 CONTINUE
DECIML=TEST*SIGN
RETURN
END
SUBROUTINE FUPDAT(NPTS)
COMMON/BLK3/M
DIMENSION M(40)
DO 12 I=1,NPTS

```

```

TEST=FLOAT(M(I))
M(I)=M(I)*10
TEST=TEST-(INT(TEST/10.0))*10.0
IFACT=0
IF(TEST.GT.5.1.AND.TEST.LT.9.0)IFACT=5
IF(TEST.GT.1.AND.TEST.LT.4.9)IFACT=5
M(I)=M(I)+IFACT
12    CONTINUE
      RETURN
      END
FUNCTION POWER(A,B)
POWER=A*(10.0**B)
RETURN
END
SUBROUTINE AVRMLT(NPTS)
COMMON/BLK1/X,Y,Z
COMMON/BLK2/SX,SY,SZ
COMMON/BLK3/M
DIMENSION X(40),Y(40),Z(40),SX(40),SY(40),SZ(40),M(40)
N=NPTS+1
DO 14 NI=2,N
I=N-NI+2
M(I)=M(I-1)
X(I)=X(I-1)
Z(I)=Z(I-1)
Y(I)=Y(I-1)
SX(I)=SX(I-1)
SY(I)=SY(I-1)
SZ(I)=SZ(I-1)
14    CONTINUE
M(1)=0
L=0
J=0
DO 15 I=2,N
IF(M(I).NE.M(I-1))GOTO 20
L=L+1
TL=FLOAT(L)
X(J)=(X(J)*TL+X(I))/(TL+1.0)
Y(J)=(Y(J)*TL+Y(I))/(TL+1.0)
Z(J)=(Z(J)*TL+Z(I))/(TL+1.0)
SX(J)=(SX(J)**2.0+SX(I)**2.0)**(1.0/2.0)
SY(J)=(SY(J)**2.0+SY(I)**2.0)**(1.0/2.0)
SZ(J)=(SZ(J)**2.0+SZ(I)**2.0)**(1.0/2.0)
15    GOTO 16
20    CONTINUE
L=0
J=J+1
X(J)=X(I)
Y(J)=Y(I)
Z(J)=Z(I)
M(J)=M(I)
SX(J)=SX(I)
SY(J)=SY(I)
SZ(J)=SZ(I)

```

```

16    CONTINUE
C    PRINT*,X(J),Y(J),Z(J)
15    CONTINUE
NPTS=J
RETURN
END
SUBROUTINE AMGNTD(NPTS)
COMMON/BLK1/X,Y,Z
COMMON/BLK4/TMAG
DIMENSION X(40),Y(40),Z(40),TMAG(40)
DO 17 I=1,NPTS
TMAG(I)=(X(I)*X(I)+Y(I)*Y(I)+Z(I)*Z(I))**(.1.0/2.0)
C    PRINT*,TMAG(I)
17    CONTINUE
RETURN
END
SUBROUTINE ZERO(NPTS)
COMMON/BLK5/T
DIMENSION T(100,60)
DO 18 I=1,100
DO 19 J=1,060
T(I,J)=0.0
19    CONTINUE
18    CONTINUE
RETURN
END
SUBROUTINE ZEROI(NPTS)
COMMON/BLK6/TI
DIMENSION TI(100,60)
DO 18 I=1,100
DO 19 J=1,060
TI(I,J)=0.0
19    CONTINUE
18    CONTINUE
RETURN
END
FUNCTION RCNVRN(K1)
RCNVRN=(FLOAT(K1)-30.0)/20.0
C    PRINT*,K1,RCNVRN
RETURN
END
INTEGER FUNCTION ICNVRN(B)
ICNVRN=IFIX((.00001+B+1.5)*20.0)
C    PRINT*,B,ICNVRN
C    PRINT*,B,ICNVRN
RETURN
END
SUBROUTINE GAUSSN(L,K,XM,YM,ZM,ITEST,TINT)
X1=RCNVRN(L)+.0000001
Y1=RCNVRN(K)+.0000001
R1=(X1*X1+Y1*Y1)**(.1./2.)
IF(R1.GT.SQRT(2.))R1=SQRT(2.)
Z1=(ABS(1.-R1*R1))**(.1./2.)
PHI1=ABS(ATAN2(R1,Z1))

```

```

PHA1=ATAN2(Y1,X1)
ITEST=00
IF(R1.LT.1.0)GOTO 21
ITEST=1
PHI1=ABS(ATAN2(R1,-Z1))
X1=SIN(PHI1)*COS(PHA1)
Y1=SIN(PHI1)*SIN(PHA1)
L=ICNVRN(X1)
K=ICNVRN(Y1)
21 CONTINUE
RM=(YM*YM+XM*XM)**(1./2.)
PHIN=ABS(ATAN2(RM,ABS(ZM)))
PHAN=ATAN2(YM,XM)
TEST=PHAN*PHA1
IF(TEST.LT.0.0)VAL=ABS(PHAN)+ABS(PHA1)
IF(TEST.LT.0.0)DELT=AMIN1(VAL,2.*3.141592654-VAL)
IF(TEST.GE.0.0)DELT=ABS(PHAN-PHA1)
RSQ=(DELT)*(DELT)+(PHI1-PHIN)*(PHI1-PHIN)
RSQ=RSQ*05.
IF(RSQ.GT.150.)RSQ=150.
TINT=(1.0/EXP(RSQ))
C PRINT997,PHI1,PHA1,X1,Y1,I,J,TINT
C PRINT996,PHIN,PHAN,XM,YM,GAUSSN
997 FORMAT(4X,4(F5.2,1X),2(I2,1X),F6.3)
996 FORMAT(3X,4(F5.2,1X),F8.6)
      RETURN
      END
SUBROUTINE RPRSNT(NPTS,UM,VM,VAL,IA)
COMMON/BLK5/T
COMMON/BLK6/TI
DIMENSION T(100,60)
DIMENSION TI(100,60)
WRITE(23,24)IA,UM,VM,VAL
24 FORMAT(2X,I4,1X,2(F11.5,1X),F12.8)
DO 40 I=10,90
U=RCNVRN(I)
DO 41 J=10,50
V=RCNVRN(J)
FT=0.0
IF(I.GT.50)FT=2.0
TEST=(U-FT)*(U-FT)+V*V
IF(TEST.GT.1.0)T(I,J)=0.0
IF(TEST.GT.1.0)TI(I,J)=0.0
PVAL=AMIN1(VAL/2.,TI(I,J))
C T(I,J)=AMIN1(T(I,J),.01)
IF(TEST.LE.1.0)T(I,J)=T(I,J)+1.0
IF(TEST.LE.1.0)TI(I,J)=TI(I,J)+1.0
IF(TEST.LE.1.0)PVAL=PVAL+1.
WRITE(10,13)U,V,T(I,J)
WRITE(21,13)U,V,TI(I,J)
WRITE(22,13)U,V,PVAL
13 FORMAT(2X,2(F11.5,1X),F12.8)
41 CONTINUE
40 CONTINUE

```

```

RETURN
END
STOP
END
SUBROUTINE GAUSNI(NPTS,UM,VM,ZM,IA,COU,VAL)
COMMON/BLK1/X,Y,Z,PX,PY,PZ
COMMON/BLK4/TMAG
COMMON/BLK5/T
DIMENSION T(60,100),X(40),Y(40),Z(40),PX(40),PY(40),PZ(40),TMAG(40
*)
DO 6 K=1,NPTS
C PRINT7
XM=UM
YM=VM
DECM=ATAN2(XM,YM)
C PRINT7
TNCM=ATAN2((XM*XM+YM*YM)**(1./2.),ZM)
C PRINT7
7 FORMAT(1X,'OK')
DO 2 I=1,60
DO 3 J=1,60
X1=RCNVRN(I)
Y1=RCNVRN(J)
TNC=(Y1+1.5)*3.14152/1.5
DEC=(X1+1.5)*3.14152*2./1.5
V1=AMIN1(ABS(2.*3.14152-ABS(DEC-DECM)),ABS(DEC-DECM))*SIN(TNC)
V2=AMIN1(ABS(2.*3.14152-ABS(TNC-TNCM)),ABS(TNC-TNCM))
RSQ=5.*(V1*V1+V2*V2)
IF(RSQ.GT.30.)RSQ=30.
C PRINT7
TVAL=(1.0/EXP(RSQ))*TMAG(K)/TMAG(1)
C PRINT7
T(I,J)=T(I,J)+TVAL
C PRINT*,T(I,J),TNC,DEC,TNCM,DECM
3 CONTINUE
2 CONTINUE
6 CONTINUE
COU=0.0
DO 4 I=1,60
DO 5 J=1,60
Y1=RCNVRN(J)
TNC=(Y1+1.5)*3.14152/1.5
IF(T(I,J).GT.VAL/2.)COU=COU+ABS(SIN(TNC))*3.14152*2.*3.14152
@/(60.*60.)
C PRINT*,T(I,J)
5 CONTINUE
4 CONTINUE
COU=COU/(3.14152*4.*.01)
RETURN
END
SUBROUTINE ZEROI(NPTS)
COMMON/BLK6/TI
DIMENSION TI(100,60)
DO 18 I=1,100

```

```

DO 19 J=1,060
TI(I,J)=0.0
19 CONTINUE
18 CONTINUE
RETURN
END
SUBROUTINE GAUSNI(NPTS,UM,VM,ZM,IA,COU,VAL)
COMMON/BLK1/X,Y,Z,PX,PY,PZ
COMMON/BLK4/TMAG
COMMON/BLK5/T
DIMENSION T(60,100),X(40),Y(40),Z(40),PX(40),PY(40),PZ(40),TMAG(40
*)
DO 6 K=1,NPTS
C PRINT7
XM=UM
YM=VM
DECM=ATAN2(XM,YM)
C PRINT7
TNCM=ATAN2((XM*XM+YM*YM)**(1./2.),ZM)
C PRINT7
7 FORMAT(1X,'OK')
DO 2 I=1,60
DO 3 J=1,60
X1=RCNVRN(I)
Y1=RCNVRN(J)
TNC=(Y1+1.5)*3.14152/1.5
DEC=(X1+1.5)*3.14152*2./1.5
V1=AMIN1(ABS(2.*3.14152-ABS(DEC-DECM)),ABS(DEC-DECM))*SIN(TNC)
V2=AMIN1(ABS(2.*3.14152-ABS(TNC-TNCM)),ABS(TNC-TNCM))
RSQ=5.* (V1*V1+V2*V2)
IF(RSQ.GT.30.)RSQ=30.
C PRINT7
TVAL=(1.0/EXP(RSQ))*TMAG(K)/TMAG(1)
C PRINT7
T(I,J)=T(I,J)+TVAL
C PRINT*,T(I,J),TNC,DEC,TNCM,DECM
3 CONTINUE
2 CONTINUE
6 CONTINUE
COU=0.0
DO 4 I=1,60
DO 5 J=1,60
Y1=RCNVRN(J)
TNC=(Y1+1.5)*3.14152/1.5
IF(T(I,J).GT.VAL/2.)COU=COU+ABS(SIN(TNC))*3.14152*2.*3.14152
@/(60.*60.)
C PRINT*,T(I,J)
5 CONTINUE
4 CONTINUE
COU=COU/(3.14152*4.*.01)
RETURN
END
SUBROUTINE ZEROI(NPTS)
COMMON/BLK6/TI

```

```

DIMENSION TI(100,60)
DO 18 I=1,100
DO 19 J=1,060
TI(I,J)=0.0
19  CONTINUE
18  CONTINUE
      RETURN
      END

```

B.1.2 Compilation of CALCOMP Procedures

The following JCL compiles and links for execution of the above source module. The object module is placed in the data set LOAD as member GO5. This is a user defined data set. This JCL uses the FORTX compiler and so can accommodate the CALCOMP routines. The particular advantage for compiling the source file separately is that the object module is available without further compilation costs.

```

//GUYE JOB '829-5,,,R=040,T=019,I=09,L=09','STROB'
//STEP1 EXEC FORTXCLG,USERLIB='SYS4.EPIC.LINK'
//FORT.SYSIN DD *
++EMBED KP2
/*
//LKED.SYSLMOD DD DSN=GEOP5.LOAD(GO5),DISP=OLD
//GO.FT01F001 DD DSN=&&FT01F001,SPACE=(6144,600),
//    DISP=(,PASS),UNIT=SYSDA,
//    DCB=(BLKSIZE=6144,RECFM=F,DSORG=DA,OPTCD=C)
//GO.FT09F001 DD DSN=SYS4.EPIC.PARMS,DISP=SHR

```

B.1.3 Execution of the Multi Step Program

The source listing that follows generates xerox outputs of the above plots. It utilizes temporary data steps between program steps. The first step executes the load module produced in the above step, while the second step executes the SAS plotting proce-

dures on the data passed to it. The raw data is contained in a separate MANTES file (in this case F0912).

```

//GUYE JOB '829-5,,,R=040,T=029,I=29,L=09','STROB',MSGCLASS=Z
//STEP1 EXEC PGM=G01
//STEPLIB DD DSN=GEOP5.LOAD,DISP=SHR
//FT05F001 DD *
++EMBED G=SPEC F0912 NOSEQ
/*
//FT06F001 DD SYSOUT=A
//GO.FT01F001 DD DSN=&&FT01F001,SPACE=(6144,600),
// DISP=(,PASS),UNIT=SYSDA,
// DCB=(BLKSIZE=6144,RECFM=F,DSORG=DA,OPTCD=C)
//GO.FT09F001 DD DSN=SYS4.EPIC.PARMS,DISP=SHR
//FT10F001 DD DSN=&&NUM1,DISP=(NEW,PASS),DCB=(LRECL=80,
// BLKSIZE=6080,RECFM=FB),VOL=SER=WORK03,UNIT=DISK,SPACE=(1600,200)
//FT21F001 DD DSN=&&NUM2,DISP=(NEW,PASS),DCB=(LRECL=80,
// BLKSIZE=6080,RECFM=FB),VOL=SER=WORK03,UNIT=DISK,SPACE=(1600,200)
//FT22F001 DD DSN=&&NUM3,DISP=(NEW,PASS),DCB=(LRECL=80,
// BLKSIZE=6080,RECFM=FB),VOL=SER=WORK03,UNIT=DISK,SPACE=(1600,200)
//FT23F001 DD DSN=GEOP5.TSO.MEAN,DISP=MOD
//FT24F001 DD DSN=GEOP5.TSO.DGTL,DISP=MOD
//FT16F001 DD DSN=GEOP5.TSO.CNVL,DISP=MOD
//FT17F001 DD DSN=GEOP5.TSO.CONF,DISP=MOD
//STEP2 EXEC XPLOT
//FT01F001 DD DSN=&&FT01F001,DISP=(OLD,DELETE)
//STEP3 EXEC SASPLOT,SIZE=2000K
//FDAT DD DSN=&&NUM1,DISP=(OLD,PASS)
//FDAT2 DD DSN=&&NUM2,DISP=(OLD,PASS)
//FDAT3 DD DSN=&&NUM3,DISP=(OLD,PASS)
//SYSIN DD *
      GOPTIONS DEVICE=XEROX HSIZE=8.25;
      OPTIONS NOSOURCE;
      TITLE;
      DATA POINT1;
      INFILE FDAT;
          INPUT X Y M;
          IF M LT 1 THEN M=.;
      OUTPUT;
      DATA POINT2;
      INFILE FDAT2;
          INPUT X Y M;
          IF M LT 1 THEN M=.;
      OUTPUT;
      DATA POINT3;
      INFILE FDAT3;

```

```

      INPUT X Y M;
      IF M LT 1 THEN M=.;

      OUTPUT;
PROC G3D DATA=POINT1 GOUT=PIC1;
PLOT X*Y=M/NOAXIS;
SYMBOL1 I=SPLINE;
PROC G3D DATA=POINT2 GOUT=PIC2;
PLOT X*Y=M/NOAXIS;
SYMBOL1 I=SPLINE;
PROC G3D DATA=POINT3 GOUT=PIC3;
PLOT X*Y=M/NOAXIS;
SYMBOL1 I=SPLINE;
DATA TOTAL;
   SET PIC1 PIC2 PIC3;
OUTPUT;
PROC GREPLAY DATA=TOTAL;
//GO.FT01F001 DD DSN=&&FT01F001,SPACE=(6144,600),
//  DISP=(,PASS),UNIT=SYSDA,
//  DCB=(BLKSIZE=6144,RECFM=F,DSORG=DA,OPTCD=C)
//STEP4 EXEC XPLOT
//

```

B.1.4 Eigenvalue Analysis

The following program generates the eigenvalues of a set of data points. It utilizes the IMSL subroutine to EIGR to do this. The output generated is the eigenvalues and vectors for each sample, then the eigenvalue and vector for all samples combined. It generates the pole position for the final eigenvector.

```

//GUYE JOB '829-5,,,R=400,,T=005,I=10,L=09','STROB'
/*TSO
//STEP1 EXEC FORTHCLG,SIZE=0256K
//FORT.SYSIN DD *
C      PROGRAM TO PRODUCE EIGENVECTORS AND EIGENVALUES OF A 3X3
C      MATRIX.  THE VECTOR ASSOCIATED WITH THE SMALLEST EIGEN VALUE
C      IS THE 'BEST FIT' VECTOR TO THE PLANE, IE., IT IS THE NORMAL
C      TO THE 'BEST FIT' PLANE.
C          INPUT
C          L=NUMBER OF VECTOR TO DETERMINE PLANE.
C          XL(I,J)=(I=1,L,J=1,3) IS THE JTH COMPONENT OF THE ITH VECTOR.
C          XE(I,J)=(I=1,L,J=1,3) IS THE JTH COMPONENT WEIGHT OF THE ITH

```

```

C VECTOR.
C OUTPUT
C XD(I)=(I=1,3) ARE THE EIGEN VALUES.
C JER=ERROR PARAMETER ( SEE IMSL EIGRS LISTING).
C XZT(I,J)=(I=1,3,J=1,3) ARE THE EIGEN VECTORS.
C DIMENSION XA(3,3),XD(3),XWK(10),XZT(3,3),XL(20,3),XE(20,3)
* ,XT(40),YT(40),ZT(40),M(40),PXT(40),PYT(40),PZT(40),
* $SXT(40),SYT(40),SZT(40),PSXT(40),PSYT(40),PSZT(40),A(10),B(10)
* ,C(10)
COMMON/BLK1/XT,YT,ZT,PXT,PYT,PZT
COMMON/BLK2/SXT,SYT,SZT,PSXT,PSYT,PSZT
COMMON/BLK3/M
ICH=1
READ*,NVALS
DO 16 K=1,NVALS
CALL READAT(NPTS,IA)
DO 20 I=1,NPTS
XT(I)=DECIML(XT(I))
YT(I)=DECIML(YT(I))
ZT(I)=DECIML(ZT(I))
SXT(I)=DECIML(SXT(I))
SYT(I)=DECIML(SYT(I))
SZT(I)=DECIML(SZT(I))
CONTINUE
20 CALL FUPDAT(NPTS)
DO 13 I=1,NPTS
XT(I)=POWER(XT(I),PXT(I))
YT(I)=POWER(YT(I),PYT(I))
ZT(I)=POWER(ZT(I),PZT(I))
SXT(I)=POWER(SXT(I),PSXT(I))
SYT(I)=POWER(SYT(I),PSYT(I))
SZT(I)=POWER(SZT(I),PSZT(I))
13 CONTINUE
JER=1
15 CONTINUE
DO 2 I=1,NPTS
XL(I,1)=XT(I)
XL(I,2)=YT(I)
XL(I,3)=ZT(I)
XE(I,1)=SXT(I)
XE(I,2)=SYT(I)
XE(I,3)=SZT(I)
XNO=(XL(I,1)*XL(I,1)+XL(I,2)*XL(I,2)+XL(I,3)*XL(I,3))**1.0/2.0
XNE=(XE(I,1)**2.0+XE(I,2)**2.0+XE(I,3)**2.0)**.5
XL(I,1)=XL(I,1)/XNO
XL(I,2)=XL(I,2)/XNO
XL(I,3)=XL(I,3)/XNO
XE(I,1)=XNE/XE(I,1)
XE(I,2)=XNE/XE(I,2)
XE(I,3)=XNE/XE(I,3)
2 CONTINUE
JZ=3
IOBN=2
IN=3

```

```

DO 5 I=1,3
DO 6 J=1,3
6 XA(I,J)=0.0
5 CONTINUE
DO 7 J=1,3
DO 8 MN=1,3
DO 9 I=1,NPTS
9 XA(J,MN)=XA(J,MN)+XL(I,J)*XL(I,MN)
8 CONTINUE
7 CONTINUE
CALL EIGRS(XA,IN,IOBN,XD,XZT,JZ,XWK,JER)
DO 12 I=1,3
12 WRITE(9,4)IA,XZT(I,1),XZT(I,2),XZT(I,3),XD(I)
CONTINUE
4 FORMAT(1X,I5,1X,3(F6.3,1X),E10.5)
17 FORMAT(1X,I5,2X,4(E8.4,2X))
IF(XD(1).GT.XD(2).AND.XD(1).GT.XD(3))ID=1
IF(XD(2).GT.XD(1).AND.XD(2).GT.XD(3))ID=2
IF(XD(3).GT.XD(2).AND.XD(3).GT.XD(1))ID=3
IF(ICH.EQ.2)GOTO 18
READ*,SLAT,SLONG
READ*,CORR,SAZ,SDEC
10 FORMAT(F4.0,1X,F3.0)
11 FORMAT(F5.2,1X,F3.0,1X,F4.1)
SLAT=SLAT/100.
SLAT=SLAT*3.14152/180.0
SLONG=SLONG*3.14152/180.0
CORR=CORR*3.14152/180.0
X=XZT(ID,1)
Y=XZT(ID,2)
Z=XZT(ID,3)
D=ATAN2(X,Y)
PI=ATAN2((X*X+Y*Y)**(1./2.),Z)
SAZ=SAZ*3.14152/180.0
SDEC=SDEC*3.14152/180.0
PI=PI+(3.14152/2.-SDEC)*COS(SAZ-D)
PI=3.141592-PI
D=D-CORR
A(K)=COS(D)*SIN(PI)
B(K)=SIN(D)*SIN(PI)
C(K)=COS(PI)
16 WRITE(10,4)IA,A(K),B(K),C(K),XD(ID)
CONTINUE
ICH=ICH+1
IA=9999
DO 14 I=1,NVALS
XT(I)=A(I)
YT(I)=B(I)
ZT(I)=C(I)
SXT(I)=1.
SYT(I)=1.
SZT(I)=1.
14 CONTINUE
NPTS=NVALS

```

```

IF(ICH.EQ.2)GOTO 15
C      WRITE*,D,PI
18      CONTINUE
      X=XZT(ID,1)
      Y=XZT(ID,2)
      Z=XZT(ID,3)
      D=ATAN2(X,Y)
      PI=ATAN2((X*X+Y*Y)**(1./2.),Z)
      BETA=ATAN2((1./2.)*TAN(PI),1.)
      BETA=3.14152/2.-BETA
      PLAT=ALAT(SLAT,D,BETA)
C      WRITE*,SLONG,D,BETA,SLAT,PLAT
      PLONG=ALONG(SLONG,D,BETA,SLAT,PLAT)
      PLAT=PLAT*180./3.14152
      PLONG=PLONG*180./3.14152
      WRITE(11,21)IA,PLONG,PLAT,PLAT,PLONG,PLONG,PLAT
1      CONTINUE
21      FORMAT(1X,I4,2X,6(F7.2,2X))
3      FORMAT(I2)
      STOP
      END
      SUBROUTINE READAT(NPTS,IA)
      DIMENSION XT(40),YT(40),ZT(40),PXT(40),PYT(40),PZT(40),SXT(40),SYT
      *(40),SZT(40),PSXT(40),PSYT(40),PSZT(40),M(40)
      COMMON/BLK1/XT,YT,ZT,PXT,PYT,PZT
      COMMON/BLK2/SXT,SYT,SZT,PSXT,PSYT,PSZT
      COMMON/BLK3/M
      READ*,NPTS
3      FORMAT(I2)
      DO 10 I=1,NPTS
      READ*,IA,M(I),YT(I),PYT(I),SYT(I),PSYT(I),XT(I),PXT(I),SXT(I)
      *,PSXT(I),
      *ZT(I),PZT(I),SZT(I),PSZT(I)
9      FORMAT(I4,1X,I2,1X,3(F4.0,1X,F3.0,1X,F4.0,1X,F3.0,1X))
10     CONTINUE
888    FORMAT(' ',8(E12.6,1X))
      RETURN
      END
      FUNCTION DECIML(A)
      SIGN=A/ABS(A)
      P=0.0
11     FC=10.0**P
      TEST=ABS(A)/FC
      IF(TEST.LE.1.0)GOTO 15
      P=P+1
      GOTO 11
15     CONTINUE
      DECIML=TEST*SIGN
      RETURN
      END
      SUBROUTINE FUPDAT(NPTS)
      COMMON/BLK3/M
      DIMENSION M(40)
      DO 12 I=1,NPTS

```

```

TEST=FLOAT(M(I))
M(I)=M(I)*10
TEST=TEST-(INT(TEST/10.0))*10.0
IFACT=0
IF(TEST.GT.5.1.AND.TEST.LT.9.9)IFACT=5
IF(TEST.GT.1.AND.TEST.LT.4.9)IFACT=5
M(I)=M(I)+IFACT
12  CONTINUE
      RETURN
      END
      FUNCTION ALAT(SLAT,D,BETA)
      BLAT=ACOS(COS(BETA)*COS(3.14152/2.-SLAT)+SIN(BETA)*SIN(3.14152
@/2.-SLAT)*COS(D))
      ALAT=3.14152/2.-BLAT
      RETURN
      END
      FUNCTION ALONG(SLONG,D,BETA,SLAT,PLAT)
      BITA=(SIN(BETA)*SIN(D)/SIN(3.14152/2.-PLAT))
      IF(ABS(BITA).GT.1.)BITA=BITA/ABS(BITA)
      BITA=ASIN(BITA)
      C   WRITE15
15  FORMAT(1X,'OK')
      IF(COS(3.14151/2.-SLAT).LE.SIN(SLAT)*SIN(PLAT))ALONG=SLONG+3.1415
@-BITA
      IF(COS(3.14151/2.-SLAT).GT.SIN(SLAT)*SIN(PLAT))ALONG=SLONG+BITA
      RETURN
      END
      FUNCTION POWER(A,B)
      POWER=A*(10.0**B)
      RETURN
      END
//GO.FT05F001 DD *
7
++EMBED G=SASP TOP4 NOSEQ
//FT09F001 DD DSN=GEOP5.DGS,DISP=OLD
//FT10F001 DD DSN=GEOP5.DGA,DISP=OLD
//FT11F001 DD DSN=GEOP5.DGC,DISP=OLD

```

B.1.5 Sun-Sight Corrections

This program corrects the compass reading for the sun-sight position. Since it can be expected that localized magnetic effects will lead to errors in the compass reading, this is an important step. Input to the program is the site latitude, longitude, Greenwich mean time, the compass bearing, and the orientation of the coring tool. Output is the correction value necessary to correct the magnetic orientation.

```

//GUYE JOB '829-5,,,R=400,F=35,T=010,I=20,L=9','STROB'
/*TSO
//STEP1 EXEC FORTHCLG,SIZE=0256K
//FORT.SYSIN DD *
C      THIS PROGRAM IS USED TO DETERMINE THE SUNS AZIMUTH AT A
C      GIVEN LATITUDE AND LONGITUDE POSITION FOR AGIVEN TIME AND
C      DATE.
C          INPUT
C      TLG=LONGITUDE IN DEGREES EG. 10120= 101DEG. 20MIN.
C      TLT=LATITUDE IN DEGREES
C      D1 =NUMBER OF DAYS SINCE JAN. 0.0 1980
C      TL =TIME EG. 1940 REPRESENTS 7.40PM
C          OUTPUT
C      A =SUNS AZIMUTH IN DEGREES AND MINUTES
C
C
READ 10,N
10 FORMAT(I3)
PRINT 20
20 FORMAT(1X,'SAMPLE',1X,'LST',1X,'SUNS AZIMUTH',1X,'SAMPLE AZIMUTH',
*,1X,' CORRECTION FACTOR',1X,' SAMPLES CORRECTED AZIMUTH')
DO 11 IZ=1,N
READ 12 ,IS,D3,TL,AZ,SAZ,TLT,TLG
D=D3/100.0
ID=AINT(D)
IF(ID.EQ.1)IU=0
IF(ID.EQ.2)IU=30
SD1=FLOAT(ID)
SD=(D-SD1)*100.0
ISD=IFIX(SD)
ID1=ISD+151+IU+2191
DI=FLOAT(ID1)
TN=(360.0/365.2422)*DI
1    CONTINUE
IF(TN.LT.0.0)TN=TN+360.0
IF(TN.GT.360.0)TN=TN-360.0
IF(TN.GT.360.0.OR.TN.LT.0.0)GOTO 1
TM=TN+278.83354-282.596403
IF(TM.LT.0.0)TM=TM+360.0
C=3.14159203/180.0
Z1=TM*C
EC=(360.0/3.14159203)*(0.016718)* SIN(Z1)
TDA=TN+EC+278.833540
IF(TDA.GT.360.0)TDA=TDA-360.0
Z1=C*23.441884
Z2=C*TDA
B=0.
DLT= SIN(B)* COS(Z1)+COS(B)*SIN(Z1)*SIN(TDA)
DLT= ARSIN(DLT)*180.0/3.14159203
Y= SIN(Z2)* COS(Z1)-TAN(B)*SIN(Z1)

```

```

X= COS(Z2)
AP= ATAN2(Y,X)
AP=(180.0/3.14159203)*AP
IF(X.GT.0.0.AND.Y.GT.0.0)U=0.0
IF(X.LT.0.0.AND.Y.GT.0.0)U=90.0
IF(X.LT.0.0.AND.Y.LT.0.0)U=180.0
IF(X.GT.0.0.AND.Y.LT.0.0)U=270.0
3 IF(AP.GT.U+90.0)AP=AP-90.0
IF(AP.LT.U)AP=AP+90.0
IF(AP.GT.U+90.0.OR.AP.LT.U)GOTO 3
PRINT*,AP
D2=-2191+D1
T0=D2*.0657098-17.411472
T=TL/100.0
IT=AINT(T)
TT=FLOAT(IT)
TT=T -TT
TT=TT/60.
TI=FLOAT(IT)
T=TI+TT
T=(T*1.002738)+T0
IF(T.GT.24.0)T=T-24.0
IF(T.LT.0.0)T=T+24.0
TLST=(T-100./15.)*15.
IF(TLST.GT.24.0)TLST=TLST-24.0
IF(TLST.LT.0.0)TLST=TLST+24.0
TH=TLST-AP
Z1=C*DLT
Z2=C*TLT
Z3=C*TH
AA= SIN(Z1)* SIN(Z2)+ COS(Z1)* COS(Z2)* COS(Z3)
AA= ARSIN(AA) *180.0/3.14159203
AT=AA*C
A=( SIN(Z1)- SIN(Z2)* SIN(AT))/(COS(Z2)* COS(AT))
A= ARCOS(A)*180.0/3.14159203
Z3=SIN(Z3)
IF(Z3.GT.0.0)A=360.0-A
TAZ=SAZ/100.0
ITAZ=AINT(TAZ)
TAZ=FLOAT(ITAZ)*100.0
SAZ=(SAZ-TAZ)/.6+TAZ
TAZ=AZ/100.0
ITAZ=AINT(TAZ)
TAZ=FLOAT(ITAZ)*100.0
AZ=(AZ-TAZ)/.6+TAZ
CR=A*100.0-SAZ
CRAZ=AZ+CR
30 IF(CR.LT.-36000.0)CR=CR+36000.0
IF(CRAZ.LT.0.0)CRAZ=CRAZ+36000.0
IF(CR.GT.36000.0)CR=CR-36000.0
IF(CRAZ.GT.36000.0)CRAZ=CRAZ-36000.0
IF(CR.LT.-36000.0.OR.CR.GT.36000.0)GOTO 30
IF(CRAZ.LT.0.0.OR.CRAZ.GT.36000.0)GOTO 30
WRITE(10,22)IS,TLST,SAZ,AZ,CR,CRAZ

```

```
22 FORMAT(1X,I5,0X,F6.2,2X,F8.2,06X,F8.2,4X,F9.2,12X,F8.2)
12 FORMAT(I5,1X,F3.0,1X,F4.0,1X,F5.0,1X,F5.0,1X,F4.0,1X,F5.0)
11 CONTINUE
C PRINT 23
23 FORMAT(1X,'NOTE THAT ALL ANGULAR MEASURES ARE IN DECIMAL DEGREES
* TIMES 100. THE LOCAL SIDHEUDRAL TIME IS GIVEN IN DECIMAL
* HOURS.')
STOP
END
//GO.SYSIN DD *
```

Appendix C

RAW DATA USED IN THIS STUDY

The raw data that was used in this study is contained in the following table. The coordinate system that was used is cartesian, with the y-axis corresponding to the north-south axis, the x-axis corresponding to the east-west axis and the z-axis the vertical component. The format used in this table includes the decimal part and the exponential part of the number in each column. This also applies to the standard deviation of each component. The data contained here represents the raw data in cartesian coordinates. For each component, the first number represents the value multiplied by 100, while the second value is the exponential (to base 10). The "field" is the maximum cleaning field strength for the reading.

Table 4: Raw data used in this report.

The following table (next page) contains the data that was obtained for this report in a field excursion in northern Manitoba. The table format is; the first column contains the sample and is identified by the first four digits referring to the sample site, the fifth digit referring to the particular sample cut from the core, the core identification is referred to by the last digit.

Sample	Field	X-value	Sigm-X	Y-Value	Sigm-Y	Z-Value	Sigm-Z
--------	-------	---------	--------	---------	--------	---------	--------

11	0	-77	-3	29	-4	-36	-3	10	-3	14	-2	63	-4
11	0	-78	-3	90	-4	-36	-3	11	-3	14	-2	68	-4
11	50	60	-5	86	-4	-55	-5	73	-4	27	-3	11	-3
11	100	-11	-3	51	-4	23	-5	66	-4	20	-3	32	-3
11	100	-10	-3	54	-4	-92	-5	77	-4	19	-3	56	-4
11	150	-33	-4	69	-4	-72	-4	97	-4	54	-4	76	-4
11	150	-31	-4	77	-4	-67	-4	93	-4	52	-4	79	-4
11	200	-17	-3	44	-4	-82	-4	85	-4	18	-3	94	-4
11	250	-25	-3	15	-3	-14	-3	40	-4	-19	-3	66	-4
11	250	-23	-3	15	-3	-14	-3	41	-4	-19	-3	61	-4
11	300	-13	-4	83	-5	-90	-4	13	-3	20	-3	12	-3
11	300	-13	-4	84	-5	-92	-4	13	-3	21	-3	12	-3
11	350	90	-4	19	-3	-29	-3	26	-3	24	-3	23	-3
11	350	99	-4	19	-3	-29	-3	26	-3	24	-3	23	-3
11	400	36	-4	11	-3	-24	-3	25	-3	-10	-3	23	-3
11	400	36	-4	11	-3	-24	-3	25	-3	-10	-3	17	-3
11	400	40	-4	12	-3	-24	-3	24	-3	-10	-3	17	-3
11	450	-99	-4	52	-4	52	-4	16	-3	-77	-4	10	-3
11	450	-97	-4	51	-4	10	-3	13	-3	-53	-4	12	-3
11	450	-19	-3	55	-4	11	-3	13	-3	-52	-4	12	-3
11	500	-19	-3	21	-3	-73	-4	33	-3	55	-4	23	-3
11	500	-19	-3	21	-3	-71	-4	33	-3	58	-4	24	-3
11	550	76	-4	23	-3	-10	-5	59	-4	49	-4	79	-4
11	550	79	-4	23	-3	37	-5	60	-4	47	-4	80	-4
11	600	-15	-3	20	-3	-15	-3	16	-3	18	-3	14	-3
11	600	-15	-3	20	-3	-15	-3	16	-3	17	-3	14	-3
11	650	-87	-4	10	-3	10	-3	14	-3	-73	-4	25	-3
11	650	-89	-4	10	-3	10	-3	14	-3	-73	-4	25	-3
11	700	-14	-3	17	-3	-54	-4	33	-3	-29	-4	24	-3
11	700	-14	-3	17	-3	-55	-4	33	-3	-27	-4	24	-3
11	750	-46	-3	88	-4	20	-3	16	-3	32	-3	14	-3
11	750	-46	-3	91	-4	21	-3	16	-3	32	-3	14	-3
11	800	68	-6	70	-4	-13	-3	20	-3	14	-3	11	-3
11	800	38	-5	73	-4	-13	-3	20	-3	11	-3	11	-3
11	850	-68	-5	91	-4	-12	-3	12	-3	31	-3	28	-3
11	850	-75	-5	92	-4	-12	-3	12	-3	31	-3	28	-3
11	900	-29	-3	20	-3	28	-3	19	-3	-67	-4	22	-3
11	900	-28	-3	19	-3	28	-3	19	-3	-65	-4	21	-3
11	950	-94	-4	17	-3	11	-4	58	-4	-18	-3	22	-3
11	950	-89	-4	18	-3	12	-4	64	-4	-18	-3	22	-3
12	0	-13	-2	51	-3	23	-3	59	-3	22	-2	30	-3
12	0	-14	-2	39	-3	12	-3	47	-3	22	-2	30	-3
12	0	-14	-2	39	-3	19	-3	47	-3	23	-2	31	-3
12	50	10	-3	31	-3	16	-3	27	-3	75	-3	20	-3
12	50	11	-3	30	-3	16	-3	28	-3	76	-3	19	-3
12	100	54	-4	19	-3	15	-3	12	-3	68	-3	84	-4
12	100	68	-4	19	-3	15	-3	12	-3	67	-3	87	-4
12	150	-20	-4	81	-4	-17	-3	13	-3	36	-3	15	-3
12	150	-20	-4	80	-4	-17	-3	13	-3	36	-3	15	-3
12	200	16	-3	15	-3	-21	-3	99	-4	41	-3	71	-4
12	200	19	-3	12	-3	-22	-3	10	-3	40	-3	61	-4
12	250	38	-4	22	-3	97	-4	21	-3	46	-3	19	-3
12	250	30	-4	20	-3	96	-4	21	-3	45	-3	18	-3
12	250	21	-4	22	-3	95	-4	21	-3	45	-3	18	-3
12	300	68	-4	25	-3	62	-4	30	-3	64	-3	35	-3

Sample	Field	X-value	Sigm-X	Y-Value	Sigm-Y	Z-Value	Sigm-Z
12	300	89	-4	24	-3	60	-4
12	300	81	-4	24	-3	52	-4
12	350	38	-4	21	-3	23	-3
12	350	13	-3	37	-3	35	-4
12	350	14	-3	37	-3	33	-4
12	400	-27	-3	25	-3	-18	-3
12	400	-26	-3	27	-3	-20	-3
12	450	-45	-3	31	-3	-29	-3
12	450	-50	-3	24	-3	-22	-3
12	550	-25	-3	14	-3	-97	-4
12	550	-24	-3	14	-3	-89	-4
12	600	48	-3	17	-3	-33	-5
12	600	49	-3	17	-3	30	-5
12	650	21	-3	13	-3	-12	-3
12	650	11	-3	20	-4	-13	-3
12	700	-17	-3	21	-3	31	-3
12	700	-17	-3	21	-3	32	-3
12	750	33	-4	50	-4	84	-5
12	750	-91	-4	13	-3	22	-4
12	750	-98	-4	13	-3	16	-4
12	800	-49	-3	25	-3	-16	-3
12	800	-48	-3	24	-3	-16	-3
12	850	-45	-3	31	-3	-16	-3
12	850	-44	-3	32	-3	-14	-3
12	900	35	-3	19	-3	-28	-3
12	900	34	-3	20	-3	-27	-3
12	950	-27	-3	28	-3	25	-3
12	950	-25	-3	29	-3	25	-3
12	950	-25	-3	29	-3	25	-3
13	0	-14	-2	46	-3	-13	-3
13	0	-13	-2	43	-3	-14	-3
13	50	48	-3	14	-3	76	-4
13	50	49	-3	12	-3	84	-4
13	400	-12	-4	17	-3	-29	-4
13	100	29	-4	19	-3	-24	-4
13	100	-80	-5	17	-3	-19	-4
13	150	23	-3	10	-3	-15	-3
13	150	32	-3	10	-3	-15	-3
13	200	21	-3	14	-3	25	-3
13	200	20	-3	14	-3	26	-3
13	250	-45	-3	67	-4	-52	-3
13	250	-45	-3	60	-4	-51	-3
13	300	-34	-3	21	-3	-24	-4
13	300	-33	-3	18	-3	-20	-4
13	350	34	-3	23	-3	-38	-4
13	350	35	-3	22	-3	15	-4
13	350	29	-3	35	-3	69	-4
13	400	13	-3	15	-3	24	-3
13	400	24	-3	84	-4	85	-4
13	400	23	-3	80	-4	85	-4
13	450	-41	-3	10	-3	86	-4
13	450	-29	-3	17	-3	-29	-4
13	450	-43	-3	10	-3	67	-4
13	500	-36	-3	10	-3	-39	-3
13	550	-62	-4	18	-3	-89	-4
13	550	-63	-4	18	-3	-10	-3

Sample	Field	X-value	Sigm-X	Y-Value	Sigm-Y	Z-Value	Sigm-Z
13	600	-65	-3	17	-3	47	-4
13	600	-68	-3	21	-3	86	-4
13	650	26	-3	88	-4	23	-3
13	650	28	-3	81	-4	19	-3
13	650	28	-3	89	-4	24	-3
13	700	-83	-4	98	-4	-24	-3
13	700	-74	-4	11	-3	-24	-3
13	750	-15	-4	14	-3	11	-3
13	750	-71	-4	86	-4	19	-3
13	750	-11	-3	94	-4	19	-3
13	800	-94	-5	45	-4	73	-4
13	800	33	-5	48	-4	75	-4
13	800	64	-5	54	-4	77	-4
13	850	34	-3	23	-3	-20	-3
13	850	34	-3	22	-3	-19	-3
13	900	-11	-3	14	-3	-11	-3
13	900	-15	-3	10	-3	-12	-3
13	900	-11	-3	14	-4	-12	-3
13	950	98	-4	17	-3	23	-3
13	950	11	-3	16	-3	23	-3
11	0	39	-5	41	-5	-66	-6
111	0	66	-5	19	-5	18	-5
111	0	66	-5	19	-5	20	-5
111	50	45	-5	20	-5	18	-5
111	50	44	-5	12	-5	18	-5
111	100	27	-5	40	-6	17	-5
111	100	27	-5	47	-6	16	-5
111	150	79	-6	62	-6	79	-6
111	150	14	-5	56	-6	76	-6
111	150	13	-5	53	-6	67	-6
111	200	46	-6	63	-6	41	-6
111	200	50	-6	73	-6	43	-6
111	250	-91	-6	91	-6	-42	-6
111	250	-90	-6	11	-5	-29	-6
111	300	-16	-6	38	-6	-61	-6
111	350	-90	-7	17	-6	24	-7
111	400	19	-6	54	-6	-66	-6
111	400	13	-6	12	-6	-61	-6
111	450	20	-6	41	-6	-20	-6
111	450	19	-6	59	-6	-13	-6
111	500	68	-6	52	-6	60	-6
111	500	67	-6	50	-6	62	-6
111	550	-17	-6	58	-6	-36	-6
111	550	-22	-6	58	-6	-34	-6
111	600	34	-6	13	-5	33	-6
111	600	23	-6	14	-5	38	-6
111	650	30	-7	46	-6	71	-7
111	650	-52	-7	45	-6	-74	-8
111	700	57	-7	10	-5	41	-6
111	700	91	-7	10	-5	38	-6
111	750	84	-6	65	-6	28	-6
111	750	87	-6	80	-6	24	-6
113	0	-36	-6	91	-6	-27	-6
113	0	-35	-6	75	-6	-26	-6
113	50	-53	-6	45	-6	-40	-6
113	50	53	-3	44	-6	-37	-6

Sample	Field	X-value	Sigm-X	Y-Value	Sigm-Y	Z-Value	Sigm-Z
113	100	-34	-6	37	-6	-36	-6
113	100	-39	-6	35	-6	-41	-6
113	150	-62	-6	61	-6	-50	-6
113	150	-61	-6	53	-6	-51	-6
113	200	-71	-6	19	-6	-36	-6
113	200	-69	-6	22	-6	-37	-6
113	250	-66	-6	35	-6	-56	-6
113	250	-62	-6	32	-6	-54	-6
113	300	-64	-6	19	-6	-26	-6
113	300	-64	-6	15	-6	-17	-6
113	350	-62	-3	16	-6	-53	-6
113	350	-62	-6	16	-6	-54	-6
113	400	35	-6	23	-6	-10	-5
113	400	35	-6	17	-6	-10	-5
113	450	46	-6	95	-7	-54	-6
113	450	51	-7	66	-6	-14	-6
113	500	10	-6	38	-6	-79	-6
113	500	-11	-8	19	-6	-76	-6
113	550	52	-3	17	-6	-99	-6
113	550	41	-3	24	-6	-10	-5
113	600	37	-6	28	-6	-98	-6
113	600	39	-6	31	-6	-99	-6
113	650	96	-7	22	-6	57	-7
113	650	21	-7	33	-6	36	-6
112	0	-69	-7	27	-5	95	-6
112	0	-34	-7	26	-5	11	-5
112	50	-10	-6	22	-5	18	-5
112	50	-37	-7	23	-5	18	-5
112	100	-30	-6	20	-5	16	-5
112	100	64	-8	19	-5	17	-5
112	150	-26	-6	13	-5	10	-5
112	150	-24	-6	14	-5	14	-5
112	200	-51	-6	52	-6	11	-5
112	200	-42	-6	59	-6	11	-5
112	200	-42	-6	59	-6	11	-5
112	250	-48	-6	33	-6	11	-5
112	250	-54	-6	38	-6	11	-5
112	300	-72	-6	70	-6	33	-6
112	300	-64	-6	96	-5	24	-6
112	300	-76	-6	69	-6	32	-6
112	350	-93	-6	12	-5	60	-6
112	350	-99	-6	45	-5	57	-6
112	400	-51	-6	20	-6	-15	-6
112	400	-48	-6	10	-6	-24	-6
112	450	-60	-6	34	-6	32	-6
112	500	-57	-6	19	-6	-32	-6
112	500	-52	-6	16	-6	-31	-6
112	550	-58	-7	58	-6	-13	-7
112	550	-45	-7	56	-6	-53	-7
112	600	-11	-6	32	-6	-44	-6
112	600	-15	-6	26	-6	-39	-6
112	700	-43	-6	30	-6	27	-6
112	700	-43	-6	30	-6	27	-6
112	700	-44	-6	26	-6	31	-6
112	800	-35	-6	23	-6	-29	-6
112	800	-36	-6	19	-6	-30	-6

Sample	Field	X-value	Sigm-X	Y-Value	Sigm-Y	Z-Value	Sigm-Z
211	0	-93	-3	41	-4	-54	-3
211	0	-91	-6	50	-4	-55	-3
211	100	-64	-3	30	-4	-60	-3
211	100	-61	-3	30	-4	-60	-3
211	100	-62	-3	25	-4	-60	-3
211	200	-92	-3	29	-4	-59	-3
211	200	-69	-3	26	-4	-59	-3
211	300	-82	-3	23	-4	-54	-3
211	300	-82	-3	24	-4	-54	-3
211	400	-70	-3	29	-4	-44	-3
211	400	-70	-3	32	-4	-44	-3
211	500	-56	-3	38	-4	-35	-3
211	500	-63	-3	81	-4	-37	-3
211	600	-50	-3	68	-4	-28	-3
211	600	-50	-3	65	-4	-28	-3
211	700	-39	-3	54	-4	-21	-3
211	700	-39	-3	51	-4	-21	-3
211	800	-31	-3	40	-4	-47	-3
211	800	-31	-3	40	-4	-17	-3
211	900	-21	-3	22	-4	-12	-3
211	900	-21	-3	22	-4	-12	-3
212	0	-10	-2	75	-4	-79	-3
212	0	-10	-2	75	-4	-79	-3
212	0	-10	-2	78	-4	-75	-3
212	50	-10	-2	74	-4	-80	-3
212	50	-10	-2	67	-4	-79	-3
212	150	-10	-2	68	-4	-80	-3
212	150	-10	-2	68	-4	-81	-3
212	250	-10	-2	58	-4	-74	-3
212	250	-10	-2	64	-4	-73	-3
212	350	-88	-3	47	-4	-62	-3
212	350	-83	-3	51	-4	-62	-3
212	450	-77	-3	12	-3	-53	-3
212	450	-77	-3	12	-3	-53	-3
212	550	-60	-3	98	-4	-40	-3
212	550	-60	-3	98	-4	-40	-3
212	650	-48	-3	75	-4	-32	-3
212	650	-48	-3	74	-4	-34	-3
212	750	-36	-3	58	-4	-23	-3
212	750	-36	-3	58	-4	-23	-3
212	850	-29	-3	47	-4	-18	-3
212	850	-29	-3	47	-4	-18	-3
212	950	-24	-3	28	-4	-14	-3
212	950	-24	-3	29	-4	-14	-3
213	0	-10	-2	37	-4	-74	-3
213	0	-11	-2	25	-4	-72	-3
213	75	-11	-2	29	-4	-70	-3
213	75	-11	-2	38	-4	-71	-3
213	175	-11	-2	31	-4	-69	-3
213	175	-11	-2	25	-4	-70	-3
213	275	-10	-2	29	-4	-65	-3
213	275	-10	-2	29	-4	-65	-3
213	375	-96	-3	10	-3	-56	-3
213	375	-96	-3	10	-3	-56	-3
213	475	-78	-3	81	-3	-44	-3
213	475	-77	-3	33	-4	-46	-3

Sample	Field	X-value	Sigm-X	Y-Value	Sigm-Y	Z-Value	Sigm-Z
213	575	-60	-3	18	-4	-35	-3
213	575	-60	-3	21	-4	-36	-3
213	675	-44	-3	19	-4	-27	-3
213	675	-44	-3	20	-4	-27	-3
213	775	-34	-3	13	-4	-16	-3
213	775	-34	-3	13	-4	-16	-3
213	875	-31	-3	68	-5	-13	-3
213	875	-31	-3	58	-5	-13	-3
213	975	-24	-3	11	-4	-11	-3
213	975	-24	-3	11	-4	-44	-3
311	0	-27	-3	11	-3	18	-3
311	0	-27	-3	12	-3	18	-3
311	50	-22	-3	84	-4	14	-3
311	50	-21	-3	82	-4	12	-3
311	100	-15	-3	66	-4	99	-4
311	100	-16	-3	51	-4	95	-4
311	150	-11	-3	42	-4	84	-4
311	150	-11	-3	44	-4	85	-4
311	200	-76	-4	30	-4	59	-4
311	200	-79	-4	34	-4	59	-4
311	250	-81	-4	36	-4	33	-4
311	250	-80	-4	36	-4	35	-4
311	300	-34	-3	36	-4	43	-4
311	300	-61	-4	37	-4	44	-4
311	350	-40	-4	20	-4	55	-4
311	350	-40	-4	23	-4	55	-4
311	400	-10	-4	27	-4	46	-4
311	400	-78	-5	29	-4	44	-4
311	450	-12	-4	29	-4	65	-4
311	450	-20	-4	32	-4	-16	-4
311	450	-18	-4	31	-4	84	-4
311	500	-41	-5	24	-4	11	-3
311	500	-38	-5	23	-4	10	-3
311	550	-99	-5	14	-4	63	-4
311	550	-12	-4	13	-4	65	-4
311	600	-80	-5	42	-4	29	-4
311	600	-80	-5	41	-4	31	-4
311	650	53	-6	13	-4	29	-4
311	650	-49	-6	14	-4	31	-4
311	700	-28	-4	16	-4	66	-4
311	700	-28	-4	17	-4	67	-4
311	750	16	-4	21	-4	17	-4
311	750	17	-4	23	-4	18	-4
311	800	-27	-4	19	-4	-23	-4
311	800	-26	-4	20	-4	-21	-4
311	800	-28	-4	20	-4	-27	-4
311	850	-20	-4	33	-4	11	-4
311	850	-20	-4	31	-4	11	-4
311	900	-13	-4	21	-4	-33	-4
311	900	-14	-4	21	-4	-33	-4
312	0	-35	-3	10	-3	24	-3
312	0	34	-3	87	-4	20	-3
312	50	-27	-3	66	-4	16	-3
312	50	-27	-3	64	-4	15	-3
312	100	-17	-3	64	-4	10	-3
312	100	-16	-3	58	-4	95	-4

Sample	Field	X-value	Sigm-X	Y-Value	Sigm-Y	Z-Value	Sigm-Z
312	150	-10 -3	64 -4	12 -3	79 -4	39 -3	10 -4
312	150	-10 -3	61 -4	12 -3	89 -4	39 -3	10 -4
312	200	-87 -4	59 -4	59 -4	51 -4	30 -3	13 -4
312	200	-95 -4	40 -4	81 -4	38 -4	35 -3	58 -4
312	250	-11 -3	33 -4	87 -4	30 -4	25 -3	34 -4
312	250	-11 -3	33 -4	86 -4	30 -4	25 -3	36 -4
312	300	-53 -4	14 -4	76 -4	33 -4	22 -3	60 -4
312	300	-58 -4	13 -4	79 -4	32 -4	21 -3	54 -4
312	350	-35 -4	17 -4	10 -3	15 -4	15 -3	32 -4
312	350	-26 -4	18 -4	10 -3	95 -5	15 -3	19 -4
312	400	-85 -4	11 -4	48 -4	20 -4	13 -3	20 -4
312	400	-86 -4	11 -4	52 -4	21 -4	13 -3	20 -4
312	450	-72 -4	23 -4	66 -4	45 -4	93 -4	51 -4
312	450	-42 -4	21 -4	66 -4	45 -4	95 -4	50 -4
312	500	-35 -4	44 -4	52 -4	25 -4	13 -3	38 -4
312	500	-35 -4	45 -4	51 -4	25 -4	12 -3	39 -4
312	550	-91 -4	43 -4	-7 -6	75 -4	84 -4	29 -4
312	550	-87 -4	44 -4	26 -5	76 -4	88 -4	29 -4
312	600	-39 -4	44 -4	34 -4	15 -4	80 -4	27 -4
312	600	-38 -4	43 -4	35 -4	24 -4	79 -4	22 -4
312	650	-48 -4	57 -4	-23 -4	19 -4	59 -4	40 -4
312	650	-45 -4	58 -4	-18 -4	18 -4	62 -4	40 -4
312	650	-40 -4	59 -4	-18 -4	17 -4	73 -4	39 -4
312	700	-42 -4	45 -4	-63 -5	30 -4	53 -4	11 -4
312	700	-40 -4	47 -4	-46 -5	30 -4	53 -4	13 -4
312	750	-31 -4	36 -4	10 -4	11 -4	33 -4	20 -4
312	750	-26 -4	37 -4	18 -5	18 -4	35 -4	19 -4
312	750	-43 -4	36 -4	11 -4	12 -4	41 -4	21 -4
312	800	-56 -4	24 -4	46 -4	24 -4	40 -4	31 -4
312	800	-52 -4	23 -4	47 -4	25 -4	41 -4	30 -4
312	850	-37 -4	68 -4	33 -5	24 -4	80 -4	38 -4
312	850	-36 -4	67 -4	79 -5	24 -4	83 -4	39 -4
312	850	-29 -4	68 -4	14 -5	25 -4	87 -4	39 -4
312	900	15 -4	15 -4	97 -5	22 -4	61 -4	27 -4
312	900	16 -4	17 -4	13 -4	19 -4	64 -4	27 -4
312	900	19 -4	17 -4	22 -4	21 -4	72 -4	27 -4
312	950	-36 -4	24 -4	-13 -5	31 -4	17 -4	22 -5
312	950	-32 -4	24 -4	22 -5	34 -4	16 -4	16 -5
312	950	-35 -4	24 -4	-53 -5	34 -4	15 -4	49 -5
312	0	-22 -3	54 -4	15 -3	60 -4	10 -2	23 -4
313	0	-20 -3	76 -4	17 -3	58 -4	10 -2	25 -4
313	0	-21 -3	73 -4	16 -3	58 -4	10 -2	29 -4
313	50	-17 -3	71 -4	12 -3	80 -4	94 -3	16 -4
313	50	-16 -3	86 -4	14 -3	49 -4	92 -3	49 -4
313	50	-18 -3	57 -4	98 -4	63 -4	92 -3	45 -4
313	100	-13 -3	70 -4	10 -3	62 -4	60 -3	32 -4
313	100	-12 -3	69 -4	10 -3	60 -4	60 -3	32 -4
313	150	-11 -3	63 -4	59 -4	57 -4	46 -3	33 -4
313	150	-11 -3	63 -4	59 -4	49 -4	46 -3	34 -4
313	200	-97 -4	52 -4	68 -4	51 -4	33 -3	23 -4
313	200	-96 -4	48 -4	66 -4	54 -4	32 -3	23 -4
313	250	-60 -4	22 -4	23 -4	22 -4	29 -3	31 -4
313	250	-63 -4	22 -4	25 -4	22 -4	30 -3	30 -4
313	300	-42 -4	10 -4	41 -4	44 -4	27 -3	21 -4
313	300	-45 -4	10 -4	40 -4	44 -4	27 -3	21 -4
313	350	-49 -4	36 -4	32 -4	27 -4	22 -3	34 -4

Sample	Field	X-value	Sigm-X	Y-Value	Sigm-Y	Z-Value	Sigm-Z
313	350	-46	-4	35	-4	36	-4
313	400	-68	-4	24	-4	72	-4
313	400	-63	-4	22	-4	74	-4
313	450	-74	-4	22	-4	32	-4
313	450	-81	-4	22	-4	36	-4
313	500	-53	-4	16	-4	-85	-5
313	500	-48	-4	14	-4	-32	-5
313	500	-54	-4	14	-4	-13	-4
313	550	-69	-4	30	-4	-17	-4
313	550	-66	-4	30	-4	-13	-4
313	600	-54	-4	33	-4	11	-5
313	600	-48	-4	32	-4	34	-5
313	600	-49	-4	31	-4	25	-5
313	650	-50	-4	11	-4	-18	-4
313	650	-47	-4	93	-5	-13	-4
313	650	-53	-4	11	-4	-21	-4
313	700	-77	-4	44	-4	-10	-4
313	700	-71	-4	40	-4	-99	-5
313	750	15	-4	12	-4	17	-4
313	750	16	-4	13	-4	22	-4
313	750	21	-4	11	-4	20	-4
313	800	-13	-4	52	-4	-23	-4
313	800	-15	-4	51	-4	-21	-4
313	800	-16	-4	53	-4	-30	-4
313	850	-45	-5	46	-4	28	-4
313	850	-12	-5	45	-4	33	-4
313	850	-51	-5	45	-4	28	-4
313	900	-13	-4	10	-4	48	-5
313	900	-26	-4	20	-4	13	-4
313	900	-28	-4	19	-4	76	-5
313	900	-34	-4	20	-4	35	-5
313	900	-42	-4	19	-4	31	-5
413	0	-53	-4	34	-4	23	-3
413	0	-40	-4	32	-4	24	-3
413	50	11	-4	96	-4	30	-3
413	50	20	-4	10	-3	29	-3
413	100	12	-4	11	-3	26	-3
413	100	88	-5	11	-3	26	-3
413	150	42	-4	65	-4	13	-3
413	150	45	-4	65	-4	13	-3
413	200	46	-4	27	-4	19	-3
413	200	46	-4	27	-4	19	-3
413	250	-41	-4	15	-4	16	-3
413	250	-41	-4	16	-4	16	-3
413	300	11	-4	55	-4	16	-3
413	300	13	-4	54	-4	17	-3
413	350	11	-5	43	-4	10	-3
413	350	95	-6	42	-4	10	-3
413	400	83	-5	11	-4	51	-4
413	400	88	-5	13	-4	53	-4
413	450	43	-4	64	-4	11	-3
413	450	45	-4	65	-4	11	-3
413	500	14	-4	26	-4	11	-3
413	500	13	-4	28	-4	11	-3
413	550	12	-4	19	-4	84	-3
413	550	15	-4	19	-4	85	-4

Sample	Field	X-value	Sigm-X	Y-Value	Sigm-Y	Z-Value	Sigm-Z
413	600	49	-4	58	-4	62	-4
413	600	55	-4	58	-4	64	-4
413	650	-69	-6	25	-4	26	-4
413	650	-23	-5	27	-4	27	-4
413	700	-28	-4	36	-4	28	-4
413	700	-31	-4	37	-4	29	-4
413	750	14	-4	13	-4	-80	-6
413	750	13	-4	14	-4	43	-5
413	850	13	-4	15	-4	41	-5
413	800	62	-4	73	-4	-35	-4
413	800	62	-4	75	-4	-36	-4
413	850	64	-5	56	-4	15	-4
746	850	81	-5	56	-4	16	-4
413	900	59	-4	19	-4	77	-4
413	900	61	-4	17	-4	76	-4
413	950	-12	-4	31	-4	-18	-4
413	950	-14	-4	32	-4	-20	-4
411	0	-19	-4	63	-4	19	-3
411	0	-33	-4	64	-4	22	-3
411	50	-20	-4	87	-4	24	-3
411	50	-22	-5	94	-4	26	-3
411	100	-20	-4	58	-4	24	-3
411	100	32	-4	48	-4	17	-3
411	100	-49	-4	36	-4	23	-3
411	150	-36	-4	49	-4	23	-3
411	150	-31	-4	53	-4	22	-3
411	200	-51	-4	62	-4	14	-3
411	200	-49	-4	66	-4	14	-3
411	250	-36	-4	47	-4	11	-3
411	250	-31	-4	48	-4	11	-3
411	300	10	-4	65	-4	98	-4
411	300	15	-4	68	-4	91	-4
411	350	-14	-4	34	-4	64	-4
411	350	-12	-4	35	-4	66	-4
411	400	82	-5	34	-4	69	-4
411	400	18	-4	32	-4	66	-4
411	400	31	-5	31	-4	59	-4
411	450	-13	-4	26	-4	58	-4
411	450	-12	-4	27	-4	57	-4
411	500	48	-5	37	-4	25	-4
411	500	11	-4	38	-4	29	-4
411	500	10	-4	37	-4	21	-4
411	550	45	-5	29	-4	50	-4
411	550	11	-4	34	-4	54	-4
411	550	19	-4	30	-4	47	-4
411	600	-85	-6	24	-4	-22	-4
411	600	29	-5	24	-4	-17	-4
411	600	-15	-5	23	-4	-26	-4
411	650	-66	-5	16	-4	54	-5
411	650	-42	-5	17	-4	12	-5
411	650	-12	-4	15	-4	-75	-5
411	700	-13	-4	13	-4	31	-4
411	700	-12	-4	14	-4	36	-4
411	750	20	-4	29	-4	19	-4
411	750	27	-4	30	-4	22	-4
411	800	-34	-4	11	-4	32	-4

Sample	Field	X-value	Sigm-X	Y-Value	Sigm-Y	Z-Value	Sigm-Z
411	800	-23	-4	11	-4	35	-4
411	800	-22	-4	13	-4	35	-4
411	850	-17	-4	17	-4	15	-4
411	850	-17	-4	16	-4	17	-4
411	900	13	-4	28	-3	16	-4
411	900	11	-4	28	-4	71	-5
411	950	-25	-4	14	-4	68	-5
411	950	-19	-4	11	-4	71	-5
412	0	45	-4	11	-3	47	-3
412	100	75	-4	14	-3	45	-3
412	100	78	-4	14	-3	45	-3
412	50	13	-3	10	-6	44	-3
412	50	13	-3	93	-4	45	-3
412	100	11	-3	56	-4	30	-3
412	100	11	-3	65	-4	30	-3
412	150	89	-4	52	-4	22	-2
412	150	94	-4	48	-4	22	-3
412	150	82	-4	39	-4	18	-3
412	200	87	-4	43	-4	18	-3
412	250	-16	-5	45	-4	13	-3
412	250	58	-5	47	-4	11	-3
412	300	94	-5	28	-4	10	-3
412	300	12	-4	43	-4	13	-3
412	350	-25	-4	13	-4	95	-4
412	350	-20	-4	14	-4	97	-4
412	400	-48	-4	36	-4	15	-4
412	400	-44	-4	36	-4	16	-4
412	450	-29	-4	60	-4	73	-4
412	450	-31	-4	60	-4	75	-4
412	500	-37	-4	13	-4	24	-4
412	500	-35	-4	13	-4	25	-4
412	550	-30	-4	49	-4	50	-4
412	550	-31	-4	51	-4	49	-4
412	600	17	-4	13	-4	-29	-5
412	600	19	-4	13	-4	-23	-5
412	600	15	-4	13	-4	-6	-5
412	650	28	-4	42	-4	55	-4
412	650	29	-4	41	-4	59	-4
412	700	-65	-4	39	-4	17	-5
412	700	-61	-4	38	-4	25	-5
412	750	-45	-4	31	-4	13	-4
412	750	-41	-4	31	-4	13	-4
412	750	-42	-4	32	-4	13	-4
412	800	30	-4	43	-4	16	-4
412	800	33	-4	47	-4	17	-4
412	850	-46	-4	97	-4	-66	-4
412	850	-48	-4	99	-4	-35	-4
412	900	16	-4	21	-4	-27	-4
412	900	14	-4	20	-4	-25	-4
412	950	-17	-4	21	-4	-13	-4
412	950	-21	-4	23	-4	-13	-4
513	0	-47	-3	28	-3	-46	-3
513	0	-49	-3	29	-3	-45	-3
513	50	-20	-5	91	-4	-22	-3
513	50	94	-5	91	-4	-21	-3
513	100	31	-4	23	-4	-10	-3

Sample	Field	X-value	Sigm-X	Y-Value	Sigm-Y	Z-Value	Sigm-Z
513	100	18 -4	50 -4	-11 -3	32 -4	93 -3	96 -4
513	100	44 -4	33 -4	-12 -3	27 -4	93 -3	90 -4
513	150	94 -5	39 -4	-13 -3	44 -4	59 -3	57 -4
513	150	26 -4	42 -4	-11 -3	41 -4	59 -3	59 -4
513	150	94 -5	40 -4	-12 -3	47 -4	59 -3	60 -4
513	200	-14 -4	47 -4	-93 -4	58 -4	38 -3	48 -4
513	200	-28 -4	49 -4	-93 -4	57 -4	38 -3	45 -4
513	200	-45 -4	80 -4	-11 -3	27 -4	46 -3	65 -4
513	250	-54 -4	63 -4	-14 -3	36 -4	38 -3	65 -4
513	250	-3 -4	67 -4	-13 -3	34 -4	39 -3	66 -4
513	300	-15 -4	49 -4	-81 -3	40 -4	29 -3	79 -4
513	300	-49 -4	53 -4	-81 -4	41 -4	29 -3	80 -4
513	300	-20 -4	51 -4	-88 -4	41 -4	28 -3	78 -4
513	350	-82 -5	26 -4	-40 -4	38 -4	25 -3	20 -4
513	350	-85 -5	22 -4	-40 -4	33 -4	26 -3	22 -4
513	400	99 -5	51 -4	-47 -4	45 -4	23 -3	61 -4
513	400	89 -5	52 -4	-48 -4	46 -4	23 -3	62 -4
513	450	-18 -4	43 -4	-24 -4	63 -4	17 -3	75 -4
513	450	-10 -4	46 -4	-48 -4	64 -4	48 -3	75 -4
513	500	-61 -4	58 -4	-73 -4	55 -4	17 -3	51 -4
513	500	-55 -4	57 -4	-73 -4	52 -4	17 -3	51 -4
513	550	-23 -4	29 -4	-10 -3	46 -4	13 -3	19 -4
513	550	-23 -4	30 -4	-11 -3	50 -4	14 -3	16 -4
513	600	-84 -4	62 -4	-96 -4	51 -4	13 -3	27 -4
513	600	-89 -4	62 -3	-89 -4	52 -4	13 -3	27 -4
513	650	24 -4	43 -3	79 -4	36 -4	53 -4	32 -4
513	650	23 -4	41 -4	77 -4	36 -4	53 -4	30 -4
513	700	26 -4	54 -4	-22 -4	67 -4	13 -3	59 -4
513	700	30 -4	52 -4	-18 -4	70 -4	13 -3	61 -4
513	750	12 -4	35 -4	-70 -4	29 -4	69 -4	30 -4
513	750	12 -4	39 -4	-67 -4	31 -4	65 -4	30 -4
513	750	-53 -5	34 -4	-80 -4	26 -4	78 -4	29 -4
513	800	-11 -4	54 -4	-13 -4	28 -4	45 -4	37 -4
513	800	-34 -5	56 -4	-78 -5	34 -4	47 -4	38 -4
513	800	-19 -4	51 -4	-23 -4	28 -4	54 -4	37 -4
513	850	-71 -5	14 -4	17 -4	23 -4	59 -4	84 -5
513	850	-80 -5	15 -4	13 -4	24 -4	62 -4	73 -5
513	900	-38 -4	39 -4	19 -5	64 -4	11 -3	31 -4
513	900	-36 -4	42 -4	73 -5	65 -4	11 -3	33 -4
513	900	-35 -4	40 -4	63 -5	66 -4	11 -3	34 -4
513	950	-20 -4	49 -4	-26 -5	27 -4	57 -5	35 -4
513	950	-22 -4	49 -4	19 -5	26 -4	49 -5	35 -4
513	950	-27 -4	48 -4	16 -5	28 -4	17 -4	33 -4
511	0	97 -4	10 -3	-65 -3	94 -4	15 -2	21 -4
511	0	13 -3	99 -4	-61 -3	10 -3	15 -2	25 -4
511	50	55 -4	48 -4	-14 -3	34 -4	11 -2	38 -4
511	50	55 -4	49 -4	-14 -3	32 -4	11 -3	45 -4
512	100	25 -4	33 -4	-13 -3	47 -4	78 -3	33 -4
511	100	20 -4	24 -4	-11 -3	41 -4	79 -3	36 -4
511	150	-52 -5	49 -4	-98 -4	38 -4	56 -3	28 -4
511	150	-1 -4	50 -4	-98 -4	47 -4	56 -3	33 -4
511	200	-35 -4	38 -4	-68 -4	45 -4	46 -3	19 -4
511	200	-33 -4	40 -4	-69 -4	45 -4	45 -3	21 -4
511	250	-81 -5	10 -4	-36 -4	13 -4	40 -3	34 -4
511	250	-32 -5	11 -4	-34 -4	13 -4	40 -3	35 -5
511	250	-10 -4	11 -4	-54 -4	18 -4	40 -3	28 -4

Sample	Field	X-value	Sigm-X	Y-Value	Sigm-Y	Z-Value	Sigm-Z
511	300	17	-4	12	-4	16	-4
511	300	20	-4	12	-4	20	-4
511	350	51	-4	25	-4	-77	-5
511	350	55	-4	22	-4	-26	-5
511	350	15	-4	25	-4	-14	-4
511	400	27	-4	25	-4	-83	-5
511	400	28	-4	24	-4	-59	-5
511	400	23	-4	27	-4	-18	-4
511	450	-32	-4	24	-4	-51	-4
511	450	-26	-4	26	-4	-50	-4
511	500	-44	-4	18	-4	-33	-4
511	500	-43	-4	23	-4	-28	-4
511	550	-24	-4	18	-4	-56	-4
511	550	-29	-4	16	-4	-55	-6
511	600	21	-4	32	-4	-69	-4
511	600	21	-4	32	-4	-68	-4
511	650	-16	-4	23	-4	-52	-4
511	650	-12	-4	24	-4	-53	-4
511	700	-50	-5	28	-4	-54	-4
511	700	-55	-5	28	-4	-55	-4
511	750	-70	-4	30	-4	-20	-4
511	750	-67	-4	31	-4	-19	-4
511	800	47	-6	33	-4	-40	-4
511	800	55	-5	33	-4	-37	-4
511	800	-47	-5	30	-4	-42	-4
511	850	41	-5	17	-4	-36	-4
511	850	50	-5	18	-4	-37	-4
511	900	-42	-6	15	-4	-28	-4
511	900	25	-6	15	-4	-26	-4
511	950	-38	-4	39	-4	-38	-4
511	950	-33	-4	39	-6	-36	-4
512	0	12	-3	31	-3	-14	-3
512	0	38	-4	20	-3	-14	-3
512	0	75	-4	19	-3	-19	-3
512	50	13	-3	81	-4	-14	-3
512	50	10	-3	10	-3	-15	-3
512	50	12	-3	77	-4	-15	-3
512	100	-31	-4	31	-4	-12	-3
512	100	11	-3	31	-4	-11	-3
512	100	11	-3	34	-4	-12	-3
512	150	80	-4	37	-4	-73	-4
512	150	85	-4	42	-4	-75	-4
512	200	70	-4	53	-4	-47	-4
512	200	75	-4	53	-4	-50	-4
512	250	96	-5	87	-4	-76	-4
512	250	13	-4	99	-4	-78	-4
512	300	46	-5	40	-4	-87	-4
512	300	88	-5	41	-4	-86	-4
512	350	15	-4	38	-4	-18	-4
512	350	20	-4	39	-4	-17	-4
512	400	96	-5	22	-4	15	-4
512	400	94	-5	22	-4	15	-4
512	450	-45	-5	10	-4	-10	-4
512	450	-32	-5	11	-4	-10	-4
512	500	62	-4	26	-4	79	-5
512	500	69	-4	26	-4	83	-5

Sample	Field	X-value	Sigm-X	Y-Value	Sigm-Y	Z-Value	Sigm-Z
512	550	-33	-4	32	-4	-10	-3
512	550	-33	-4	29	-4	-86	-4
512	550	-29	-4	28	-4	-84	-4
512	650	29	-4	68	-5	-41	-4
512	650	26	-4	74	-5	-39	-4
512	700	30	-4	37	-4	-90	-4
512	700	33	-4	36	-4	-88	-4
512	750	10	-4	22	-4	26	-4
511	750	80	-5	23	-4	28	-4
512	750	28	-5	22	-4	27	-4
512	800	-27	-4	40	-4	85	-5
512	800	-24	-4	39	-4	10	-4
212	800	-23	-4	40	-4	43	-5
512	850	45	-5	43	-4	-38	-4
512	850	84	-5	41	-4	-37	-4
512	850	19	-5	44	-4	-58	-4
512	900	14	-4	24	-4	-15	-4
512	900	12	-4	23	-4	-16	-4
512	900	98	-5	24	-4	-21	-4
512	950	16	-6	33	-4	-21	-4
512	950	42	-5	34	-4	-18	-4
512	950	11	-4	37	-4	-91	-5
611	0	-15	-5	32	-5	18	-4
611	0	-41	-5	22	-5	20	-4
611	0	-50	-6	43	-5	23	-4
611	50	-47	-5	50	-5	89	-5
611	50	-44	-5	46	-5	80	-5
611	500	-44	-5	50	-5	89	-5
611	100	-44	-5	59	-5	10	-5
611	100	-44	-5	60	-5	59	-6
611	150	-53	-5	51	-5	-52	-5
611	150	-56	-5	50	-5	-53	-5
611	200	-59	-5	66	-5	-21	-5
611	200	-56	-5	68	-5	-20	-5
611	250	-46	-5	51	-5	-22	-5
611	250	-48	-5	49	-5	-24	-5
611	300	-44	-5	44	-5	-39	-5
611	300	-57	-5	25	-5	-27	-5
611	300	-44	-5	42	-5	-27	-5
611	350	-35	-5	-26	-5	-92	-6
611	350	-34	-5	29	-5	-24	-5
611	350	-34	-5	26	-5	-11	-5
611	400	-26	-5	44	-5	-15	-5
611	400	-27	-5	46	-5	-15	-5
611	450	86	-6	49	-5	-52	-5
611	450	95	-6	47	-5	-50	-5
611	500	30	-5	33	-5	-66	-5
611	500	30	-5	33	-5	-66	-5
611	600	-44	-6	32	-5	-40	-5
611	600	-45	-6	31	-5	-41	-5
611	700	79	-6	35	-5	-50	-5
611	700	82	-6	35	-5	-48	-5
611	800	-25	-5	33	-5	-52	-5
611	800	-26	-5	34	-5	-51	-5
611	900	-27	-5	25	-5	-22	-5
611	900	-25	-5	25	-5	-21	-5

Sample	Field	X-value	Sigm-X	Y-Value	Sigm-Y	Z-Value	Sigm-Z
611	900	-28	-5	25 -5	-24 -5	69 -5	55 -6
612	0	-86	-5	95 -5	83 -5	24 -5	10 -3
612	0	-83	-5	93 -5	78 -5	25 -5	10 -3
612	50	-86	-5	55 -5	47 -5	32 -5	68 -4
612	50	-85	-5	62 -5	45 -5	33 -5	68 -4
612	100	-72	-5	38 -5	29 -5	38 -5	32 -4
612	100	-71	-5	43 -5	29 -5	35 -5	32 -4
612	150	-43	-5	37 -5	-17 -5	23 -5	17 -4
612	150	-42	-5	33 -5	-17 -5	24 -5	16 -4
612	200	-40	-5	61 -5	-58 -5	21 -5	12 -4
612	200	-48	-5	48 -5	-48 -5	23 -5	14 -4
612	200	-43	-5	59 -5	-55 -5	16 -5	11 -5
612	250	-42	-5	45 -5	16 -5	44 -5	81 -5
612	250	-41	-5	47 -5	16 -5	45 -5	82 -5
612	300	-53	-5	49 -5	-32 -5	34 -5	31 -5
612	300	-52	-5	48 -5	-33 -5	32 -5	31 -5
612	350	-22	-5	23 -5	-55 -5	18 -5	46 -5
612	350	-24	-5	20 -5	-53 -5	19 -5	43 -5
612	400	-53	-5	60 -5	-17 -5	56 -5	31 -5
612	400	-55	-5	60 -5	-14 -5	54 -5	33 -5
612	500	15	-5	18 -5	-60 -5	32 -5	44 -5
612	500	15	-5	17 -5	-59 -5	32 -5	42 -5
612	600	-18	-5	19 -5	-18 -5	32 -5	16 -5
612	600	-31	-6	42 -5	-15 -5	20 -5	13 -5
612	700	-59	-6	32 -5	-19 -5	29 -5	39 -5
612	700	-69	-6	33 -5	-19 -5	28 -5	39 -5
612	800	-31	-5	53 -5	14 -5	61 -5	61 -5
612	800	-32	-5	48 -5	50 -6	37 -5	52 -5
612	800	-35	-5	51 -5	-99 -7	47 -5	61 -5
613	0	-13	-5	28 -5	-13 -4	85 -5	11 -3
613	0	-13	-4	26 -5	-34 -5	11 -4	10 -3
613	0	-13	-4	35 -5	-24 -5	12 -4	10 -3
613	100	-74	-5	60 -5	-61 -5	76 -5	28 -4
613	100	-71	-5	56 -5	-57 -5	80 -5	28 -4
613	200	-46	-5	13 -5	-16 -5	53 -5	93 -5
613	200	-45	-5	13 -5	-17 -5	52 -5	94 -5
613	300	-30	-5	53 -5	-53 -5	25 -5	83 -5
613	300	-32	-5	54 -5	-50 -5	28 -5	86 -5
613	400	-41	-5	45 -5	-81 -5	13 -5	39 -5
613	400	-54	-5	29 -5	-92 -5	22 -5	23 -5
613	400	-54	-5	29 -5	-93 -5	21 -5	24 -5
613	500	-54	-5	42 -5	-34 -5	18 -5	16 -5
613	500	-41	-5	23 -5	-34 -5	18 -5	16 -5
613	500	-42	-5	23 -5	-35 -5	18 -5	59 -6
613	600	-63	-6	41 -5	-13 -5	56 -5	-36 -5
613	600	-81	-6	43 -5	-14 -5	55 -5	-39 -5
613	700	80	-6	12 -5	24 -6	27 -5	-17 -5
613	700	79	-6	12 -5	22 -6	26 -5	-17 -5
613	800	-29	-5	19 -5	-44 -5	17 -5	22 -5
613	800	-31	-5	19 -5	-45 -5	17 -5	23 -5
613	900	-12	-7	13 -5	-96 -6	23 -5	-16 -5
613	900	-10	-5	21 -5	-14 -5	24 -5	-18 -5
613	900	-10	-5	20 -5	-87 -6	23 -5	-12 -5
711	0	18	-5	41 -5	34 -5	65 -5	60 -5
711	0	56	-6	39 -5	36 -5	73 -5	61 -4
711	0	42	-6	40 -5	35 -5	72 -5	60 -4
711	0	42	-6	40 -5	35 -5	72 -5	34 -5

Sample	Field	X-value	Sigm-X	Y-Value	Sigm-Y	Z-Value	Sigm-Z
711	50	-10	-5	39	-5	22	-5
711	50	-10	-5	40	-5	31	-5
711	50	-11	-5	38	-5	24	-5
711	100	-24	-5	28	-5	19	-5
711	100	-26	-5	28	-5	19	-5
711	150	-54	-5	32	-5	-13	-5
711	150	-52	-5	31	-5	-11	-5
711	200	-12	-5	18	-5	33	-5
711	200	-62	-5	15	-5	68	-7
711	200	-10	-5	15	-5	-71	-6
711	250	-11	-5	27	-6	-65	-7
711	250	-12	-5	30	-6	-22	-7
711	300	30	-6	25	-5	10	-7
711	300	31	-6	26	-5	-12	-5
711	300	27	-6	26	-5	-36	-6
711	400	23	-5	87	-6	51	-5
711	400	23	-5	88	-6	52	-5
711	500	-22	-5	40	-5	16	-5
711	500	-24	-5	49	-5	13	-5
711	500	-21	-5	39	-5	15	-5
711	600	14	-5	34	-5	38	-5
711	600	13	-5	35	-5	39	-5
711	700	-21	-5	29	-5	27	-5
711	700	-20	-5	29	-5	26	-5
711	800	-37	-5	27	-5	26	-5
711	800	-36	-5	27	-5	23	-5
711	800	-37	-5	29	-5	19	-5
712	0	29	-5	97	-5	-47	-5
712	0	27	-5	95	-5	-47	-5
712	100	28	-5	52	-5	-56	-6
712	100	25	-5	55	-5	66	-6
712	100	36	-5	59	-5	19	-5
712	200	35	-5	27	-5	48	-5
712	200	37	-5	26	-5	49	-5
712	300	53	-6	32	-5	37	-5
712	300	41	-6	32	-5	28	-5
712	400	-12	-6	11	-5	16	-5
712	400	-11	-6	11	-5	18	-5
712	500	56	-6	25	-5	30	-5
712	500	54	-6	25	-5	21	-5
712	500	59	-6	25	-5	30	-5
712	600	35	-7	17	-5	26	-5
712	600	15	-6	17	-5	29	-5
712	600	30	-7	17	-5	26	-5
712	700	15	-5	13	-5	22	-5
712	700	15	-5	12	-5	22	-5
712	800	-13	-5	16	-5	-29	-5
712	800	-12	-5	15	-5	-29	-5
712	900	16	-5	26	-5	25	-5
712	900	17	-5	26	-5	24	-5
713	0	40	-5	93	-5	33	-5
713	0	39	-5	90	-5	35	-5
713	100	-21	-5	44	-5	23	-5
713	100	-24	-5	42	-5	21	-5
713	100	-33	-5	35	-5	22	-5
713	200	35	-6	15	-5	28	-5

Sample	Field	X-value	Sigm-X	Y-Value	Sigm-Y	Z-Value	Sigm-Z
713	200	20	-6	16	-5	28	-5
713	200	38	-6	17	-5	27	-5
713	300	-15	-5	18	-5	-64	-6
713	300	-19	-5	17	-5	-54	-6
713	300	-19	-5	17	-5	-61	-6
713	400	-22	-5	16	-5	40	-5
713	400	-22	-5	16	-5	41	-5
713	400	-23	-5	17	-5	42	-5
713	500	-30	-6	23	-5	13	-5
713	500	-20	-6	23	-5	15	-6
713	500	-17	-6	22	-5	77	-7
713	600	-40	-5	18	-5	20	-6
713	600	-41	-5	19	-5	22	-6
713	700	-34	-5	14	-5	13	-5
713	700	-32	-5	16	-5	12	-5
713	800	-50	-5	29	-5	-12	-5
713	800	-50	-5	29	-5	-11	-5
713	900	-35	-5	81	-5	32	-6
713	900	-34	-5	85	-6	33	-6
811	0	-10	-5	16	-5	-27	-6
811	0	-10	-5	16	-4	-26	-6
811	100	-42	-6	13	-5	48	-6
811	100	-25	-6	16	-5	46	-6
811	100	-32	-6	16	-5	46	-6
811	200	-99	-6	22	-5	87	-5
811	200	-10	-5	23	-5	99	-6
811	200	-97	-6	22	-5	97	-6
811	300	72	-6	13	-5	58	-6
811	300	74	-6	13	-5	47	-6
811	300	76	-6	12	-5	84	-6
811	400	55	-6	18	-5	59	-6
811	400	65	-6	17	-5	86	-6
811	400	65	-6	18	-5	76	-6
811	500	-15	-5	23	-5	20	-5
811	500	-17	-5	23	-5	20	-5
811	600	-24	-6	99	-6	23	-5
811	600	-17	-6	95	-6	24	-5
811	700	-39	-5	16	-5	23	-7
811	700	-32	-6	16	-5	85	-7
811	700	-37	-6	17	-5	42	-7
811	800	-11	-6	12	-5	15	-5
811	800	-17	-6	12	-5	16	-5
811	900	-17	-6	19	-5	-98	-8
811	900	-15	-6	20	-5	38	-6
811	900	-16	-6	19	-5	31	-6
812	0	-23	-5	16	-5	18	-5
812	0	-24	-5	16	-5	17	-5
812	100	-23	-5	81	-6	87	-6
812	100	-24	-5	86	-6	91	-6
812	200	-26	-5	19	-5	30	-5
812	200	-25	-5	18	-5	29	-5
812	300	-27	-5	19	-5	37	-5
812	300	-27	-5	20	-5	38	-5
812	400	-31	-5	29	-5	12	-5
812	400	-30	-5	28	-5	11	-5
812	400	-29	-5	28	-5	12	-5

Sample	Field	X-value	Sigm-X	Y-Value	Sigm-Y	Z-Value	Sigm-Z
812	500	-32	-5	27	-5	-40	-6
812	500	-33	-5	27	-5	-26	-6
812	600	-15	-6	17	-5	-38	-6
812	600	-15	-6	17	-5	-30	-6
812	700	14	-6	38	-5	-15	-6
812	700	17	-6	38	-5	-65	-6
812	800	-32	-5	19	-5	33	-5
812	800	-32	-5	19	-5	34	-5
812	900	-57	-5	17	-5	27	-5
812	900	-58	-5	16	-5	26	-5
813	0	-26	-5	12	-5	18	-5
813	0	-31	-5	63	-6	20	-5
813	100	-29	-5	66	-6	56	-6
813	100	-30	-5	64	-6	58	-6
813	200	-41	-5	12	-5	-27	-5
813	200	-41	-5	14	-5	-25	-5
813	300	-47	-5	14	-5	-35	-5
813	300	-16	-5	13	-5	-35	-5
813	400	-56	-6	17	-5	13	-5
813	400	-63	-6	16	-5	12	-5
813	400	-79	-6	15	-5	12	-5
813	500	-21	-5	26	-5	48	-6
813	500	-24	-5	29	-5	44	-6
813	600	-33	-5	15	-5	80	-6
813	600	-34	-5	15	-5	75	-6
813	700	11	-5	10	-5	26	-5
813	700	12	-5	10	-5	26	-5
813	800	-60	-6	49	-6	14	-5
813	800	-53	-6	43	-6	14	-5
813	900	-14	-5	84	-6	68	-6
813	900	-90	-6	63	-6	37	-6
813	900	-15	-5	90	-6	61	-6
911	0	-29	-3	80	-4	42	-4
911	0	-30	-3	81	-4	44	-4
911	200	-67	-4	23	-4	85	-5
911	200	-64	-4	23	-4	79	-5
911	300	-14	-4	14	-4	25	-6
911	300	-12	-4	15	-4	70	-6
911	300	-16	-4	11	-4	-16	-4
911	400	-89	-5	94	-5	-13	-4
911	400	-70	-5	85	-5	-12	-4
911	400	-88	-5	11	-4	-16	-4
911	500	-35	-4	14	-5	-14	-4
911	500	-32	-4	13	-4	-14	-4
911	600	-43	-4	16	-4	11	-4
911	600	-43	-4	15	-4	11	-4
911	700	-26	-4	22	-4	16	-4
911	700	-25	-4	22	-4	15	-4
911	800	61	-5	17	-4	-79	-5
911	800	49	-5	17	-4	-53	-5
911	800	20	-6	17	-4	-94	-5
911	900	-22	-4	23	-4	15	-5
911	900	-20	-4	22	-4	35	-5
911	900	-20	-4	22	-4	-70	-6
911	900	-20	-4	22	-4	24	-5
912	0	-52	-3	33	-4	46	-3

Sample	Field	X-value	Sigm-X	Y-Value	Sigm-Y	Z-Value	Sigm-Z
912	0	-54	-3	48	-4	47	-3
912	50	-19	-3	60	-4	71	-4
912	50	-19	-3	63	-4	68	-4
912	100	-64	-4	43	-4	17	-4
912	100	-10	-3	38	-4	15	-4
912	150	-65	-4	30	-4	73	-5
912	200	29	-5	12	-4	-18	-4
912	200	22	-5	12	-4	-18	-4
912	200	26	-5	12	-4	-23	-4
912	250	-29	-4	28	-4	-52	-4
912	250	-28	-4	29	-4	-53	-4
912	300	-17	-4	33	-4	-96	-4
912	300	-13	-4	35	-4	-95	-4
912	350	-47	-4	36	-4	-28	-4
912	350	-38	-4	34	-4	-27	-4
912	350	-40	-4	34	-4	-31	-4
912	450	-26	-5	28	-4	-54	-5
912	450	-18	-5	25	-4	-41	-5
912	450	-76	-6	26	-4	-42	-5
912	550	-42	-4	30	-4	22	-4
912	550	-40	-4	30	-4	22	-4
912	650	-21	-4	34	-4	-45	-6
912	650	-22	-4	34	-4	20	-5
912	650	-26	-4	33	-4	-47	-5
912	750	-44	-5	46	-4	-18	-4
912	750	-14	-5	43	-4	-15	-4
912	750	-17	-5	43	-4	-18	-4
912	850	-25	-4	46	-4	-33	-4
912	850	-22	-4	47	-4	-36	-4
912	950	-16	-4	32	-4	81	-7
912	950	-19	-4	32	-8	-48	-5
913	0	-22	-3	73	-4	-13	-3
913	0	-20	-3	-37	-4	-12	-3
913	75	-69	-4	66	-4	-18	-4
913	75	-68	-4	61	-4	-15	-4
913	175	-46	-5	20	-4	96	-5
913	175	-24	-4	15	-4	-94	-5
913	175	-34	-4	16	-4	-14	-4
913	275	-27	-4	31	-4	12	-4
913	275	-25	-4	32	-4	13	-4
913	375	-44	-4	13	-4	13	-4
913	375	-43	-4	13	-4	13	-4
913	475	-25	-4	13	-4	59	-6
913	475	-23	-4	13	-4	16	-5
913	475	-23	-4	13	-4	-20	-5
913	575	-47	-5	28	-4	23	-4
913	575	-35	-5	27	-4	23	-4
913	575	-33	-5	27	-4	30	-4
913	675	15	-4	20	-4	-26	-4
913	675	16	-4	19	-4	-24	-4
913	775	11	-4	14	-4	-11	-4
913	775	12	-4	14	-4	-12	-4
913	875	-17	-4	27	-4	75	-5
1011	0	-25	-5	60	-4	-35	-4
1011	0	11	-5	61	-4	-42	-4
1011	0	-11	-4	56	-4	-50	-4

Sample	Field	X-value	Sigm-X	Y-Value	Sigm-Y	Z-Value	Sigm-Z
1011	50	-38	-4	54	-4	-45	-4
1011	50	-35	-4	47	-4	-42	-4
1011	100	-26	-4	80	-5	-26	-4
1011	100	-17	-4	22	-4	-19	-4
1011	150	-10	-4	15	-4	-35	-4
1011	150	-11	-4	14	-4	-41	-4
1011	200	-16	-3	11	-4	-18	-4
1011	200	-10	-4	82	-5	-16	-4
1011	250	-85	-5	39	-5	41	-5
1011	250	-47	-5	42	-5	43	-5
1011	300	-33	-4	62	-5	-15	-4
1011	300	-38	-4	58	-5	-56	-5
1011	350	-13	-4	31	-5	-30	-5
1011	350	-11	-4	44	-5	16	-5
1011	400	-52	-5	58	-5	23	-5
1011	400	-54	-5	49	-5	26	-4
1011	450	18	-5	10	-4	83	-5
1011	450	-25	-5	78	-5	12	-4
1011	500	-73	-5	17	-5	26	-4
1011	500	-81	-5	20	-5	28	-5
1012	0	-69	-5	83	-4	-17	-3
1012	0	46	-5	87	-4	-17	-3
1012	50	-15	-4	32	-4	-28	-4
1012	50	-26	-4	17	-4	-24	-4
1012	100	-33	-4	13	-4	-52	-5
1012	100	-33	-4	13	-4	-12	-5
1012	150	-37	-4	93	-5	-80	-5
1012	150	-35	-4	88	-5	-65	-5
1012	200	-31	-4	13	-4	-68	-5
1012	200	-31	-4	15	-4	-62	-5
1012	200	-30	-4	12	-4	-66	-6
1012	250	-30	-4	30	-4	-26	-5
1012	250	-28	-4	28	-4	-59	-5
1012	300	-41	-4	26	-4	16	-5
1012	300	-37	-4	20	-4	11	-5
1012	350	-24	-4	19	-4	-50	-4
1012	350	-27	-4	18	-4	-48	-4
1012	400	85	-6	14	-4	-46	-4
1012	400	14	-5	14	-4	-41	-4
1012	450	26	-5	12	-4	-34	-4
1012	450	-10	-5	11	-4	-33	-4
1012	500	16	-4	22	-4	-25	-4
1012	500	12	-4	19	-4	-22	-4
1012	550	-25	-4	70	-5	-23	-4
1012	550	-26	-4	72	-5	-20	-4
1012	600	25	-5	61	-5	-28	-5
1012	600	-34	-5	31	-5	-28	-4
1012	650	-28	-4	32	-4	-86	-4
1012	650	-29	-4	35	-4	-85	-4
1012	700	-20	-4	23	-4	-13	-4
1012	700	-18	-4	21	-4	-14	-4
1013	0	-62	-4	64	-4	-21	-3
1013	0	-60	-4	57	-4	-20	-3
1013	50	-87	-4	39	-4	-14	-3
1013	50	-93	-4	39	-4	-14	-3
1013	100	-96	-4	51	-4	-75	-4

Sample	Field	X-value	Sigm-X	Y-Value	Sigm-Y	Z-Value	Sigm-Z
1013	100	-95	-4	55	-4	-73	-4
1013	150	-50	-4	25	-4	-15	-4
1013	150	14	-4	11	-3	-11	-4
1013	200	-55	-4	72	-4	87	-5
1013	200	-57	-4	75	-4	12	-4
1013	250	34	-5	29	-4	-74	-5
1013	250	43	-5	29	-4	-71	-5
1013	300	40	-4	18	-4	-22	-4
1013	300	39	-4	16	-4	-17	-4
1013	350	48	-5	38	-4	-95	-6
1013	350	51	-5	36	-4	10	-5
1013	400	88	-5	22	-4	68	-7
1013	400	87	-5	22	-4	21	-5
1013	450	16	-5	34	-4	26	-5
1013	450	24	-6	31	-4	53	-5
1013	500	17	-6	48	-4	14	-4
1013	500	20	-6	17	-4	19	-4
1112	0	-10	-3	49	-3	63	-4
1112	0	93	-4	15	-3	29	-4
1112	0	75	-4	14	-3	30	-4
1112	100	24	-4	49	-4	23	-4
1112	100	28	-4	47	-4	23	-4
1112	100	19	-4	44	-4	45	-4
1112	200	19	-4	10	-4	19	-4
1112	200	21	-4	12	-4	22	-4
1112	300	11	-5	28	-4	29	-5
1112	300	36	-5	31	-4	55	-5
1112	300	42	-5	31	-4	-26	-5
1112	400	16	-4	19	-4	-22	-5
1112	400	19	-4	19	-4	-63	-6
1112	400	18	-4	19	-4	-27	-5
1112	400	17	-4	20	-4	-10	-4
1112	500	-13	-4	49	-4	71	-5
1112	500	-10	-4	47	-4	93	-5
1112	500	-18	-4	52	-4	41	-6
1112	500	-17	-4	51	-4	-39	-5
1112	600	-20	-6	45	-4	18	-4
1113	600	35	-6	18	-4	41	-4
1112	600	39	-5	19	-4	40	-4
1112	700	-16	-4	34	-4	10	-4
1112	700	-16	-4	35	-4	14	-4
1112	700	-18	-4	32	-4	12	-4
1112	800	14	-4	24	-4	28	-4
1112	800	18	-4	23	-4	32	-4
1113	0	22	-4	29	-4	20	-4
1113	0	16	-4	32	-4	20	-4
1113	0	35	-4	35	-4	22	-4
1113	50	-45	-5	17	-4	11	-4
1113	50	-32	-5	17	-4	14	-4
1211	0	29	-3	18	-3	56	-4
1211	0	29	-3	18	-3	74	-4
1211	0	30	-3	19	-3	54	-4
1211	100	10	-3	75	-4	18	-4
1211	100	11	-3	76	-4	20	-4
1211	200	57	-4	30	-4	10	-4
1211	200	59	-4	29	-4	15	-4

Sample	Field	X-value	Sigm-X	Y-Value	Sigm-Y	Z-Value	Sigm-Z
1211	200	55	-4	30	-4	96	-5
1211	300	24	-4	27	-4	-13	-4
1211	300	28	-4	27	-4	-11	-4
1211	300	26	-4	26	-4	-17	-4
1211	400	-46	-5	21	-4	-16	-4
1211	400	87	-7	50	-4	-13	-4
1211	400	-57	-5	21	-4	-29	-4
1211	500	53	-4	31	-4	-32	-4
1211	500	47	-4	29	-4	-40	-5
1211	500	45	-4	29	-4	-41	-4
1211	600	29	-5	64	-5	-47	-5
1211	600	11	-4	60	-5	-62	-5
1211	600	61	-5	73	-5	-10	-4
1211	600	56	-6	75	-5	-14	-4
1211	600	-23	-6	80	-5	-18	-4
1211	600	50	-5	73	-5	-97	-5
1211	600	87	-5	81	-5	-50	-5
1211	600	11	-4	70	-5	-24	-5
1211	600	11	-4	60	-5	-20	-5
1211	600	11	-4	67	-5	-50	-6
1211	600	12	-4	71	-5	76	-6
1211	700	-19	-5	82	-5	60	-5
1211	700	-13	-5	92	-5	72	-5
1211	800	87	-5	22	-4	-10	-4
1211	800	10	-4	21	-4	-50	-5
1211	800	10	-4	21	-4	-28	-5
1211	800	-48	-4	38	-4	-52	-4
1212	0	-49	-4	40	-4	-51	-4
1212	50	10	-4	29	-4	16	-4
1212	50	12	-4	29	-4	14	-4
1212	50	11	-4	29	-4	75	-5
1212	150	15	-4	34	-4	34	-4
1212	150	12	-4	35	-4	35	-4
1212	250	74	-5	23	-4	34	-4
1212	250	88	-5	23	-4	34	-4
1212	350	-49	-7	67	-5	13	-5
1212	350	34	-5	70	-5	22	-5
1212	350	78	-6	59	-5	-67	-5
1212	450	-94	-5	29	-4	-32	-5
1212	450	-65	-5	30	-4	-14	-5
1212	550	-24	-4	12	-4	16	-4
1212	550	-21	-4	13	-4	16	-4
1212	650	15	-4	25	-4	75	-5
1212	650	13	-4	25	-4	54	-5
1212	750	34	-5	22	-4	-15	-4
1212	750	70	-5	24	-4	-13	-4
1212	750	67	-5	24	-4	-13	-4
1212	850	20	-4	65	-5	17	-4
1212	850	22	-4	65	-5	18	-4
1212	950	88	-5	97	-5	-34	-5
1212	950	63	-5	82	-5	-98	-5
1212	950	66	-5	91	-5	-11	-4
1213	0	31	-4	19	-4	-89	-5
1213	0	37	-4	19	-4	-67	-5
1213	100	41	-4	37	-4	25	-4
1213	100	43	-4	37	-4	25	-4

Sample	Field	X-value	Sigm-X	Y-Value	Sigm-Y	Z-Value	Sigm-Z
1213	175	-90	-6	22	-4	27	-4
1213	175	18	-5	22	-4	28	-4
1213	275	14	-4	20	-4	-13	-4
1213	275	15	-4	21	-4	-10	-4
1213	275	14	-4	21	-4	-17	-4
1213	375	-22	-4	37	-4	35	-4
1213	375	-19	-4	37	-4	35	-4
1213	475	-84	-5	20	-4	93	-5
1213	475	-86	-5	20	-4	45	-5
1213	575	44	-4	24	-4	24	-4
1213	575	45	-4	24	-4	24	-4
1213	675	-19	-5	14	-4	-32	-4
1213	675	-43	-5	13	-4	-31	-4
1213	775	-48	-5	17	-4	-14	-4
1213	775	-17	-5	18	-4	-12	-4
1213	775	-65	-5	20	-4	-19	-4
1213	875	-47	-4	35	-4	-83	-5
1213	875	-44	-4	35	-4	-63	-5
1213	975	-44	-4	38	-4	29	-4
1213	975	-43	-4	34	-4	25	-4
1313	0	-13	-4	14	-4	32	-5
1313	0	-11	-4	14	-4	29	-5
1313	100	-49	-6	10	-4	-48	-5
1313	100	-64	-7	10	-4	-46	-5
1313	200	31	-5	69	-5	-10	-4
1313	200	34	-5	64	-5	-10	-4
1313	300	-26	-5	58	-5	-71	-5
1313	300	-24	-5	55	-5	-63	-5
1313	300	-29	-5	60	-5	-69	-5
1313	400	-69	-5	34	-5	-28	-6
1313	400	-73	-5	36	-5	-43	-7
1313	500	53	-6	47	-5	-15	-5
1313	500	24	-5	43	-5	-10	-5
1313	500	30	-5	53	-5	-12	-5
1313	500	48	-5	51	-5	-75	-6
1313	600	26	-5	51	-5	-52	-6
1313	600	22	-5	46	-5	44	-6
1313	600	22	-5	45	-5	-12	-5
1313	700	-35	-5	60	-5	-29	-5
1313	700	-32	-5	60	-5	-29	-5
1313	700	-23	-5	69	-5	-27	-5
1313	800	-47	-7	41	-5	10	-6
1313	800	-14	-6	43	-5	-67	-7
1313	800	-13	-6	40	-5	-27	-6
1313	800	-38	-6	14	-5	-62	-6
1312	0	36	-5	60	-5	91	-7
1312	0	29	-5	77	-5	-72	-6
1312	0	45	-5	65	-5	-46	-6
1312	50	43	-5	40	-5	12	-6
1312	50	44	-5	39	-5	45	-6
1312	150	48	-5	41	-5	-23	-5
1312	150	48	-4	39	-5	-23	-5
1312	250	89	-5	24	-5	-74	-6
1312	250	90	-5	22	-5	-61	-6
1312	350	15	-5	26	-5	55	-6
1312	350	16	-5	25	-5	50	-6

Sample	Field	X-value	Sigm-X	Y-Value	Sigm-Y	Z-Value	Sigm-Z
1312	450	66	-6	53	-5	-98	-6
1312	450	16	-5	17	-5	91	-6
1312	450	17	-5	16	-5	61	-6
1312	550	-35	-5	36	-5	-39	-5
1312	550	-34	-5	36	-5	-37	-5
1312	650	32	-5	19	-5	57	-6
1312	650	34	-5	22	-5	51	-6
1312	750	19	-5	35	-5	53	-5
1312	750	17	-5	35	-5	54	-5
1312	850	-64	-6	33	-5	57	-5
1312	850	-59	-6	32	-5	57	-5
1312	850	-33	-5	32	-5	42	-5
1312	950	49	-5	66	-5	-84	-5
1312	950	54	-5	76	-5	-93	-5
1311	0	-35	-4	36	-4	-21	-4
1311	0	-36	-4	36	-4	-20	-4
1311	750	-17	-4	22	-4	-11	-4
1311	75	-16	-4	20	-4	-10	-4
1311	75	-15	-4	19	-4	-11	-4
1311	175	45	-5	10	-4	18	-5
3111	175	52	-5	10	-4	26	-5
1311	275	54	-5	84	-5	81	-5
1311	275	60	-5	77	-5	82	-5
1311	375	75	-5	12	-4	57	-5
1311	375	76	-5	12	-4	45	-5
1311	375	76	-5	11	-4	61	-5
1311	475	-40	-5	16	-4	50	-5
1311	475	-18	-5	15	-4	51	-5
1311	475	-36	-4	16	-4	31	-5
1311	475	-42	-5	17	-4	24	-5
1311	575	-81	-5	13	-4	78	-7
1311	575	-74	-5	12	-5	-13	-6
1311	675	-84	-5	14	-4	68	-6
1311	675	-92	-5	14	-4	10	-5
1311	775	-99	-5	10	-4	33	-5
1311	775	-11	-4	93	-5	38	-5
1311	875	-21	-4	24	-4	-12	-4
1311	875	-20	-4	24	-4	-12	-4
1311	975	43	-5	62	-5	-18	-6
1311	975	46	-5	62	5	10	-6
1311	975	56	-5	62	-5	57	-6
1412	0	48	-5	22	-4	-40	-5
1412	0	58	-5	24	-4	-37	-5
1412	0	30	-5	22	-4	-58	-5
1412	100	-15	-4	18	-4	97	-5
1412	100	-16	-4	19	-4	99	-5
1412	200	-88	-5	79	-5	-11	-4
1412	200	-75	-5	85	-5	-11	-4
1412	300	-36	-4	24	-4	53	-5
1412	300	-36	-4	24	-4	41	-5
1412	400	90	-5	49	-5	74	-5
1412	400	99	-5	49	-5	70	-5
1412	500	-91	-5	27	-4	-33	-5
1412	500	-86	-5	28	-4	-51	-6
1412	500	-64	-5	24	-4	-40	-5
1412	600	-17	-5	48	-4	-56	-5

Sample	Field	X-value	Sigm-X	Y-Value	Sigm-Y	Z-Value	Sigm-Z
1412	600	-11	-5	48 -4	-57 -5	13 -4	16 -4
1412	700	-87	-5	14 -4	11 -4	11 -4	23 -5
1412	700	-65	-5	14 -4	12 -4	10 -4	17 -5
1412	700	-64	-5	14 -4	12 -4	11 -4	17 -5
1412	800	-34	-5	19 -4	-44 -5	96 -5	92 -5
1412	800	-58	-5	14 -4	-28 -5	11 -4	-78 -6
1411	0	77	-4	55 -4	43 -4	32 -4	45 -3
1411	0	81	-4	55 -4	43 -4	31 -4	44 -3
1411	50	81	-4	55 -4	43 -4	31 -4	44 -3
1411	50	49	-4	42 -4	22 -4	40 -4	18 -3
1411	50	47	-4	44 -4	23 -4	41 -4	18 -3
1411	150	26	-4	17 -4	-93 -5	35 -4	56 -4
1411	150	26	-4	18 -4	-83 -5	35 -4	56 -4
1411	250	35	-4	18 -4	-10 -4	37 -4	36 -4
1411	250	38	-4	17 -4	-93 -5	37 -4	40 -4
1411	350	22	-5	26 -4	-16 -4	22 -4	19 -4
1411	350	24	-5	26 -4	-15 -5	22 -4	20 -4
1411	450	-30	-5	12 -4	-90 -5	11 -4	10 -4
1411	450	-30	-5	12 -4	-67 -5	12 -4	69 -5
1411	450	-48	-5	12 -4	-98 -5	11 -4	43 -5
1411	550	17	-4	14 -4	-11 -4	87 -5	17 -4
1411	550	18	-4	14 -4	-11 -4	84 -5	-18 -4
1411	650	47	-5	23 -4	14 -4	30 -4	31 -4
1411	650	78	-5	24 -4	15 -4	30 -4	32 -4
1411	750	-22	-5	18 -4	-17 -4	11 -4	21 -4
1411	750	-22	-5	18 -4	-16 -4	11 -4	21 -4
1411	850	-22	-4	23 -4	-89 -5	13 -4	28 -4
1411	850	-21	-4	24 -4	-96 -5	14 -4	30 -4
1411	950	-32	-5	57 -4	-15 -4	13 -4	36 -6
1411	950	-22	-5	56 -5	-14 -4	13 -4	11 -5
1413	0	83	-4	33 -4	26 -4	44 -4	20 -3
1413	0	90	-4	32 -4	28 -4	46 -4	21 -3
1413	75	38	-4	22 -4	16 -4	16 -4	18 -3
1413	75	38	-4	22 -4	16 -4	17 -4	18 -3
1413	175	10	-4	91 -5	97 -5	65 -5	60 -4
1413	175	97	-5	90 -5	10 -4	61 -5	60 -4
1413	175	10	-4	96 -5	10 -4	58 -5	60 -4
1413	275	-33	-5	12 -4	28 -5	70 -5	12 -4
1413	275	-32	-5	13 -4	21 -5	71 -5	13 -4
1413	375	-92	-5	22 -4	-22 -4	15 -4	55 -4
1413	375	-68	-5	24 -4	-22 -4	14 -4	56 -4
1413	375	-72	-5	24 -4	-24 -4	14 -4	56 -4
1413	475	-52	-4	11 -4	-20 -4	27 -4	22 -4
1413	475	-52	-4	13 -4	-19 -4	29 -4	24 -4
1413	575	-25	-4	26 -4	-52 -5	14 -4	-31 -4
1413	575	-24	-4	25 -4	-58 -5	14 -4	-31 -4
1413	675	88	-5	20 -4	-88 -5	99 -5	55 -4
1413	675	97	-5	21 -4	-80 -5	96 -5	55 -4
1413	775	-22	-4	22 -4	14 -4	16 -4	20 -4
1413	775	-19	-4	22 -4	13 -4	15 -4	18 -4
1413	875	-13	-4	18 -4	91 -4	43 -4	42 -4
1413	875	-13	-4	18 -4	-12 -4	41 -4	42 -4
1413	975	32	-4	14 -4	27 -4	18 -4	28 -4
1413	975	31	-4	12 -4	27 -4	17 -4	28 -4
5021	0	-31	-3	17 -3	-60 -3	19 -3	32 -3
5021	0	-34	-3	14 -3	-67 -3	15 -3	30 -3

Sample	Field	X-value	Sigm-X	Y-Value	Sigm-Y	Z-Value	Sigm-Z
5021	100	-52	-4	89	-4	-62	-4
5021	100	84	-4	89	-4	-58	-4
5021	200	-52	-4	30	-4	24	-4
5021	200	-53	-4	30	-4	-25	-4
5021	300	-24	-4	25	-4	-21	-4
5021	300	-25	-4	25	-4	-20	-4
5021	400	-21	-4	16	-4	19	-4
5021	400	-20	-4	16	-4	-18	-4
5021	500	-41	-5	17	-4	-78	-6
5021	500	-31	-5	17	-4	-31	-6
5021	600	-15	-4	13	-4	73	-6
5021	600	-16	-4	12	-4	11	-5
5021	700	-78	-5	92	-5	-21	-4
5021	700	-75	-5	85	-4	-21	-4
5021	800	-51	-5	85	-5	-11	-4
5021	800	-77	-5	84	-5	-11	-4
5021	900	15	-4	40	-5	76	-5
5021	900	14	-4	41	-5	78	-5
5022	0	16	-4	10	-4	14	-4
5022	150	-15	-4	13	-4	62	-5
5022	150	-15	-4	13	-4	63	-5
5022	250	-99	-5	13	-4	66	-5
5022	250	-74	-5	12	-4	58	-5
5022	350	-99	-5	16	-4	55	-5
5022	350	-89	-5	16	-4	55	-5
5022	450	-13	-4	59	-5	32	-5
5022	550	-22	-5	35	-5	13	-5
5022	650	-26	-5	75	-5	30	-5
5022	750	-34	-5	77	-5	-10	-5
5022	850	-55	-5	69	-5	52	-5
5022	950	10	-5	31	-5	72	-5
5023	0	30	-4	38	-4	-20	-4
5023	0	31	-4	38	-4	-20	-4
5023	175	-30	-6	13	-4	45	-5
5023	175	-57	-6	14	-4	43	-5
5023	275	-56	-6	10	-4	50	-5
5023	275	10	-5	11	-4	52	-5
5023	375	25	-5	75	-6	-86	-5
5023	375	25	-5	70	-5	-85	-5
5023	475	-11	-5	16	-4	-63	-5
5023	575	-21	-5	12	-4	-70	-5
5023	675	-35	-6	63	-5	35	-5
5023	775	24	-5	82	-5	56	-5
5023	875	10	-4	73	-5	86	-5
5023	975	77	-5	16	-5	-65	-6
5121	0	-91	-4	13	-3	65	-5
5121	0	-67	-4	84	-4	19	-4
5121	100	-60	-4	27	-4	82	-4
5121	100	-6	-4	28	-4	91	-4
5121	200	-26	-4	27	-4	-43	-4
5121	200	-21	-4	28	-4	-29	-4
5121	300	-48	-4	50	-4	-64	-4
5121	300	-47	-4	47	-4	-50	-4
5121	400	-18	-4	38	-4	-59	-5
5121	400	-21	-4	37	-4	78	-6
5121	500	22	-4	52	-4	-45	-4

Sample	Field	X-value	Sigm-X	Y-Value	Sigm-Y	Z-Value	Sigm-Z
5121	500	24	-4	48	-4	-33	-4
5121	600	-41	-4	23	-4	-69	-4
5121	600	-37	-4	22	-4	54	-4
5121	700	54	-4	56	-4	-47	-4
5121	700	46	-4	53	-4	-41	-4
5121	800	22	-4	39	-4	-25	-4
5121	800	15	-4	38	-4	-18	-4
5121	900	-31	-4	49	-4	16	-4
5121	900	-19	-4	44	-4	37	-4
5122	0	24	-3	13	-3	28	-3
5122	0	24	-3	14	-3	30	-3
5122	150	35	-4	60	-4	39	-4
5122	150	38	-4	59	-4	47	-4
5122	250	73	-4	74	-4	-16	-4
5122	250	78	-4	72	-4	-10	-4
5122	350	24	-5	61	-4	-57	-4
5122	350	92	-5	61	-4	-20	-4
5122	450	31	-4	35	-4	-31	-4
5122	450	34	-4	35	-4	-25	-4
5122	550	-10	-3	16	-4	-10	-3
5122	550	-10	-3	18	-4	-97	-4
5122	650	49	-4	45	-4	-72	-6
5122	650	54	-4	44	-4	77	-6
5122	750	-31	-4	54	-4	-13	-4
5122	750	-31	-4	67	-4	-53	-5
5122	850	63	-4	46	-4	88	-5
5122	850	66	-4	45	-4	15	-4
5122	950	15	-4	60	-4	-31	-4
5122	950	19	-4	61	-4	-21	-4
5123	0	-20	-3	62	-4	-27	-4
5123	0	-16	-3	54	-4	36	-5
5123	175	-64	-5	69	-4	39	-6
5123	175	-96	-5	75	-4	71	-5
5123	275	63	-4	36	-4	-58	-4
5123	275	61	-4	37	-4	-45	-4
5123	375	67	-4	45	-4	-26	-4
5123	375	60	-4	46	-4	-20	-4
5123	475	-28	-4	54	-4	-80	-5
5123	475	-24	-4	59	-4	-23	-5
5123	575	-40	-4	47	-4	-35	-4
5123	575	-28	-4	36	-4	-30	-4
5123	675	13	-4	48	-5	-71	-4
5123	675	45	-4	56	-5	-63	-4
5123	775	37	-6	24	-4	-16	-5
5123	775	63	-5	26	-4	69	-5
5123	875	30	-4	41	-4	-94	-4
5123	875	35	-4	40	-4	-86	-4
5123	975	28	-4	42	-4	-59	-4
5123	975	29	-4	43	-4	-53	-4
5221	0	-58	-4	34	-3	-45	-3
5221	0	-53	-4	16	-3	-45	-3
5221	100	-10	-3	93	-4	-14	-3
5221	100	-97	-4	89	-4	-13	-3
5221	200	-10	-3	25	-4	87	-4
5221	200	-11	-3	28	-4	96	-4
5221	600	-96	-4	72	-4	-24	-4

Sample	Field	X-value	Sigm-X	Y-Value	Sigm-Y	Z-Value	Sigm-Z
5221	300	-95	-4	69	-4	-14	-4
5221	400	-51	-4	82	-4	-18	-3
5221	400	-50	-4	82	-4	-17	-3
5221	500	-62	-4	51	-4	84	-5
5221	500	-61	-4	51	-4	16	-4
5221	600	-26	-4	55	-4	-99	-4
5221	600	-25	-4	54	-4	-89	-4
5221	700	-36	-4	11	-3	-12	-3
5221	700	-36	-4	10	-3	-12	-3
5221	800	20	-4	37	-4	-17	-4
5221	800	-12	-4	35	-4	-12	-4
5221	900	-11	-3	10	-3	-15	-3
5221	900	-11	-3	99	-4	-14	-3
5222	0	29	-3	19	-3	-55	-4
5222	0	29	-3	18	-3	-49	-4
5222	150	86	-5	32	-4	-36	-4
5222	250	-94	-6	53	-4	-10	-3
5222	250	-27	-5	52	-4	-98	-4
5222	350	60	-5	24	-4	-11	-4
5222	350	53	-5	24	-4	-56	-5
5222	450	-72	-4	26	-4	-78	-4
5222	450	-75	-4	25	-4	-75	-4
5222	550	20	-5	25	-4	-3	-5
5222	550	-29	-5	21	-4	81	-7
5222	650	44	-4	14	-4	27	-4
5222	650	48	-4	16	-4	29	-4
5222	750	85	-4	29	-4	-49	-5
5222	750	10	-4	27	-4	-52	-4
5222	850	39	-4	40	-4	-10	-3
5222	850	38	-4	39	-4	-96	-4
5222	950	90	-4	42	-4	-83	-4
5222	950	84	-4	41	-4	-79	-4
5223	0	-25	-4	34	-4	-37	-4
5223	0	-54	-4	18	-4	-33	-4
5223	175	-34	-4	20	-4	-15	-4
5223	175	-33	-4	20	-4	-14	-4
5223	275	82	-5	34	-4	-48	-4
5223	275	61	-5	32	-4	78	-4
5223	375	-45	-4	16	-4	-45	-4
5223	375	-34	-4	33	-4	-45	-4
5223	475	-61	-4	38	-4	56	-5
5223	475	-64	-4	36	-4	61	-5
5223	575	-32	-4	50	-4	61	-5
5223	575	-32	-4	49	-4	69	-5
5223	675	-86	-7	-5	-4	39	-4
5223	675	-85	-4	40	-4	19	-4
5223	775	-18	-4	33	-4	-18	-4
5223	775	-17	-4	33	-4	-15	-4
5223	875	-40	-4	34	-4	13	-4
5223	875	-40	-4	34	-4	18	-4
5622	0	43	-6	59	-6	32	-6
5622	0	-26	-6	76	-6	33	-7
5622	0	-76	-3	43	-4	-60	-6
5622	0	-75	-3	31	-4	-52	-3
5622	100	-96	-4	45	-4	18	-4
5622	100	-94	-4	46	-4	25	-4

Sample	Field	X-value	Sigm-X	Y-Value	Sigm-Y	Z-Value	Sigm-Z
5622	200	-61	-4	35	-4	-12	-4
5622	200	-12	-4	47	-4	-18	-4
5622	300	-44	-4	13	-4	-90	-4
5622	300	-37	-4	11	-4	-72	-4
5622	400	-34	-4	18	-4	-95	-5
5622	400	-32	-4	17	-4	61	-5
5622	500	-59	-4	26	-4	-45	-4
5622	500	-51	-4	25	-4	-30	-4
5622	600	-13	-3	64	-4	-58	-4
5622	600	-14	-3	62	-4	-49	-4
5622	700	-26	-4	52	-4	-89	-4
5622	700	-18	-4	50	-4	-72	-4
5622	800	-13	-3	20	-4	52	-4
5622	800	-13	-3	20	-4	61	-4
5622	900	-27	-4	20	-4	-85	-4
5622	900	-20	-4	19	-4	-74	-4
5623	0	-66	-4	39	-3	-32	-3
5623	0	58	-5	28	-3	-33	-3
5623	150	-82	-4	93	-4	-93	-4
5623	150	-89	-4	81	-4	-89	-4
5623	250	-73	-4	78	-4	-11	-4
5623	250	-64	-4	74	-4	-70	-5
5623	250	-61	-4	56	-4	-90	-4
5623	350	-61	-4	56	-4	-90	-4
5623	350	-70	-4	52	-4	-10	-3
5622	450	-49	-4	54	-4	-93	-4
5623	450	-58	-4	56	-4	-97	-4
5623	550	-14	-4	87	-4	-15	-3
5623	550	-95	-5	84	-4	-15	-3
5623	650	-55	-4	50	-4	-11	-3
5623	650	-52	-4	48	-4	-10	-3
5623	750	-99	-6	35	-4	-66	-4
5623	750	-31	-5	30	-4	-43	-4
5623	850	-25	-4	70	-4	-24	-4
5623	850	-41	-4	87	-5	-20	-4
5623	950	-88	-5	62	-4	-84	-4
5623	950	-10	-4	68	-4	-66	-4
5522	0	19	-3	21	-3	-10	-3
5522	0	85	-4	97	-4	-85	-4
5522	100	-80	-4	40	-4	89	-6
5522	100	-83	-4	42	-4	78	-5
5522	200	54	-6	51	-4	39	-4
5522	200	19	-5	52	-4	43	-4
5522	300	62	-4	63	-4	-10	-4
5522	300	33	-4	12	-4	30	-4
5522	400	-30	-4	32	-4	-57	-5
5522	400	-29	-4	31	-4	-32	-5
5522	500	-29	-4	21	-4	67	-4
5522	500	-27	-4	19	-4	51	-4
5522	600	-72	-4	36	-4	29	-5
5522	600	-58	-4	41	-4	-42	-5
5522	700	-48	-4	72	-4	-23	-4
5522	700	-52	-4	75	-4	-26	-4
5522	800	-15	-3	90	-4	96	-5
5522	800	-15	-3	91	-4	15	-4
5522	900	-74	-4	48	-4	-26	-4

Sample	Field	X-value	Sigm-X	Y-Value	Sigm-Y	Z-Value	Sigm-Z
5522	900	-79	-4	46	-4	-24	-4
5523	0	-96	-5	71	-5	-24	-4
5523	0	-10	-4	76	-4	-25	-4
5523	150	-65	-4	10	-4	37	-5
5523	150	-73	-4	16	-5	24	-5
5523	250	-54	-4	21	-4	-12	-4
5523	250	-54	-4	21	-4	13	-4
5523	250	-54	-4	21	-4	-92	-5
5523	350	-10	-3	28	-4	-25	-4
5523	350	-10	-3	27	-4	-23	-4
5523	450	-47	-3	12	-4	-17	-4
5523	450	-17	-3	11	-4	-14	-4
5523	550	-21	-3	35	-4	21	-5
5523	550	-21	-3	36	-4	42	-5
5523	650	-23	-3	11	-4	13	-4
5523	650	-24	-3	10	-4	15	-4
5523	750	-11	-3	45	-4	-34	-5
5523	750	-11	-3	45	-4	-11	-5
5523	850	-36	-3	26	-4	70	-4
5523	850	-36	-3	25	-4	72	-4
5523	850	-36	-3	25	-4	70	-4
5523	950	-87	-4	16	-4	-12	-4
5523	950	-87	-4	17	-4	-75	-5
5721	0	-39	-4	16	-3	-13	-3
5721	0	-37	-4	16	-3	-13	-3
5721	100	-24	-4	10	-3	-11	-3
5721	100	-28	-4	10	-3	-10	-3
5721	200	-16	-4	99	-4	-10	-3
5721	200	-15	-4	97	-4	-10	-3
5721	300	-29	-4	83	-4	-99	-4
5721	300	-24	-4	86	-4	-10	-3
5721	400	-14	-4	82	-4	-86	-4
5721	400	-17	-4	82	-4	-86	-4
5721	500	-10	-4	82	-4	-11	-3
5721	500	-14	-4	78	-4	-10	-3
5721	600	81	-5	76	-4	-95	-4
5721	600	58	-5	73	-4	-92	-4
5721	700	10	-4	75	-4	-97	-4
5721	700	58	-5	73	-4	-94	-4
5721	800	-19	-4	60	-4	-83	-4
5721	800	-18	-4	60	-4	-79	-4
5721	900	-22	-5	78	-4	-12	-3
5721	900	-18	-4	73	-4	-12	-3
5722	0	-12	-3	33	-3	42	-4
5722	0	-12	-3	32	-3	47	-4
5722	150	-54	-4	18	-3	70	-5
5722	150	-58	-4	18	-3	79	-5
5722	250	-38	-4	15	-3	29	-4
5722	250	-40	-4	15	-3	35	-4
5722	350	-38	-4	15	-3	30	-4
5722	350	-40	-4	15	-3	32	-4
5722	450	-41	-4	13	-3	30	-4
5722	450	-43	-4	12	-3	31	-4
5722	550	-40	-4	14	-3	42	-4
5722	550	-43	-4	14	-3	44	-4
5722	650	18	-4	99	-4	60	-4
5722	650	-19	-5	10	-3	57	-4

Sample	Field	X-value	Sigm-X	Y-Value	Sigm-Y	Z-Value	Sigm-Z	
5722	750	-18	-4	10 -3	-49 -6	21 -4	16 -3	38 -4
5722	750	-22	-4	10 -3	25 -5	21 -4	16 -3	38 -4
5722	850	-81	-5	59 -4	-90 -5	22 -4	13 -3	25 -4
5722	850	-12	-4	59 -4	-76 -5	22 -4	12 -3	25 -4
5722	950	-15	-4	65 -4	98 -5	27 -4	12 -3	28 -4
5722	950	-13	-4	64 -4	13 -4	27 -4	12 -3	28 -4
5723	0	-25	-4	24 -3	-22 -4	20 -3	-47 -3	78 -4
5723	0	-26	-4	24 -3	-19 -4	20 -3	-47 -3	76 -4
5723	175	-21	-4	22 -4	-17 -4	16 -4	37 -4	11 -4
5723	175	-21	-4	23 -4	-15 -4	15 -4	38 -4	12 -4
5723	275	-28	-4	21 -4	-3 -6	10 -4	59 -4	11 -4
5723	275	-28	-4	21 -4	15 -5	10 -4	59 -4	11 -4
5723	375	-16	-4	19 -4	77 -5	56 -5	75 -4	52 -5
5723	375	-17	-4	20 -4	62 -5	54 -5	73 -4	54 -5
5723	475	-11	-4	17 -4	-15 -4	19 -4	57 -4	21 -4
5723	475	-13	-4	17 -4	-14 -4	18 -4	56 -4	21 -4
5723	575	-76	-5	96 -5	-70 -5	13 -4	41 -4	51 -5
5723	575	-89	-5	96 -5	-64 -5	18 -4	41 -4	54 -5
5723	675	-17	-4	18 -4	-13 -4	92 -5	59 -4	82 -5
5723	675	-19	-4	20 -4	-14 -4	83 -5	58 -4	84 -5
5723	775	-45	-4	82 -5	-19 -5	11 -4	49 -4	10 -4
5723	775	-46	-4	96 -5	68 -6	11 -4	47 -4	10 -4
5723	875	-23	-4	17 -4	-21 -4	63 -5	42 -4	14 -4
5723	875	-55	-4	17 -4	-20 -4	65 -5	41 -4	13 -4
5723	975	-31	-4	16 -4	33 -5	60 -5	37 -4	12 -4
5723	975	-27	-4	14 -4	42 -5	41 -5	36 -4	12 -4
521	0	-20	-3	85 -4	-21 -3	53 -4	1 -2	37 -4
521	0	-68	-4	80 -4	-21 -3	51 -4	99 -3	37 -4
521	100	-95	-5	56 -4	-11 -3	72 -4	49 -3	20 -4
521	100	-4	-5	54 -4	-11 -3	58 -4	48 -3	22 -4
521	200	-16	-4	51 -4	-75 -4	56 -4	26 -3	12 -4
521	200	-13	-4	46 -4	-72 -4	54 -4	26 -3	10 -4
521	300	-23	-5	13 -4	-52 -4	24 -4	19 -3	29 -4
521	300	-69	-5	20 -4	-51 -4	24 -4	2 -3	29 -4
521	400	-14	-4	16 -4	-48 -4	25 -4	13 -3	19 -4
521	400	-15	-4	16 -4	-48 -4	25 -4	13 -3	19 -4
521	500	-12	-4	20 -4	-42 -4	23 -4	10 -3	95 -5
521	500	-12	-4	20 -4	-41 -4	23 -4	10 -3	99 -5
521	600	-17	-4	22 -4	-27 -4	20 -4	81 -4	75 -5
521	600	-16	-4	21 -4	-25 -4	20 -4	82 -4	76 -5
521	700	-12	-4	10 -4	-22 -4	14 -4	65 -4	48 -5
521	700	-13	-4	10 -4	-21 -4	14 -4	66 -4	51 -5
521	800	-42	-5	84 -5	-10 -4	79 -5	46 -4	38 -5
521	800	-60	-5	90 -5	-10 -4	86 -5	46 -4	43 -5
521	900	-14	-4	16 -4	-18 -4	43 -5	28 -4	11 -4
521	900	-14	-4	15 -4	-18 -4	39 -5	27 -4	11 -4
522	0	10	-3	82 -4	-34 -3	12 -3	11 -2	82 -4
522	0	58	-4	82 -4	-30 -3	97 -4	11 -2	78 -4
522	150	31	-4	61 -4	-11 -3	86 -4	50 -3	48 -4
522	150	31	-4	60 -4	-10 -3	86 -4	50 -3	52 -4
522	250	73	-5	33 -4	-69 -4	78 -4	29 -3	37 -4
522	250	60	-5	59 -4	-65 -4	56 -4	38 -3	97 -4
522	350	36	-4	25 -4	-48 -4	88 -5	23 -3	64 -4
522	350	37	-4	25 -4	-48 -4	92 -5	23 -3	64 -4
522	450	21	-4	25 -4	-36 -4	26 -4	14 -3	52 -4
522	450	19	-4	24 -4	-35 -4	26 -4	14 -3	50 -4

Sample	Field	X-value	Sigm-X	Y-Value	Sigm-Y	Z-Value	Sigm-Z
522	550	-49	-5	17	-4	-75	-5
522	550	-67	-5	16	-4	-73	-5
522	650	48	-5	22	-4	-18	-4
522	650	18	-5	23	-4	-18	-4
522	750	55	-5	15	-4	-15	-4
522	750	42	-5	15	-4	-14	-4
522	750	35	-5	15	-4	-13	-4
522	850	77	-5	16	-4	-30	-4
522	850	56	-5	16	-4	-32	-4
522	950	-18	-5	17	-4	-10	-5
522	950	-20	-5	17	-4	10	-6
523	0	-35	-3	10	-3	-34	-3
523	0	-34	-3	99	-4	-33	-3
523	175	-43	-4	6	-4	-12	-3
523	175	-43	-4	59	-4	-19	-3
523	275	-55	-4	21	-4	-69	-4
523	275	-57	-4	23	-4	-69	-4
523	375	-35	-4	40	-4	-52	-4
523	375	-37	-4	40	-4	-51	-4
523	475	-48	-4	92	-5	-51	-4
6821	0	10	-6	36	-5	-15	-5
6821	100	65	-7	31	-5	-14	-5
6821	200	93	-7	30	-5	-13	-5
6821	300	-37	-6	12	-5	-11	-5
6821	400	-84	-6	18	-5	-16	-5
6821	500	21	-6	17	-5	10	-5
6821	600	14	-5	22	-5	-23	-6
6821	700	-44	-6	13	-5	-17	-5
6821	800	-31	-6	97	-6	46	-6
6821	900	12	-5	20	-5	-74	-6
6821	900	12	-5	14	-5	-60	-6
6822	0	12	-5	20	-5	-74	-6
6822	0	12	-5	14	-5	-60	-6
6822	150	12	-5	14	-5	-43	-6
6822	250	11	-5	10	-5	-21	-6
6822	350	46	-6	91	-6	68	-6
6822	450	12	-5	11	-5	65	-6
6822	550	68	-6	11	-5	55	-6
6822	650	57	-7	10	-5	45	-6
6822	750	13	-5	11	-5	95	-7
6822	850	-12	-6	12	-5	-71	-6
6822	950	-53	-6	10	-5	14	-6
6823	0	21	-6	21	-5	-11	-5
6823	175	-19	-6	97	-6	-20	-6
6823	275	84	-7	12	-5	-24	-6
6823	375	20	-6	12	-5	-51	-6
6823	475	21	-7	11	-5	-47	-6
6823	575	-69	-7	95	-6	-34	-6
6823	675	-92	-8	12	-5	31	-8
6823	775	-55	-7	11	-5	78	-7
6823	875	33	-6	13	-5	-37	-8
6921	0	23	-6	14	-5	-17	-7
6921	0	-61	-6	15	-5	-49	-6
9621	100	-34	-6	12	-5	-31	-7
6921	200	25	-6	16	-5	-18	-8
6921	300	-63	-6	13	-5	13	-6

Sample	Field	X-value	Sigm-X	Y-Value	Sigm-Y	Z-Value	Sigm-Z
6921	400	26	-6	17	-5	62	-6
6921	500	-55	-6	15	-5	71	-7
6921	600	-99	-6	13	-5	-56	-8
6921	700	49	-6	13	-5	44	-6
6921	800	-56	-7	17	-5	-15	-8
6921	900	-39	-6	14	-5	23	-6
6922	0	-37	-6	13	-5	31	-6
6922	150	-22	-6	12	-5	-96	-7
6922	250	22	-7	14	-5	-62	-6
6922	350	-58	-6	87	-6	93	-7
6922	450	-47	-6	82	-6	-17	-7
6922	550	-31	-6	11	-5	-11	-6
6922	650	-22	-6	10	-5	23	-6
6922	750	-74	-6	11	-5	34	-6
6922	850	-12	-6	10	-5	-80	-7
6923	0	44	-6	12	-5	26	-6
6923	175	38	-6	11	-5	21	-6
6923	275	-39	-7	13	-5	18	-6
6923	375	45	-7	10	-5	-37	-7
6723	475	33	-7	12	-5	76	-7
6923	575	-13	-6	11	-5	28	-6
6923	675	11	-6	16	-5	57	-7
6923	775	-72	-7	10	-5	-15	-7
6923	875	24	-6	16	-5	42	-6
6923	975	-16	-6	12	-5	41	-6
6221	0	64	-5	68	-5	-10	-5
6221	0	66	-5	71	-5	-11	-5
6221	100	25	-5	48	-5	-17	-5
6221	100	23	-5	44	-5	-16	-5
6221	200	-13	-5	29	-5	-96	-7
6221	300	11	-5	23	-5	12	-5
6221	400	-16	-5	31	-5	38	-5
6221	500	-27	-5	42	-5	-59	-6
6221	600	23	-5	46	-5	-12	-5
6221	700	-56	-5	22	-5	36	-6
6221	800	-82	-5	12	-5	-37	-6
6221	900	65	-6	30	-5	-40	-7
6222	0	-12	-4	23	-4	-20	-4
6222	0	-11	-4	23	-4	-19	-4
6222	150	-14	-4	16	-4	-10	-4
6222	150	-15	-4	16	-4	-10	-4
6222	250	-37	-5	15	-4	-42	-5
6222	350	-73	-5	38	-5	-12	-4
6222	450	-22	-4	20	-4	-14	-4
6222	550	-48	-5	86	-5	-61	-5
6222	650	-46	-5	47	-5	12	-4
6222	750	36	-5	49	-5	44	-5
6222	825	-85	-5	97	-5	-75	-5
6222	950	-13	-4	10	-4	43	-5
6223	0	96	-5	53	-4	96	-5
6323	175	-49	-5	71	-5	20	-4
6223	275	-36	-5	81	-6	-59	-5
6223	375	-58	-5	13	-5	-16	-5
6223	475	-23	-6	95	-5	99	-5
6223	575	-50	-5	63	-5	-12	-4
6223	675	11	-4	18	-5	49	-5

Sample	Field	X-value	Sigm-X	Y-Value	Sigm-Y	Z-Value	Sigm-Z
6223	775	34	-5	33	-5	22	-6
6223	875	-74	-6	71	-5	76	-5
4511	0	-15	-5	38	-4	13	-4
4511	0	-4	-5	41	-4	13	-4
4511	0	-55	-5	39	-4	11	-4
4511	0	-73	-5	42	-4	84	-5
4511	100	-83	-5	26	-4	-81	-5
4511	100	-80	-5	26	-4	-78	-5
4511	200	-18	-4	32	-4	-17	-5
4511	200	-19	-4	36	-4	-16	-5
4511	300	-68	-5	23	-4	-24	-5
4511	300	-80	-5	26	-4	-60	-5
4511	300	-70	-5	23	-4	-64	-5
4511	400	-86	-5	19	-4	-25	-5
4511	400	-86	-5	19	-4	-21	-5
4511	500	-11	-4	22	-4	-12	-4
4511	500	-11	-4	22	-4	-15	-4
4511	600	-19	-4	33	-4	-26	-4
4511	600	-19	-4	36	-4	-25	-4
4511	700	-86	-5	15	-4	81	-5
4511	700	-83	-5	15	-4	77	-5
4511	800	-83	-5	11	-4	-95	-5
4511	800	-92	-5	12	-4	-10	-4
4511	800	-82	-5	13	-4	-10	-4
4511	900	-66	-5	14	-4	-15	-5
4511	900	-65	-5	13	-4	-38	-6
4511	900	-82	-5	14	-4	-31	-5
4511	900	-70	-5	44	-4	-70	-5
4511	900	-74	-5	13	-4	-41	-5
4511	900	-64	-5	13	-4	-30	-5
4512	0	41	-4	72	-4	46	-4
4512	0	36	-4	68	-4	49	-4
4512	0	35	-4	65	-4	49	-4
4512	500	31	-4	50	-4	29	-4
4511	500	28	-4	45	-4	31	-4
4511	500	25	-4	45	-4	29	-4
4512	150	25	-4	46	-4	27	-4
4512	150	36	-4	51	-4	31	-4
4512	150	36	-4	50	-4	33	-4
4512	250	37	-4	48	-4	33	-4
4512	250	38	-4	49	-4	33	-4
4512	350	23	-4	31	-4	29	-4
4512	350	23	-4	31	-4	30	-4
4512	450	14	-4	12	-4	19	-4
4512	450	14	-4	12	-4	20	-4
4512	550	17	-4	23	-4	11	-4
4512	550	17	-4	23	-4	16	-4
4512	650	95	-5	12	-4	90	-5
4512	650	10	-4	13	-4	100	-4
4512	750	23	-4	61	-5	-10	-4
4512	750	25	-4	65	-5	-98	-5
4512	850	47	-5	61	-5	-10	-4
4512	850	45	-5	51	-5	-10	-4
4512	950	28	-5	93	-5	-23	-5
4512	950	38	-5	94	-5	-34	-5
4513	0	87	-5	54	-4	-21	-4

Sample	Field	X-value	Sigm-X	Y-Value	Sigm-Y	Z-Value	Sigm-Z
4513	0	15	-4	53	-4	-18	-4
4513	0	13	-4	51	-4	-22	-4
4513	50	-67	-5	38	-4	57	-6
4513	50	-78	-5	38	-4	44	-5
4513	750	-79	-5	37	-4	-15	-6
4513	175	39	-5	37	-4	-52	-5
4513	175	53	-5	37	-4	-45	-5
4513	275	-17	-4	33	-4	26	-5
4513	275	-15	-4	34	-4	32	-5
4513	375	43	-6	41	-4	-19	-4
4513	375	11	-5	42	-4	-18	-4
4513	475	-20	-4	28	-4	-42	-5
4513	475	-19	-4	28	-4	93	-5
4513	575	-84	-5	16	-4	-11	-4
4513	575	-80	-5	15	-4	-11	-4
4513	675	-79	-5	13	-4	-45	-5
4513	675	-73	-5	15	-4	-56	-5
4513	675	-70	-5	15	-4	-54	-5
4513	775	-25	-5	26	-4	-2	-6
4513	775	-60	-5	26	-4	11	-5
4513	775	-31	-5	26	-4	-40	-5
4513	875	-15	-4	21	-4	35	-4
4513	875	-15	-4	22	-4	30	-5
4513	975	79	-5	26	-4	10	-5
4513	975	97	-5	26	-4	18	-5
4611	0	44	-2	82	-3	-21	-2
4621	0	44	-2	81	-3	-21	-2
4621	100	25	-3	12	-3	-14	-3
4621	100	25	-3	12	-3	-14	-3
4621	200	22	-3	96	-4	-92	-4
4621	200	21	-3	11	-3	-83	-4
4621	300	74	-4	10	-3	-54	-4
4621	300	75	-4	10	-3	-49	-4
4621	400	-74	-4	73	-4	-39	-4
4621	400	77	-4	73	-4	-35	-4
4621	500	-74	-4	37	-4	-23	-4
4621	500	-70	-4	34	-4	-17	-4
4621	600	60	-4	30	-4	-80	-4
4621	600	67	-4	27	-4	78	-4
4621	700	48	-4	10	-4	-68	-4
4621	700	42	-4	85	-5	-67	-4
4621	800	-66	-4	31	-4	-76	-4
4621	800	-56	-4	26	-4	-66	-4
4621	900	89	-5	37	-4	-98	-4
4621	900	13	-4	35	-4	-91	-4
4622	0	85	-4	52	-4	18	-3
4622	0	91	-4	55	-4	18	-3
4622	50	43	-4	63	-4	10	-3
4622	50	44	-4	59	-4	10	-3
4622	150	15	-4	38	-4	61	-4
4622	150	20	-4	37	-4	61	-4
4622	250	26	-4	20	-4	-94	-5
4622	250	26	-4	16	-4	-33	-5
4622	350	-34	-4	48	-4	21	-4
4622	350	-22	-4	42	-4	26	-4
4622	450	32	-4	75	-4	14	-4

Sample	Field	X-value	Sigm-X	Y-Value	Sigm-Y	Z-Value	Sigm-Z
4622	450	34	-4	73	-4	21	-4
4622	550	-12	-4	36	-4	-34	-4
4622	550	-15	-4	36	-4	-27	-4
4622	650	93	-4	17	-4	-89	-5
4622	650	77	-4	16	-4	-61	-5
4622	750	83	-4	52	-4	33	-4
4622	***	80	-4	53	-4	44	-4
4622	850	67	-4	11	-4	23	-4
4622	850	78	-4	99	-5	20	-4
4622	950	10	-4	57	-4	-53	-5
4622	950	19	-4	55	-4	-68	-5
4623	0	10	-4	46	-4	-18	-3
4623	0	18	-4	47	-4	-17	-3
4623	75	45	-4	30	-4	-90	-4
4623	75	46	-4	30	-4	-85	-4
4623	175	-77	-4	46	-4	-10	-3
4623	175	76	-4	45	-4	-97	-4
4623	275	25	-4	54	-4	-66	-4
4623	275	28	-4	61	-4	-62	-4
4623	375	50	-4	55	-4	-42	-4
4623	375	69	-4	55	-4	-37	-4
4623	475	91	-5	19	-4	-34	-4
4623	475	15	-4	23	-4	-30	-4
4623	575	-83	-4	21	-4	-18	-4
4623	575	-78	-4	19	-4	-13	-4
4623	675	-46	-4	32	-4	-29	-5
4623	675	-45	-4	81	-4	13	-5
4623	775	-36	-4	27	-4	-39	-4
4623	775	-4	-4	27	-4	-37	-4
4623	875	41	-4	40	-4	-10	-4
4623	975	-56	-5	33	-4	-71	-5
4623	975	-46	-5	32	-4	-20	-5
5113	0	26	-3	63	-4	-33	-3
5113	0	25	-3	54	-4	-37	-3
5113	75	17	-4	40	-4	-46	-4
5113	75	18	-4	36	-4	-40	-4
5113	175	78	-5	13	-4	-42	-4
5113	175	34	-5	24	-4	-21	-4
5113	275	-33	-5	67	-5	37	-4
5113	275	10	-5	77	-5	41	-4
5113	275	-14	-4	17	-4	36	-4
5113	375	14	-4	21	-4	-33	-4
5113	375	96	-5	22	-4	-30	-4
5113	475	-81	-4	62	-4	-49	-4
5113	475	-78	-4	61	-4	-51	-4
5113	575	60	-5	72	-4	71	-4
5113	575	15	-4	71	-4	78	-4
5113	575	-27	-5	69	-4	70	-4
5113	***	26	-4	66	-4	-54	-4
5113	675	31	-4	64	-4	-34	-4
5113	675	26	-4	63	-4	-44	-4
5113	775	39	-4	63	-4	-43	-4
5113	775	31	-4	61	-4	-43	-4
5113	875	1	-4	21	-4	42	-4
5113	875	11	-4	21	-4	47	-4
5113	975	47	-4	19	-4	10	-4

Sample	Field	X-value	Sigm-X	Y-Value	Sigm-Y	Z-Value	Sigm-Z
5113	975	55	-4	15	-4	21	-4
5113	975	49	-4	18	-4	18	-4
5112	0	24	-3	18	-3	80	-4
5112	0	20	-3	72	-4	92	-4
5112	50	67	-4	30	-4	-32	-4
5112	50	83	-4	55	-4	-38	-4
5112	150	-16	-5	14	-4	-12	-4
5112	150	71	-5	16	-4	-61	-5
5112	150	23	-5	20	-4	-26	-4
5112	250	-67	-5	14	-4	95	-5
5112	250	-17	-5	14	-4	11	-4
5112	250	25	-5	18	-4	18	-5
5112	350	30	-4	43	-4	-36	-4
5112	350	29	-4	41	-4	-25	-4
5112	350	34	-4	43	-4	-24	-4
5112	450	-47	-5	41	-4	-79	-4
5112	450	-24	-5	42	-4	-68	-4
5112	550	59	-5	51	-4	-49	-4
5112	550	29	-5	50	-4	-54	-4
5112	650	93	-5	19	-4	-47	-4
5112	650	83	-5	20	-4	-40	-4
5112	650	32	-5	20	-4	-52	-4
5112	750	35	-4	29	-4	-23	-4
5112	750	34	-4	30	-4	-14	-4
5112	750	10	-4	27	-4	-47	-4
5112	850	14	-4	26	-4	-36	-4
5112	850	-22	-6	26	-4	-40	-4
5112	950	-46	-5	22	-4	-41	-4
5112	950	-16	-5	19	-4	-31	-4
5111	0	67	-3	15	-3	-23	-3
5111	0	28	-3	12	-3	-22	-3
5111	100	66	-4	67	-4	-39	-4
5111	100	78	-4	69	-4	-35	-4
5111	200	-10	-4	28	-4	-33	-4
5111	200	26	-5	30	-4	24	-4
5111	300	19	-4	65	-4	-13	-3
5111	300	33	-4	54	-4	-10	-3
5111	300	21	-4	62	-4	-11	-3
5111	400	18	-4	69	-5	-22	-4
5111	400	27	-4	97	-5	-18	-4
5111	400	19	-4	72	-5	-31	-4
5111	500	15	-4	11	-4	-53	-4
5111	500	-5	-7	37	-4	-15	-3
5111	500	-15	-6	36	-4	-15	-3
5111	600	22	-5	72	-4	-50	-4
5111	600	-72	-4	74	-4	-27	-3
5111	600	-64	-5	68	-4	-12	-3
5111	700	-16	-3	97	-4	-12	-3
5111	700	-15	-3	96	-4	-12	-3
5111	800	51	-4	66	-4	30	-4
5111	800	56	-4	65	-4	45	-4
5111	900	-65	-4	32	-4	-91	-4
5111	900	-88	-4	41	-4	-13	-3
5511	0	11	-4	54	-4	-20	-3
5511	0	60	-5	48	-4	-30	-3
5511	100	-11	-3	20	-4	-43	-4

Sample	Field	X-value	Sigm-X	Y-Value	Sigm-Y	Z-Value	Sigm-Z
5511	100	-11	-3	22	-4	-43	-4
5511	200	-12	-3	32	-4	-25	-4
5511	200	-12	-3	33	-4	-26	-4
5511	300	-15	-3	26	-4	-47	-4
5511	300	-15	-3	26	-4	-46	-4
5511	400	-78	-4	19	-4	-52	-4
5511	400	-74	-4	19	-4	-52	-4
5511	500	-13	-3	35	-4	-23	-4
5511	600	-13	-3	37	-4	-22	-4
5511	500	10	-4	30	-4	-60	-5
5511	600	80	-5	39	-4	-32	-5
5511	600	65	-5	29	-4	-70	-5
5511	700	23	-4	33	-4	-30	-5
5511	700	25	-4	33	-4	-68	-6
5511	800	25	-3	63	-4	-14	-4
5511	800	24	-3	64	-4	-10	-4
5511	900	-23	-3	27	-4	-81	-5
5511	900	-23	-3	28	-4	-64	-5
5512	0	-71	-4	13	-3	-42	-3
5512	0	-70	-4	15	-3	-42	-3
5512	500	-26	-3	51	-4	-11	-3
5512	500	-25	-3	48	-4	-11	-3
5512	150	-13	-3	36	-4	-73	-4
5512	150	-13	-3	35	-4	-73	-4
5512	250	-15	-3	29	-4	-17	-4
5512	250	-14	-3	33	-4	-15	-4
5512	350	-56	-4	39	-4	-86	-4
5512	350	-54	-4	41	-4	-85	-4
5512	450	62	-4	39	-4	-12	-3
5512	450	65	-4	36	-4	-12	-3
5512	550	-16	-3	27	-4	-49	-4
5512	550	-15	-3	29	-4	-42	-4
5512	650	-24	-3	53	-4	-12	-3
5512	650	-24	-3	53	-4	-12	-3
5512	750	-34	-3	54	-4	-1	-3
5512	750	-31	-3	46	-4	-10	-3
5512	850	83	-4	36	-4	14	-3
5512	850	82	-4	33	-4	-13	-3
5512	950	-55	-3	81	-4	30	-4
5512	950	-54	-3	79	-4	29	-4
5513	0	26	-3	12	-3	-50	-4
5513	0	27	-3	12	-3	-57	-4
5513	750	20	-3	63	-4	-14	-3
5513	750	19	-3	64	-4	-14	-3
5513	175	14	-3	42	-4	-14	-3
5513	175	14	-3	41	-4	-14	-3
5513	275	19	-3	40	-4	-15	-3
5513	275	20	-3	39	-4	-15	-3
5513	375	92	-4	44	-4	-15	-3
5513	375	96	-4	41	-4	-15	-3
5513	475	81	-4	69	-4	-37	-4
5513	475	78	-4	70	-4	-33	-4
5513	575	100	-3	69	-4	-10	-3
5513	575	99	-4	63	-4	-10	-3
5513	675	32	-4	49	-4	-57	-4
5513	675	31	-4	50	-4	-54	-4

Sample	Field	X-value	Sigm-X	Y-Value	Sigm-Y	Z-Value	Sigm-Z
5513	775	39	-4	33	-4	-12	-3
5513	775	39	-4	33	-4	-12	-3
5513	875	-31	-3	33	-4	-56	-4
5513	875	-30	-3	35	-4	-55	-4
5513	975	-38	-3	59	-4	11	-4
5513	975	-38	-3	59	-4	99	-5
5513	975	-38	-3	59	-4	53	-4
5211	0	36	-4	54	-4	-54	-4
5211	0	37	-4	53	-4	-53	-4
5211	100	-28	-4	27	-4	38	-4
5211	100	-25	-4	27	-4	39	-4
5211	200	11	-4	11	-4	26	-4
5211	200	13	-4	11	-4	28	-4
5211	300	17	-4	32	-4	-65	-4
5211	300	18	-4	31	-4	-52	-5
5211	400	60	-4	22	-4	98	-5
5211	400	63	-4	22	-4	86	-5
5211	500	75	-5	13	-4	89	-4
5211	500	75	-5	11	-4	86	-4
5211	600	-36	-4	34	-4	18	-4
5211	600	-30	-4	34	-4	17	-4
5211	700	-28	-4	57	-4	-17	-4
5211	700	-31	-4	56	-4	-15	-4
5211	800	-36	-5	81	-4	41	-4
5211	800	-29	-5	80	-4	44	-4
5211	900	-82	-5	50	-4	-97	-5
5211	900	-62	-5	50	-4	-12	-4
5212	0	-16	-3	47	-4	96	-6
5212	0	-16	-3	46	-4	27	-5
5212	50	-61	-4	33	-4	-33	-4
5212	50	-61	-4	34	-4	-26	-4
5212	150	-41	-4	56	-4	-32	-4
5212	150	-47	-4	56	-4	-32	-4
5212	250	-25	-4	32	-4	10	-4
5212	250	-25	-4	33	-4	14	-4
5212	350	-20	-4	14	-4	-51	-4
5212	350	-19	-4	14	-4	-51	-4
5212	450	93	-5	53	-4	52	-4
5212	450	53	-5	51	-4	52	-4
5212	550	-45	-4	62	-4	76	-4
5212	550	-41	-4	63	-4	80	-4
5212	650	-65	-4	48	-4	65	-5
5212	650	-61	-4	46	-4	99	-5
5212	750	-22	-4	60	-4	87	-4
5212	750	-26	-4	58	-4	-84	-4
5212	850	-69	-4	31	-4	38	-4
5212	850	-69	-4	30	-4	38	-4
5212	950	11	-4	23	-4	-18	-4
5212	950	20	-4	34	-4	-15	-4
5212	950	22	-4	35	-4	-13	-4
5213	0	-3	-4	65	-4	-72	-4
5213	0	-28	-4	66	-4	-71	-4
5213	75	-17	-4	16	-4	-68	-4
5213	75	-20	-4	13	-4	-68	-4
5213	175	11	-4	25	-4	-94	-5
5213	175	14	-4	24	-4	-34	-5
5213	175	77	-5	27	-4	-11	-4

Sample	Field	X-value	Sigm-X	Y-Value	Sigm-Y	Z-Value	Sigm-Z
5213	275	-33	-5	27	-4	-63	-4
5213	275	-33	-5	26	-4	-51	-4
5213	375	12	-4	51	-4	-19	-4
5213	375	-13	-4	51	-4	-20	-4
5213	475	-11	-4	23	-4	-32	-4
5213	475	-10	-4	22	-4	-31	-4
5213	575	69	-4	55	-4	90	-5
5213	575	90	-4	55	-4	10	-4
5213	675	-45	-5	56	-4	-26	-4
5213	675	-25	-4	47	-4	-26	-4
5213	775	-79	-4	29	-4	-42	-4
5213	775	-80	-4	28	-4	-41	-4
5213	875	11	-4	26	-4	-29	-4
5213	875	12	-4	25	-4	-28	-4
5213	975	-13	-4	59	-4	-36	-4
5213	975	-12	-4	59	-4	-38	-4
5621	0	85	-4	12	-3	-10	-2
5621	0	10	-3	10	-3	-10	-2
5621	100	-59	-5	43	-4	-40	-3
5621	100	62	-7	34	-4	-39	-3
5621	200	-46	-4	34	-4	-41	-3
5621	200	-11	-3	98	-4	-47	-3
5621	200	-13	-3	10	-3	-48	-3
5621	300	17	-4	52	-4	-37	-3
5621	300	58	-5	52	-4	-36	-3
5621	400	-12	-3	64	-4	-31	-3
5621	400	-12	-3	-36	-4	-30	-3
5621	500	-76	-4	87	-4	-26	-3
5621	500	-74	-4	88	-4	-25	-3
5621	600	-68	-5	44	-4	-25	-3
5621	600	-83	-5	43	-4	-23	-3
5621	700	-21	-4	16	-4	-12	-3
5621	700	-27	-4	18	-4	-10	-3
5621	800	-35	-4	48	-4	-17	-3
5621	800	-26	-4	52	-4	-16	-3
5621	900	-57	-5	60	-4	-17	-3
5621	900	31	-5	60	-4	-17	-3
5612	0	36	-3	55	-4	-53	-3
5612	0	66	-6	64	-4	-50	-3
5612	50	10	-3	42	-4	-26	-3
5612	50	10	-3	43	-4	-26	-3
5612	150	52	-4	65	-4	-20	-3
5612	150	51	-4	64	-4	-18	-3
5612	250	-16	-4	41	-4	-22	-3
5612	250	-18	-4	42	-4	-21	-3
5612	350	34	-4	52	-4	-19	-3
5612	685	30	-4	52	-4	-17	-3
5612	450	-22	-4	59	-4	-14	-3
5612	450	-25	-4	42	-4	-21	-3
5612	550	-45	-4	49	-4	-19	-3
5612	550	-41	-4	52	-4	-18	-3
5612	650	-31	-5	33	-4	-14	-3
5612	650	42	-5	37	-4	-14	-3
5612	750	42	-4	53	-4	-16	-3
5612	750	33	-4	56	-4	-15	-3
5612	850	-27	-4	16	-4	-12	-3

Sample	Field	X-value	Sigm-X	Y-Value	Sigm-Y	Z-Value	Sigm-Z
5612	850	-25	-4	17	-4	-11	-3
5612	950	-39	-4	44	-4	-91	-4
5612	950	-31	-4	46	-4	-92	-4
5613	0	49	-3	12	-3	-71	-3
5613	0	45	-3	93	-4	-42	-3
5613	75	12	-3	89	-4	-20	-3
5613	75	13	-3	84	-4	-20	-3
5613	175	51	-4	73	-4	-11	-3
5613	175	44	-4	77	-4	-10	-3
5613	275	45	-4	71	-4	-39	-4
5613	275	49	-4	71	-4	-40	-4
5613	375	24	-4	46	-4	-96	-4
5613	375	23	-4	45	-4	-90	-4
5613	475	2	-4	48	-4	-45	-4
5613	475	12	-4	47	-4	-39	-4
5613	575	18	-4	75	-4	-76	-4
5613	575	21	-4	73	-4	-67	-4
5613	675	70	-4	51	-4	-66	-5
5613	675	63	-4	49	-4	-18	-5
5613	775	18	-4	39	-4	-89	-4
5613	775	15	-4	39	-4	-86	-4
5613	875	29	-4	38	-4	85	-5
5613	875	27	-4	38	-4	11	-4
5712	0	94	-4	59	-4	-22	-4
5712	0	96	-4	59	-4	-2	-4
5712	100	74	-5	24	-4	-49	-4
5712	100	97	-5	25	-4	-48	-4
5712	200	-92	-5	11	-4	-34	-4
5712	200	-74	-5	13	-4	-33	-4
5712	300	54	-5	18	-4	-13	-4
5712	300	96	-5	21	-4	-13	-4
5712	400	-32	-4	22	-4	-49	-4
5712	400	-33	-4	24	-4	-48	-4
5712	500	-11	-3	23	-4	-21	-4
5712	500	-11	-3	22	-4	-21	-4
5712	600	-59	-5	39	-4	-29	-5
5712	600	-43	-5	38	-4	-95	-6
5712	700	1	-4	46	-4	-88	-5
5712	700	88	-5	16	-4	-61	-5
5712	700	63	-5	15	-4	-86	-5
5712	800	-1	-4	46	-4	-25	-4
5712	800	-11	-4	44	-4	-21	-4
5712	800	-14	-4	45	-4	-23	-4
5712	900	11	-5	13	-4	-13	-4
5712	900	16	-5	12	-4	-12	-4
5711	0	-14	-3	71	-4	-38	-4
5711	0	-14	-3	67	-4	-35	-4
5711	50	-24	-4	40	-4	-11	-5
5711	50	-25	-4	40	-4	19	-5
5711	50	-24	-4	38	-4	-21	-5
5711	150	1	-4	13	-4	35	-4
5711	150	11	-4	14	-4	39	-4
5711	250	41	-4	32	-4	54	-5
5711	250	39	-4	32	-4	71	-5
5711	350	23	-4	48	-4	45	-4
5711	350	26	-4	48	-4	45	-4

Sample	Field	X-value	Sigm-X	Y-Value	Sigm-Y	Z-Value	Sigm-Z	
5711	450	16	-4	4	-4	-14	-4	
5711	450	13	-4	41	-4	-12	-4	
5711	550	6	-4	22	-4	-11	-5	
5711	550	61	-4	21	-4	16	-5	
5711	650	-11	-4	25	-4	-68	-5	
5711	650	-86	-5	24	-4	-81	-5	
5711	650	750	-18	-4	25	-4	-32	-4
5711	750	-15	-4	25	-4	-3	-4	
5711	850	-49	-4	22	-4	-25	-5	
5711	850	-47	-4	22	-4	-19	-5	
5711	950	-14	-4	21	-4	56	-4	
5711	950	-11	-4	21	-4	59	-4	
6012	0	-79	-3	17	-3	-38	-3	
6012	0	-77	-3	13	-3	-39	-3	
6012	100	-11	-4	75	-4	35	-3	
6012	100	12	-3	15	-3	37	-3	
6012	200	-14	-3	23	-3	43	-3	
6012	200	-21	-3	18	-3	46	-3	
6012	300	33	-3	29	-3	27	-3	
6012	300	31	-3	29	-3	31	-3	
6012	300	23	-3	27	-3	33	-3	
6012	400	-27	-3	13	-3	43	-3	
6012	400	-26	-3	13	-3	46	-3	
6012	500	-79	-3	88	-4	49	-3	
6012	500	-74	-3	12	-3	48	-3	
6012	600	-24	-3	31	-3	42	-3	
6012	600	-20	-3	34	-3	4	-3	
6012	700	11	-3	12	-3	15	-3	
6012	700	13	-3	14	-3	18	-3	
6012	800	-36	-3	13	-3	30	-3	
6012	800	-34	-3	14	-4	33	-3	
6012	900	-32	-3	27	-3	28	-3	
6012	900	-34	-3	26	-3	31	-3	
6013	0	39	-3	13	-3	-19	-3	
6013	0	36	-3	10	-3	-23	-3	
6013	50	-21	-4	64	-4	14	-3	
6013	50	-81	-5	57	-4	15	-3	
6013	50	-25	-5	59	-4	14	-3	
6013	150	13	-3	47	-4	41	-3	
6013	150	14	-3	42	-4	41	-3	
6013	250	22	-3	38	-4	31	-3	
6013	250	21	-3	31	-4	31	-3	
6013	350	15	-3	47	-4	19	-3	
6013	350	17	-3	55	-4	19	-3	
6013	450	15	-3	50	-4	21	-3	
6013	450	16	-3	46	-4	21	-3	
6013	550	66	-4	44	-4	51	-3	
6013	550	67	-4	45	-4	5	-3	
6013	650	-24	-4	15	-3	38	-4	
6013	650	-35	-4	16	-3	39	-3	
6013	750	50	-3	7	-4	27	-3	
6013	750	47	-3	5	-4	28	-3	
6013	850	-3	-3	12	-3	36	-3	
6013	850	-29	-3	12	-3	36	-3	
6013	950	-37	-4	62	-4	36	-3	
6013	950	-62	-4	43	-4	35	-3	

Sample	Field	X-value	Sigm-X	Y-Value	Sigm-Y	Z-Value	Sigm-Z
6111	0	-61	-3	26	-3	-14	-2
6111	0	-61	-3	25	-3	-14	-2
6111	100	-6	-3	25	-3	-13	-2
6111	100	-61	-3	25	-3	-13	-2
6111	200	-6	-3	26	-3	-14	-2
6111	200	-61	-3	25	-3	-14	-2
6111	300	-58	-3	28	-3	-14	-2
6111	300	-58	-3	29	-3	-14	-2
6111	400	-61	-3	25	-3	-13	-2
6111	400	-61	-3	26	-3	-13	-2
6111	500	-65	-3	24	-3	-13	-2
6111	500	-65	-3	25	-3	-13	-2
6111	600	-64	-3	25	-3	-14	-2
6111	600	-64	-3	25	-3	-14	-2
6111	700	-68	-3	24	-3	-14	-2
6111	700	-66	-3	24	-3	-13	-2
6111	800	-67	-3	24	-3	-13	-2
6111	800	-66	-3	23	-3	-13	-2
6111	900	-69	-3	22	-3	-14	-2
6111	900	-69	-3	23	-3	-14	-2
6113	0	-84	-3	11	-3	-11	-2
6113	0	-84	-3	13	-3	-1	-2
6113	50	-85	-3	99	-4	-11	-2
6113	50	-84	-3	11	-3	-11	-2
6113	150	-82	-4	12	-3	-1	-2
6111	150	-83	-3	12	-3	-1	-2
6113	250	-83	-3	11	-3	-11	-2
6112	250	-93	-3	12	-3	-11	-2
6112	350	-83	-3	11	-3	-11	-2
6112	350	-82	-3	11	-3	-11	-2
6112	450	-84	-3	11	-3	-11	-2
6112	450	-84	-3	11	-3	-11	-3
6112	550	-85	-3	11	-3	-11	-2
6112	550	-85	-3	11	-3	-11	-2
6112	650	-86	-3	11	-3	-11	-2
6112	650	-84	-3	12	-3	-11	-2
6112	750	-87	-3	12	-3	-11	-2
6112	750	-87	-3	12	-3	-11	-2
6112	850	-89	-3	13	-3	-11	-2
6112	850	-92	-3	15	-3	-11	-2
6112	950	-92	-3	13	-3	-11	-2
6112	950	-93	-3	13	-3	-11	-2
6113	0	-27	-3	15	-3	-84	-3
6113	0	-27	-3	15	-3	-85	-3
6113	75	-27	-4	26	-3	-91	-3
6113	75	-14	-3	14	-3	-91	-3
6113	175	-14	-3	18	-3	-91	-3
6113	175	-22	-3	19	-3	-9	-3
6113	275	-21	-3	14	-3	-88	-3
6113	275	-2	-3	14	-3	-9	-3
6113	375	-19	-3	15	-3	-93	-3
6113	375	-18	-3	14	-3	-91	-3
6113	475	-19	-3	13	-3	-87	-3
6113	475	-18	-3	14	-3	-87	-3
6113	575	-19	-3	15	-3	-89	-3
6113	575	-18	-3	14	-3	-90	-3

Sample	Field	X-value	Sigm-X	Y-Value	Sigm-Y	Z-Value	Sigm-Z
6113	675	-24	-3	15	-3	-55	-3
6113	675	-23	-3	15	-3	-87	-3
6113	775	-25	-3	14	-3	-91	-3
6113	775	-24	-3	14	-3	-92	-3
6113	875	-26	-3	14	-3	-95	-3
6113	875	-27	-3	14	-3	-95	-3
6113	975	-29	-3	16	-3	-95	-3
6113	975	-28	-3	16	-3	-99	-3
6213	0	-92	-5	18	-4	24	-4
6213	0	-90	-5	18	-4	24	-4
6213	100	-98	-5	17	-5	-33	-5
6213	100	-98	-5	13	-5	-32	-5
6213	200	-66	-5	38	-5	-10	-4
6213	200	-65	-5	38	-5	-10	-4
6213	300	-73	-5	34	-5	-12	-5
6213	300	-73	-5	35	-5	-15	-6
6213	400	-60	-5	18	-5	-33	-5
6213	400	-59	-5	18	-5	-33	-5
6213	500	-75	-5	17	-5	98	-6
6213	500	-76	-5	17	-5	86	-6
6213	600	-21	-5	23	-5	28	-5
6213	600	-21	-5	24	-5	29	-5
6213	700	-24	-5	27	-5	13	-7
6213	800	-18	-5	36	-5	39	-5
6213	900	-35	-5	22	-5	-38	-5
6211	0	-5	-4	11	-3	14	-3
6211	0	-46	-4	11	-3	14	-3
6211	50	-28	-4	24	-4	68	-5
6211	50	-28	-4	24	-4	85	-5
6211	150	-15	-4	14	-4	-41	-5
6211	250	-43	-4	90	-5	-72	-5
6211	250	-42	-4	77	-5	-60	-5
6211	350	16	-4	19	-4	79	-5
6211	350	19	-4	20	-4	75	-5
6211	450	92	-4	10	-4	-35	-5
6211	450	-22	-4	99	-5	-28	-5
6211	550	-22	-4	39	-4	-73	-5
6211	550	-19	-4	40	-4	-39	-5
6211	650	-39	-4	21	-4	48	-5
6211	650	-36	-4	21	-4	46	-5
6211	750	-25	-4	19	-4	-21	-4
6211	750	-26	-4	18	-4	-18	-4
6211	850	-88	-5	14	-4	-56	-5
6211	850	-10	-4	11	-4	-26	-5
6211	950	-3	-6	86	-5	-39	-5
6211	950	-13	-5	82	-5	-24	-5
6212	0	-26	-4	15	-4	-14	-4
6212	0	-20	-5	15	-4	-14	-4
6212	75	-62	-5	30	-5	-35	-5
6212	175	23	-6	27	-5	94	-6
6212	275	-86	-5	18	-5	-14	-5
6212	375	85	-6	46	-5	-71	-5
6212	475	-52	-5	13	-5	-46	-5
6212	575	-11	-4	17	-5	-40	-5
6212	675	41	-5	62	-5	-46	-5
6212	775	-23	-5	72	-5	-52	-5

Sample	Field	X-value	Sigm-X	Y-Value	Sigm-Y	Z-Value	Sigm-Z
6212	875	-75	-6	79	-5	-99	-6
4913	0	-32	-3	16	-3	92	-5
4913	0	-32	-3	16	-3	11	-4
4913	100	-13	-3	86	-3	88	-4
4913	100	-12	-3	15	-3	93	-4
4913	200	-20	-3	87	-4	71	-5
4913	200	-19	-3	79	-4	15	-3
4913	300	-27	-3	25	-3	-22	-3
4913	300	-28	-3	26	-3	-23	-3
4913	400	83	-4	60	-4	-10	-3
4913	400	83	-4	58	-4	-10	-3
4913	500	25	-3	94	-4	-20	-4
4913	500	25	-3	89	-4	-18	-4
4913	600	-83	-4	31	-4	65	-4
4913	600	-82	-4	30	-4	55	-4
4913	700	-25	-3	10	-3	-15	-3
4913	700	-25	-3	10	-3	-16	-3
4913	700	17	-3	18	-3	26	-3
4913	800	31	-3	37	-3	34	-3
4913	800	31	-3	38	-3	34	-3
4913	900	42	-4	52	-4	44	-3
4913	900	50	-4	60	-4	44	-3
6511	0	-65	-5	10	-4	14	-5
6511	0	-70	-5	10	-4	12	-5
6511	100	-88	-5	10	-4	-94	-6
6511	100	-89	-5	11	-4	65	-6
6511	100	-90	-5	12	-4	56	-6
6511	200	-37	-5	67	-5	-23	-5
6511	200	-36	-5	65	-5	-24	-5
6511	300	-74	-5	96	-5	-33	-5
6511	300	-69	-5	94	-5	-32	-5
6511	400	-42	-5	12	-4	-28	-5
6511	400	-40	-5	12	-4	-38	-5
6511	400	-43	-5	12	-4	-11	-5
6511	500	-56	-5	76	-5	-27	-5
6511	500	-56	-5	87	-6	-27	-5
6511	600	-53	-6	1	-4	-91	-6
6511	600	-41	-6	99	-5	-15	-5
6511	600	-64	-6	10	-4	-18	-5
6511	700	-22	-5	72	-5	75	-6
6511	700	-27	-5	75	-5	84	-6
6511	800	21	-5	54	-5	22	-5
6511	800	-10	-5	28	-5	23	-5
6511	800	-87	-6	27	-5	24	-5
6511	900	-32	-5	60	-5	68	-5
6511	900	-34	-5	40	-5	68	-5
6512	0	17	-5	76	-5	-26	-5
6512	0	20	-5	79	-5	-25	-5
6512	50	10	-5	65	-5	-23	-5
6512	50	22	-5	59	-5	-26	-5
6512	50	23	-5	59	-5	-28	-5
6512	150	19	-5	68	-5	55	-5
6512	150	17	-5	71	-5	-56	-5
6512	250	-17	-5	58	-5	-22	-5
6512	250	-18	-5	56	-5	-23	-5
6512	350	-10	-5	46	-5	-23	-5

Sample	Field	X-value	Sigm-X	Y-Value	Sigm-Y	Z-Value	Sigm-Z
6512	350	-12	-5	47	-5	-22	-5
6512	450	-34	-5	36	-5	-56	-5
6512	450	-38	-5	36	-5	-52	-5
6512	550	51	-6	72	-5	20	-6
6911	0	66	-6	-20	-6	66	-6
6911	0	49	-6	93	-6	51	-7
6913	0	-76	-6	44	-6	84	-6
6711	0	44	-6	70	-6	-17	-6
6711	200	35	-6	59	-6	-24	-6
6711	200	65	-6	52	-5	-92	-6
6712	0	18	-5	18	-5	29	-6
6712	0	-49	-7	27	-6	-32	-6
						20	-5
						69	-5
						60	-5
						11	-5
						28	-6
						73	-6
						53	-6
						34	-6
						11	-5
						-97	-6
						76	-6
						10	-5
						-11	-4
						-12	-4
						-16	-4
						10	-6
						42	-7
						37	-6
						59	-6
						34	-6
						-97	-6
						11	-6
						76	-6
						94	-6
						11	-6
						32	-7

Appendix D**APPARENT POLE POSITIONS**

This appendix contains the pole positions determined in this project by applying the methods developed here. There are four tables. The first table contains the positions for the DGTL approach using magnitude weight. The second table contains the positions determined by applying the CNVL method using magnitude weight. The third and fourth tables contain the corresponding results for unit weighting. The fifth table contains the results for conventional analysis.

Table 5: Apparent pole positions using the DGTL method using magnitude over the reduced spectrum.

The following table contains the apparent pole positions,(next page) for the DGTL method when applied to the spectrum restricted to the range from 100-300oe. Included in this table are the associated areas of uncertainty and the number of points used in the calculations.

Sample	Uncorrected Mean		Corrected Mean		Prob Area	No. of Points
	Latitude	Longitude	Latitude	Longitude		
11	-10.0	55.9	-11.6	60.0	18.6875	4
12	4.1	55.9	2.4	52.2	26.8218	3
13	-41.2	38.3	-43.2	45.6	10.2442	3
111	-36.4	41.9	-35.9	40.0	14.2594	3
113	-36.4	41.9	-35.9	40.0	15.0037	3
112	-36.4	41.9	-35.9	40.0	99.8954	3
211	-38.5	40.4	-42.7	54.6	17.3605	3
212	-38.5	40.4	-42.7	54.6	16.2379	2
213	-38.5	40.4	-42.7	54.6	16.5079	2
311	-33.8	43.7	-34.9	47.5	99.8954	4
312	-33.8	43.7	-34.9	47.5	99.8954	3
313	-33.8	43.7	-34.9	47.5	99.8954	3
412	8.0	54.1	7.0	51.8	99.8954	3
411	-40.1	39.2	-41.3	43.4	99.8954	3
413	-40.1	39.2	-41.3	43.4	99.8954	3
513	-20.4	16.1	-18.0	10.0	28.9536	3
511	-44.1	28.6	-41.8	10.0	29.5342	3
512	9.6	53.4	11.3	57.6	35.5146	3
611	-38.5	40.4	-37.9	38.3	27.0236	3
612	-38.5	40.4	-37.9	38.3	22.9756	3
613	-38.5	40.4	-37.9	38.3	23.1869	3
711	-34.7	43.1	-27.1	10.0	27.3564	3
712	3.8	56.0	9.0	70.0	99.8954	3
713	-34.7	43.1	-27.1	10.0	28.3716	3
811	7.6	54.3	6.1	51.0	99.8954	3
812	-32.9	44.3	-34.5	49.4	32.7472	3
813	-32.9	44.3	-34.5	49.4	15.5747	3
911	-44.6	35.5	-45.1	37.8	17.2419	2
912	-40.9	31.7	-41.5	34.1	13.6677	4
913	-44.6	35.5	-45.1	37.8	32.3979	2
011	-40.3	39.1	-42.2	45.7	19.8555	3
012	-40.3	39.1	-42.2	45.7	24.9767	3
112	1.7	57.0	0.6	54.6	38.6499	3
211	3.0	56.4	1.2	52.4	34.3657	3
212	3.0	56.4	1.2	52.4	99.8954	2
213	3.0	56.4	1.2	52.4	34.6024	3
313	-16.9	13.5	-17.9	16.3	22.3085	3
312	10.4	53.0	9.6	51.3	18.5572	2
311	10.4	53.0	9.6	51.3	99.8954	2
412	-48.2	31.9	-50.1	40.2	17.2419	3
411	7.2	54.5	5.6	51.0	26.7240	2
413	-48.2	31.9	-50.1	40.2	99.8954	2
021	-38.5	40.3	-38.5	40.3	19.5392	3
022	-38.5	40.3	-38.5	40.3	26.8118	2
023	6.2	60.2	6.2	60.2	99.8954	2
121	-42.0	37.6	-39.6	26.4	25.2062	3
122	-4.5	59.9	-2.8	63.7	26.3564	2
123	-4.5	59.9	-2.8	63.7	32.6125	2
221	-46.0	26.4	-45.4	22.4	16.3393	3
222	-23.0	26.5	-22.3	26.6	18.6023	2
223	-48.5	31.3	-47.9	27.9	18.6860	2
622	-38.6	33.5	-38.8	34.2	21.5768	3
623	-41.4	38.1	-41.6	38.8	26.1884	2
522	-33.7	43.7	-34.9	47.6	16.0482	3
523	-1.5	59.6	-2.5	61.9	19.6261	2

Sample	Uncorrected Mean Latitude	Uncorrected Mean Longitude	Corrected Mean Latitude	Corrected Mean Longitude	Prob Area	No. of Points
5721	-12.4	10.3	-0.3	23.8	30.0049	3
5722	-33.9	43.5	-22.6	10.0	99.8954	2
5723	-33.9	43.5	-22.6	10.0	22.9153	2
521	-20.1	15.9	-19.7	15.1	30.5959	3
523	-38.6	33.6	-38.3	32.4	24.2975	2
5821	-17.6	14.1	-17.6	14.1	19.7070	3
5822	39.4	36.1	39.4	36.1	20.6827	2
5823	-7.5	57.1	-7.5	57.1	13.5055	2
5921	-38.6	40.2	-38.6	40.2	32.2312	3
5922	-14.2	19.8	-14.2	19.8	17.7973	2
5923	4.4	55.9	4.4	55.9	39.3985	2
6221	3.5	56.3	1.5	52.1	36.7961	3
6222	-33.5	43.8	-35.7	50.7	24.4034	2
6223	-33.5	43.8	-35.7	50.7	23.2305	2
511	-31.5	45.1	-17.1	10.0	32.3236	3
512	3.8	56.1	11.8	81.7	99.8954	2
513	3.8	56.1	11.8	81.7	99.8954	2
621	4.3	55.9	4.3	55.9	25.7313	3
622	4.3	55.9	4.3	55.9	37.6799	2
623	-14.2	19.8	-14.2	19.8	18.6459	2
113	-4.4	17.0	-1.0	21.2	29.1218	2
112	-4.4	17.0	-1.0	21.2	36.5914	1
111	-4.4	17.0	-1.0	21.2	23.2269	3
512	-34.9	42.9	-35.8	45.5	14.5463	2
513	3.7	56.2	3.0	54.6	17.2101	2
211	2.6	56.7	1.7	54.7	29.9028	3
212	-4.3	58.5	-5.1	60.5	19.7165	2
213	-13.5	19.2	-14.7	19.5	23.1325	2
621	-14.8	20.2	-15.0	20.2	21.4420	3
612	-12.2	18.4	-14.3	19.2	24.0977	2
613	0.8	38.9	-1.1	35.8	27.4437	2
712	-15.6	24.8	-3.2	41.1	13.9688	3
711	6.7	54.8	14.3	77.9	31.6314	2
012	-2.3	58.8	5.7	84.4	31.6314	3
013	34.1	40.1	45.3	79.3	99.8954	2
111	-44.6	28.0	-28.1	10.0	23.8914	3
112	-27.5	22.2	-12.3	35.2	10.3880	2
113	-27.5	22.2	-12.3	35.2	27.5787	2
213	-37.5	41.1	-40.0	49.6	25.1679	3
211	-37.5	41.1	-40.0	49.6	17.7469	2
212	-37.5	41.1	-40.0	49.6	23.5951	2
913	-38.5	40.3	-38.5	40.3	15.8121	3
511	-7.5	57.1	-7.5	57.1	30.8450	3
512	-7.5	57.1	-7.5	57.1	30.7184	2
013	-40.3	39.1	-42.2	45.7	27.7062	3
522	-14.7	24.0	-14.3	24.2	32.5669	2
511	-34.9	42.9	-35.8	45.5	13.7645	3

Table 6: Apparent pole positions using the CNVL method, and magnitude weight over the reduced spectrum.

The following table contains the apparent pole positions, (next page) obtained using the CNVL method, using magnitude weight and over the spectrum ranging from 100oe. to 300oe. Included in this table are the dimensions of the ellipses of confidence for each point. The table contains the results for data that was not corrected for error in the compass reading, as well as the corrected results.

mple	Lat	Long	Uncorrected Mean			Lat	Corrected Mean			Major		
			Confidence				Confidence					
			Radius (Circle)	Minor Axes	Major Axes		Radius (Circle)	Minor Axes	Major Axes			
1	-8.9	53.8	1.000	1.000	1.000	-10.5	57.9	1.000	1.000	1.000		
2	58.4	39.4	1.000	1.000	1.000	56.4	35.2	1.000	1.000	1.000		
3	61.3	46.7	1.000	1.000	1.000	59.4	34.4	1.000	1.000	1.000		
11	17.2	170.9	1.000	1.000	1.000	16.6	172.5	1.000	1.000	1.000		
13	-12.1	64.8	1.000	1.000	1.000	-11.8	63.6	1.000	1.000	1.000		
12	12.9	158.8	1.000	1.000	1.000	12.4	158.1	1.000	1.000	1.000		
11	2.3	68.3	1.000	1.000	1.000	-0.1	76.0	1.000	1.000	1.000		
12	-2.3	67.6	1.000	1.000	1.000	-4.8	75.6	1.000	1.000	1.000		
13	-3.5	72.0	1.000	1.000	1.000	-5.6	80.1	1.000	1.000	1.000		
11	33.7	115.7	1.000	1.000	1.000	34.1	116.9	1.000	1.000	1.000		
12	27.3	124.1	1.000	1.000	1.000	27.9	125.4	1.000	1.000	1.000		
13	40.4	111.0	1.000	1.000	1.000	40.7	111.9	1.000	1.000	1.000		
12	26.6	183.2	1.000	1.000	1.000	28.0	179.9	1.000	1.000	1.000		
11	29.8	151.7	1.000	1.000	1.000	30.9	152.5	1.000	1.000	1.000		
13	34.1	166.6	1.000	1.000	1.000	35.4	166.2	1.000	1.000	1.000		
13	36.1	50.8	1.000	1.000	1.000	37.9	50.0	1.000	1.000	1.000		
11	34.4	61.3	1.000	1.000	1.000	36.0	60.0	1.000	1.000	1.000		
12	57.6	97.3	1.000	1.000	1.000	57.7	97.5	1.000	1.000	1.000		
11	26.7	83.7	1.000	1.000	1.000	26.9	83.0	1.000	1.000	1.000		
12	20.8	87.3	1.000	1.000	1.000	20.9	86.6	1.000	1.000	1.000		
13	18.1	71.4	1.000	1.000	1.000	18.4	70.6	1.000	1.000	1.000		
11	33.4	99.5	1.000	1.000	1.000	34.0	92.3	1.000	1.000	1.000		
12	46.5	189.5	1.000	1.000	1.000	38.0	190.0	1.000	1.000	1.000		
13	32.8	123.1	1.000	1.000	1.000	30.0	115.7	1.000	1.000	1.000		
11	23.1	177.5	1.000	1.000	1.000	25.0	176.2	1.000	1.000	1.000		
12	6.9	134.8	1.000	1.000	1.000	8.1	137.4	1.000	1.000	1.000		
13	-6.7	76.1	1.000	1.000	1.000	-7.4	79.3	1.000	1.000	1.000		
11	-22.5	91.2	1.000	1.000	1.000	-22.6	92.4	1.000	1.000	1.000		
12	2.4	38.9	1.000	1.000	1.000	1.9	39.8	1.000	1.000	1.000		
13	-1.1	112.1	1.000	1.000	1.000	-0.9	113.1	1.000	1.000	1.000		
11	2.2	83.6	1.000	1.000	1.000	1.7	86.8	1.000	1.000	1.000		
12	-6.4	91.6	1.000	1.000	1.000	-6.7	95.1	1.000	1.000	1.000		
12	48.5	162.1	1.000	1.000	1.000	49.9	156.5	1.000	1.000	1.000		
11	75.9	97.9	1.000	1.000	1.000	75.5	83.7	1.000	1.000	1.000		
12	35.4	181.4	1.000	1.000	1.000	38.0	174.6	1.000	1.000	1.000		
13	77.7	188.4	1.000	1.000	1.000	80.3	152.6	1.000	1.000	1.000		
13	31.5	37.3	1.000	1.000	1.000	30.6	37.5	1.000	1.000	1.000		
12	46.8	93.4	1.000	1.000	1.000	46.6	90.8	1.000	1.000	1.000		
11	61.5	185.9	1.000	1.000	1.000	62.4	175.2	1.000	1.000	1.000		
12	-8.4	99.3	1.000	1.000	1.000	-8.4	102.8	1.000	1.000	1.000		
11	78.4	35.9	1.000	1.000	1.000	76.4	10.0	1.000	1.000	1.000		
13	51.0	122.2	1.000	1.000	1.000	51.8	122.5	1.000	1.000	1.000		
12	4.1	65.5	1.000	1.000	1.000	4.1	65.5	1.000	1.000	1.000		
12	-2.9	124.7	1.000	1.000	1.000	-2.9	124.7	1.000	1.000	1.000		
13	39.2	156.8	1.000	1.000	1.000	39.2	156.8	1.000	1.000	1.000		
21	22.8	96.7	1.000	1.000	1.000	23.0	93.8	1.000	1.000	1.000		
22	51.9	136.1	1.000	1.000	1.000	50.1	144.8	1.000	1.000	1.000		
23	65.1	15.8	1.000	1.000	1.000	67.9	36.4	1.000	1.000	1.000		
21	-35.3	92.1	1.000	1.000	1.000	-35.2	90.6	1.000	1.000	1.000		
22	18.4	19.2	1.000	1.000	1.000	19.1	19.7	1.000	1.000	1.000		
23	25.3	123.7	1.000	1.000	1.000	25.0	123.0	1.000	1.000	1.000		
22	5.7	75.9	1.000	1.000	1.000	5.7	76.2	1.000	1.000	1.000		
23	16.7	73.4	1.000	1.000	1.000	16.6	73.6	1.000	1.000	1.000		

mple	Uncorrected Mean						Corrected Mean						
	Lat	Long	Confidence			Lat	Long	Confidence			Radius (Circle)	Minor Axes	Major Axes
			Radius (Circle)	Minor Axes	Major Axes			Radius (Circle)	Minor Axes	Major Axes			
522	-14.8	181.2	1.000	1.000	1.000	-13.3	181.1	1.000	1.000	1.000	1.000	1.000	1.000
523	-47.1	94.8	1.000	1.000	1.000	-47.2	98.7	1.000	1.000	1.000	1.000	1.000	1.000
721	52.7	83.6	1.000	1.000	1.000	56.4	83.4	1.000	1.000	1.000	1.000	1.000	1.000
722	34.2	111.1	1.000	1.000	1.000	32.9	100.8	1.000	1.000	1.000	1.000	1.000	1.000
723	16.8	85.5	1.000	1.000	1.000	21.3	71.9	1.000	1.000	1.000	1.000	1.000	1.000
21	40.2	51.9	1.000	1.000	1.000	40.4	51.9	1.000	1.000	1.000	1.000	1.000	1.000
23	18.2	52.1	1.000	1.000	1.000	18.5	51.8	1.000	1.000	1.000	1.000	1.000	1.000
321	17.8	28.2	1.000	1.000	1.000	17.8	28.2	1.000	1.000	1.000	1.000	1.000	1.000
322	20.3	84.7	1.000	1.000	1.000	20.3	84.7	1.000	1.000	1.000	1.000	1.000	1.000
323	-2.1	26.0	1.000	1.000	1.000	-2.1	26.0	1.000	1.000	1.000	1.000	1.000	1.000
921	39.8	103.4	1.000	1.000	1.000	39.8	103.4	1.000	1.000	1.000	1.000	1.000	1.000
922	16.9	40.7	1.000	1.000	1.000	16.9	40.7	1.000	1.000	1.000	1.000	1.000	1.000
923	60.0	181.2	1.000	1.000	1.000	60.0	181.2	1.000	1.000	1.000	1.000	1.000	1.000
221	81.2	114.7	1.000	1.000	1.000	81.6	100.9	1.000	1.000	1.000	1.000	1.000	1.000
222	28.1	76.4	1.000	1.000	1.000	27.1	78.9	1.000	1.000	1.000	1.000	1.000	1.000
223	6.9	130.8	1.000	1.000	1.000	8.4	134.3	1.000	1.000	1.000	1.000	1.000	1.000
511	42.1	92.1	1.000	1.000	1.000	45.5	84.2	1.000	1.000	1.000	1.000	1.000	1.000
512	55.8	173.9	1.000	1.000	1.000	40.4	190.0	1.000	1.000	1.000	1.000	1.000	1.000
513	36.7	97.1	1.000	1.000	1.000	39.0	86.1	1.000	1.000	1.000	1.000	1.000	1.000
521	63.3	43.1	1.000	1.000	1.000	63.3	43.1	1.000	1.000	1.000	1.000	1.000	1.000
522	53.4	185.1	1.000	1.000	1.000	53.4	185.1	1.000	1.000	1.000	1.000	1.000	1.000
523	26.2	17.6	1.000	1.000	1.000	26.2	17.6	1.000	1.000	1.000	1.000	1.000	1.000
113	41.4	153.5	1.000	1.000	1.000	38.8	153.0	1.000	1.000	1.000	1.000	1.000	1.000
112	52.9	58.2	1.000	1.000	1.000	55.1	59.4	1.000	1.000	1.000	1.000	1.000	1.000
111	58.4	85.1	1.000	1.000	1.000	59.3	85.8	1.000	1.000	1.000	1.000	1.000	1.000
512	-17.2	82.1	1.000	1.000	1.000	-17.5	83.9	1.000	1.000	1.000	1.000	1.000	1.000
513	38.5	45.1	1.000	1.000	1.000	37.7	42.2	1.000	1.000	1.000	1.000	1.000	1.000
211	49.1	150.1	1.000	1.000	1.000	50.1	149.7	1.000	1.000	1.000	1.000	1.000	1.000
212	-51.0	98.9	1.000	1.000	1.000	-51.0	102.3	1.000	1.000	1.000	1.000	1.000	1.000
213	3.3	27.3	1.000	1.000	1.000	2.1	25.1	1.000	1.000	1.000	1.000	1.000	1.000
521	25.3	32.6	1.000	1.000	1.000	25.1	32.7	1.000	1.000	1.000	1.000	1.000	1.000
522	37.2	35.2	1.000	1.000	1.000	35.4	34.9	1.000	1.000	1.000	1.000	1.000	1.000
523	59.7	35.0	1.000	1.000	1.000	57.8	29.4	1.000	1.000	1.000	1.000	1.000	1.000
712	22.3	13.5	1.000	1.000	1.000	35.8	43.4	1.000	1.000	1.000	1.000	1.000	1.000
711	71.3	155.9	1.000	1.000	1.000	58.4	190.0	1.000	1.000	1.000	1.000	1.000	1.000
712	11.1	184.9	1.000	1.000	1.000	-5.3	172.7	1.000	1.000	1.000	1.000	1.000	1.000
713	-4.0	156.9	1.000	1.000	1.000	-19.4	168.9	1.000	1.000	1.000	1.000	1.000	1.000
111	15.9	47.4	1.000	1.000	1.000	30.8	40.6	1.000	1.000	1.000	1.000	1.000	1.000
12	4.3	28.5	1.000	1.000	1.000	20.8	31.2	1.000	1.000	1.000	1.000	1.000	1.000
13	24.5	41.7	1.000	1.000	1.000	39.9	44.1	1.000	1.000	1.000	1.000	1.000	1.000
113	22.3	82.9	1.000	1.000	1.000	21.5	86.1	1.000	1.000	1.000	1.000	1.000	1.000
111	-14.9	88.6	1.000	1.000	1.000	-15.4	94.0	1.000	1.000	1.000	1.000	1.000	1.000
112	11.2	142.0	1.000	1.000	1.000	13.3	145.6	1.000	1.000	1.000	1.000	1.000	1.000
113	-19.1	94.0	1.000	1.000	1.000	-19.1	94.0	1.000	1.000	1.000	1.000	1.000	1.000
111	-78.0	63.3	1.000	1.000	1.000	-78.0	63.3	1.000	1.000	1.000	1.000	1.000	1.000
112	-55.0	80.7	1.000	1.000	1.000	-55.0	80.7	1.000	1.000	1.000	1.000	1.000	1.000
113	10.3	90.2	1.000	1.000	1.000	9.9	93.0	1.000	1.000	1.000	1.000	1.000	1.000
12	51.1	49.7	1.000	1.000	1.000	51.4	49.9	1.000	1.000	1.000	1.000	1.000	1.000
111	-20.2	82.7	1.000	1.000	1.000	-20.4	84.5	1.000	1.000	1.000	1.000	1.000	1.000

Table 7: Apparent polar positions using conventional analysis over the reduced spectrum.

The pole positions that are contained in the table in the following pages, (next page) are those obtained in using the conventional methods that are currently used. This table contains the sample identifier and the pole postions.

Sample	Latitude	Longitude
112	98.82	-30.89
211	78.54	-4.35
1013	64.75	-17.56
4512	148.38	15.96
4513	167.01	7.55
5523	28.80	-42.50
5612	36.64	50.26
5613	93.61	37.97
5621	99.50	-36.13
5721	73.64	-22.67
5722	129.63	26.98
311	188.54	0.82
522	98.27	39.28
312	18.44	0.31
313	111.94	44.37
412	104.00	38.10
1011	106.95	-38.42
5022	128.80	-10.04
6213	85.06	-29.13
6211	186.76	1.35
6112	99.11	-32.84
5623	39.43	-20.10
5511	22.38	12.21
5223	122.18	-12.29
5213	43.58	19.14
5212	50.69	-46.82
5112	77.10	33.30
4623	33.39	15.48
4622	189.64	26.98
4621	46.80	59.16
1413	158.65	44.47
1411	129.45	40.36
1311	178.34	45.32
1112	161.05	44.45
913	83.10	-41.76
912	128.52	-8.28
712	169.72	32.43
711	125.07	-28.07
613	55.08	-24.04
611	162.49	-11.11
523	97.29	-16.62
511	103.87	46.21
413	118.40	54.06

Table 8: Apparent polar positions using DGTL analysis with unit weighting over the reduced spectrum.

The pole positions that are contained in the table, (next page) in the following pages, are those obtained in using the DGTL method with a unit weighting scheme over the spectrum ranging from 100oe. to 300oe. This table contains the sample identifier, the pole positions, the area of confidence, and the number of points available in the calculations.

Sample	Uncorrected Mean Latitude	Uncorrected Mean Longitude	Corrected Mean Latitude	Corrected Mean Longitude	Prob Area	No. of Points
11	6.0	42.5	4.1	45.7	3.3587	4
12	49.4	18.6	47.0	10.0	2.4646	3
13	-41.2	38.3	-43.2	45.6	0.0731	3
111	46.6	145.8	46.1	147.8	3.3154	3
113	-12.2	66.9	-11.9	65.8	0.9299	3
112	15.5	159.8	15.0	159.1	2.3862	3
211	3.6	67.6	1.2	75.1	0.9026	3
212	-3.6	66.7	-6.1	74.9	0.8360	2
213	-2.5	70.1	-4.8	78.2	0.8180	2
311	31.3	117.8	31.7	119.0	0.8815	4
312	28.4	123.0	28.9	124.3	1.4607	3
313	45.9	107.3	46.1	108.0	1.0841	3
412	33.4	181.9	34.8	178.1	1.4750	3
411	29.5	150.3	30.6	151.1	1.1995	3
413	40.7	171.5	42.0	169.8	2.1031	3
513	36.2	51.6	38.0	50.8	0.7190	3
511	37.5	60.0	39.1	58.9	0.6519	3
512	59.8	94.8	60.0	95.4	1.1785	3
611	26.1	84.6	26.3	83.9	0.5758	3
612	18.2	75.7	18.5	74.9	1.4348	3
613	18.2	75.7	18.5	74.9	0.7139	3
711	33.4	100.0	33.9	92.8	1.8597	3
712	36.3	186.7	27.8	190.0	2.5489	3
713	28.8	122.0	26.2	113.7	2.9731	3
811	-3.9	174.0	-1.9	177.5	4.1924	3
812	5.3	137.6	6.5	140.3	3.2396	3
813	-8.1	61.3	-9.3	64.7	1.7696	3
911	-22.9	91.9	-23.0	93.1	0.7051	2
912	0.5	24.5	-0.1	25.4	1.1528	4
913	-4.9	120.8	-4.7	121.8	2.5176	2
011	-20.8	88.9	-21.2	93.0	1.9300	3
012	-7.5	90.6	-7.8	94.2	0.7428	3
112	45.6	165.5	46.9	159.8	0.3400	3
211	73.7	122.4	74.5	109.5	1.0225	3
212	38.0	183.0	40.6	174.3	1.8640	2
213	42.6	152.4	44.6	152.2	2.7006	3
313	32.8	35.3	31.9	35.3	1.3569	3
312	31.0	100.0	31.0	97.9	0.1240	2
311	50.7	182.0	51.7	174.8	2.9609	2
412	-41.4	100.0	-41.3	105.0	1.7926	3
411	79.8	32.5	77.8	10.0	1.0636	2
413	61.2	110.8	61.6	110.0	1.5963	2
021	-4.1	66.6	-4.1	66.6	1.6550	3
022	-2.6	126.6	-2.6	126.6	1.8303	2
023	38.7	157.5	38.7	157.5	1.4827	2
121	13.9	57.9	15.8	54.9	1.3393	3
122	36.6	167.8	34.1	180.0	3.9798	2
123	56.2	30.5	58.7	43.2	1.8463	2
221	-39.3	156.7	-39.9	154.7	1.5057	3
222	9.4	16.4	10.1	16.5	1.5393	2
223	-20.1	73.7	-19.7	72.4	1.3190	2
622	0.4	86.1	0.4	86.4	1.4686	3
623	19.3	73.9	19.2	74.1	0.7486	2
522	-29.2	100.0	-29.2	103.1	1.7926	3
523	-48.2	94.8	-48.3	98.7	1.0916	2

Sample	Uncorrected Mean Latitude	Uncorrected Mean Longitude	Corrected Mean Latitude	Corrected Mean Longitude	Prob Area	No. of Points
6721	54.0	87.4	56.8	87.4	0.6018	3
6722	36.0	108.0	35.3	98.4	1.9768	2
6723	16.7	76.6	22.9	63.7	1.8393	2
521	35.8	49.2	36.0	49.1	0.3902	3
523	19.5	52.6	19.8	52.3	0.8376	2
6821	22.1	25.9	22.1	25.9	0.8419	3
6822	21.3	86.8	21.3	86.8	0.7106	2
6823	-7.5	57.1	-7.5	57.1	0.3638	2
6921	23.9	100.0	23.9	100.0	2.4843	3
6922	18.3	84.7	18.3	84.7	1.5344	2
923	58.7	151.5	58.7	151.5	3.0799	2
221	60.2	188.3	62.9	165.8	2.9635	3
222	28.4	76.7	27.4	79.2	0.5965	2
223	-10.3	183.0	-7.6	181.5	2.4019	2
511	50.1	93.9	52.4	90.3	1.0225	3
512	53.7	175.4	38.2	190.0	1.4169	2
513	62.9	82.9	66.4	93.0	1.6821	2
621	63.5	46.4	63.5	46.4	0.6471	3
622	26.5	189.3	26.5	189.3	3.7925	2
623	28.0	15.7	28.0	15.7	1.2435	2
113	13.3	168.8	10.2	165.4	3.4069	2
112	57.2	87.3	58.0	87.7	0.9322	1
111	42.8	31.2	46.0	35.2	1.6244	3
512	-18.0	84.2	-18.3	86.0	1.1032	2
513	39.6	46.3	38.8	43.4	0.9594	2
211	6.1	148.1	7.0	149.7	4.4291	3
212	-44.5	47.7	-45.5	51.5	1.3525	2
213	21.2	29.9	20.0	30.5	2.3651	2
621	23.6	32.7	23.4	32.8	0.8798	3
612	36.4	33.2	34.5	32.7	1.0584	2
613	60.2	32.2	58.3	24.7	1.1765	2
712	-2.8	11.9	10.4	34.6	1.3545	3
711	70.2	152.4	57.6	190.0	1.5877	2
012	4.4	141.6	-9.0	165.0	2.5642	3
013	-3.0	155.3	-18.3	169.0	1.9098	2
111	14.6	46.2	29.6	39.4	1.0804	3
112	-1.3	12.8	15.1	36.9	1.2012	2
113	25.9	42.0	41.3	45.0	0.7727	2
213	21.1	91.3	20.7	94.7	0.9264	3
211	-14.5	87.0	-15.1	92.4	1.6208	2
212	-6.8	89.8	-7.2	94.7	3.8849	2
913	-33.8	100.0	-33.8	100.0	4.2383	3
511	-77.7	41.6	-77.7	41.6	0.9700	3
512	-63.0	46.1	-63.0	46.1	1.4981	2
013	-12.5	109.1	-12.1	112.8	4.6412	3
522	48.7	43.8	49.0	44.0	0.6605	2
511	-18.9	81.0	-19.2	82.8	1.1142	3

Table 9: Apparent polar positions using CNVL analysis with unit weighting over the reduced spectrum.

The pole positions that are contained in the table in the following pages, are those obtained in using the CNVL method with a unit weighting scheme over the spectrum ranging from 100oe. to 300oe (next page). This table contains the sample identifier, the pole positions, the area of confidence, and the number of points available in the calculations.

Sample	Lat	Long	Uncorrected Mean			Corrected Mean					
			Confidence			Lat	Long	Confidence			Radius (Circle)
			Radius (Circle)	Minor Axes	Major Axes			Radius (Circle)	Minor Axes	Major Axes	
11	-8.9	53.8	1.000	1.000	1.000	-10.5	57.9	1.000	1.000	1.000	1.000
12	58.4	39.4	1.000	1.000	1.000	56.4	35.2	1.000	1.000	1.000	1.000
13	61.3	46.7	1.000	1.000	1.000	59.4	34.4	1.000	1.000	1.000	1.000
111	17.2	170.9	1.000	1.000	1.000	16.6	172.5	1.000	1.000	1.000	1.000
113	-12.1	64.8	1.000	1.000	1.000	-11.8	63.6	1.000	1.000	1.000	1.000
112	12.9	158.8	1.000	1.000	1.000	12.4	158.1	1.000	1.000	1.000	1.000
211	2.3	68.3	1.000	1.000	1.000	-0.1	76.0	1.000	1.000	1.000	1.000
212	-2.3	67.6	1.000	1.000	1.000	-4.8	75.6	1.000	1.000	1.000	1.000
213	-3.5	72.0	1.000	1.000	1.000	-5.6	80.1	1.000	1.000	1.000	1.000
311	33.7	115.7	1.000	1.000	1.000	34.1	116.9	1.000	1.000	1.000	1.000
312	27.3	124.1	1.000	1.000	1.000	27.9	125.4	1.000	1.000	1.000	1.000
313	40.4	111.0	1.000	1.000	1.000	40.7	111.9	1.000	1.000	1.000	1.000
412	26.6	183.2	1.000	1.000	1.000	28.0	179.9	1.000	1.000	1.000	1.000
411	29.8	151.7	1.000	1.000	1.000	30.9	152.5	1.000	1.000	1.000	1.000
413	34.1	166.6	1.000	1.000	1.000	35.4	166.2	1.000	1.000	1.000	1.000
513	36.1	50.8	1.000	1.000	1.000	37.9	50.0	1.000	1.000	1.000	1.000
511	34.4	61.3	1.000	1.000	1.000	36.0	60.0	1.000	1.000	1.000	1.000
512	57.6	97.3	1.000	1.000	1.000	57.7	97.5	1.000	1.000	1.000	1.000
511	26.7	83.7	1.000	1.000	1.000	26.9	83.0	1.000	1.000	1.000	1.000
512	20.8	87.3	1.000	1.000	1.000	20.9	86.6	1.000	1.000	1.000	1.000
513	18.1	71.4	1.000	1.000	1.000	18.4	70.6	1.000	1.000	1.000	1.000
111	33.4	99.5	1.000	1.000	1.000	34.0	92.3	1.000	1.000	1.000	1.000
112	46.5	189.5	1.000	1.000	1.000	38.0	190.0	1.000	1.000	1.000	1.000
113	32.8	123.1	1.000	1.000	1.000	30.0	115.7	1.000	1.000	1.000	1.000
111	23.1	177.5	1.000	1.000	1.000	25.0	176.2	1.000	1.000	1.000	1.000
112	6.9	134.8	1.000	1.000	1.000	8.1	137.4	1.000	1.000	1.000	1.000
113	-6.7	76.1	1.000	1.000	1.000	-7.4	79.3	1.000	1.000	1.000	1.000
111	-22.5	91.2	1.000	1.000	1.000	-22.6	92.4	1.000	1.000	1.000	1.000
112	2.4	38.9	1.000	1.000	1.000	1.9	39.8	1.000	1.000	1.000	1.000
113	-1.1	112.1	1.000	1.000	1.000	-0.9	113.1	1.000	1.000	1.000	1.000
011	2.2	83.6	1.000	1.000	1.000	1.7	86.8	1.000	1.000	1.000	1.000
012	-6.4	91.6	1.000	1.000	1.000	-6.7	95.1	1.000	1.000	1.000	1.000
112	48.5	162.1	1.000	1.000	1.000	49.9	156.5	1.000	1.000	1.000	1.000
211	75.9	97.9	1.000	1.000	1.000	75.5	83.7	1.000	1.000	1.000	1.000
212	35.4	181.4	1.000	1.000	1.000	38.0	174.6	1.000	1.000	1.000	1.000
213	77.7	188.4	1.000	1.000	1.000	80.3	152.6	1.000	1.000	1.000	1.000
313	31.5	37.3	1.000	1.000	1.000	30.6	37.5	1.000	1.000	1.000	1.000
312	46.8	93.4	1.000	1.000	1.000	46.6	90.8	1.000	1.000	1.000	1.000
311	61.5	185.9	1.000	1.000	1.000	62.4	175.2	1.000	1.000	1.000	1.000
412	-8.4	99.3	1.000	1.000	1.000	-8.4	102.8	1.000	1.000	1.000	1.000
411	78.4	35.9	1.000	1.000	1.000	76.4	10.0	1.000	1.000	1.000	1.000
413	51.0	122.2	1.000	1.000	1.000	51.8	122.5	1.000	1.000	1.000	1.000
021	4.1	65.5	1.000	1.000	1.000	4.1	65.5	1.000	1.000	1.000	1.000
022	-2.9	124.7	1.000	1.000	1.000	-2.9	124.7	1.000	1.000	1.000	1.000
023	39.2	156.8	1.000	1.000	1.000	39.2	156.8	1.000	1.000	1.000	1.000
121	22.8	96.7	1.000	1.000	1.000	23.0	93.8	1.000	1.000	1.000	1.000
122	51.9	136.1	1.000	1.000	1.000	50.1	144.8	1.000	1.000	1.000	1.000
123	65.1	15.8	1.000	1.000	1.000	67.9	36.4	1.000	1.000	1.000	1.000
221	-35.3	92.1	1.000	1.000	1.000	-35.2	90.6	1.000	1.000	1.000	1.000
222	18.4	19.2	1.000	1.000	1.000	19.1	19.7	1.000	1.000	1.000	1.000
223	25.3	123.7	1.000	1.000	1.000	25.0	123.0	1.000	1.000	1.000	1.000
622	5.7	75.9	1.000	1.000	1.000	5.7	76.2	1.000	1.000	1.000	1.000
623	16.7	73.4	1.000	1.000	1.000	16.6	73.6	1.000	1.000	1.000	1.000

mple	Lat	Long	Uncorrected Mean			Lat	Long	Corrected Mean				
			Confidence		Major			Confidence		Major		
			Radius (Circle)	Minor Axes				Radius (Circle)	Minor Axes	Axes		
522	-14.8	181.2	1.000	1.000	1.000	-13.3	181.1	1.000	1.000	1.000		
523	-47.1	94.8	1.000	1.000	1.000	-47.2	98.7	1.000	1.000	1.000		
721	52.7	83.6	1.000	1.000	1.000	56.4	83.4	1.000	1.000	1.000		
722	34.2	111.1	1.000	1.000	1.000	32.9	100.8	1.000	1.000	1.000		
723	16.8	85.5	1.000	1.000	1.000	21.3	71.9	1.000	1.000	1.000		
21	40.2	51.9	1.000	1.000	1.000	40.4	51.9	1.000	1.000	1.000		
23	18.2	52.1	1.000	1.000	1.000	18.5	51.8	1.000	1.000	1.000		
321	17.8	28.2	1.000	1.000	1.000	17.8	28.2	1.000	1.000	1.000		
322	20.3	84.7	1.000	1.000	1.000	20.3	84.7	1.000	1.000	1.000		
323	-2.1	26.0	1.000	1.000	1.000	-2.1	26.0	1.000	1.000	1.000		
921	39.8	103.4	1.000	1.000	1.000	39.8	103.4	1.000	1.000	1.000		
922	16.9	40.7	1.000	1.000	1.000	16.9	40.7	1.000	1.000	1.000		
923	60.0	181.2	1.000	1.000	1.000	60.0	181.2	1.000	1.000	1.000		
221	81.2	114.7	1.000	1.000	1.000	81.6	100.9	1.000	1.000	1.000		
222	28.1	76.4	1.000	1.000	1.000	27.1	78.9	1.000	1.000	1.000		
223	6.9	130.8	1.000	1.000	1.000	8.4	134.3	1.000	1.000	1.000		
511	42.1	92.1	1.000	1.000	1.000	45.5	84.2	1.000	1.000	1.000		
512	55.8	173.9	1.000	1.000	1.000	40.4	190.0	1.000	1.000	1.000		
513	36.7	97.1	1.000	1.000	1.000	39.0	86.1	1.000	1.000	1.000		
521	63.3	43.1	1.000	1.000	1.000	63.3	43.1	1.000	1.000	1.000		
522	53.4	185.1	1.000	1.000	1.000	53.4	185.1	1.000	1.000	1.000		
523	26.2	17.6	1.000	1.000	1.000	26.2	17.6	1.000	1.000	1.000		
113	41.4	153.5	1.000	1.000	1.000	38.8	153.0	1.000	1.000	1.000		
112	52.9	58.2	1.000	1.000	1.000	55.1	59.4	1.000	1.000	1.000		
111	58.4	85.1	1.000	1.000	1.000	59.3	85.8	1.000	1.000	1.000		
512	-17.2	82.1	1.000	1.000	1.000	-17.5	83.9	1.000	1.000	1.000		
513	38.5	45.1	1.000	1.000	1.000	37.7	42.2	1.000	1.000	1.000		
211	49.1	150.1	1.000	1.000	1.000	50.1	149.7	1.000	1.000	1.000		
212	-51.0	98.9	1.000	1.000	1.000	-51.0	102.3	1.000	1.000	1.000		
213	3.3	27.3	1.000	1.000	1.000	2.1	25.1	1.000	1.000	1.000		
221	25.3	32.6	1.000	1.000	1.000	25.1	32.7	1.000	1.000	1.000		
212	37.2	35.2	1.000	1.000	1.000	35.4	34.9	1.000	1.000	1.000		
213	59.7	35.0	1.000	1.000	1.000	57.8	29.4	1.000	1.000	1.000		
212	22.3	13.5	1.000	1.000	1.000	35.8	43.4	1.000	1.000	1.000		
211	71.3	155.9	1.000	1.000	1.000	58.4	190.0	1.000	1.000	1.000		
212	11.1	184.9	1.000	1.000	1.000	-5.3	172.7	1.000	1.000	1.000		
213	-4.0	156.9	1.000	1.000	1.000	-19.4	168.9	1.000	1.000	1.000		
111	15.9	47.4	1.000	1.000	1.000	30.8	40.6	1.000	1.000	1.000		
12	4.3	28.5	1.000	1.000	1.000	20.8	31.2	1.000	1.000	1.000		
13	24.5	41.7	1.000	1.000	1.000	39.9	44.1	1.000	1.000	1.000		
213	22.3	82.9	1.000	1.000	1.000	21.5	86.1	1.000	1.000	1.000		
211	-14.9	88.6	1.000	1.000	1.000	-15.4	94.0	1.000	1.000	1.000		
212	11.2	142.0	1.000	1.000	1.000	13.3	145.6	1.000	1.000	1.000		
213	-19.1	94.0	1.000	1.000	1.000	-19.1	94.0	1.000	1.000	1.000		
211	-78.0	63.3	1.000	1.000	1.000	-78.0	63.3	1.000	1.000	1.000		
212	-55.0	80.7	1.000	1.000	1.000	-55.0	80.7	1.000	1.000	1.000		
213	10.3	90.2	1.000	1.000	1.000	9.9	93.0	1.000	1.000	1.000		
2	51.1	49.7	1.000	1.000	1.000	51.4	49.9	1.000	1.000	1.000		
11	-20.2	82.7	1.000	1.000	1.000	-20.4	84.5	1.000	1.000	1.000		

Table 10: Apparent polar positions using DGTL analysis with unit weighting over the full spectrum.

The pole positions that are contained in the table in the following pages, are those obtained in using the DGTL method with a unit weighting scheme over the spectrum ranging from 000oe. to 900oe. (next page). This table contains the sample identifier, the pole positions, the area of confidence, and the number of points available in the calculations.

Sample	Uncorrected Mean		Corrected Mean		Prob Area	No. of Points
	Latitude	Longitude	Latitude	Longitude		
111	46.6	145.8	46.1	147.8	2.8647	15
312	16.7	129.4	17.4	131.0	0.0	20
911	-26.3	107.9	-26.2	109.2	1.6366	8
111	46.6	145.8	46.1	147.8	2.8647	15
312	16.7	129.4	17.4	131.0	0.0	20
911	-26.3	107.9	-26.2	109.2	1.6366	8
411	32.0	157.2	33.2	157.6	0.0	18
1211	60.7	45.4	58.5	31.6	1.0563	8
1512	57.0	181.0	41.5	190.0	1.0889	10
611	26.1	84.6	26.3	83.9	0.1660	14
1313	-42.5	37.3	-43.4	40.6	1.7571	8
1212	61.4	27.5	59.0	10.0	1.2662	10
5021	1.5	45.4	1.5	45.4	1.2337	9
711	19.4	123.9	16.6	113.9	3.4974	11
612	33.7	108.7	33.6	108.2	1.0573	12
613	-9.8	46.4	-9.2	45.2	0.9401	9
5113	25.9	42.0	41.3	45.0	0.8732	10
713	-50.5	105.4	-49.6	82.1	4.3499	9
1211	11.2	61.2	13.0	57.9	2.2309	9
912	-12.7	110.9	-12.5	112.0	0.5288	13
011	22.8	153.2	24.5	154.8	2.5322	10
913	-4.8	100.0	-4.8	101.0	1.3808	9
311	-28.0	114.2	-27.8	116.2	2.9927	10
522	-29.2	100.0	-29.2	103.1	3.9194	9
722	31.0	117.7	28.5	106.3	1.5939	9
721	49.5	70.5	56.0	71.1	0.4816	9
1111	24.5	27.8	27.7	28.7	1.7120	9
723	27.1	79.4	32.6	69.3	1.8949	9
5111	50.1	93.9	52.4	90.3	0.8154	9
623	42.4	17.8	42.4	17.8	1.6594	10
1112	50.5	57.1	52.9	58.0	0.8510	10
522	49.4	34.1	49.7	34.6	0.2289	8
221	75.4	25.6	72.9	10.0	2.3235	9
913	4.3	55.9	4.3	55.9	1.2337	9
822	3.2	141.0	3.2	141.0	1.8156	9
823	-0.0	190.0	-0.0	190.0	4.1933	8
921	14.8	104.9	14.8	104.9	2.7369	9
922	18.3	84.7	18.3	84.7	2.0939	8
511	-74.2	56.7	-74.2	56.7	1.1558	9
512	-57.8	27.5	-57.8	27.5	1.6254	6
111	14.6	46.2	29.1	39.2	0.8366	9
513	40.5	100.0	41.8	90.4	2.1513	11
612	27.6	30.6	25.7	30.9	0.4421	10
523	-29.3	100.0	-29.2	103.1	3.9194	9
412	-10.0	141.5	-9.1	143.8	0.0	20
521	31.1	53.6	31.3	53.4	0.0	9
222	-4.5	59.9	-2.8	63.7	2.5673	9
11	1.4	189.1	3.8	185.7	0.0	21
12	-40.8	71.9	-41.8	77.6	0.0	19
13	-41.2	38.3	-43.2	45.6	2.4395	18
113	2.1	56.8	2.5	57.8	1.0459	13
112	-39.6	156.8	-40.1	154.9	1.7678	14
211	-2.5	70.1	-4.8	78.2	0.4347	9
212	-6.6	67.8	-9.0	76.3	0.2349	10
213	-5.6	71.1	-7.7	79.5	0.2316	10

Sample	Uncorrected Mean		Corrected Mean		Prob Area	No. of Points
	Latitude	Longitude	Latitude	Longitude		
311	10.1	165.8	11.5	167.2	2.2970	18
313	31.3	117.8	31.7	119.0	0.0	17
413	19.6	185.0	20.9	181.9	0.0	22
513	26.2	46.9	28.2	45.5	0.0	19
511	27.3	50.3	29.2	48.8	0.0	20
512	62.3	78.1	63.2	79.4	0.0	18
611	36.4	88.2	36.0	89.7	0.5357	15
811	0.5	178.3	2.5	181.0	4.0360	9
1012	-7.5	90.6	-7.8	94.2	1.7263	14
1013	67.4	100.0	67.4	98.1	2.0420	10
1112	-10.9	139.8	-10.0	137.9	1.5697	8
1213	-40.1	157.2	-37.9	165.7	1.0448	10
1312	72.1	107.2	72.2	105.6	1.7040	10
1412	-45.6	161.7	-43.7	170.5	2.3386	8
1411	45.6	38.3	43.7	29.5	0.0	10
1413	59.7	105.1	59.9	104.6	2.4426	10
5123	16.2	26.3	18.8	32.7	2.3561	9
5221	-8.7	37.8	-8.1	36.5	1.3128	9
5223	-6.4	134.9	-6.8	133.8	5.1272	8
5623	17.6	60.0	17.4	60.2	1.0902	5
523	12.4	58.2	12.7	57.8	0.4574	4
5821	5.7	29.6	5.7	29.6	1.8146	9
5923	65.0	161.9	65.0	161.9	3.8218	9
5222	0.2	55.6	-1.6	59.7	1.6718	9
5223	39.2	152.9	41.3	145.6	2.2457	8
5622	54.9	141.0	54.9	141.0	3.2777	11
5113	59.9	76.4	61.2	77.9	2.0246	11
5111	16.3	21.3	15.3	21.5	1.7120	9
5512	-8.5	73.8	-8.9	75.4	1.8803	10
5513	38.7	36.6	37.9	33.3	1.8688	10
5621	20.6	35.7	20.4	35.8	0.3600	9
5613	52.2	37.8	50.4	35.3	0.4413	9
5712	-15.0	53.7	-3.6	26.7	1.6918	9
5711	67.2	143.4	55.3	190.0	2.2024	10
5012	0.4	137.1	-6.4	111.2	2.6306	9
5013	0.4	137.1	-6.4	111.2	4.7123	10
5213	13.2	96.0	13.1	99.8	0.5646	9
5211	-31.2	100.0	-31.0	106.4	1.7926	10
5212	-7.9	61.9	-9.6	67.0	2.1352	9
5622	0.4	86.1	0.4	86.4	1.7925	9
5213	14.5	38.4	13.4	39.7	2.4720	15

Table 11: Apparent polar positions using CNVL analysis with unit weighting over the full spectrum.

The pole positions that are contained in the table in the following pages, are those obtained in using the CNVL method with a unit weighting scheme over the spectrum ranging from 000oe. to 900oe. (next page). This table contains the sample identifier, the pole positions, and the dimensions of the ellipse of confidence.

Sample	Lat	Long	Uncorrected Mean			Corrected Mean			Major Axes	
			Confidence		Lat	Confidence				
			Radius (Circle)	Minor Axes		Major Axes	Radius (Circle)	Minor Axes		
11	-29.3	105.7	1.000	1.000	1.000	-29.4	106.3	1.000	1.000	1.000
112	16.0	133.4	1.000	1.000	1.000	16.9	135.0	1.000	1.000	1.000
111	-30.1	82.2	1.000	1.000	1.000	-30.3	83.6	1.000	1.000	1.000
11	-29.3	105.7	1.000	1.000	1.000	-29.4	106.3	1.000	1.000	1.000
112	16.0	133.4	1.000	1.000	1.000	16.9	135.0	1.000	1.000	1.000
111	-30.1	82.2	1.000	1.000	1.000	-30.3	83.6	1.000	1.000	1.000
11	42.8	152.6	1.000	1.000	1.000	43.9	152.5	1.000	1.000	1.000
211	72.9	14.1	1.000	1.000	1.000	70.3	10.0	1.000	1.000	1.000
.512	63.2	170.7	1.000	1.000	1.000	47.9	190.0	1.000	1.000	1.000
111	20.4	53.8	1.000	1.000	1.000	20.9	53.2	1.000	1.000	1.000
313	19.8	43.5	1.000	1.000	1.000	19.0	44.3	1.000	1.000	1.000
212	64.1	181.9	1.000	1.000	1.000	66.6	164.8	1.000	1.000	1.000
021	3.8	70.8	1.000	1.000	1.000	3.8	70.8	1.000	1.000	1.000
11	28.0	132.6	1.000	1.000	1.000	24.0	124.2	1.000	1.000	1.000
12	12.4	70.0	1.000	1.000	1.000	12.7	69.1	1.000	1.000	1.000
13	-14.9	44.5	1.000	1.000	1.000	-14.4	43.1	1.000	1.000	1.000
113	24.3	42.6	1.000	1.000	1.000	39.6	44.1	1.000	1.000	1.000
13	-12.8	120.7	1.000	1.000	1.000	-14.7	105.7	1.000	1.000	1.000
121	30.5	61.7	1.000	1.000	1.000	32.3	59.8	1.000	1.000	1.000
12	-6.0	61.8	1.000	1.000	1.000	-6.4	62.8	1.000	1.000	1.000
011	6.6	98.3	1.000	1.000	1.000	6.6	101.3	1.000	1.000	1.000
13	0.4	101.9	1.000	1.000	1.000	0.5	102.8	1.000	1.000	1.000
311	-0.5	124.6	1.000	1.000	1.000	-0.1	126.1	1.000	1.000	1.000
522	-34.7	120.4	1.000	1.000	1.000	-34.2	123.8	1.000	1.000	1.000
722	32.2	120.7	1.000	1.000	1.000	29.1	109.7	1.000	1.000	1.000
721	50.7	72.1	1.000	1.000	1.000	56.8	73.0	1.000	1.000	1.000
111	39.8	47.5	1.000	1.000	1.000	42.5	47.5	1.000	1.000	1.000
723	18.0	88.8	1.000	1.000	1.000	21.9	75.3	1.000	1.000	1.000
511	48.4	93.0	1.000	1.000	1.000	51.0	88.4	1.000	1.000	1.000
623	41.7	40.3	1.000	1.000	1.000	41.7	40.3	1.000	1.000	1.000
112	57.6	73.0	1.000	1.000	1.000	59.1	74.1	1.000	1.000	1.000
22	49.7	38.4	1.000	1.000	1.000	50.1	38.8	1.000	1.000	1.000
221	33.9	104.1	1.000	1.000	1.000	34.1	106.3	1.000	1.000	1.000
913	0.1	133.9	1.000	1.000	1.000	0.1	133.9	1.000	1.000	1.000
822	7.3	119.9	1.000	1.000	1.000	7.3	119.9	1.000	1.000	1.000
823	-6.6	20.5	1.000	1.000	1.000	-6.6	20.5	1.000	1.000	1.000
921	34.5	121.8	1.000	1.000	1.000	34.5	121.8	1.000	1.000	1.000
922	12.3	91.7	1.000	1.000	1.000	12.3	91.7	1.000	1.000	1.000
511	-74.5	107.7	1.000	1.000	1.000	-74.5	107.7	1.000	1.000	1.000
512	-55.5	63.5	1.000	1.000	1.000	-55.5	63.5	1.000	1.000	1.000
111	13.4	47.5	1.000	1.000	1.000	27.8	39.0	1.000	1.000	1.000
513	38.1	98.6	1.000	1.000	1.000	40.0	88.1	1.000	1.000	1.000
612	26.0	31.6	1.000	1.000	1.000	24.1	32.2	1.000	1.000	1.000
523	-36.7	98.1	1.000	1.000	1.000	-36.7	101.5	1.000	1.000	1.000
12	8.9	163.5	1.000	1.000	1.000	10.2	165.0	1.000	1.000	1.000
21	27.5	54.9	1.000	1.000	1.000	27.8	54.6	1.000	1.000	1.000
222	36.4	22.7	1.000	1.000	1.000	39.0	32.9	1.000	1.000	1.000
1	-11.0	58.0	1.000	1.000	1.000	-12.5	62.1	1.000	1.000	1.000
2	9.3	100.5	1.000	1.000	1.000	9.4	103.6	1.000	1.000	1.000
3	-55.3	137.5	1.000	1.000	1.000	-53.7	145.6	1.000	1.000	1.000
13	10.4	24.6	1.000	1.000	1.000	11.0	24.1	1.000	1.000	1.000
12	-1.5	116.2	1.000	1.000	1.000	-1.7	115.2	1.000	1.000	1.000
11	-3.3	69.2	1.000	1.000	1.000	-5.6	77.4	1.000	1.000	1.000

mple	Lat	Long	Uncorrected Mean			Lat	Long	Corrected Mean				
			Confidence		Major			Confidence		Major		
			Radius (Circle)	Minor Axes				Radius (Circle)	Minor Axes			
12	-5.1	68.8	1.000	1.000	1.000	-7.4	77.2	1.000	1.000	1.000		
13	-5.9	71.0	1.000	1.000	1.000	-8.1	79.4	1.000	1.000	1.000		
11	30.2	137.4	1.000	1.000	1.000	31.1	138.5	1.000	1.000	1.000		
13	29.4	115.6	1.000	1.000	1.000	29.8	117.0	1.000	1.000	1.000		
13	32.5	180.6	1.000	1.000	1.000	33.9	177.6	1.000	1.000	1.000		
13	32.6	43.1	1.000	1.000	1.000	34.6	42.5	1.000	1.000	1.000		
11	32.9	42.5	1.000	1.000	1.000	35.0	42.1	1.000	1.000	1.000		
12	51.7	49.2	1.000	1.000	1.000	53.6	50.6	1.000	1.000	1.000		
11	39.1	69.6	1.000	1.000	1.000	38.1	70.8	1.000	1.000	1.000		
11	12.6	168.3	1.000	1.000	1.000	14.4	169.8	1.000	1.000	1.000		
012	7.8	52.2	1.000	1.000	1.000	6.2	55.1	1.000	1.000	1.000		
013	37.3	79.5	1.000	1.000	1.000	36.6	81.0	1.000	1.000	1.000		
112	27.5	180.2	1.000	1.000	1.000	29.0	174.4	1.000	1.000	1.000		
213	37.9	107.0	1.000	1.000	1.000	38.3	108.8	1.000	1.000	1.000		
312	85.3	177.4	1.000	1.000	1.000	86.2	149.5	1.000	1.000	1.000		
412	-2.7	101.3	1.000	1.000	1.000	-2.6	104.6	1.000	1.000	1.000		
411	44.5	21.5	1.000	1.000	1.000	42.5	10.0	1.000	1.000	1.000		
413	16.5	124.1	1.000	1.000	1.000	17.4	126.5	1.000	1.000	1.000		
123	35.9	14.3	1.000	1.000	1.000	38.6	27.5	1.000	1.000	1.000		
221	-17.9	50.8	1.000	1.000	1.000	-17.4	49.5	1.000	1.000	1.000		
223	-26.0	107.6	1.000	1.000	1.000	-26.1	106.3	1.000	1.000	1.000		
523	20.3	58.5	1.000	1.000	1.000	20.2	58.7	1.000	1.000	1.000		
23	15.1	56.5	1.000	1.000	1.000	15.4	56.1	1.000	1.000	1.000		
321	18.2	10.1	1.000	1.000	1.000	18.2	10.1	1.000	1.000	1.000		
923	52.5	175.8	1.000	1.000	1.000	52.5	175.8	1.000	1.000	1.000		
222	1.9	81.1	1.000	1.000	1.000	1.1	85.0	1.000	1.000	1.000		
223	-7.4	188.7	1.000	1.000	1.000	-4.7	190.0	1.000	1.000	1.000		
522	61.9	143.7	1.000	1.000	1.000	61.9	143.7	1.000	1.000	1.000		
113	67.8	83.5	1.000	1.000	1.000	68.7	87.1	1.000	1.000	1.000		
111	27.9	34.3	1.000	1.000	1.000	27.0	34.6	1.000	1.000	1.000		
512	-14.1	63.2	1.000	1.000	1.000	-14.7	65.0	1.000	1.000	1.000		
513	33.9	23.0	1.000	1.000	1.000	32.9	17.6	1.000	1.000	1.000		
521	20.9	34.3	1.000	1.000	1.000	20.7	34.5	1.000	1.000	1.000		
513	63.2	36.4	1.000	1.000	1.000	61.4	29.6	1.000	1.000	1.000		
712	-9.7	22.3	1.000	1.000	1.000	3.9	10.0	1.000	1.000	1.000		
711	60.0	104.1	1.000	1.000	1.000	58.7	107.0	1.000	1.000	1.000		
012	-5.7	172.6	1.000	1.000	1.000	-19.9	142.5	1.000	1.000	1.000		
013	-9.3	168.0	1.000	1.000	1.000	-25.6	166.0	1.000	1.000	1.000		
213	15.6	97.5	1.000	1.000	1.000	15.5	101.2	1.000	1.000	1.000		
211	-21.0	78.8	1.000	1.000	1.000	-21.9	84.5	1.000	1.000	1.000		
212	4.1	56.2	1.000	1.000	1.000	2.1	60.5	1.000	1.000	1.000		
522	0.4	73.8	1.000	1.000	1.000	0.3	74.1	1.000	1.000	1.000		
213	13.3	41.3	1.000	1.000	1.000	12.2	42.7	1.000	1.000	1.000		

Table 12: Apparent polar positions using DGTL analysis with magnitude weighting over the full spectrum.

The pole positions that are contained in the table in the following pages, are those obtained in using the DGTL method with a magnitude weighting scheme over the spectrum ranging from 000oe. to 900oe. (next page). This table contains the sample identifier, the pole positions, the area of confidence, and the number of points available in the calculations.

sample	Uncorrected Mean Latitude	Mean Longitude	Corrected Mean Latitude	Corrected Mean Longitude	Prob Area	No. of Points
111	49.5	134.8	49.1	136.7	23.4393	15
312	-9.2	183.9	-7.7	183.3	0.0	20
911	-23.9	108.2	-23.8	109.4	22.4854	8
411	6.6	185.6	7.9	185.0	1.7839	18
211	73.7	122.4	74.5	109.5	14.8554	8
512	57.0	181.0	41.5	190.0	16.8995	10
611	56.2	100.9	56.2	100.9	21.8471	14
313	47.8	57.1	47.1	57.1	14.4813	8
212	59.0	169.1	61.4	161.8	17.4347	10
021	31.0	17.3	31.0	17.3	13.7070	9
711	25.1	120.4	22.8	111.4	26.2174	11
612	44.9	107.9	44.8	107.5	21.4988	12
613	-6.7	45.2	-6.2	44.0	14.7512	9
113	25.9	42.0	41.3	45.0	7.4804	10
713	-50.5	105.4	-49.6	82.1	29.9418	9
121	11.2	61.2	13.0	57.9	12.2989	9
912	-10.2	117.4	-10.0	118.4	18.2243	13
011	27.8	68.5	26.7	70.4	11.3776	10
913	-0.7	92.0	-0.8	93.0	10.4169	9
311	-42.5	37.3	-43.4	40.6	13.8338	10
522	-29.2	100.0	-29.2	103.1	27.2645	9
722	31.0	117.7	28.5	106.3	18.2570	9
721	49.5	70.5	56.0	71.1	9.8104	9
111	24.5	27.8	27.7	28.7	12.3330	9
723	27.1	79.4	32.6	69.3	12.7818	9
511	50.1	93.9	52.4	90.3	11.0934	9
523	44.0	12.6	44.0	12.6	12.8007	10
112	56.4	84.2	57.3	84.5	11.4959	10
522	52.5	49.0	52.7	49.2	10.3739	8
221	71.6	10.9	68.9	10.0	18.2874	9
913	-7.7	184.8	-7.7	184.8	22.4960	9
322	45.0	157.1	45.0	157.1	26.3305	9
323	2.8	51.5	2.8	51.5	22.3899	8
921	10.7	104.6	10.7	104.6	29.7564	9
922	-0.5	107.9	-0.5	107.9	32.6714	8
511	-74.2	56.7	-74.2	56.7	12.7663	9
512	-57.8	27.5	-57.8	27.5	14.3308	6
111	14.6	46.2	29.1	39.2	7.2102	9
513	40.5	100.0	41.8	90.4	19.3220	11
512	33.2	30.2	31.3	29.7	10.1798	10
523	-29.3	100.0	-29.2	103.1	24.6915	9
112	-9.0	184.0	-7.6	183.5	1.1463	20
521	35.8	49.2	36.0	49.1	9.7866	9
222	-4.5	59.9	-2.8	63.7	15.2525	9
11	1.4	189.1	3.8	185.7	3.8519	21
12	-6.3	185.8	-3.9	184.1	0.8209	19
13	61.4	88.5	61.0	87.7	8.5442	18
113	40.2	100.0	40.2	101.5	15.8873	13
112	11.1	165.1	10.6	164.4	29.2653	14
211	-2.5	70.1	-4.8	78.2	8.4875	9
212	-3.6	66.7	-6.1	74.9	8.1439	10
213	-5.6	71.1	-7.7	79.5	8.1730	10
311	43.5	58.8	42.6	54.7	13.2360	18
313	6.4	185.7	7.8	185.0	0.1660	17
313	6.6	185.6	7.9	185.0	0.4961	22

ample	Uncorrected Mean		Corrected Mean		Prob Area	No. of Points
	Latitude	Longitude	Latitude	Longitude		
513	1.3	189.1	-1.1	185.6	0.0	19
511	1.3	189.1	-1.1	185.6	0.8631	20
512	-1.3	10.9	1.1	14.4	2.0967	18
611	38.2	132.5	39.3	133.5	20.6708	15
311	-1.6	176.1	0.4	179.2	31.2284	9
012	-5.5	94.9	-5.6	98.4	12.0946	14
013	-3.2	51.1	-4.8	54.6	11.9507	10
112	50.3	181.4	51.9	171.7	18.3017	8
213	-40.1	157.2	-37.9	165.7	22.3591	10
312	31.0	100.0	31.0	97.9	21.1305	10
412	24.7	120.5	25.5	122.7	21.2821	8
411	63.5	108.1	63.7	107.0	16.1508	10
413	63.5	108.1	63.7	107.0	17.2100	10
123	16.2	26.3	18.8	32.7	14.6839	9
221	-8.7	37.8	-8.1	36.5	11.7957	9
223	-68.0	119.4	-68.2	116.6	24.8099	8
523	17.6	60.0	17.4	60.2	10.2982	5
523	15.9	55.6	16.2	55.2	10.0878	4
321	8.0	27.3	8.0	27.3	17.5798	9
923	31.6	149.8	31.6	149.8	31.9746	9
222	16.4	70.3	15.1	73.5	13.7019	9
223	39.2	152.9	41.3	145.6	22.5201	8
522	54.9	141.0	54.9	141.0	18.6087	11
113	56.3	99.6	56.3	99.6	12.6736	11
111	16.3	21.3	15.3	21.5	12.3330	9
512	-10.5	80.6	-10.8	82.2	11.5850	10
513	40.8	42.2	40.0	39.0	13.6779	10
521	20.6	35.7	20.4	35.8	9.3386	9
513	50.8	28.3	48.8	22.9	10.7630	9
712	-15.0	53.7	-3.6	26.7	12.9271	9
711	25.9	100.0	27.5	86.6	19.0640	10
012	0.4	137.1	-6.4	111.2	18.6191	9
013	0.4	137.1	-6.4	111.2	21.2109	10
213	30.3	90.5	29.9	93.3	12.3003	9
211	-31.2	100.0	-31.0	106.4	28.0896	10
212	-10.7	73.2	-12.0	78.4	15.3205	9
522	1.0	109.3	1.0	109.6	21.2238	9
213	31.7	56.5	30.9	57.3	12.9438	15

Table 13: Apparent polar positions using CNVL analysis with magnitude weighting, over the full spectrum.

The pole positions that are contained in the table in the following pages, are those obtained in using the CNVL method with a magnitude weighting scheme over the spectrum ranging from 000oe. to 900oe. (next page). This table contains the sample identifier, the pole positions, and the dimensions of the ellipse of confidence.

mple	Uncorrected Mean						Corrected Mean					
	Lat	Long	Confidence			Lat	Long	Confidence			Radius (Circle)	Minor Axes
			Radius (Circle)	Minor Axes	Major Axes			Radius (Circle)	Minor Axes	Major Axes		
11	-29.3	105.7	1.000	1.000	1.000	-29.4	106.3	1.000	1.000	1.000	1.000	1.000
12	16.0	133.4	1.000	1.000	1.000	16.9	135.0	1.000	1.000	1.000	1.000	1.000
11	-30.1	82.2	1.000	1.000	1.000	-30.3	83.6	1.000	1.000	1.000	1.000	1.000
11	42.8	152.6	1.000	1.000	1.000	43.9	152.5	1.000	1.000	1.000	1.000	1.000
211	72.9	14.1	1.000	1.000	1.000	70.3	10.0	1.000	1.000	1.000	1.000	1.000
512	63.2	170.7	1.000	1.000	1.000	47.9	190.0	1.000	1.000	1.000	1.000	1.000
11	20.4	53.8	1.000	1.000	1.000	20.9	53.2	1.000	1.000	1.000	1.000	1.000
313	19.8	43.5	1.000	1.000	1.000	19.0	44.3	1.000	1.000	1.000	1.000	1.000
212	64.1	181.9	1.000	1.000	1.000	66.6	164.8	1.000	1.000	1.000	1.000	1.000
021	3.8	70.8	1.000	1.000	1.000	3.8	70.8	1.000	1.000	1.000	1.000	1.000
11	28.0	132.6	1.000	1.000	1.000	24.0	124.2	1.000	1.000	1.000	1.000	1.000
12	12.4	70.0	1.000	1.000	1.000	12.7	69.1	1.000	1.000	1.000	1.000	1.000
13	-14.9	44.5	1.000	1.000	1.000	-14.4	43.1	1.000	1.000	1.000	1.000	1.000
113	24.3	42.6	1.000	1.000	1.000	39.6	44.1	1.000	1.000	1.000	1.000	1.000
13	-12.8	120.7	1.000	1.000	1.000	-14.7	105.7	1.000	1.000	1.000	1.000	1.000
121	30.5	61.7	1.000	1.000	1.000	32.3	59.8	1.000	1.000	1.000	1.000	1.000
12	-6.0	61.8	1.000	1.000	1.000	-6.4	62.8	1.000	1.000	1.000	1.000	1.000
011	6.6	98.3	1.000	1.000	1.000	6.6	101.3	1.000	1.000	1.000	1.000	1.000
13	0.4	101.9	1.000	1.000	1.000	0.5	102.8	1.000	1.000	1.000	1.000	1.000
311	-0.5	124.6	1.000	1.000	1.000	-0.1	126.1	1.000	1.000	1.000	1.000	1.000
522	-34.7	120.4	1.000	1.000	1.000	-34.2	123.8	1.000	1.000	1.000	1.000	1.000
722	32.2	120.7	1.000	1.000	1.000	29.1	109.7	1.000	1.000	1.000	1.000	1.000
721	50.7	72.1	1.000	1.000	1.000	56.8	73.0	1.000	1.000	1.000	1.000	1.000
111	39.8	47.5	1.000	1.000	1.000	42.5	47.5	1.000	1.000	1.000	1.000	1.000
723	18.0	88.8	1.000	1.000	1.000	21.9	75.3	1.000	1.000	1.000	1.000	1.000
511	48.4	93.0	1.000	1.000	1.000	51.0	88.4	1.000	1.000	1.000	1.000	1.000
623	41.7	40.3	1.000	1.000	1.000	41.7	40.3	1.000	1.000	1.000	1.000	1.000
112	57.6	73.0	1.000	1.000	1.000	59.1	74.1	1.000	1.000	1.000	1.000	1.000
22	49.7	38.4	1.000	1.000	1.000	50.1	38.8	1.000	1.000	1.000	1.000	1.000
221	33.9	104.1	1.000	1.000	1.000	34.1	106.3	1.000	1.000	1.000	1.000	1.000
913	0.1	133.9	1.000	1.000	1.000	0.1	133.9	1.000	1.000	1.000	1.000	1.000
322	7.3	119.9	1.000	1.000	1.000	7.3	119.9	1.000	1.000	1.000	1.000	1.000
323	-6.6	20.5	1.000	1.000	1.000	-6.6	20.5	1.000	1.000	1.000	1.000	1.000
921	34.5	121.8	1.000	1.000	1.000	34.5	121.8	1.000	1.000	1.000	1.000	1.000
922	12.3	91.7	1.000	1.000	1.000	12.3	91.7	1.000	1.000	1.000	1.000	1.000
511	-74.5	107.7	1.000	1.000	1.000	-74.5	107.7	1.000	1.000	1.000	1.000	1.000
512	-55.5	63.5	1.000	1.000	1.000	-55.5	63.5	1.000	1.000	1.000	1.000	1.000
111	13.4	47.5	1.000	1.000	1.000	27.8	39.0	1.000	1.000	1.000	1.000	1.000
513	38.1	98.6	1.000	1.000	1.000	40.0	88.1	1.000	1.000	1.000	1.000	1.000
512	26.0	31.6	1.000	1.000	1.000	24.1	32.2	1.000	1.000	1.000	1.000	1.000
523	-36.7	98.1	1.000	1.000	1.000	-36.7	101.5	1.000	1.000	1.000	1.000	1.000
12	8.9	163.5	1.000	1.000	1.000	10.2	165.0	1.000	1.000	1.000	1.000	1.000
21	27.5	54.9	1.000	1.000	1.000	27.8	54.6	1.000	1.000	1.000	1.000	1.000
222	36.4	22.7	1.000	1.000	1.000	39.0	32.9	1.000	1.000	1.000	1.000	1.000
1	-11.0	58.0	1.000	1.000	1.000	-12.5	62.1	1.000	1.000	1.000	1.000	1.000
2	9.3	100.5	1.000	1.000	1.000	9.4	103.6	1.000	1.000	1.000	1.000	1.000
3	-55.3	137.5	1.000	1.000	1.000	-53.7	145.6	1.000	1.000	1.000	1.000	1.000
13	10.4	24.6	1.000	1.000	1.000	11.0	24.1	1.000	1.000	1.000	1.000	1.000
12	-1.5	116.2	1.000	1.000	1.000	-1.7	115.2	1.000	1.000	1.000	1.000	1.000
11	-3.3	69.2	1.000	1.000	1.000	-5.6	77.4	1.000	1.000	1.000	1.000	1.000
12	-5.1	68.8	1.000	1.000	1.000	-7.4	77.2	1.000	1.000	1.000	1.000	1.000
13	-5.9	71.0	1.000	1.000	1.000	-8.1	79.4	1.000	1.000	1.000	1.000	1.000
11	30.2	137.4	1.000	1.000	1.000	31.1	138.5	1.000	1.000	1.000	1.000	1.000

Sample	Lat	Long	Uncorrected Mean			Corrected Mean				
			Confidence			Lat	Long	Confidence		
			Radius (Circle)	Minor Axes	Major Axes			Radius (Circle)	Minor Axes	Major Axes
313	29.4	115.6	1.000	1.000	1.000	29.8	117.0	1.000	1.000	1.000
413	32.5	180.6	1.000	1.000	1.000	33.9	177.6	1.000	1.000	1.000
513	32.6	43.1	1.000	1.000	1.000	34.6	42.5	1.000	1.000	1.000
511	32.9	42.5	1.000	1.000	1.000	35.0	42.1	1.000	1.000	1.000
512	51.7	49.2	1.000	1.000	1.000	53.6	50.6	1.000	1.000	1.000
511	39.1	69.6	1.000	1.000	1.000	38.1	70.8	1.000	1.000	1.000
311	12.6	168.3	1.000	1.000	1.000	14.4	169.8	1.000	1.000	1.000
1012	7.8	52.2	1.000	1.000	1.000	6.2	55.1	1.000	1.000	1.000
1013	37.3	79.5	1.000	1.000	1.000	36.6	81.0	1.000	1.000	1.000
1112	27.5	180.2	1.000	1.000	1.000	29.0	174.4	1.000	1.000	1.000
1213	37.9	107.0	1.000	1.000	1.000	38.3	108.8	1.000	1.000	1.000
312	85.3	177.4	1.000	1.000	1.000	86.2	149.5	1.000	1.000	1.000
412	-2.7	101.3	1.000	1.000	1.000	-2.6	104.6	1.000	1.000	1.000
411	44.5	21.5	1.000	1.000	1.000	42.5	10.0	1.000	1.000	1.000
413	16.5	124.1	1.000	1.000	1.000	17.4	126.5	1.000	1.000	1.000
5123	35.9	14.3	1.000	1.000	1.000	38.6	27.5	1.000	1.000	1.000
5221	-17.9	50.8	1.000	1.000	1.000	-17.4	49.5	1.000	1.000	1.000
5223	-26.0	107.6	1.000	1.000	1.000	-26.1	106.3	1.000	1.000	1.000
6223	20.3	58.5	1.000	1.000	1.000	20.2	58.7	1.000	1.000	1.000
523	15.1	56.5	1.000	1.000	1.000	15.4	56.1	1.000	1.000	1.000
5821	18.2	10.1	1.000	1.000	1.000	18.2	10.1	1.000	1.000	1.000
5923	52.5	175.8	1.000	1.000	1.000	52.5	175.8	1.000	1.000	1.000
5222	1.9	81.1	1.000	1.000	1.000	1.1	85.0	1.000	1.000	1.000
5223	-7.4	188.7	1.000	1.000	1.000	-4.7	190.0	1.000	1.000	1.000
6222	61.9	143.7	1.000	1.000	1.000	61.9	143.7	1.000	1.000	1.000
5113	67.8	83.5	1.000	1.000	1.000	68.7	87.1	1.000	1.000	1.000
5111	27.9	34.3	1.000	1.000	1.000	27.0	34.6	1.000	1.000	1.000
512	-14.1	63.2	1.000	1.000	1.000	-14.7	65.0	1.000	1.000	1.000
513	33.9	23.0	1.000	1.000	1.000	32.9	17.6	1.000	1.000	1.000
5621	20.9	34.3	1.000	1.000	1.000	20.7	34.5	1.000	1.000	1.000
5613	63.2	36.4	1.000	1.000	1.000	61.4	29.6	1.000	1.000	1.000
5712	-9.7	22.3	1.000	1.000	1.000	3.9	10.0	1.000	1.000	1.000
5711	60.0	104.1	1.000	1.000	1.000	58.7	107.0	1.000	1.000	1.000
5012	-5.7	172.6	1.000	1.000	1.000	-19.9	142.5	1.000	1.000	1.000
5013	-9.3	168.0	1.000	1.000	1.000	-25.6	166.0	1.000	1.000	1.000
5213	15.6	97.5	1.000	1.000	1.000	15.5	101.2	1.000	1.000	1.000
5211	-21.0	78.8	1.000	1.000	1.000	-21.9	84.5	1.000	1.000	1.000
5212	4.1	56.2	1.000	1.000	1.000	2.1	60.5	1.000	1.000	1.000
5622	0.4	73.8	1.000	1.000	1.000	0.3	74.1	1.000	1.000	1.000
5213	13.3	41.3	1.000	1.000	1.000	12.2	42.7	1.000	1.000	1.000

Appendix E

LATITUDE AND LONGITUDE POSITIONS OF THE SAMPLE SITES.

The following table contains the Latitude and Longitude position for each core.

Table 14: Latitudinal and longitudinal positions of the sites

The following table contains the latitude and longitude positions of the sample sites. Contained, as well, are the compass bearing readings and the GMT time. This traverse was conducted as a preliminary survey, intended to identify areas for further study. It appears that a survey conducted in this manner produces more significant results than one that is focused on one formation.

Sample	Date	Time	Sample Azimuth	Suns Azimuth	Latitude	Longitude
80001	123	1940	24700	21000	5645	10000
80002	123	1944	22300	20630	5645	10000
80201	123	2042	30430	23700	5645	10000
80202	123	2048	31200	23130	5645	10000
80101	123	1955	27600	21030	5645	10000
80102	123	2000	200	22800	5645	10000
80301	123	2057	33500	23500	5645	10000
80302	123	2106	1800	23730	5645	10000
80401	123	2118	6100	24100	5645	10000
80402	123	2129	15900	24430	5645	10000
80501	123	2139	24200	24000	5645	10000
80502	125	1520	19000	11100	5645	10000
80601	123	2154	0	24700	5644	10000
80602	123	2206	31330	25000	5644	10000
80701	123	2215	9030	23800	5645	10000
80702	123	2223	3900	26000	5645	10000
80801	123	100	23430	29100	5644	10000
80802	123	104	7200	29000	5644	10000
80901	123	114	830	29130	5644	10000
80902	123	120	16200	29400	5644	10000
81001	123	129	25100	29700	5644	10000
81002	123	134	14630	29700	5644	10000
81101	123	150	10030	30000	5644	10000
81102	123	156	2930	30200	5644	10000
81201	123	206	6200	30500	5644	10000
81202	123	210	3200	30300	5644	10000
81401	123	220	5900	30700	5645	10000
81402	123	223	20430	30700	5645	10000
81601	123	235	1930	30230	5644	10000
81602	123	238	18500	3080	5644	10000
81301	125	1545	17600	12000	5644	10000
81302	125	1540	16700	11830	5644	10000
81501	125	1555	15000	12330	5645	10000
81502	125	1600	18400	12400	5645	10000
81701	125	1640	2500	13700	5645	10000
81702	125	1635	2830	13500	5645	10000
8181	125	1655	1400	14400	5644	10000
8182	125	1700	5330	14430	5644	10000
81901	125	1720	21430	15030	5644	10000
81902	125	1725	21700	15200	5644	10000
82001	125	2110	34330	23730	5640	10000
82002	125	2115	30330	24000	5640	10000
82101	125	2135	7100	24500	5640	10000
82102	125	2140	4000	24600	5640	10000
82201	125	2210	9830	25400	5639	10000
82202	125	2215	7430	25700	5639	10000
82301	125	2240	8200	26200	5639	10000
82302	125	2230	9030	26200	5639	10000
83501	125	123	20600	29600	5634	10000
83502	125	127	25200	29730	5634	10000
83401	125	134	8100	29630	5634	10000
83402	125	149	6100	29730	5634	10000
83301	125	145	3730	29930	5635	10000
82701	125	230	26200	30900	5638	10000
82702	125	241	6330	30630	5638	10000

Sample	Date	Time	Sample Azimuth	Suns Azimuth	Latitude	Longitude
83302	126	1320	34130	8700	5635	10000
83201	126	1340	1100	8830	5635	10000
83202	126	1345	10200	9000	5635	10000
83101	126	1400	930	9530	5637	10000
83001	126	1410	7430	9700	5637	10000
83002	126	1415	4600	9900	5638	10000
82801	126	1430	11100	10130	5638	10000
82802	126	1435	6030	10400	5638	10000
82401	126	1710	30500	14700	5638	10000
82402	126	1737	31100	15700	5638	10000
82501	126	1750	27800	16230	5638	10000
82502	126	1755	33200	16400	5638	10000
82601	126	1805	28500	16800	5638	10000
82602	126	1812	27200	17200	5638	10000
82901	126	1825	25500	17730	5637	10000
82902	126	1830	25500	18000	5637	10000
83601	129	2320	14930	26900	5625	10000
83602	130	1234	13900	7700	5625	10000
83701	130	1255	7700	8100	5625	10000
83702	130	1300	15400	8200	5625	10000
83801	130	1335	34530	9030	5621	10000
83802	130	1350	2130	8200	5621	10000
83901	130	1400	29000	9400	5621	10000
83902	130	1410	5500	9530	5621	10000
84001	130	1425	5700	9900	5620	10000
84002	130	1430	22530	10100	5620	10000
84101	130	1107	1630	12700	5619	10000
84102	130	1117	300	12800	5619	10000
84201	130	1141	4830	13900	5619	10000
84202	130	1150	5800	14000	5619	10000
84301	130	1210	9000	14630	5619	10000
84302	130	1217	7930	14830	5619	10000
84401	130	1243	8430	15800	5618	10000
84402	130	1252	6630	16000	5618	10000
84501	130	115	1900	17200	5618	10000
84502	130	110	3900	17000	5618	10000
84601	130	151	13000	18600	5618	10000
84701	130	204	7200	19130	5617	10000
84702	130	211	7200	19600	5617	10000
84801	130	233	9230	20200	5617	10000
84802	130	735	5830	28330	5617	10000
84902	130	757	8200	28800	5617	10000
85001	130	300	16700	21700	5617	10000
85101	130	320	28900	21900	5616	10000
85102	130	329	7300	22200	5616	10000
85201	130	347	24200	23300	5616	10000
85202	130	821	1430	29200	5616	10000
85302	130	417	11130	24030	5615	10000
85401	130	447	13800	24700	5615	10000
85402	130	455	8400	25100	5615	10000
85501	130	511	2400	25100	5614	10000
85502	130	517	3400	25330	5614	10000
85601	130	543	19100	26030	5614	10000
85602	130	854	14530	30100	5614	10000
86401	201	343	5900	22900	5606	10000
86402	201	347	10600	23000	5606	10000

Sample	Date	Time	Sample Azimuth	Suns Azimuth	Latitude	Longitude
86301	201	413	21100	23900	5608	10000
86302	201	416	30800	24000	5608	10000
86201	201	437	3400	24700	5609	10000
86202	201	440	33500	24700	5609	10000
86101	201	459	12830	25600	5610	10000
86102	201	504	26200	25400	5610	10000
85301	202	910	24700	9600	5615	10000
85701	202	932	8030	10430	5613	10000
85702	202	1057	20700	12430	5613	10000
85801	202	1001	12330	10830	5613	10000
85802	202	1008	8630	10900	5613	10000
85901	202	1021	3000	12100	5612	10000
85902	202	1030	8130	12200	5612	10000
86001	202	1040	32130	11300	5612	10000
86002	202	1045	30330	11730	5612	10000
86601	202	1126	34500	13000	5604	10000
86701	202	1136	7900	13500	5602	10000
86702	202	1143	6530	13930	5602	10000
87201	202	1206	27800	14800	5602	10000

Appendix F**COMPASS ERROR CORRECTIONS**

The following table contains the correction factors for the compass error. These values were determined by taking a sun-sight reading and a GMT reading and applying the calculations described here.

Table 15: Compass error due to local field abnormalities.

This table contains the correction factor for the error in the compass reading due to local influences on the earth's field. These values were used to correct the orientations of the magnetic remanences of the samples.

Sample	LST	Samples Azimuth	Suns Azimuth	Correction Factor	Corrected Azimuth
80001	7.11	210.00	247.00	4.23	242.77
80002	7.17	206.30	223.00	-1.01	224.01
80201	8.14	237.00	304.30	9.28	295.01
80202	8.24	231.30	312.00	1.69	310.31
80101	7.36	210.30	276.00	-1.17	277.17
80102	7.44	228.00	2.00	14.69	-12.69
80301	8.39	235.00	335.00	2.61	332.39
80302	8.54	237.30	18.00	2.22	15.78
80401	8.74	241.00	61.00	2.45	58.55
80402	8.93	244.30	159.00	2.68	156.32
80501	9.10	240.00	242.00	-4.31	246.31
80502	2.89	111.00	190.00	-0.63	190.63
80601	9.35	247.00	0.0	-1.22	1.22
80602	9.55	250.00	313.30	-1.22	314.52
80701	9.70	238.00	90.30	-15.40	105.70
80702	9.83	260.00	39.00	4.69	34.31
80801	12.39	291.00	234.30	3.60	230.70
80802	12.46	290.00	72.00	1.82	70.18
80901	12.62	291.30	8.30	1.15	7.15
80902	12.72	294.00	162.00	2.68	159.32
81001	12.87	297.00	251.00	3.91	247.09
81002	12.96	297.00	146.30	2.93	143.37
81101	13.22	300.00	100.30	2.77	97.53
81102	13.32	302.00	29.30	3.59	25.71
81201	13.49	305.00	62.00	4.61	57.39
81202	13.56	303.00	32.00	1.81	30.19
81401	13.73	307.00	59.00	3.82	55.18
81402	13.78	307.00	204.30	3.22	201.08
81601	13.98	302.30	19.30	-3.90	23.20
81602	14.03	308.00	185.00	1.20	183.80
81301	3.31	120.00	176.00	1.80	174.20
81302	3.23	118.30	167.00	1.45	165.55
81501	3.48	123.30	150.00	2.31	147.69
81502	3.56	124.00	184.00	1.59	182.41
81701	4.23	137.00	25.00	2.33	22.67
81702	4.15	135.00	28.30	1.96	26.34
81801	4.48	144.00	14.00	4.30	9.70
81802	4.56	144.30	53.30	2.87	50.43
81901	4.90	150.30	214.30	1.65	212.65
81902	4.98	152.00	217.00	1.47	215.53
82001	8.74	237.30	343.30	1.14	342.16
82002	8.83	240.00	303.30	2.40	300.90
82101	9.16	245.00	71.00	1.85	69.15
82102	9.24	246.00	40.00	1.51	38.49
82201	9.74	254.00	98.30	1.88	96.42
82202	9.83	257.00	74.30	3.67	70.63
82301	10.25	262.00	82.00	2.83	79.17
82302	10.08	262.00	90.30	5.12	85.18
83501	12.90	296.00	206.00	4.16	201.84
83502	12.97	297.30	252.00	4.68	247.32
83401	13.09	296.30	81.00	2.30	78.70
83402	13.34	297.30	61.00	0.35	60.65
83301	13.27	299.30	37.30	3.14	34.16
82701	14.02	309.00	262.00	3.90	258.10
82702	14.21	306.30	63.30	-1.01	64.31

Sample	LST	Samples Azimuth	Suns Azimuth	Correction Factor	Corrected Azimuth
83302	0.95	87.00	341.30	2.24	339.06
83201	1.29	88.30	11.00	-0.56	11.56
83202	1.37	90.00	102.00	0.10	101.90
83101	1.62	95.30	9.30	2.23	7.07
83001	1.79	97.00	74.30	1.78	72.52
83002	1.87	99.00	46.00	2.69	43.31
82801	2.12	101.30	111.00	1.67	109.33
82802	2.21	104.00	60.30	3.24	57.06
82401	4.80	147.00	305.00	2.12	302.88
82402	5.25	157.00	311.00	1.98	309.02
82501	5.47	162.30	278.00	2.14	275.86
82502	5.55	164.00	332.00	1.82	330.18
82601	5.72	168.00	285.00	1.73	283.27
82602	5.83	172.00	272.00	2.83	269.17
82901	6.05	177.30	255.00	2.69	252.31
82902	6.13	180.00	255.00	3.28	251.72
83601	11.18	269.00	149.30	1.26	148.04
83602	0.45	77.00	139.00	1.51	137.49
83701	0.80	81.00	77.00	1.36	75.64
83702	0.88	82.00	154.00	1.36	152.64
83801	1.47	90.30	345.30	2.61	342.69
83802	1.72	82.00	21.30	-8.80	30.10
83901	1.88	94.00	290.00	1.09	288.91
83902	2.05	95.30	55.00	0.24	54.76
84001	2.30	99.00	57.00	0.67	56.33
84002	2.39	101.00	225.30	1.55	223.75
84101	22.99	127.00	16.30	-21.37	37.67
84102	23.16	128.00	3.00	-22.35	25.35
84201	23.56	139.00	48.30	-16.08	64.38
84202	23.71	140.00	58.00	-16.85	74.85
84301	0.05	146.30	90.00	-14.47	104.47
84302	0.16	148.30	79.30	-13.84	93.14
84401	0.60	158.00	84.30	-9.24	93.54
84402	0.75	160.00	66.30	-9.02	75.32
84501	13.10	172.00	19.00	-28.00	47.00
84502	13.02	170.00	39.00	-29.03	68.03
84601	13.70	186.00	130.00	-21.07	151.07
84701	13.92	191.30	72.00	-18.34	90.34
84702	14.04	196.00	72.00	-15.02	87.02
84801	14.40	202.00	92.30	-13.42	105.72
84802	19.45	283.30	58.30	0.59	57.71
84902	19.82	288.00	82.00	0.22	81.78
85001	14.85	217.00	167.00	-3.90	170.90
85101	15.19	219.00	289.00	-6.03	295.03
85102	15.34	222.00	73.00	-4.91	77.91
85201	15.64	233.00	242.00	2.29	239.71
85202	20.22	292.00	14.30	-1.24	15.54
85302	16.14	240.30	111.30	3.12	108.18
85401	16.64	247.00	138.00	3.18	134.82
85402	16.78	251.00	84.00	5.39	78.61
85501	17.04	251.00	24.00	1.77	22.23
85502	17.14	253.30	34.00	2.70	31.30
85601	17.58	260.30	191.00	3.73	187.27
85602	20.77	301.00	145.30	0.39	144.91
86401	15.64	229.00	59.00	-0.80	59.80

Sample	LST	Samples Azimuth	Suns Azimuth	Correction Factor	Corrected Azimuth
86402	15.71	230.00	106.00	-0.65	106.65
86301	16.14	239.00	211.00	2.75	208.25
86302	16.19	240.00	308.00	3.10	304.90
86201	16.54	247.00	34.00	5.48	28.52
86202	16.59	247.00	335.00	4.81	330.19
86101	16.91	256.00	128.30	9.55	118.75
86102	16.99	254.00	262.00	6.42	255.58
85301	21.17	96.00	247.00	-28.06	275.06
85701	21.54	104.30	80.30	-24.51	104.81
85702	22.96	124.30	207.00	-22.05	229.05
85801	22.02	108.30	123.30	-26.62	149.92
85802	22.14	109.00	86.30	-27.38	113.68
85901	22.36	121.00	30.00	-18.06	48.06
85902	22.51	122.00	81.30	-18.90	100.20
86001	22.67	113.00	321.30	-29.93	351.23
86002	22.76	117.30	303.30	-26.64	329.94
86601	23.44	130.00	345.00	-22.10	367.10
86701	23.61	135.00	79.00	-19.06	98.06
86702	23.73	139.30	65.30	-16.14	81.44
87201	0.11	148.00	278.00	-11.94	289.94

Appendix G

RESULTS OF THE EIGENVALUE ANALYSIS

This table contains the results from the eigenvalue analysis. The pole position that was determined in this manner is 23°S 0° S and 146°W. The values contained in the table are the normals to the best-fit plane. They have been corrected for core orientation.

Table 16: Eigenvalue analysis of selected samples.

This table contains the eigenvalue results. Contained in the table are the vector normals of the best fit planes. The last value (denoted as 999), is the results from a subsequent eigenvalue analysis done on the normals. The sample that indicated a sweep behavior were chosen to be suitable for this analysis.

Sample	X-value	Y-value	Z-value
112	-0.259	-0.832	0.490
212	0.335	-0.782	0.526
211	0.628	0.661	-0.412
1013	0.649	0.590	-0.479
111	0.132	0.043	-0.990
6221	-0.256	-0.184	-0.949
5112	-0.214	0.181	-0.960
9999	146.26	-23.51	

Appendix H**CORING TOOL ORIENTATION**

This table contains the orientation of the coring tool as it was in the drilling procedure. All values in this study were corrected using these results. At some sample sites, the sun-sight position was unavailable due to weather conditions.

Table 17: Coring tool orientation in situ.

The data contained in this table is the sample orientations as they were cored. These values were considered in the calculations of the orientation of the magnetic moments of the samples in the reference frame of the earth.

Sample Site	GMT	Compass North	Date	Core Declination	Core Inclination
002	1940	210	123	247	86
001	1944	206.5	123	223	85
022	2042	237	123	304.5	86
021	2048	231.5	123	312	85
012	1955	210.5	123	276	83
011	2000	228	123	2	85
032	2057	235	123	335	85
031	2106	237.5	123	18	80
042	2118	241	123	61	90
041	2129	244.5	123	159	82.5
052	2139	240	123	242	85
051	520	111	125	190	72
062	2154	247	123	0	85
061	2206	250	123	313.5	83
072	2215	238	123	90.5	79
071	2223	260	123	39	83
082	100	291	123	234.5	81
081	104	290	123	72	78
092	114	291.5	123	8.5	81
091	120	294	123	162	67
102	129	297	123	251	71
101	134	297	123	146.5	73
112	150	300	123	100.5	65
111	156	302	123	29.5	73
122	206	305	123	62	80
121	210	303	123	32	80
142	220	307	123	59	75
141	223	307	123	204.5	73
162	235	302.5	123	19.5	81
161	238	308	123	185	71
132	545	120	125	176	79
131	540	118.5	125	167	76.5
152	1555	123.5	125	150	72.5
151	1600	124	125	184	77
172	1640	137	125	25	80
171	1635	135	125	28.5	79
182	1655	144	125	14	85
181	1700	144.5	125	53.5	83
192	1720	150.5	125	214.5	77
191	1725	152	125	217	78
202	910	237.5	125	343.5	82
201	915	240	125	303.5	81
212	910	237.5	125	343.5	82
211	915	240	125	303.5	81
212	935	245	125	71	86
211	940	246	125	40	80
222	1010	254	125	98.5	83
221	1015	257	125	74.5	85
232	1040	262	125	82	78
231	1030	262	125	90.5	85
352	123	296	125	206	71
351	127	297.5	125	252	63
342	134	296.5	125	81	77
341	149	297.5	125	61	76
332	145	299.5	125	37.5	80

Sample Site	GMT	Compass North	Date	Core Declination	Core Inclination
272	230	309	125	262	78
271	241	306.5	125	63.5	75
331	1320	87	126	341.5	79
322	1340	88.5	126	11	84
321	1345	90	126	102	75
312	1400	95.5	126	9.5	79
302	1410	97	126	74.5	75
301	1415	99	126	46	75
282	1430	101.5	126	111	84
281	1435	104	126	60.5	82
242	1710	147	126	305	82
241	1737	157	126	311	82
252	1750	162.5	126	278	77
251	1755	164	126	332	80
262	1805	168	126	285	84
261	1812	172	126	272	86
292	1825	177.5	126	255	80
291	1830	180	126	255	80
362	320	269	129	149.5	80
361	1234	77	130	139	79
372	1255	81	130	77	79
371	1300	82	130	154	80
382	1335	90.5	130	345.5	74
381	1350	82	130	21.5	78
392	1400	94	130	290	75
391	1410	95.5	130	55	75
402	1425	99	130	57	81
401	1430	101	130	225.5	74
412	1107	127	130	16.5	82
411	1117	128	130	3	76
422	1141	139	130	48.5	81
421	1150	140	130	58	80
432	1220	146.5	130	90	85
431	1217	148.5	130	79.5	85
442	1243	158	130	84.5	83
441	1252	160	130	66.5	85
452	115	172	130	19	81
451	110	170	130	39	76
462	151	186	130	130	76
472	204	191.5	130	72	79
471	211	196	130	72	80
482	1933	202	130	92.5	70
481	35	283.5	130	58.5	79
491	057	288	130	82	77
502	30	217	130	167	70
512	320	219	130	289	76
511	329	222	130	73	72
522	347	233	130	242	73
521	821	292	130	14.5	84
531	417	240.5	130	111.5	84
542	447	247	130	138	83
541	455	251	130	84	76
552	511	251	130	24	80
551	517	253.5	130	34	83
562	543	260.5	130	191	84

Sample Site	GMT	Compass North	Date	Core Declination	Core Inclination
561	854	30.1	130	145.5	83
712	201	NA	NA	82	81
711	201	NA	NA	86	77
702	201	NA	NA	71	83
701	201	NA	NA	241	76
692	201	NA	NA	236.5	72
691	201	NA	NA	62	82
682	201	NA	NA	249	65
652	201	NA	NA	47.5	82
651	201	NA	NA	39.5	72
642	343	229	201	59	85
641	347	230	201	106	89
632	413	239	201	211	68
631	416	240	201	308	65
622	437	247	201	34	80
621	440	247	201	335	84
612	459	256	201	128.5	85
611	504	254	201	262	73
532	910	96	202	247	74
572	932	104.5	202	80.5	79
571	1057	124.5	202	207	75
582	1001	108.5	202	123.5	81
581	1008	109	202	86.5	86
592	1021	121	202	30	89
591	1030	122	202	81.5	84
602	1040	113	202	321.5	76
601	1040	117.5	202	303.5	80
662	1126	130	202	345	85
672	1636	135	202	79	85
671	1643	139.5	202	65.5	83
722	1206	148	202	278	80

Appendix I**DATA CORRECTIONS DUE TO COMPASS ERRORS**

The realistic setting for palaeomagnetic sampling is in the presence of local magnetization that can lead to errors in compass orientation. In areas where the surveying of the roads is inadequate, or where such significant land sights are non-existent, sun-sight readings are required. With a sun-sight position, and the corresponding Greenwich mean time that the sight was made at, an accurate determination of the true north position can be made for the longitudinal position of the samples' location.

The calculations are based on the orbital and rotational motion of the earth relative to the sun. These calculations are complicated because of the complexity of this motion. However, they are far from being an unusual procedure since they have been used for centuries in navigational applications.

The principle in their use here, is to determine the true sun's position at that particular time and longitudinal position in the reference frame of the observer (horizontal reference frame). Since the orbital motion of the earth around the sun is accurately known, the apparent motion of the sun to the observer can be calculated and compared to the position that is measured with the compass (the sun-

sight position). This difference is then subtracted from the samples orientation to give its correction factor.

The earth's position in it's orbit around the sun is described in elliptic coordinates. The elliptic is the plane of the earth's orbit. In this particular reference frame, the principle latitude of the sun is zero. The sun "orbits" through 360 degrees, during the course of one year, and it's intermediate position is determined by the date. This position of the sun is determined in the elliptic coordinate frame by the following steps (Duffet-Smith, 1981);

1. Find the number of days since January 0.0 at the beginning of the year, then add 365 days for every year since 1980 (add one day for each leap year).
2. Convert to degrees.
3. Calculate;

$$M = N + \epsilon - \omega$$

where; ϵ = ecliptic longitude at epoch

ω = ecliptic longitude at perigee

then convert to the interval 0-360 by adding or subtracting multiples of 360.

4. The geocentric elliptic is determined by the relationship;

$$l/l_0 = N + 360 / \pi \times \sin M + \epsilon$$

then convert to the interval 0-360 as above.

The next step is to convert to right ascension and declination, the coordinate system that is fixed relative to the center of the earth, with the declination the measure off of the equatorial plane.

5. Calculate;

$$s = \arcsin \langle \sin \beta \times \cos \xi + \cos \beta \times \sin \epsilon \times \sin \lambda_0 \rangle$$

6. The right ascension is given as;

$$a = \arctan \langle \sin \lambda \times \cos \xi - \tan \beta \times \sin \xi \rangle / \langle \cos \lambda_0 \rangle$$

The tan function confuses the correct sign of the ascension; it can be recovered using the "CAST" rule.

The next step in the procedure is to convert from equatorial to horizon coordinates. This system uses the horizon as the plane of reference.

7. The hour angle H is given as;

$$H = LST - a$$

and is calculated as follows;

- Greenwich sidereal time (GST) is determined by the following calculations;

$$GST = DS \times A - B + C \times GMT$$

where DS = number of days since Jan. 0.0
and date of interest.

A,B,C = are constants determined from table
values.

The result is converted to the interval 0-24 by
adding or subtracting multiples of 24.

8. Calculate;

$$a = \arcsin(\sin \alpha \times \sin \theta + \cos \alpha \times \cos \phi \times \cos H)$$

where ϕ = geographic latitude

a = altitude

9. Calculate;

$$A = \arccos(\sin \alpha - \sin \theta \times \sin a) / (\cos \theta \times \cos a)$$

if $\sin(H) > 0$ then $A = 360 - A$

The value of the azimuthal angle A , is the correct value of the sun-sight position. The difference between this value and the measured value represents the error of the reading.¹¹ All inclination measurements made relative to compass north are then corrected using this value.

¹¹ Due to magnetic deviation of the compass bearing.